Optoelectronic Components (OC)

When: Mon 08:00–09:30 Lecture (beginning 13.04.15)
Thu 09:45–11:15 Lecture
Fri 11:30–12:15 Tutorial (beginning 24.04.15)
Detailed dates and examinations on next page

Where: Kleiner HS A, Build. 30.22 (L)
HS II, Build. 30.41 (T)

Lecturer: Prof. Dr. W. Freude (Build. 30.10 R.3.34)

Tutors: Dipl.-Ing. S. Wolf
Dipl.-Phys. W. Hartmann

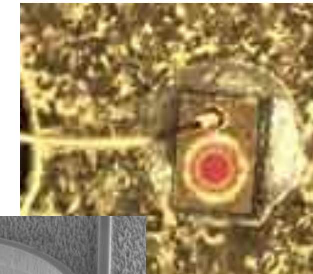

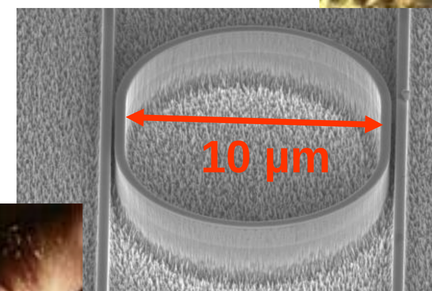

Contents:

- Optical communications overview
- Slab, strip, and fibre waveguides
- Light-emitting and laser diodes
- Optical amplifiers
- Pin photodiodes
- Noise
- Receivers and detection errors

Pl avoid unnecessary emails.
However, I am more than ready for Q&A.

Lectures (Kl. HS A, Build. 30.22)

1. Mon 13.04.15 08:00
2. Thu 16.04.15 09:45
3. Mon 20.04.15 08:00
4. Thu 23.04.15 09:45
5. Mon 27.04.15 08:00
6. Thu 30.04.15 09:45
7. Mon 04.05.15 08:00
8. Thu 07.05.15 09:45
9. Mon 11.05.15 08:00
10. Mon 18.05.15 08:00
11. Thu 21.05.15 09:45
12. Mon 01.06.15 08:00
13. Mon 08.06.15 08:00
14. Thu 11.06.15 09:45
15. Mon 15.06.15 08:00
16. Thu 18.06.15 09:45

A. Mon 22.06.15 08:00 (Q&A 1)
B. Thu 25.06.15 09:45 (Q&A 2)

Tutorial (HS II, Build. 30.41)

First Fri 24.04.15 11:30–12:15
Last Fri 10.07.15 11:30–12:15
Total of 11 tutorials

Examinations (in my office)

1. Wed 15.07.15 13:00–19:00
2. ??? ???
3. *Aug* none
4. *Normally* once a month

Lab Tour OC & NLO (IPQ)

1. Tue ???
2. Thu ???

LECTURE 1

LECTURE 1 — Introduction

Why optical communications?

- Based on inexpensive extremely broadband glass fibres
- Fast transmitters with semiconductor lasers
- Fast receivers with semiconductor photodetectors
- Optical broadband amplifiers available

Lightwave technology developed over the last 40 years has greatly infuenced our needs for communication. Resources made accessible in the World Wide Web (WWW) have changed our attitude towards information acquisition, which is being regarded as an everyday's necessity, and even as a natural right for everybody. Today's undersea and underground optical cables provide large-capacity links carrying more than 90 % of the communication traffic.

An Optical Network the Size of a Football Ground

Data centres (Google, Facebook, Microsoft, Apple, . . .)

- Size of a data centre, for example YouTube

  100 h video files / min uploaded in May 2013 → 375 PB

  Volume increases by 185 TB / d, annual growth rate is 70 %.

  540 TB storage per rack & increase for 1 a → 1 200 racks,
  good for 30 000 servers including mass storage of 632 PB.

  1 200 racks require an area of $30\,\text{m} \times 100\,\text{m} = 3\,000\,\text{m}^2$.

http://www.autonomoussystem.net/ — Posted 1st July 2013 by Nathan Owens

Facebook´s data center in Luleå, Sweden: On-line 06/2013

Luleå [ˈlʉːleo]

An Optical Network the Size of a Football Ground — Interior

- Internal data network with high-density data traffic
  Server connected by switches with $30\,000 \times 3 = 90\,000$ 10 G-ports,
  i. e., by 90 000 cables, each with a capacity of 10 Gbit/s.
  The aggregate internal data rate amounts to 900 Tbit/s.

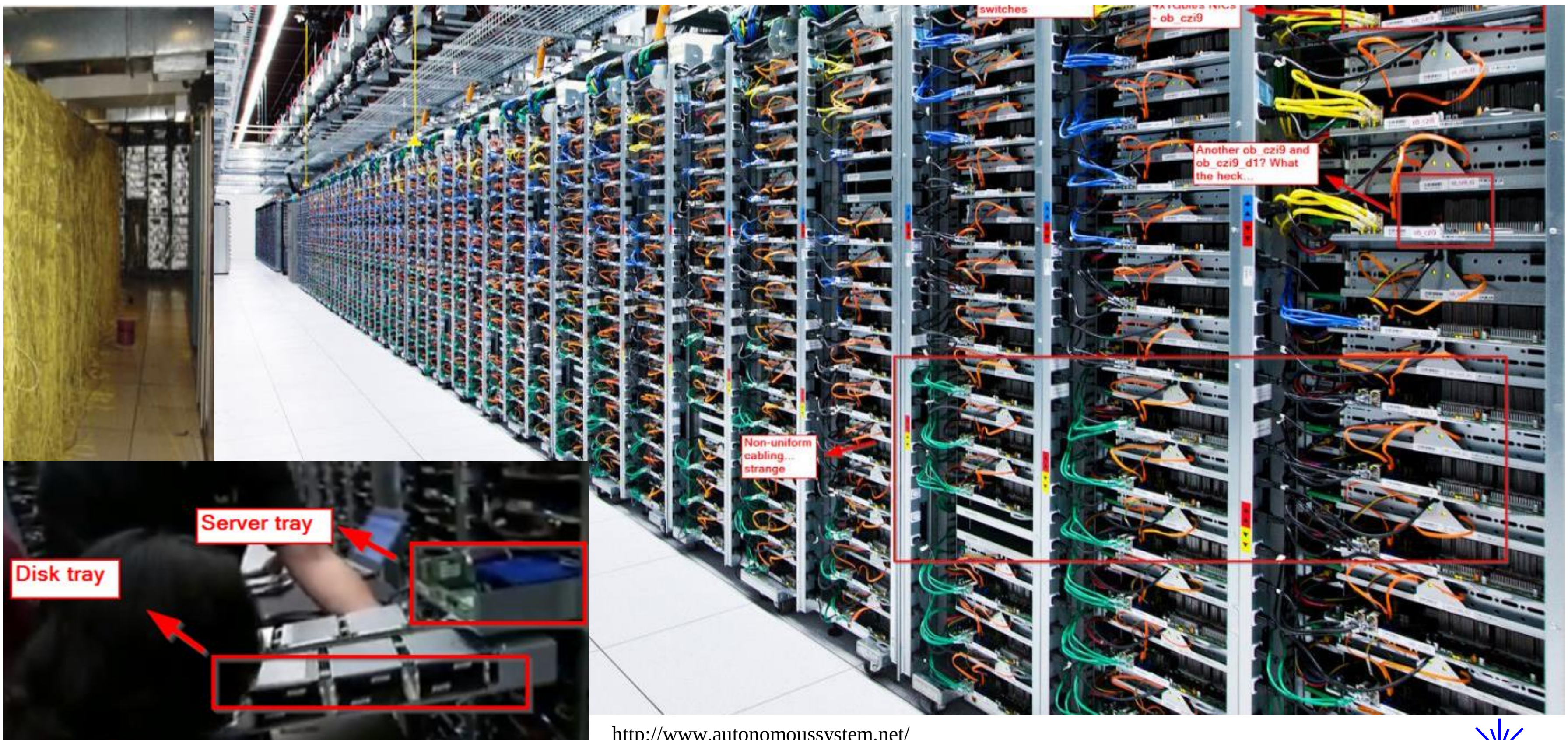

http://www.autonomoussystem.net/

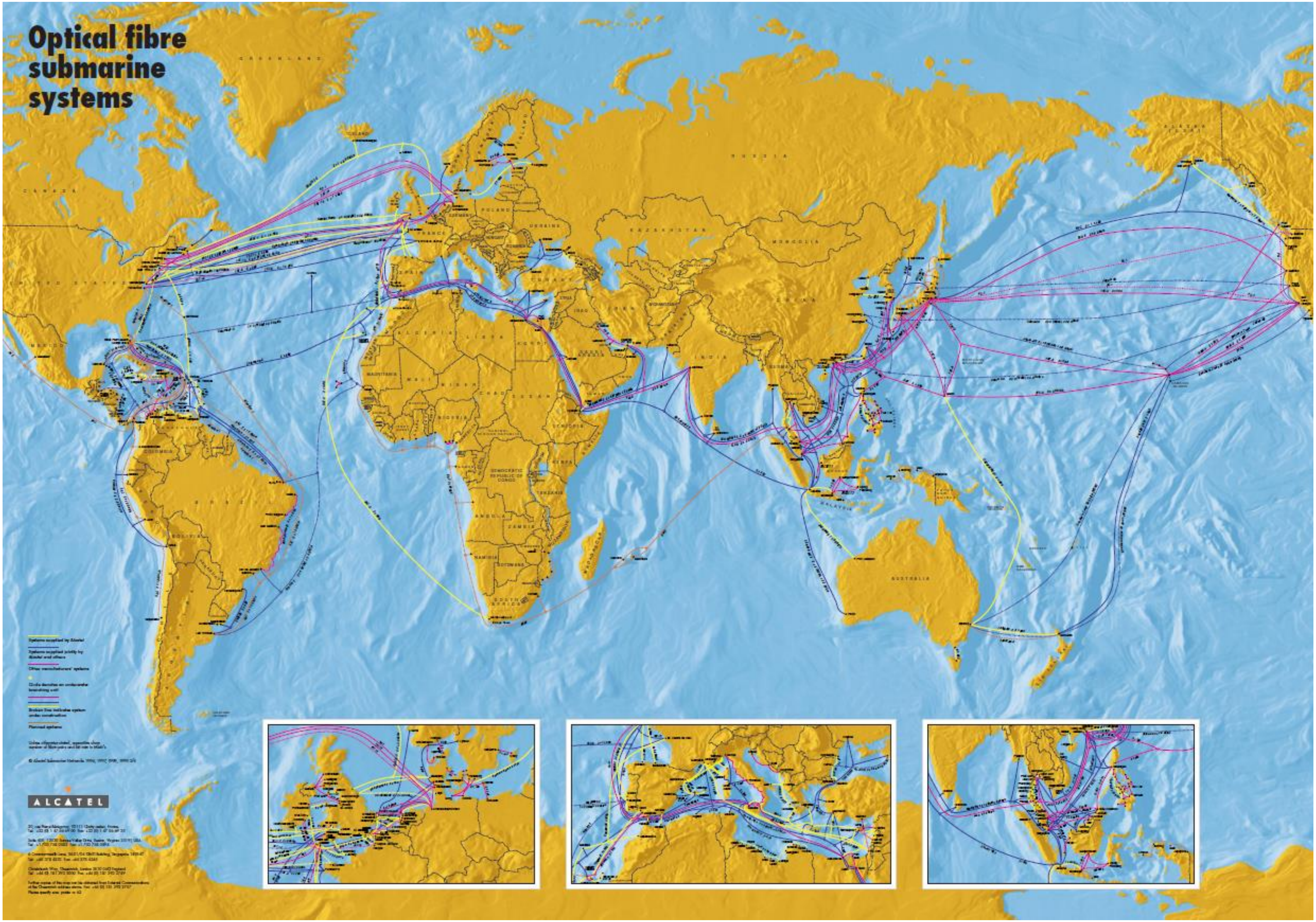
Optical fibre submarine systems
ALCATEL

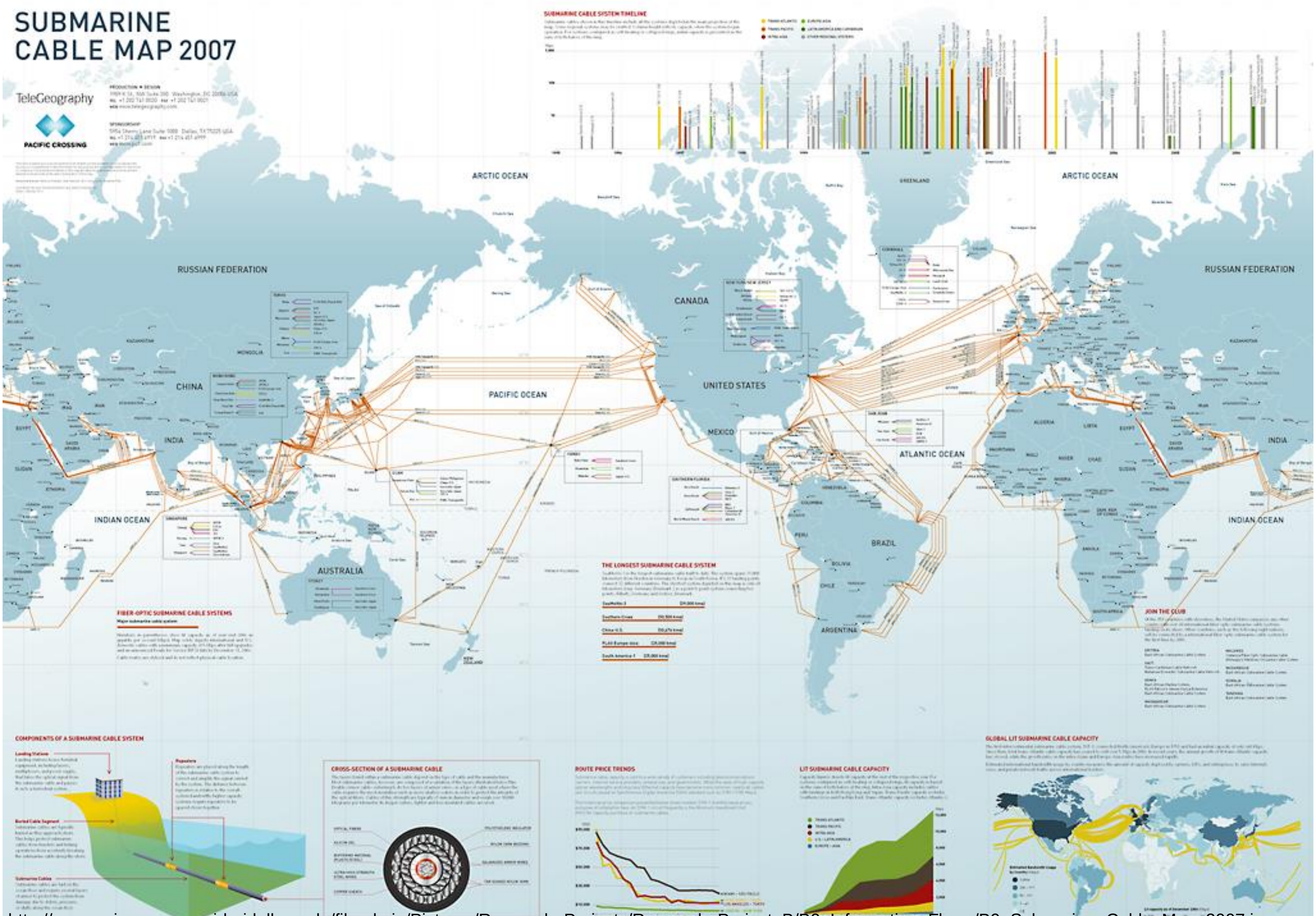

http://www.asia-europe.uni-heidelberg.de/fileadmin/Pictures/Research_Projects/Research_Project_B/B9_Information_Flows/B9_Submarine_Cable_Map_2007.jpg

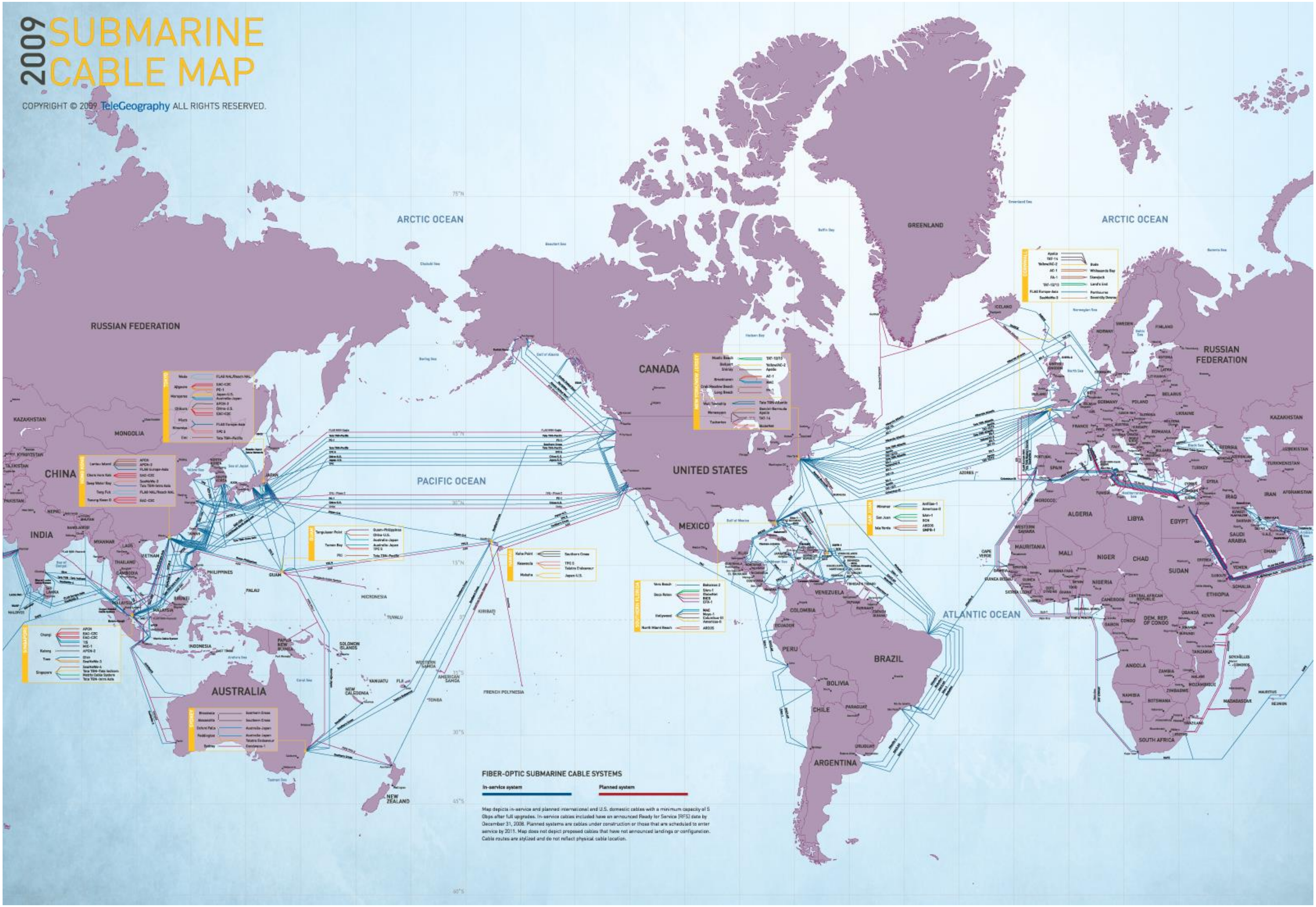

http://www.telegeography.com/product-info/map_cable/index.php

Submarine Cable Map (2010)

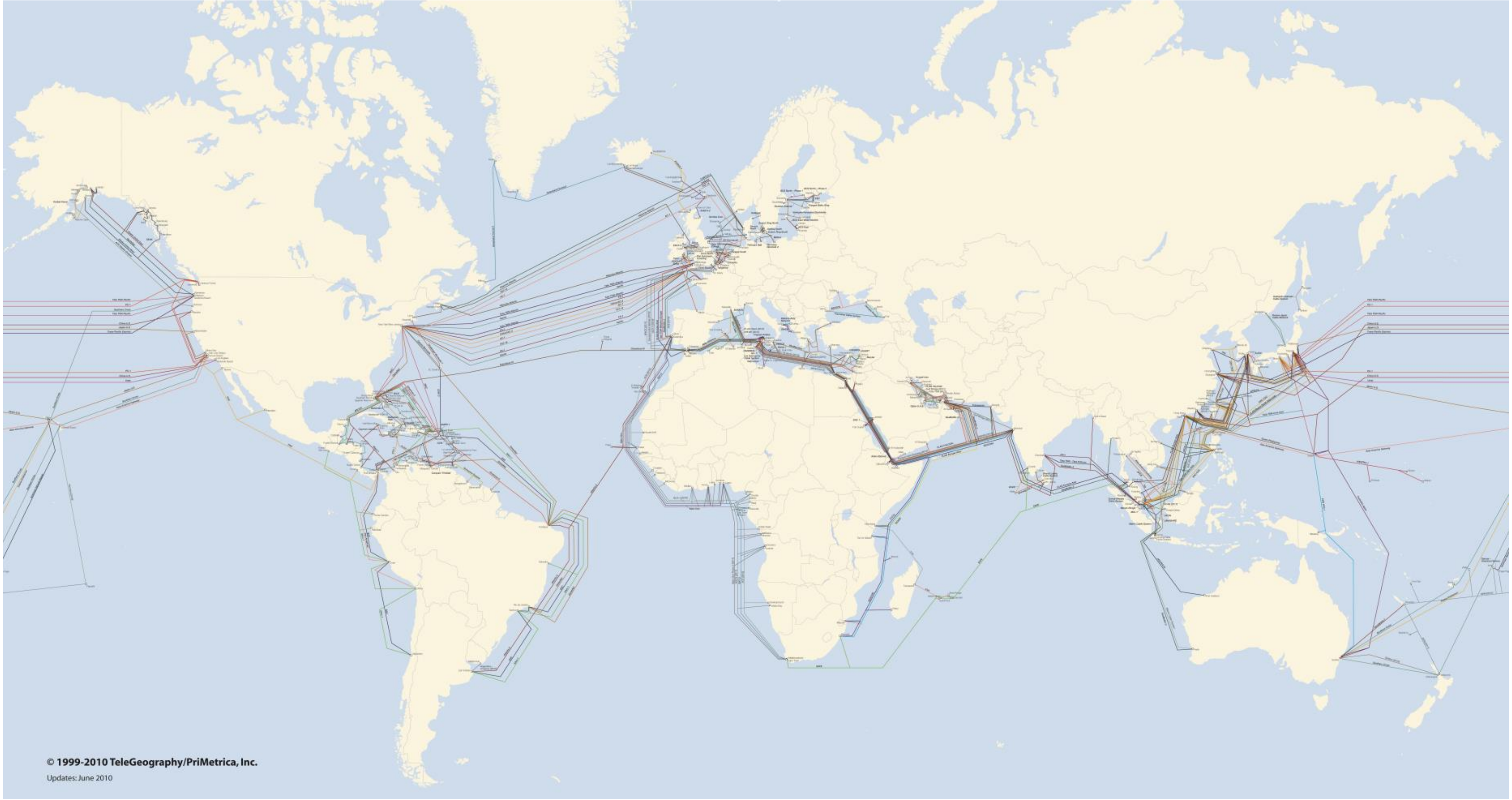

http://www.telegeography.com/product-info/map_cable/index.php

Submarine Cable Map (2011)

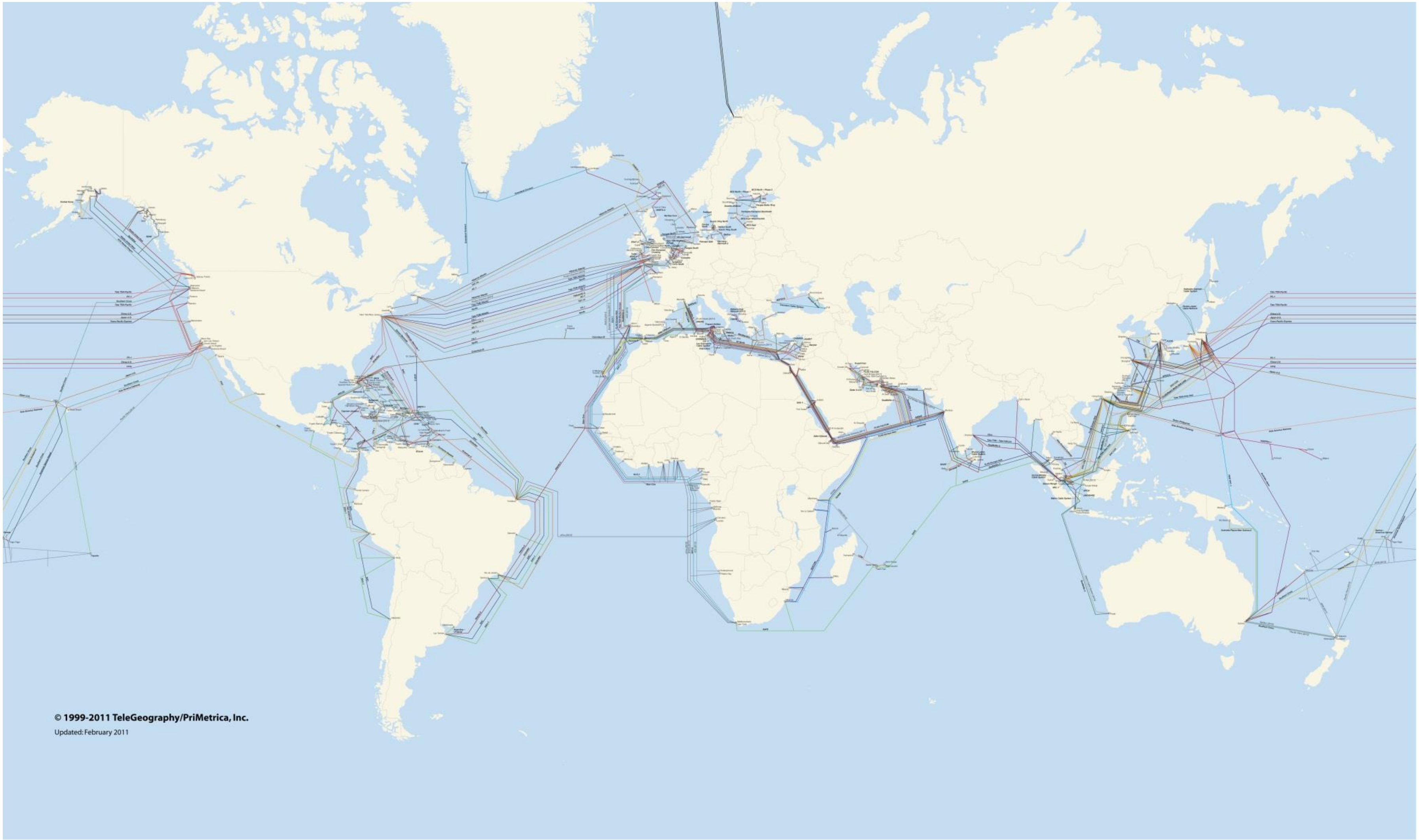

http://www.telegeography.com/product-info/map_cable/index.php

Submarine Cable Map (2013)

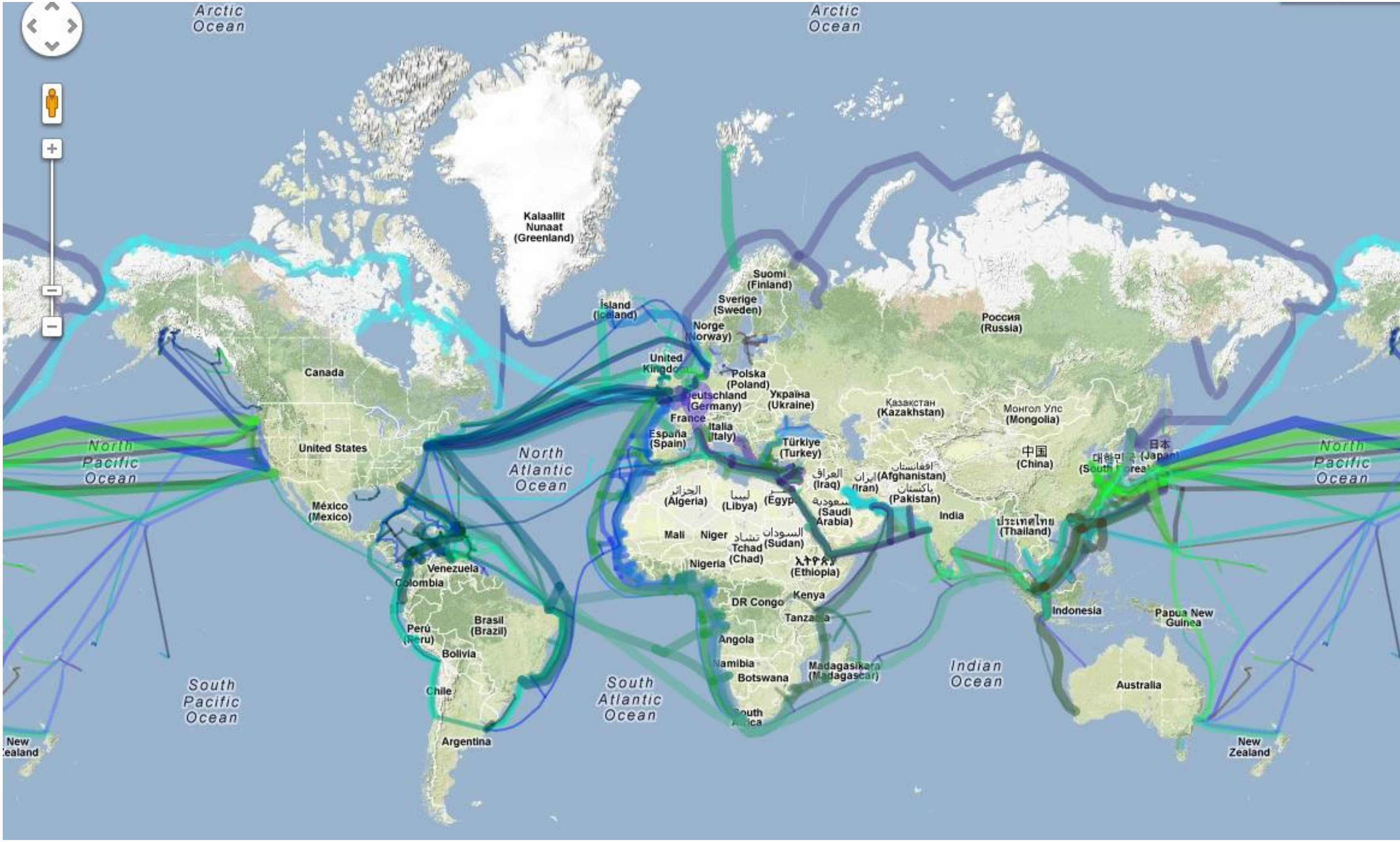

http://www.cablemap.info/

Submarine Cable Map (2014)

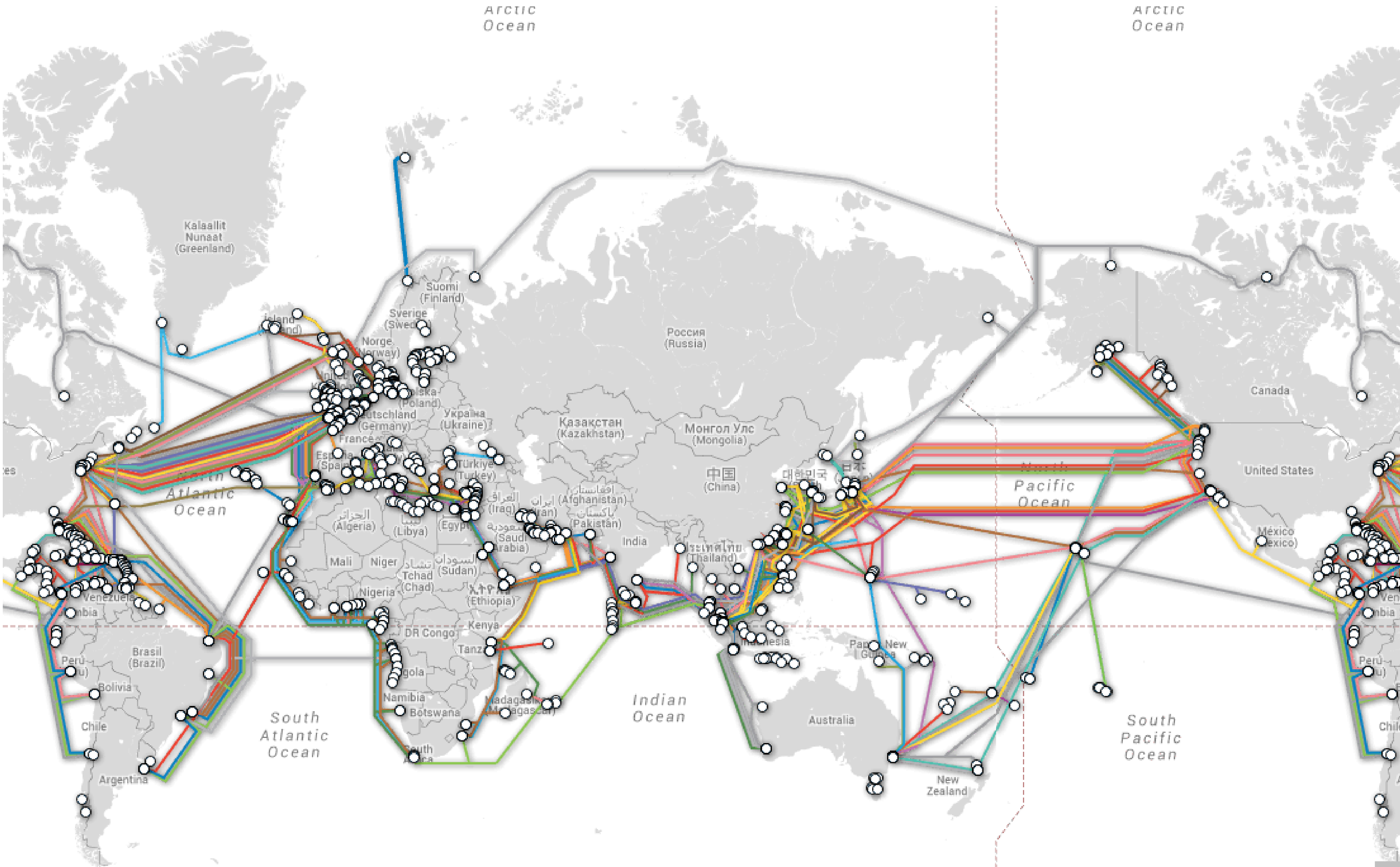

http://www.submarinecablemap.com/#/

Submarine Communication Systems — Laying the Cable

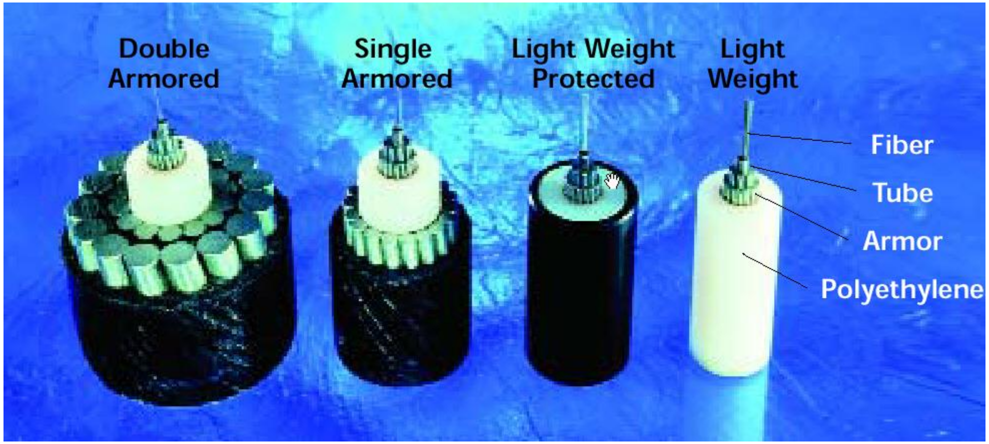

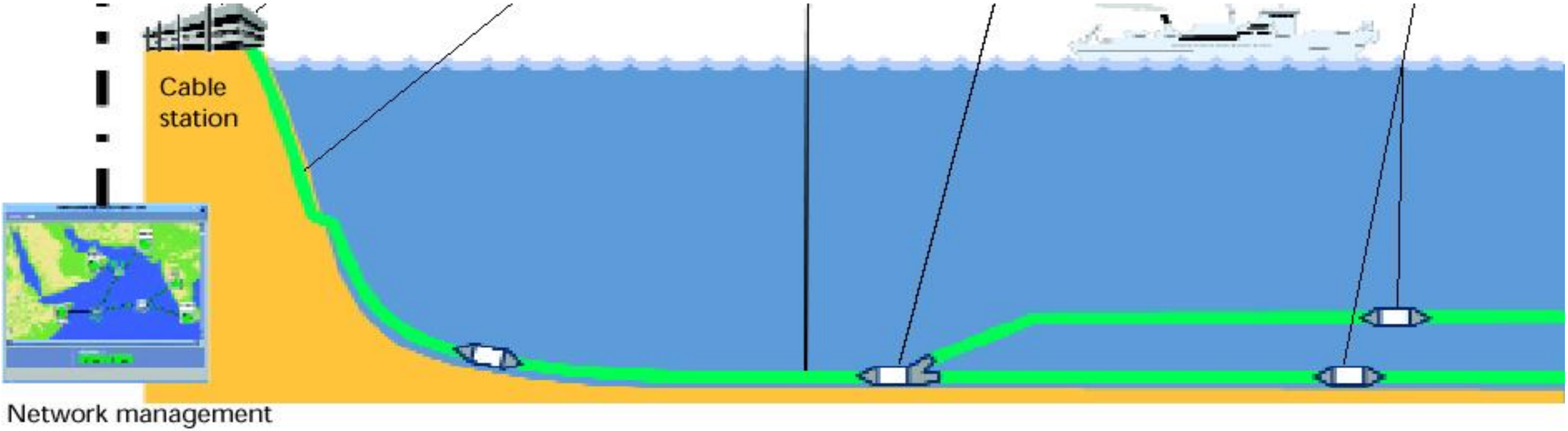

Submarine Communications Cable

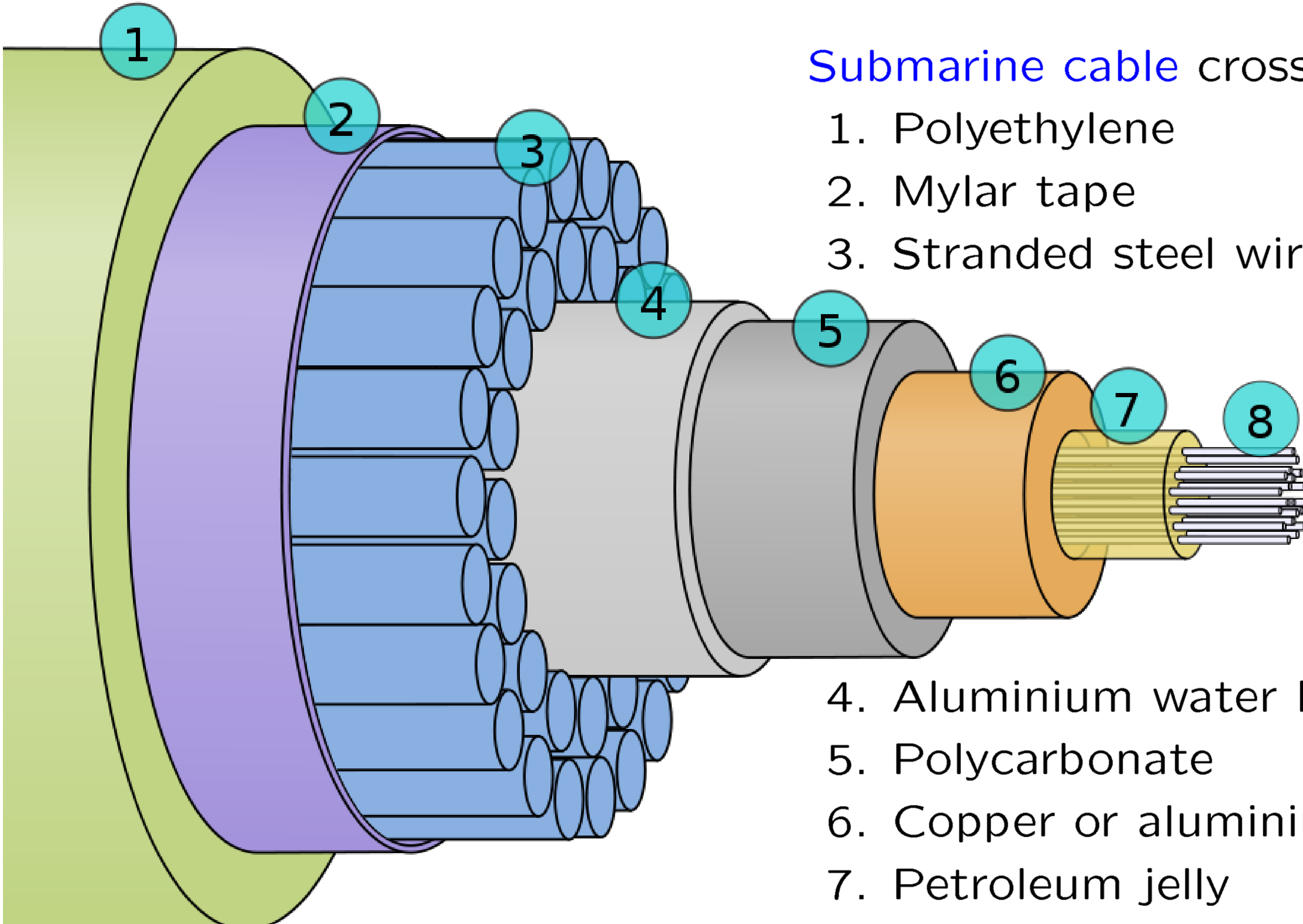

Submarine cable cross-section:

1. Polyethylene
2. Mylar tape
3. Stranded steel wires
4. Aluminium water barrier
5. Polycarbonate
6. Copper or aluminium tube
7. Petroleum jelly
8. Optical fibers

http://en.wikipedia.org/wiki/Submarine_communications_cable

Submarine Umbilicals

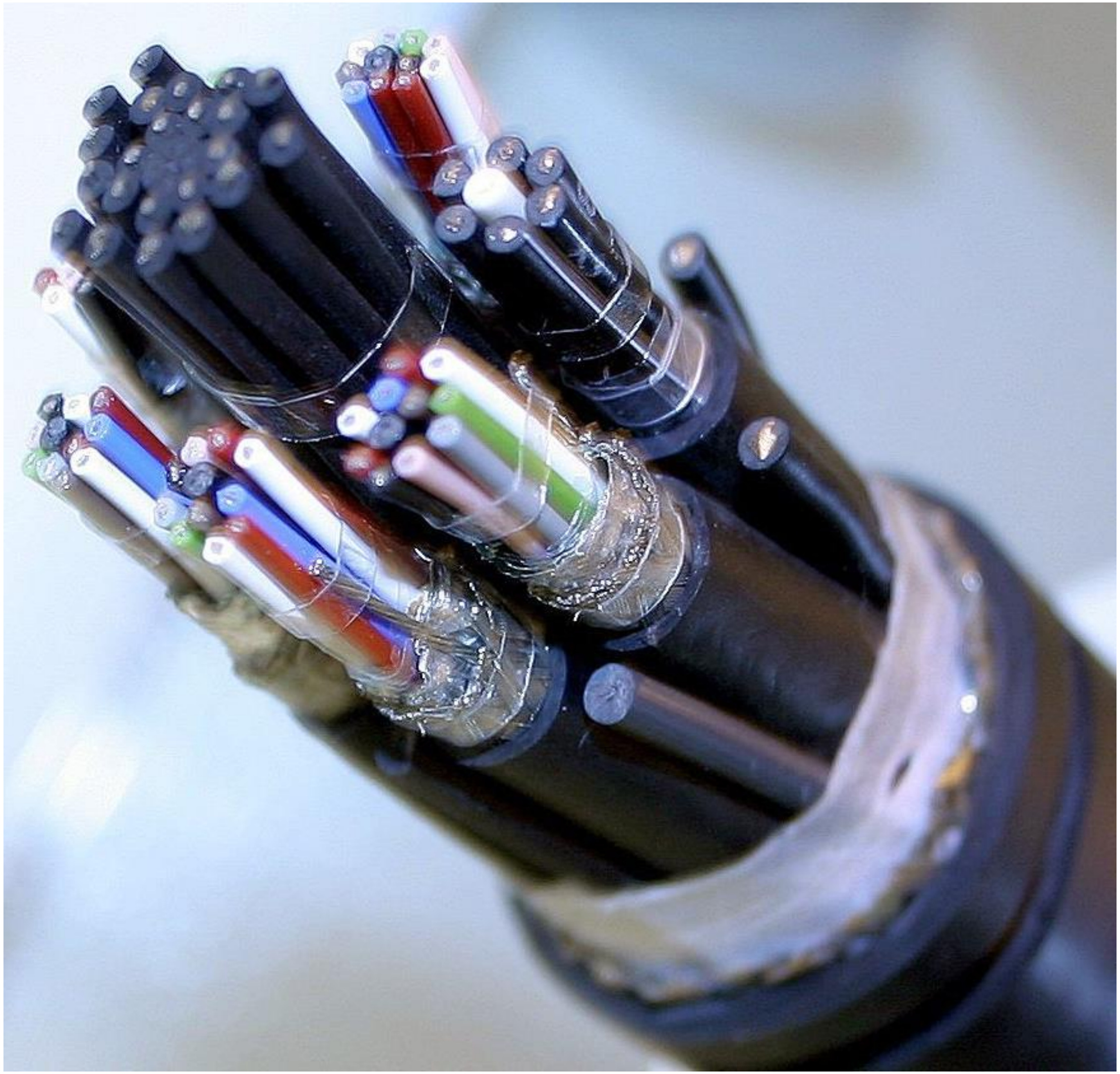

http://www.directindustry.com/prod/lapp-muller/submarine-umbilical-cable-17976-259620.html

Submarine umbilicals with electrical, optical, hydraulic, mechanical functions for submarine and offshore works

Umbilical cord

1a cord arising from the navel that connects the fetus with the placenta, and through which respiratory gases, nutrients, and wastes pass

1b yolk stalk

2 tethering or supply line (as for an astronaut outside a spacecraft or a diver underwater)

3 necessary, supportive, or nurturing link or connection

Optical Network Infrastructure — Abbreviations & Buzz Words

SONET Synchronous optical network (ANSI)
American National Standards Institute
SDH Synchroneous digital hierachy (ITU)
International Telecommunication Union

MAN Metropolitan area net.
LAN Local area network
AP Access point
ISP Internet service provdr
POP Post office protocol
CO Central office

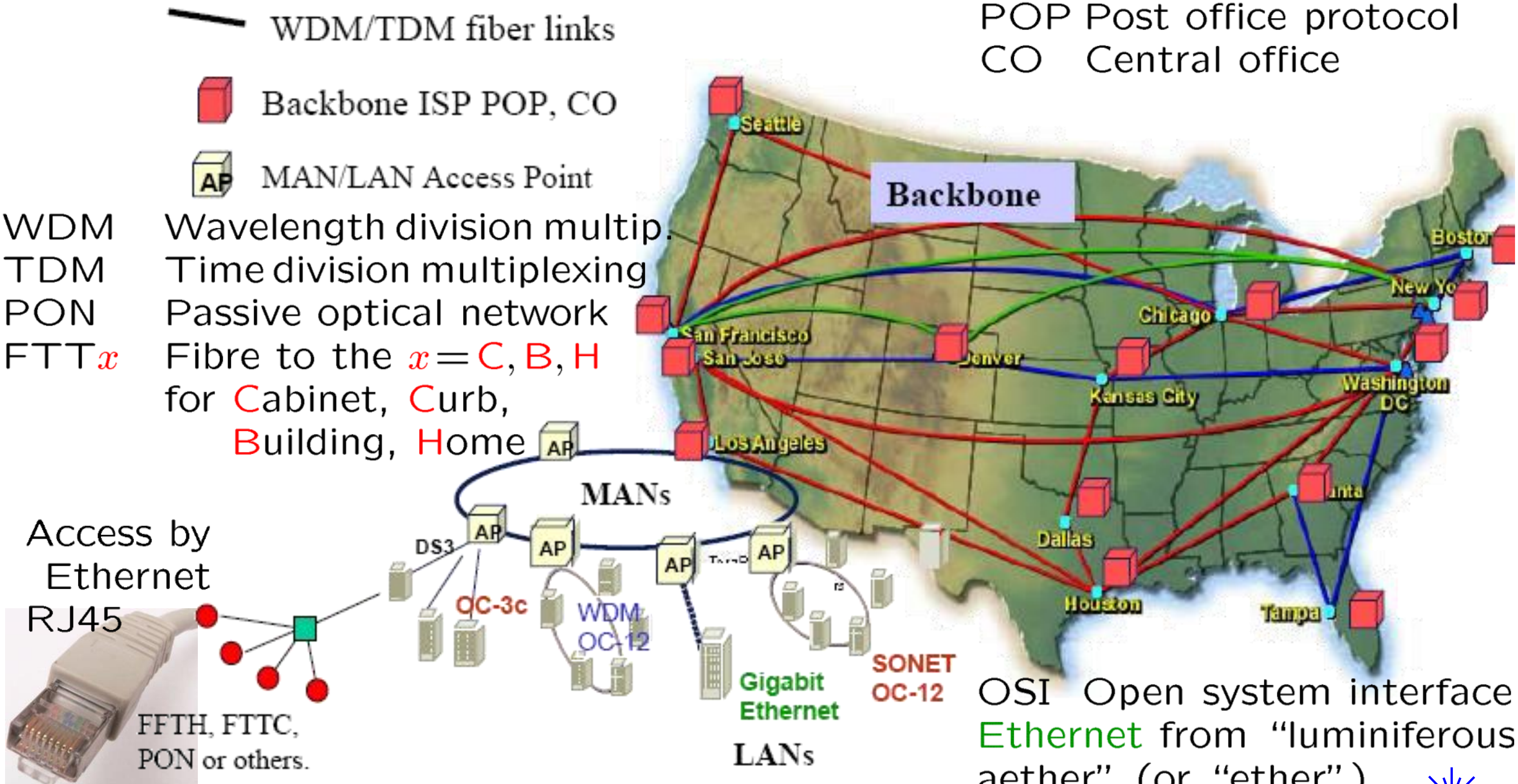

WDM Wavelength division multip.
TDM Time division multiplexing
PON Passive optical network
FTTx Fibre to the $x =$ C, B, H
for Cabinet, Curb,
Building, Home

Access by Ethernet RJ45

OSI Open system interface
Ethernet from "luminiferous aether" (or "ether")

Communication With Light

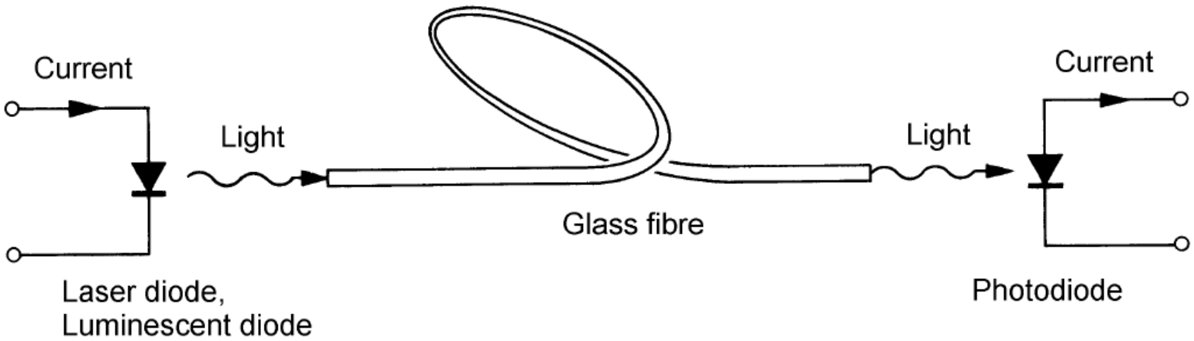

Fig. 1.1. Optical point-to-point transmission link with an intensity-modulated carrier centered at a wavelength λ and direct (incoherent) detection

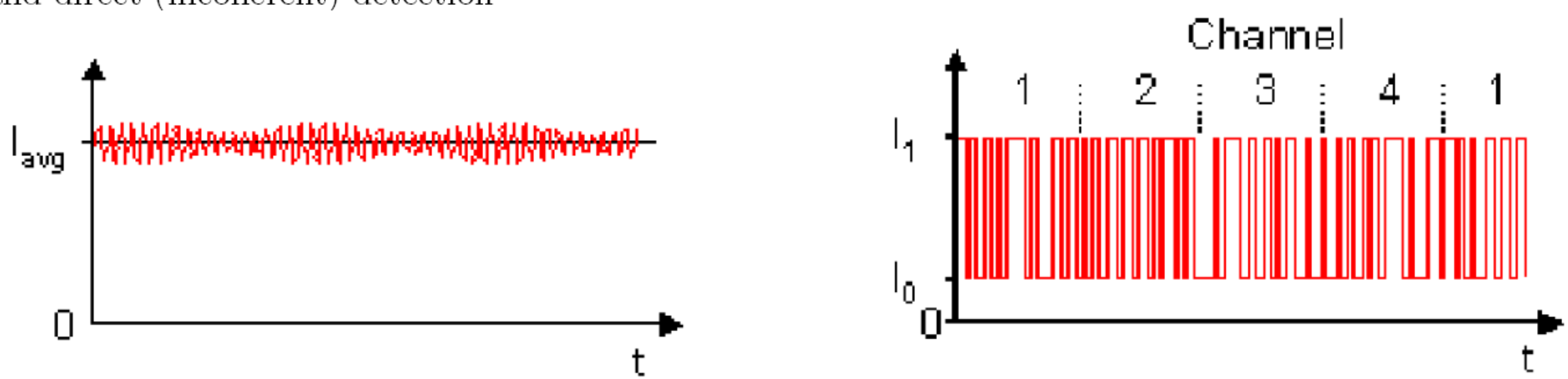

(a) Analogue intensity modulation

(b) Digital intensity modulation with TDM

Fig. 1.2. Modulation formats (a) Analogue intensity modulation around an operating point I_{avg} (b) Digital intensity modulation between an off (I_0) and an on value (I_1). For a 4-channel *t*ime *d*ivision *m*ultiplexing scheme (TDM) individual transmission time slots 1 . . . 4 are assigned to each data source

Light Guidance by Total Internal Reflection or by Index Gradient

Snell's law (1621, by Willebrord van Roijen Snell, also called Snellius, ⋆1580 † 1626, Dutch astronomer and mathematician)

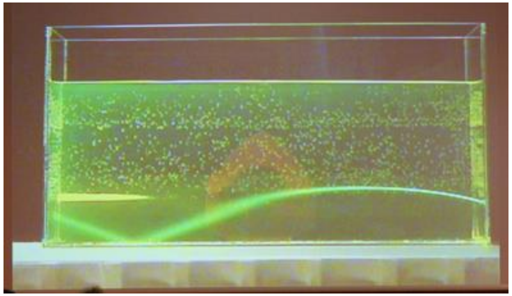

Water with sugar solution acts as graded-index light guide.

Gießen, H.: Öffentliche Vorlesung über Tarnkappen im Mercedes Museum am 22.7.2008. http://www.pi4.uni-stuttgart.de/

Total internal reflection (TIR) at transition from optically denser medium (larger refractive index n_1) to medium with lesser density (smaller refractive index $n_2 < n_1$)

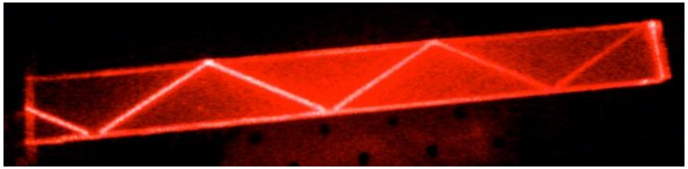

http://en.wikipedia.org/wiki/File:Total_internal_reflection_of_Chelonia_mydas_.jpg

http://en.wikipedia.org/wiki/File:TIR_in_PMMA.jpg

Fibre Types

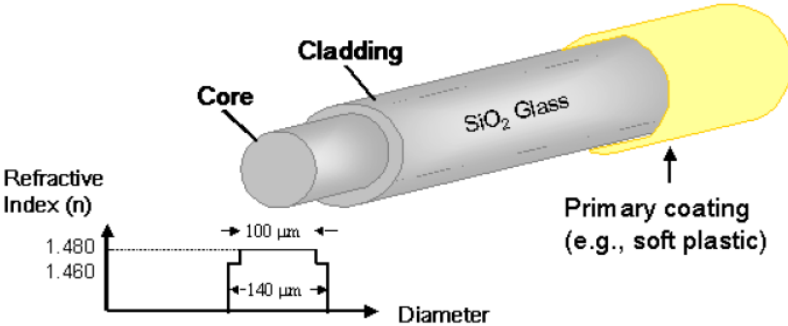

(a) Multimode fibre with step-index profile

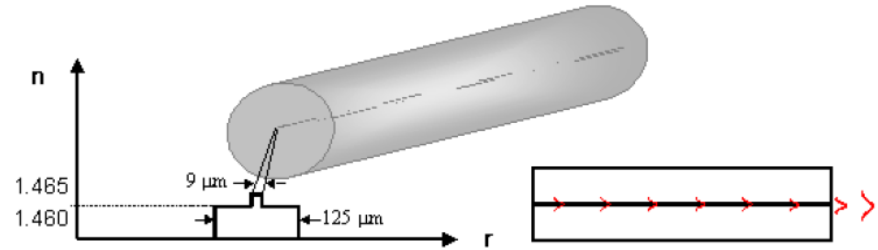

(b) Single-mode fibre with step-index profile

Fig. 1.3. Fibre types with step-shaped refractive index profile comprising a higher-index core and a lower-index cladding (a) Fat-core step-index multimode fibre with a relative refractive index difference $\Delta \approx 1.3\,\%$ (b) Long-haul step-index single-mode communication fibre with $\Delta \approx 0.33\ \%$

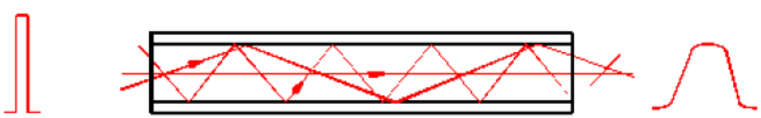

(a) Multimode fibre with step-index profile

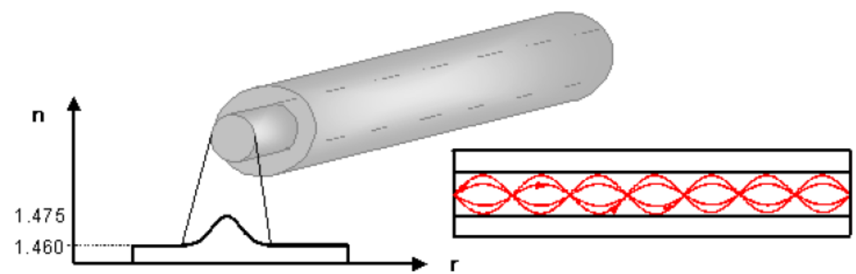

(b) Multimode fibre with graded-index profile

Fig. 1.4. Intermodal dispersion for multimode fibres. (a) Step-index profile with significant group delay differences (b) Graded-index profile, where geometrical path length differences are compensated by radial variations in the refractive index

Chromatic Dispersion

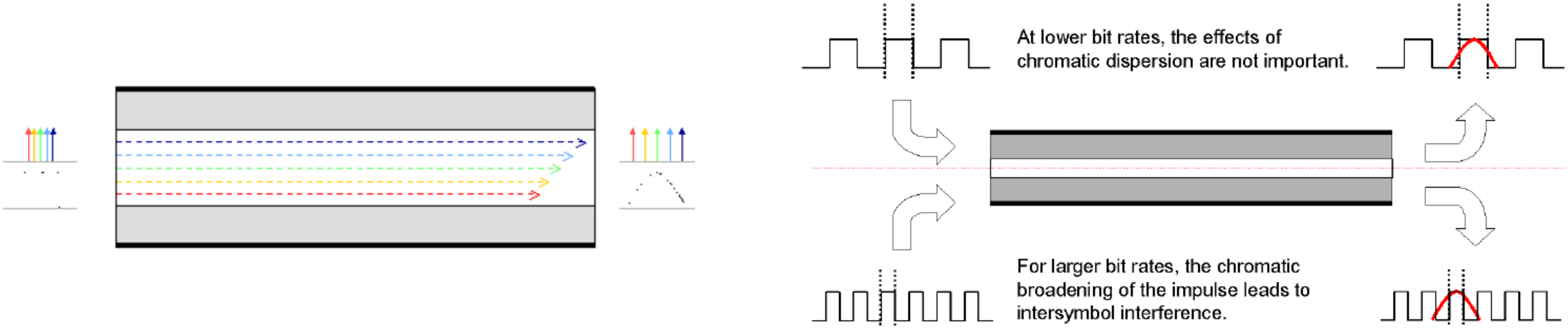

(a) Chromatic dispersion in a single-mode fibre (b) Group delay dispersion and intersymbol interference

Fig. 1.5. Group delay dispersion and bit error probability (bit error rate BER). (a) Different wavelengths ("colours", therefore "chromatic") inside the same mode propagate with different velocities, thereby increasing the output impulse width (b) Broadening of the transmitted impulse leads to bit detection errors

Optical Communications

Rapid extension of internet communication requires systems having higher transmission capacity.

Demands increase 100 % to 200 % per year. Systems are based on **photonic networks with WDM technology** (*w*avelength *d*ivision *m*ultiplexing).

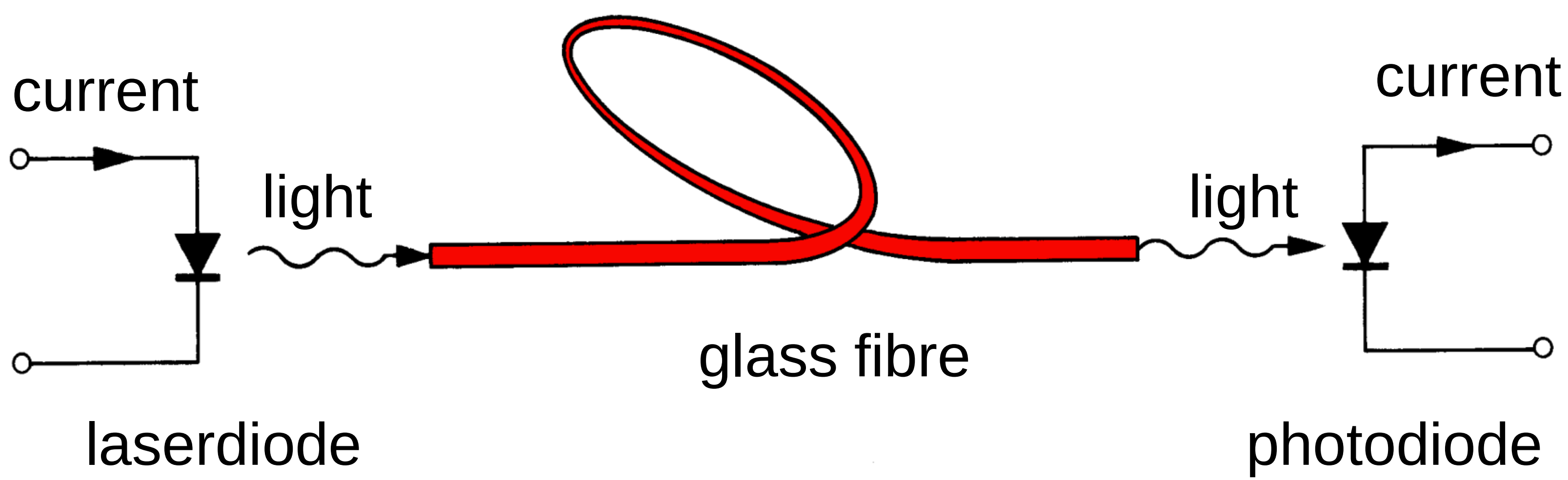

Services and Available Bitrates

Bitrates of typical services:

Voice (ISDN) 64 kbit/s (compressed < 10 kbit/s)

Picture (TV) 140 Mbit/s (compressed 2…6 Mbit/s)

Loss: 40 % for 10 km quartz glass fibre (like 20 m coax cable)

Bitrates of transmission media:

Twisted pair	6 Mbit/s (6 km); coax 650 Mbit/s (1.5 km)		
Glass fibre	40 Gbit/s (1 Mio km)		Bell / IPQ 2002
Glass fibre	1.28 Tbit/s single channel (240 km)		HHI 2006
Fibre+OFDM	13.5 Tbit/s	135 OFDM ch (6 248 km)	NTT 2009
Fibre+OFDM	26.0 Tbit/s	325 OFDM ch (50 km)	IPQ 2011
Fibre+Nyquist	32.5 Tbit/s	325 Nyquist ch (227 km)	IPQ 2012
Bible	100 Mbit	$\Rightarrow$ 325,000 bibles/s (250,000 full TV)	

J. Leuthold, G. Raybon, Y. Su, R. Essiambre, S. Cabot, J. Jaques, M. Kauer: 40 Gbit/s transmission and cascaded all-optical wavelength conversion over 1 000 000 km. Electron. Lett. vol. 38 no. 15, July 2002

H. G. Weber, S. Ferber, M. Kroh, C. Schmidt-Langhorst, R. Ludwig, V. Marembert, C. Boerner, F. Futami, S. Watanabe, C. Schubert: Single channel 1.28 Tbit/s and 2.56 Tbit/s DQPSK transmission. Electron. Lett. Vol. 42 No. 3, Feb. 2006

H. Masuda, E. Yamazaki, A. Sano, T. Yoshimatsu, T. Kobayashi, E. Yoshida, Y. Miyamoto, S. Matsuoka, Y. Takatori, M. Mizoguchi, K. Okada, K. Hagimoto, T. Yamada, S. Kamei: 13.5-Tb/s (135 x 111-Gb/s/ch) No-guard-interval coherent OFDM transmission over 6,248 km using SNR maximized second-order DRA in the extended L-Band. OFC 2009, PDPB5

Optical Wavelength Division Multiplexing (WDM)

- Internet: Need for bandwidth B

- Optical transmission systems

  fibres: $B \approx$ 65 THz (450 nm)

  amplifiers: $B \approx$ 10 THz (80 nm)

  wavelength division multiplexing

  channels: $\Delta f \approx$ 5, 10, 25, 50, 100 GHz

  capacity: 40 Gbit/s $\times$ 100 ch = 4 Tbit/s

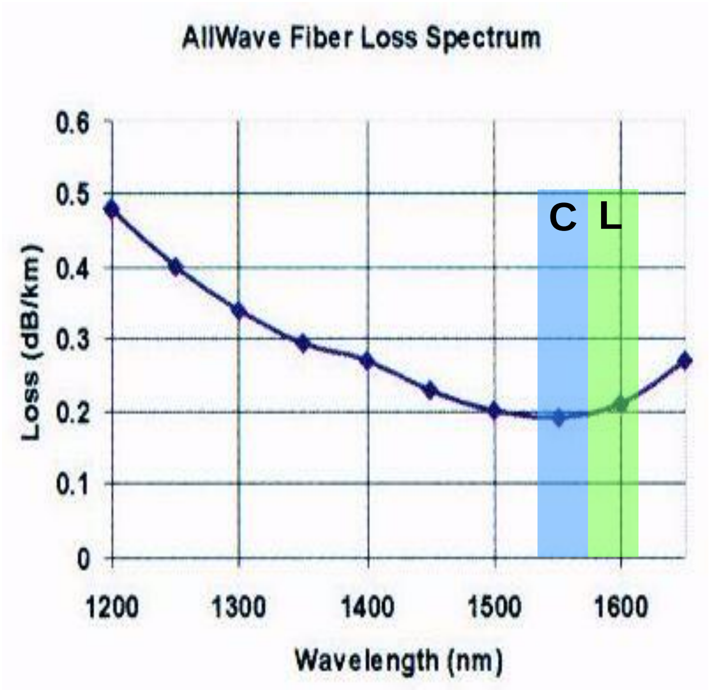

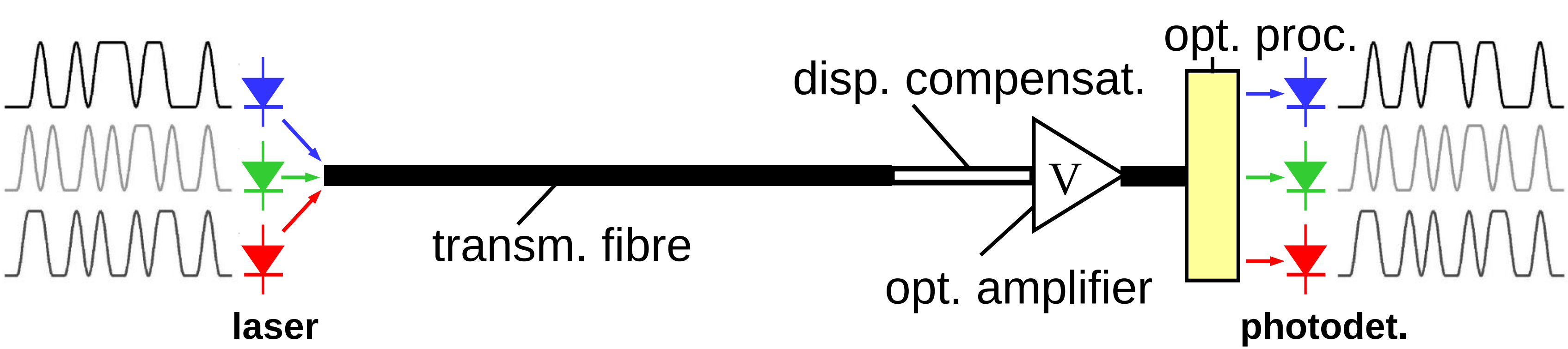

Wavelength Division Multiplexing

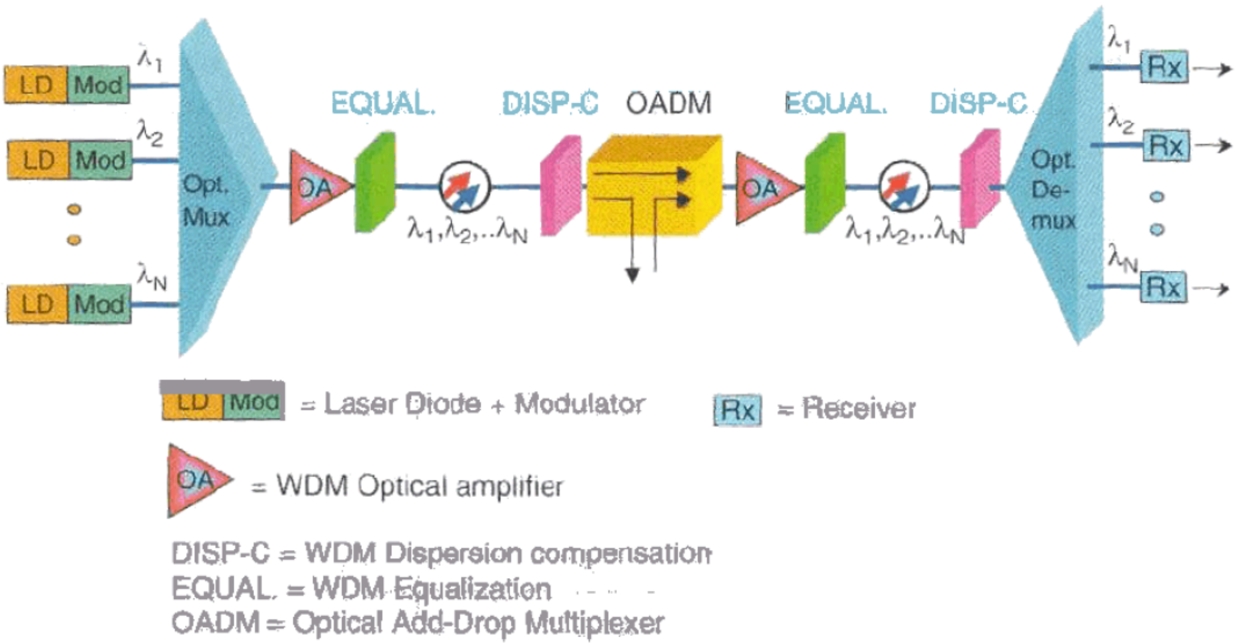

Fig. 1.6. Wavelength division multiplexing transmission scheme. The path from LD MOD(λ_i) to Rx(λ_i) corresponds to the simplified point-to-point transmission depicted in Fig. 1.1. [after Fig. iii on Page xxiv in reference Footnote 10 on Page 4]

12.8Tbit/s Transmission of 160 PDM-QPSK (160x2x40Gbit/s) Channels with Coherent Detection over 2,550km

Gabriel Charlet[1], Jérémie Renaudier[1], Haik Mardoyan[1], Oriol Bertran Pardo[1], Frédéric Cérou[2], Patrice Tran[1], Sébastien Bigo[1]

1 : Alcatel-Lucent, Research and Innovation, Centre de Villarceaux, 91620, Nozay, France,

2 : IRISA/INRIA de Rennes, Campus universitaire de Beaulieu, 35042 Rennes, France

Gabriel.Charlet@alcatel-lucent.fr

ECOC'07 PDP 1.6

Abstract: *A 12.8Tbit/s ultra-high capacity transmission is demonstrated over an ultra-long distance of 2,550km thanks to coherent detection and powerful signal processing against chromatic dispersion, PMD and narrow optical filtering.*

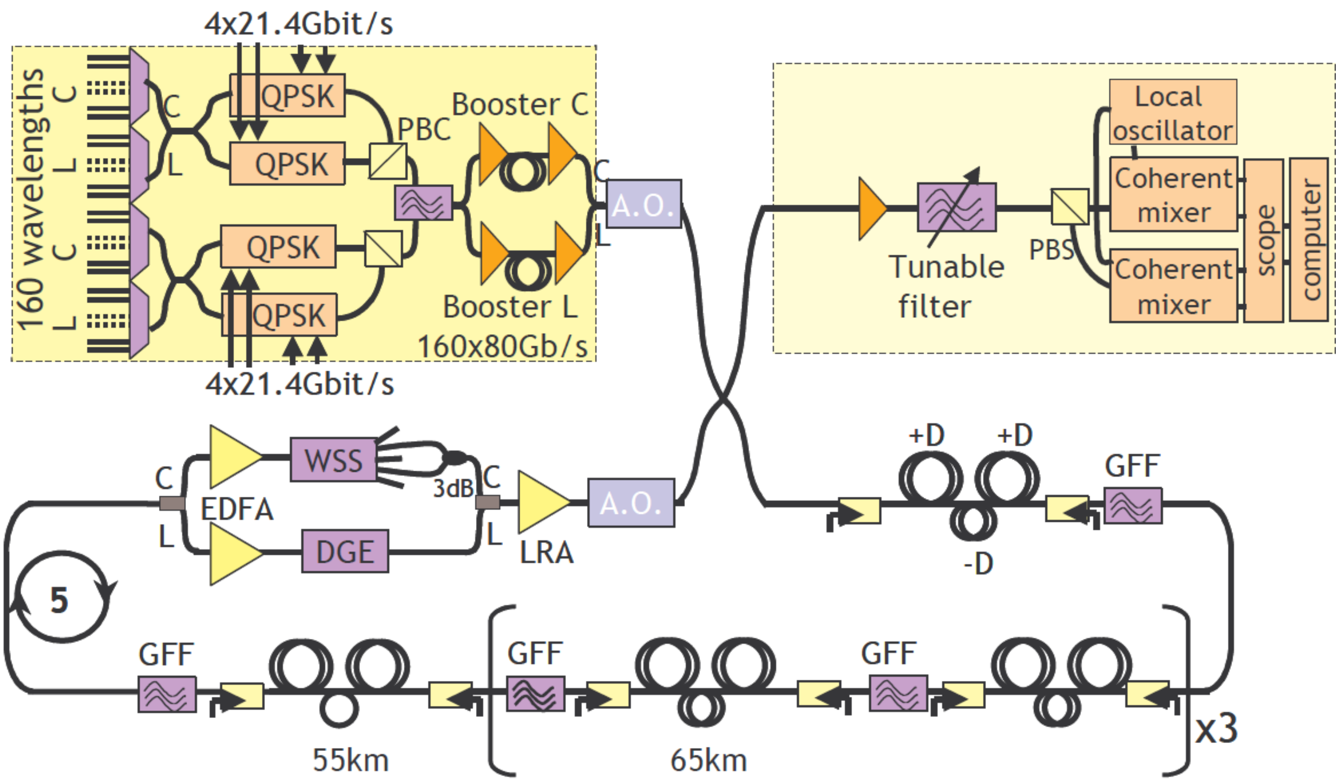

25.6-Tb/s C+L-Band Transmission of Polarization-Multiplexed RZ-DQPSK Signals

A. H. Gnauck(1), G. Charlet(2), P. Tran(2), P. J. Winzer(1), C. R. Doerr(1), J. C. Centanni(1), E. C. Burrows(1), T. Kawanishi(3),T. Sakamoto(3), and K. Higuma(4)

(1) Alcatel-Lucent, Bell Labs, Holmdel, New Jersey 07733, USA, Email: gnauck@lucent.com
(2) Alcatel-Lucent, Research and Innovation, Centre de Villarceaux, Route de Villejust, 91620 NOZAY, France
(3) National Inst. of Information and Communications Technologies (NICT), 4-2-1 Nukui-Kita, Koganei, Tokyo 184-8795, Japan
(4) Sumitomo Osaka Cement, 585 Toyotomi, Funabashi, Chiba 274-8601, Japan

OFC'07 PDP 19

Abstract: We demonstrate record 25.6-Tb/s transmission over 240 km using 160 WDM channels on a 50-GHz grid in the C+L bands. Each channel contains two polarization-multiplexed 85.4-Gb/s RZ-DQPSK signals, yielding a spectral efficiency of 3.2 b/s/Hz in each band.

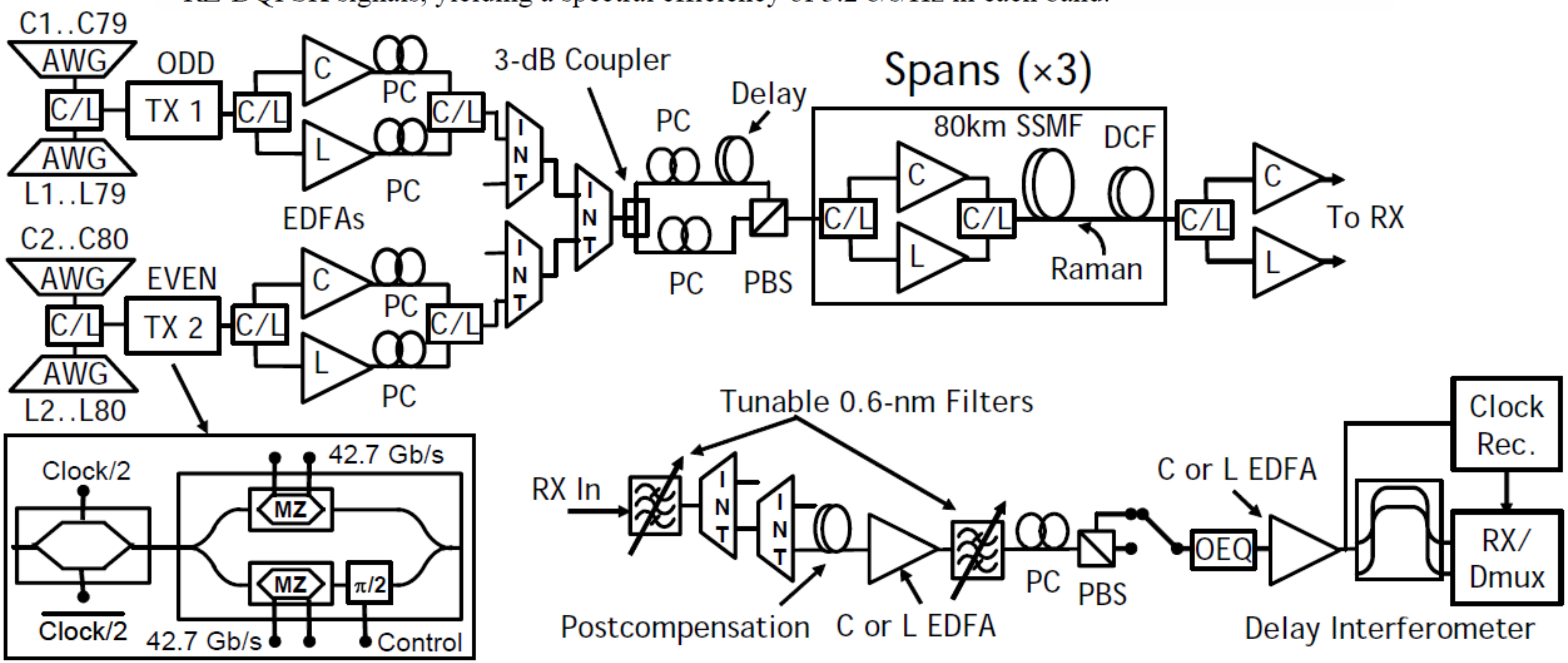

Fig. 1. Experimental setup. AWG: Arrayed Waveguide Grating Router. C/L: C-band/L-band splitter or combiner. INT: 50GHz/100GHz interleaver or de-interleaver. PC: Polarization controller. PBS: Polarization beamsplitter. OEQ: Optical equalizer.

32-bit/s/Hz Spectral Efficiency WDM Transmission over 177-km Few-Mode Fiber

R. Ryf[1], S. Randel[1], N. K. Fontaine[1], M. Montoliu[1,2], E. Burrows[1], S. Corteselli[1], S. Chandrasekhar[1], A. H. Gnauck[1], C. Xie[1], R.-J. Essiambre[1], P. J. Winzer[1], R. Delbue[3], P. Pupalaikis[3], A. Sureka[3], Y. Sun[4], L. Grüner-Nielsen[5], R. V. Jensen[5], and R. Lingle, Jr.[4]

[1]*Bell Laboratories, Alcatel-Lucent, 791 Holmdel-Keyport Rd, Holmdel, NJ, 07733, USA.*
[2]*Universitat Politècnica de Catalunya (ETSETB), Barcelona, Spain*
[3]*LeCroy Corporation, 700 Chestnut Ridge Road, Chestnut Ridge, NY 10977, USA*
[4]*OFS, 2000 Northeast Expressway, Norcross, GA 30071, USA*
[5]*OFS Fitel Denmark, Priorparken 680, 2605 Brondby, Denmark.*

Roland.Ryf@alcatel-lucent.com

OFC'13 PDP 5A.1

Abstract: We transmit 32 WDM channels over 12 spatial and polarization modes of 177 km few-mode fiber at a record spectral efficiency of 32 bit/s/Hz. The transmitted signals are strongly coupled and recovered using 12×12 multiple-input multiple-output digital signal

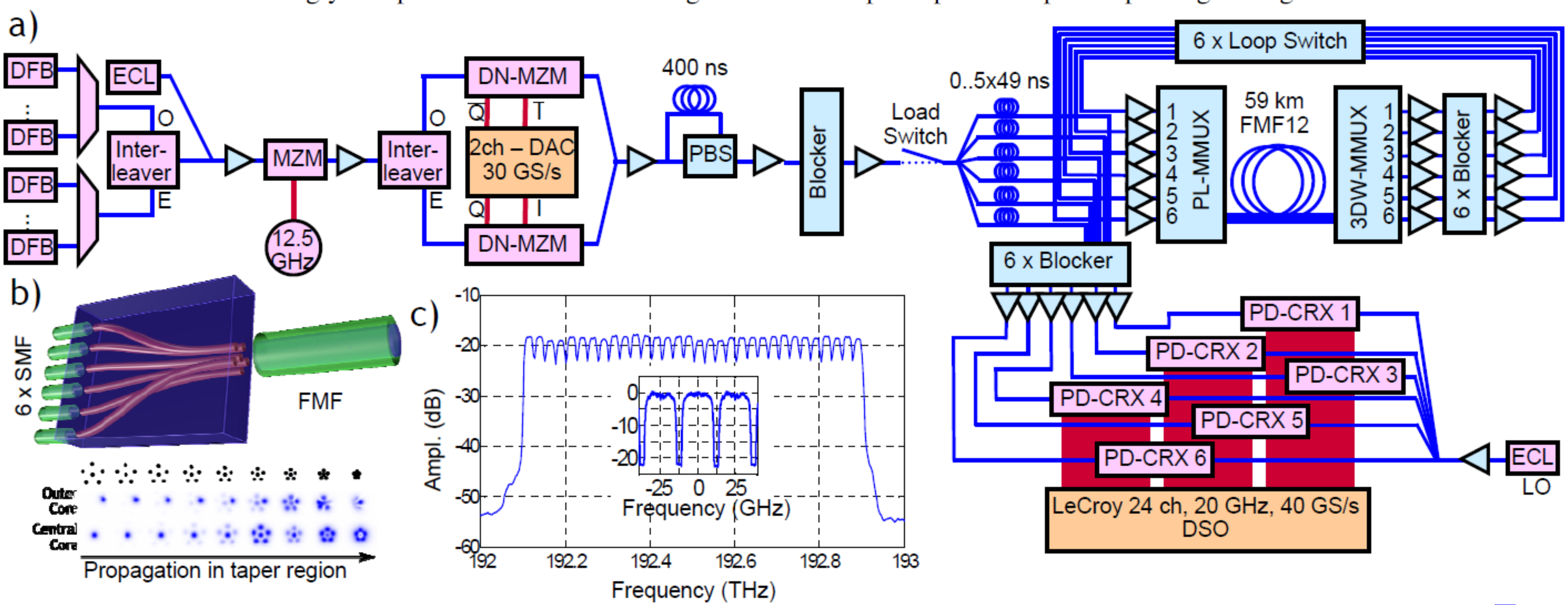

Polymer Fibres for In-house Cabling

In future broadband connections become standard:

- Telephone replaced by VoIP (Voice over Internet Protocol)
- Besides TV broadcast, Video/Channel on Demand (IP-TV) becomes important
- Data rates $\geq 100\,\mathrm{Mbit/s}$
- Glass fibre closer to the subscriber (VDSL, FTTB, FTTH)
- UMTS-HSxPA, WiMax and satellites fill in the voids

Disadvantages of Cu cables:

- Cu cables in houses prone to interferences (motors, switched power supplies, computers, starter for gas discharge lamps)
- Many connections only to the building
- New cables require new slots — who pays?

Solution:

- Plastic optical fibre (POF)

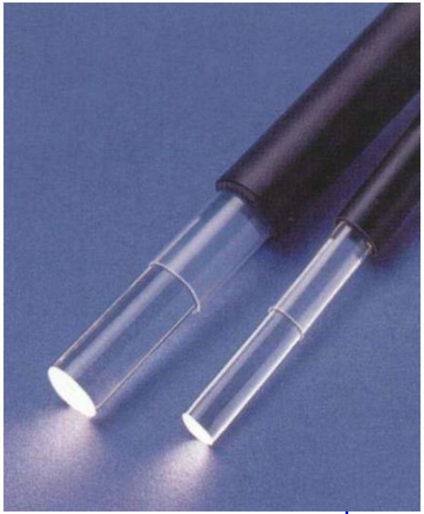

Attenuation of Glass and Polymer Fibres

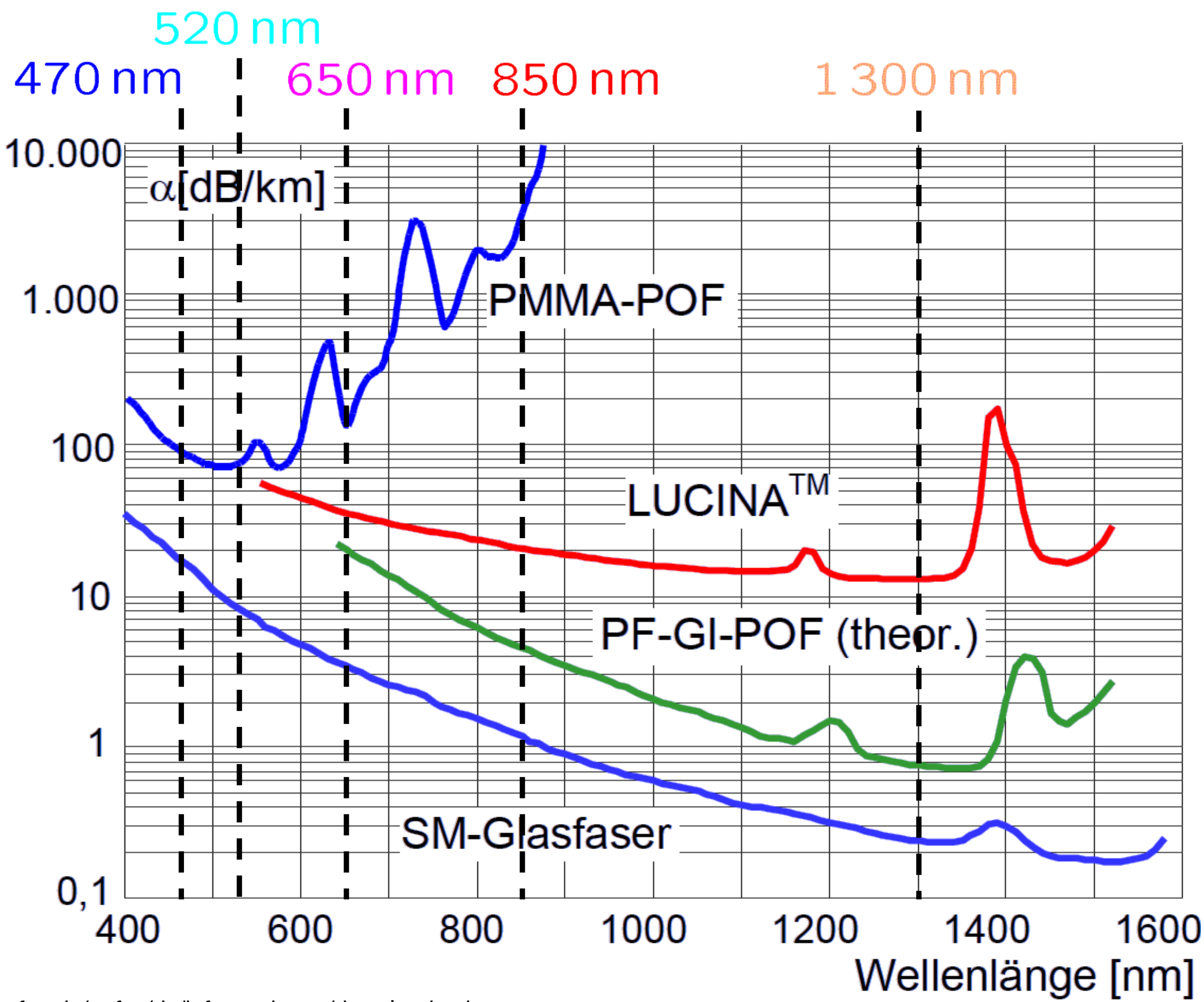

http://www.pofac.de/pofac/de/informationen/downloads.php

Network Architecture in Buildings Using Multimode Waveguides

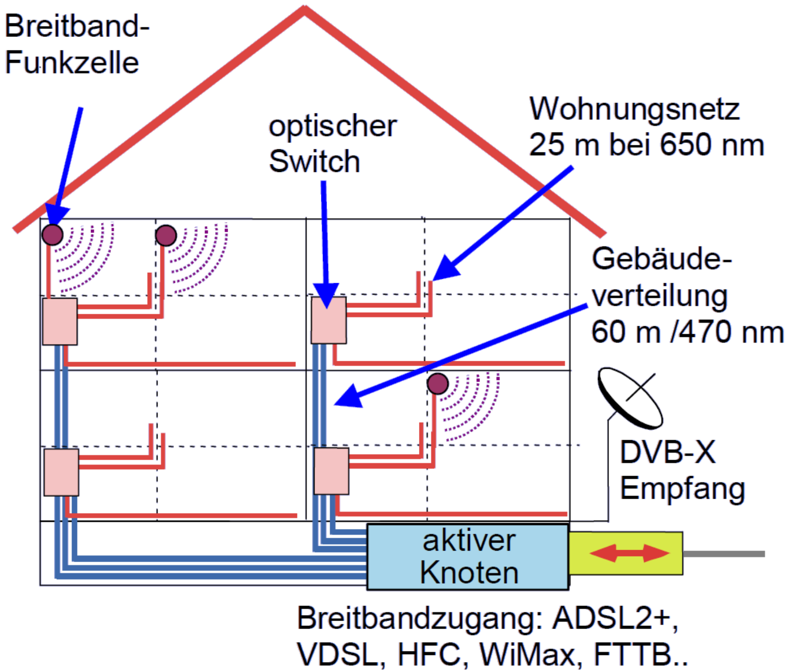

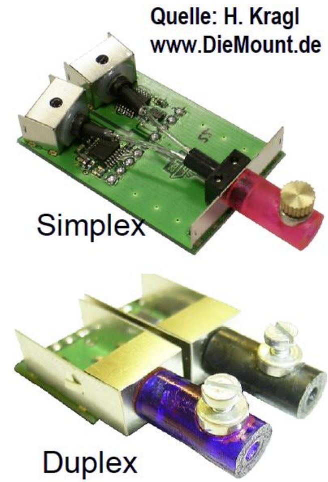

Ethernet, 1 core,
red LED, $\leq 30\,\mathrm{m}$

Ethernet, 2 cores,
blue LED, $\leq 120\,\mathrm{m}$

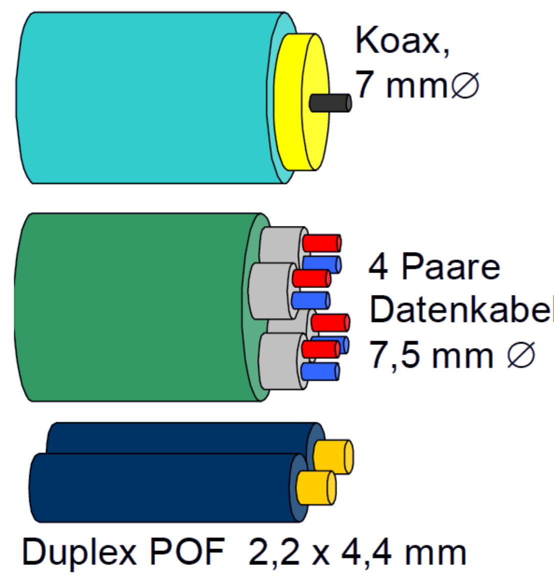

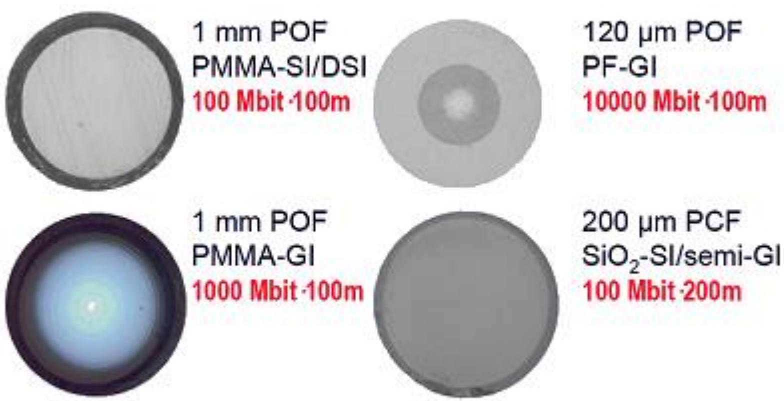

Cross-sections and cables

http://www.pofac.de/pofac/de/informationen/downloads.php

The Logarithmic Scale

dB $= 10 \log_{10} (P_1 / P_0)$		dBm $= 10 \log_{10} (P / 1\ mW)$	
0 dB	= 1	0 dBm	= 1 mW
+ 0.1 dB	= 1.023 (+2.3%)	3 dBm	= 2 mW
+ 3 dB	= 2	5 dBm	= 3 mW
+ 5 dB	= 3	10 dBm	= 10 mW
+ 10 dB	= 10	20 dBm	= 100 mW
-3 dB	= 0.5	-3 dBm	= 0.5 mW
-10 dB	= 0.1	-10 dBm	= 100 μW
-20 dB	= 0.01	-30 dBm	= 1 μW
-30 dB	= 0.001	-60 dBm	= 1 nW

Optical Power

Power (P):

– *Transmitter: typ. -6 to +17 dBm (0.25 to 50 mW)*

– *Receiver: typ. -3 to -35 dBm (500 down to 0.3 μW)*

– *Optical Amplifier: typ. +3 to +20 dBm (2 to 100 mW)*

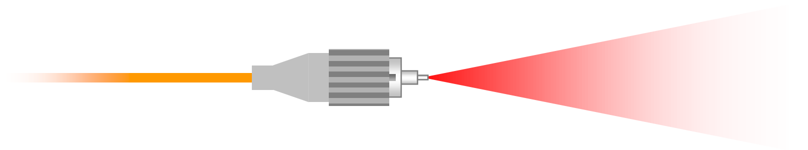

Laser safety

– International standard: IEC 825-1

– United States (FDA): 21 CFR 1040.10

– Both standards consider **class I** safe under reasonable forseeable conditions of operation (e.g., without using optical instruments, such as lenses or microscopes)

Why need amplifiers be distributed along a transmission distance?

Due to attenuation in the transmitting fibre the optical signal decays exponentially with the transmission span. Practical spans without amplification are about 70 km. Why are the spans so short?

A transatlantic transmission from New York to London experiences an attenuation of about 1 400 dB (7 000 km @ 0.2 dB / km). Thus, for receiving one photon in London we have to inject 10^{140} photons into the optical fibre end in New York. If all the mass of our sun ($m_{\text{sun}} = 2 \times 10^{33}\,\text{g}$) having an energy equivalent of $W_{\text{sun}} = mc^2 = 1.8 \times 10^{47}\,\text{Ws}$ could be converted into photons with a photon energy $hf = 6 \times 10^{-34}\,\text{Ws}^2 \times 200\,\text{THz} = 1.2 \times 10^{-19}\,\text{Ws}$, we had generated 1.5×10^{66} photons at a wavelength of $1.55\,\mu\text{m}$ ($f \approx 200\,\text{THz}$), and could bridge a span with 660 dB loss, corresponding to a transmission distance of 3 300 km only. For a direct transmission New York – London we thus had to evaporate $10^{140}/10^{66} = 10^{74}$ suns.

Calculations stimulated by an oral presentation of N. J. Doran (S. K. Turitsyn, M. P. Fedoruk, N. J. Doran and W. Forysiak: Optical soliton transmission in fiber lines with short-scale dispersion management. 25th European Conf. on Optical Communication (ECOC'99), Nice, France, September 26–30, 1999)

Why need amplifiers be distributed along a transmission distance?

10^{74} suns are quite a bit. The (observable) universe is estimated to have an extension of 14×10^{9} light years. Its mean density is supposed to be $3 \times 10^{-30}\,\mathrm{g}\,/\,\mathrm{cm}^3$ (`http://curious.astro.cor nell.edu/question.php?num ber=342`).

So, the universe's mass (comprising not only suns) is $m_{\text{univ}} = 7 \times 10^{54}\,\mathrm{g}$, and its energy equivalent is $W_{\text{univ}} = m_{\text{univ}} c^2 = 6 \times 10^{68}\,\mathrm{Ws}$ corresponding to 4.7×10^{87} photons at a wavelength of $1.55\,\mu\mathrm{m}$. If we are able to receive one photon then the maximum span will be $877\,\mathrm{dB}\,/(0.2\,\mathrm{dB}\,/\,\mathrm{km}) = 4\,385\,\mathrm{km}$.

However, for bridging the distance New York – London in one go we had to burn $10^{140}/10^{87} = 10^{53}$ universes!

How come — NY supernova not visible in London? Spherical $\sim (bL)^2$, fibre $\sim \exp(\alpha L)$:

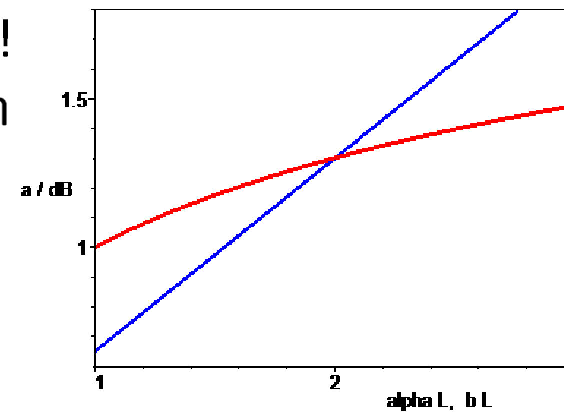

$$a_{\text{free space}}/\,\mathrm{dB} \sim 10\,\lg\left[(bL)^2\right] = 20 \lg (bL)$$

$$a_{\text{fibre}}/\,\mathrm{dB} = 10\,\lg\left[\exp(\alpha L)\right] = 4.34 (\alpha L)$$

Universe's mass calculations and web address contributed by Dipl.-Phys. Jan Brückner, DFG Research Training Group 786 "Mixed Fields and Nonlinear Interactions" (http://www.gkmf.uni-karlsruhe.de), Karlsruhe, Germany, June 23, 2005

LECTURE 2

LW Transmission Bands

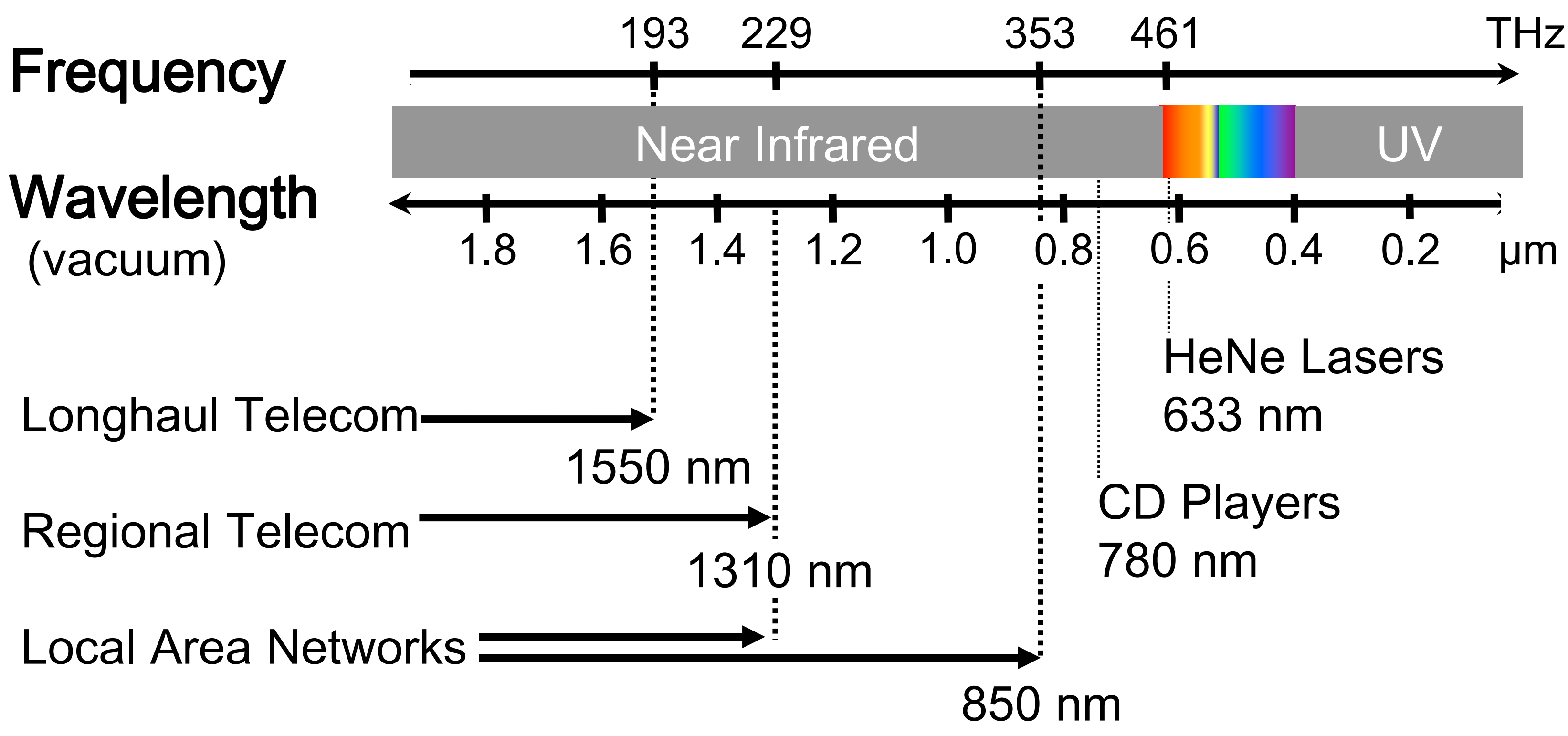

LW Transmission Bands - ITU Proposed Assignment

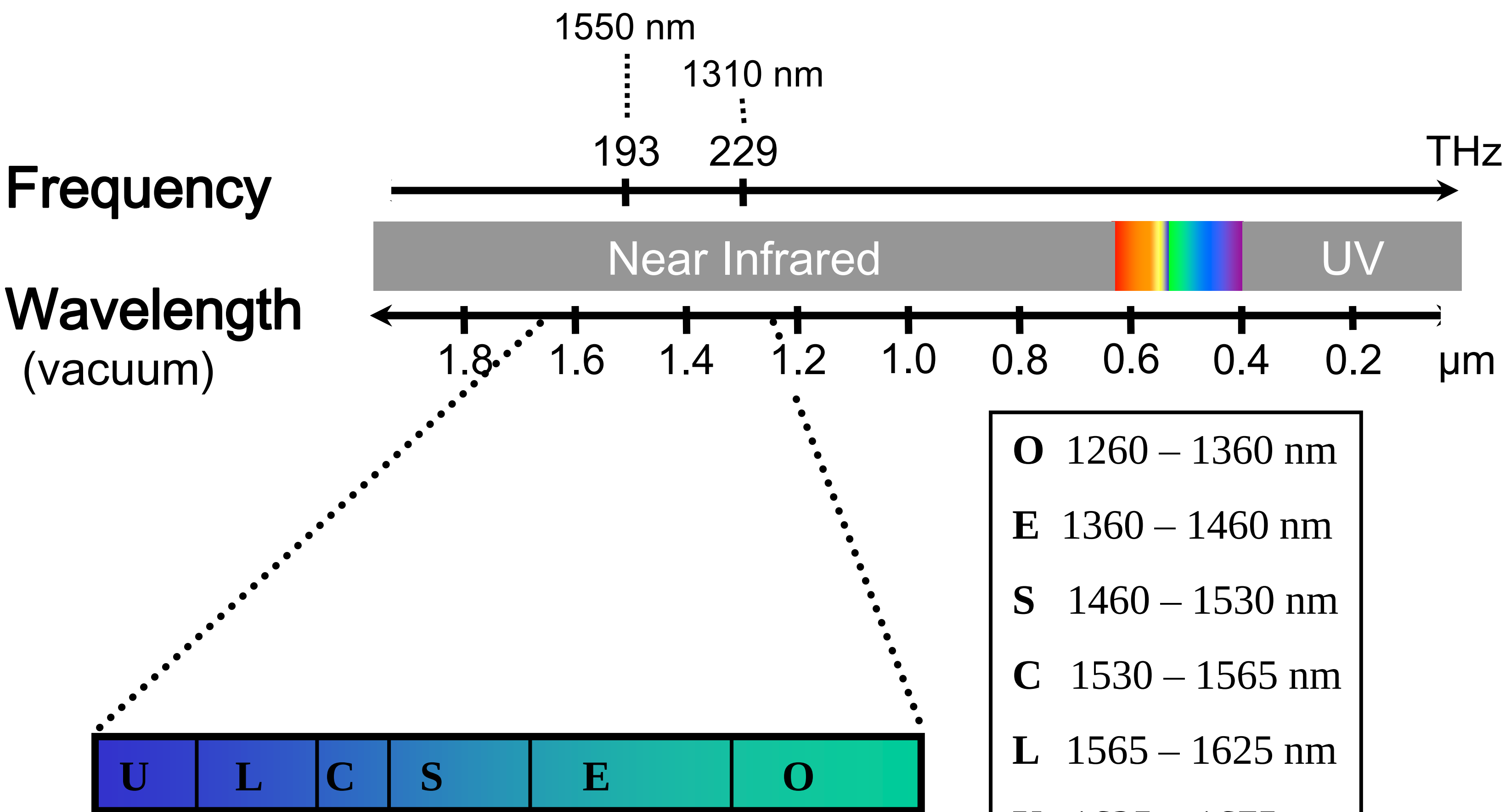

O	1260 – 1360 nm
E	1360 – 1460 nm
S	1460 – 1530 nm
C	1530 – 1565 nm
L	1565 – 1625 nm
U	1625 – 1675 nm

Transmission Bands

Designation of 40-nm bands ($\lambda/\,\mu$m) at $\lambda = 1.550\,\mu$m										
	S+		**S**		**C**		**L**		**L+**	
1.450	**1.470**	1.490	**1.510**	1.530	**1.550**	1.570	**1.590**	1.610	**1.630**	1.650

Table 1.1. Designation of bands at $\lambda = 1.550\,\mu$m

Wavelength table for the C-band (DWDM ITU-T grid)					
$\lambda_{\mathrm{ITU}}/\,$nm	$\lambda_{\mathrm{ITU}}/\,$nm	$\lambda_{\mathrm{ITU}}/\,$nm	$\lambda_{\mathrm{ITU}}/\,$nm	$\lambda_{\mathrm{ITU}}/\,$nm	$\lambda_{\mathrm{ITU}}/\,$nm
1 527.99	1 534.25	1 540.56	1 546.92	1 553.33	1 559.78
1 528.77	1 535.04	1 541.35	1 547.72	1 554.13	1 560.61
1 529.55	1 535.82	1 542.14	1 548.51	1 554.94	1 561.42
1 530.33	1 536.61	1 542.94	1 549.32	1 555.75	1 562.23
1 531.12	1 537.40	1 543.73	1 550.12	1 556.55	1 563.05
1 531.90	1 538.19	1 544.53	1 550.92	1 557.36	$\Delta = 0.79$
1 532.68	1 538.98	1 545.32	1 551.72	1 558.17	**all:**
1 533.47	1 539.77	1 546.12	1 552.52	1 558.98	**±0.1**

Table 1.2. DWDM ITU-T grid at $\lambda = 1.550\,\mu$m. Channel spacing corresponds to frequency grid $\Delta f = 100\,$GHz

Standard ITU Channel Grid

CH	Frequency(THz)	Wavelength(nm	CH	Frequency(THz)	Wavelength(nm)
15	191.500	1,565.4961	44	194,400	1,542.1425
16	191.600	1,564.6790	45	194.500	1,541.3496
17	191.700	1,563.8628	46	194,600	1,540.5576
18	191.800	1,563.0475	47	194.700	1,539.7663
19	191.900	1,562.2329	48	194.800	1,538.9759
20	192.000	1,561.4193	49	194.900	1,538.1863
21	192.100	1,560.6065	50	195,000	1,537.3974
22	192.200	1,559.7945	51	195.100	1,536.6094
23	192.300	1,558.9834	52	195.200	1,535.8222
24	192.400	1,558.1731	53	195.300	1,535.0358
25	192.500	1,557.3636	54	195.400	1,534.2503
26	192.600	1,556.5550	55	195.500	1,533.4655
27	192.700	1,555.7473	56	195.600	1,532.6815
28	192.800	1,554.9404	57	195.700	1,531.8983
29	192.900	1,554.1343	58	195.800	1,531.1159
30	193.000	1,553.3290	59	195.900	1,530.3344
31	193.100	1,552.5246	60	196.000	1,529.5536
32	193.200	1,551.7210	61	196.100	1,528.7736
33	193.300	1,550.9183	62	196,200	1,527.9944
34	193.400	1,550.1163	63	196.300	1,527.2160
35	193.500	1,549.3153	64	196.400	1,526.4384
36	193.600	1,548.5150	65	196.500	1,525.6616
37	193.700	1,547.7155	66	196.600	1,524.8856
38	193.800	1,546.9169	67	196.700	1,524.1103
39	193.900	1,546.1191	68	196.800	1,523.3359
40	194.000	1,545.3222	69	196.900	1,522.5622
41	194.100	1,544.5260	70	197.000	1,521.7893
42	194.200	1,543.7307	71	197.100	1,521.0200
43	194.300	1,542.9362	72	197.200	1,520.2500

Reference frequency: 195 THz

Basic grid: 100 GHz (≈ 0.79 nm)

Subdivisions: 50 GHz or 25 GHz

CWDM Channel Grid

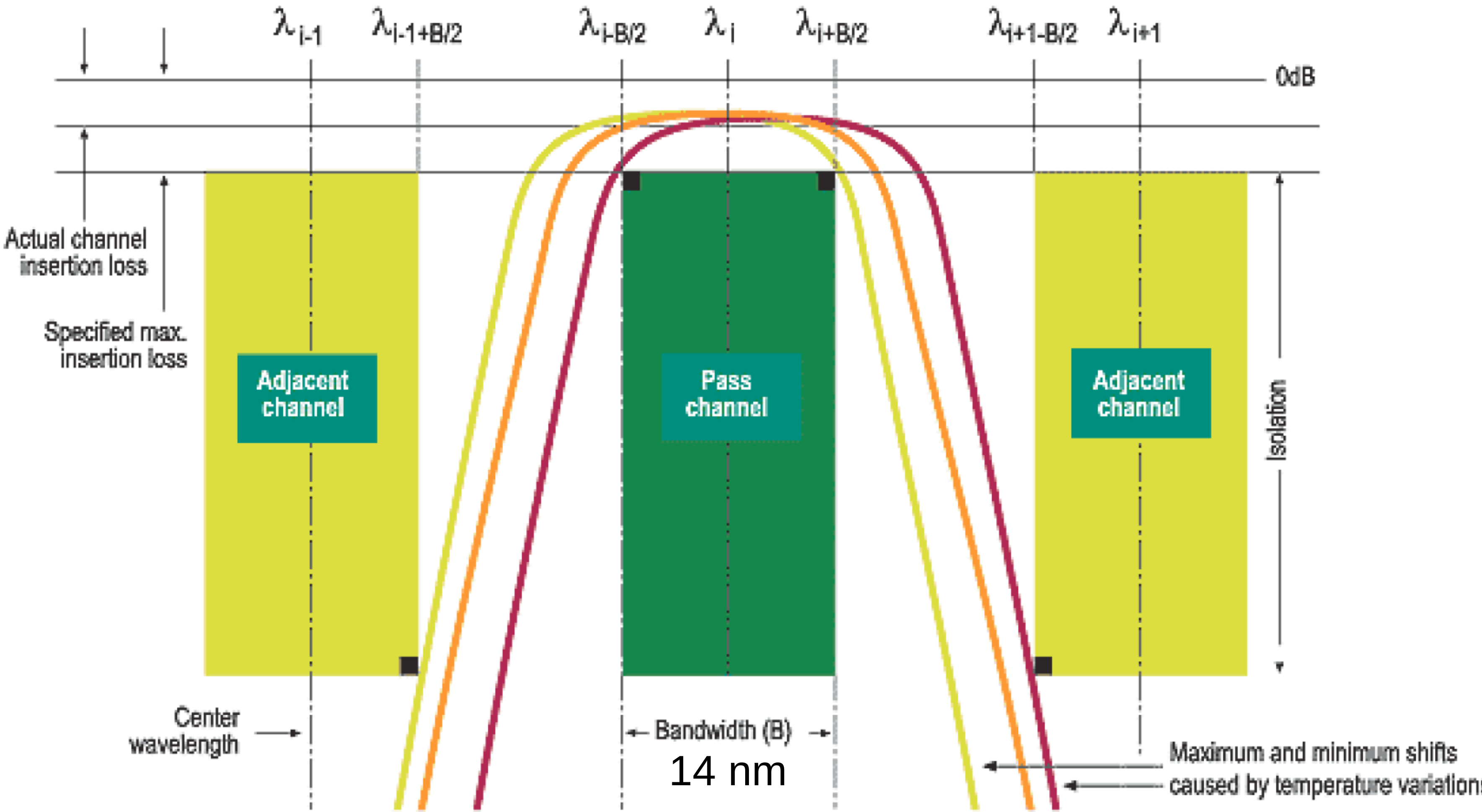

*C*oarse *w*avelength *d*ivision *m*ultiplexing: Channel grid with $\Delta\lambda$ = 20 nm, i.e., filter allows ±6.7 nm laser drift (thermal/aging), guard band width is 6.7 nm.

Advantages of Optical Communications

- Large transmission capacity because of the large fibre bandwidth in the order of (250 …190) THz = 60 THz
- Low fibre loss, about 2.2, 0.35, 0.15 dB/km at λ = 0.85, 1.3, 1.55 μm, i. e., down to 3 dB loss for a fibre length of L = 20 km corresponding to a power attenuation by a factor of only 2
- Immunity to interference because of the high carrier frequency, and because of the strong confinement of the light inside the fibre

Organization of Course

1. Introduction
2. Light Waveguides
3. Light sources
4. Optical amplifiers
5. Pin photodiode
6. Noise
7. Receivers and detection errors

Summaries, problems and quizzes

Photonics: Basic Components

Probe, laser bar, fibre — glass fibres — photodiode, eye of a needle

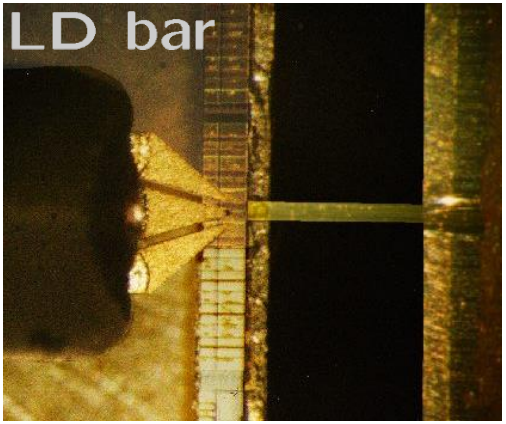

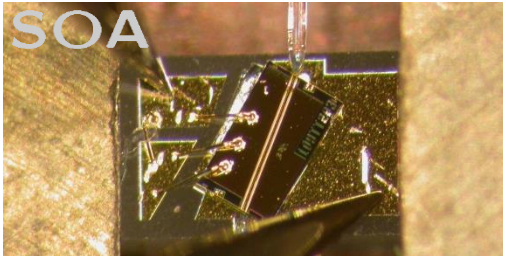

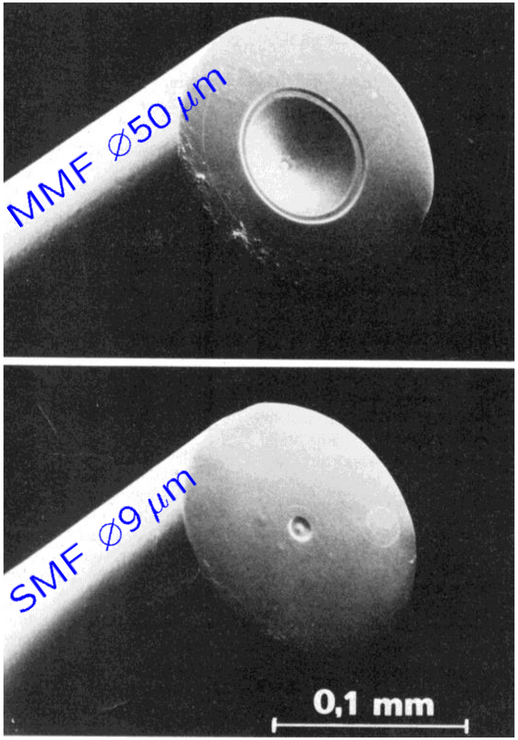

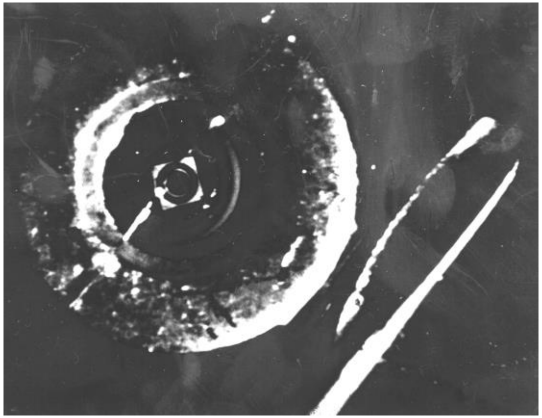

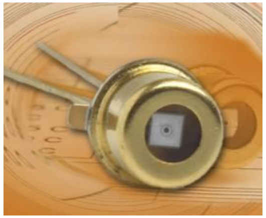

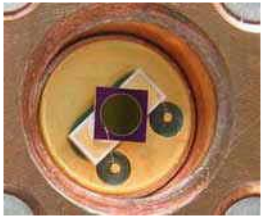

Multimode fibre

$2a = 65\,\mu\mathrm{m}$

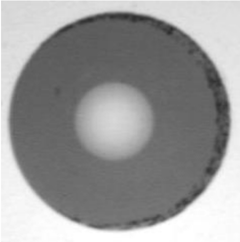

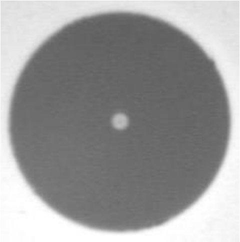

Single-mode fibre

$2a = 9\,\mu\mathrm{m}$

LECTURE 3

Fundamentals of Wave Propagation

Maxwell's Equations

$$\text{curl}\,\vec{H} = \frac{\partial \vec{D}}{\partial t}\,, \qquad \text{curl}\,\vec{E} = -\frac{\partial \vec{B}}{\partial t}\,,$$

$$\text{div}\,\vec{D} = 0\,, \qquad \text{div}\,\vec{B} = 0\,,$$

$$\vec{D} = \epsilon_0 \vec{E} + \vec{P}\,, \qquad \vec{B} = \mu_0 \vec{H}$$

Fourier Transform

$$\Psi(t) = \int\limits_{-\infty}^{+\infty} \tilde{\Psi}(f)\,\mathrm{e}^{+\mathrm{j}\,2\pi f t}\,\mathrm{d}f, \qquad \tilde{\Psi}(f) = \int\limits_{-\infty}^{+\infty} \Psi(t)\,\mathrm{e}^{-\mathrm{j}\,2\pi f t}\,\mathrm{d}t$$

Medium Properties

$$\vec{P}(t,\vec{r}) = \epsilon_0 \int_0^\infty \chi_t(\tau,\vec{r})\,\vec{E}(t-\tau,\vec{r})\,\mathrm{d}\tau\,,$$

$$\vec{P}(f) = \epsilon_0 \underline{\chi}(f)\vec{E}(f), \qquad \underline{\chi}(f) = \int_0^\infty \chi_t(t)\,\mathrm{e}^{-\mathrm{j}\,2\pi f t}\,\mathrm{d}t\,,$$

$$\underline{\chi}(f) = \chi(f) + \mathrm{j}\,\chi_i(f) = \epsilon_r(f) - 1 - \mathrm{j}\,\epsilon_{ri}(f), \quad \underline{\chi}(f) = \underline{\chi}^*(-f)$$

Refractive Index and Dielectric Constant $\bar{\epsilon}_r = \bar{n}^2$

$$\bar{n} = n - \mathrm{j}\,n_i, \qquad \bar{\epsilon}_r = \epsilon_r - \mathrm{j}\,\epsilon_{ri},$$

$$\epsilon_r = n^2 - n_i^2, \qquad \epsilon_{ri} = 2nn_i,$$

$$n^2 = \tfrac{1}{2}\epsilon_r\left(1 + \sqrt{1 + \epsilon_{ri}^2/\epsilon_r^2}\right), \qquad n_i = \epsilon_{ri}/(2n),$$

$$n \approx \sqrt{\epsilon_r} \quad (\text{for } |\epsilon_{ri}| \ll \epsilon_r) \qquad n_i \approx \epsilon_{ri}/(2\sqrt{\epsilon_r}\,),$$

$$n \approx \sqrt{|\epsilon_{ri}|/2} \quad (\text{for } |\epsilon_{ri}| \gg \epsilon_r) \qquad n_i \approx \mathrm{sgn}(\epsilon_{ri})\sqrt{|\epsilon_{ri}|/2}$$

Causal Time Functions and Analytic Spectra

Because of causality: Real and imaginary parts interconnected by so-called Hilbert transform and its inverse, $\breve{\Psi} = \mathcal{H}_F\{\breve{\Psi}\}$ and $\breve{\Psi} = \mathcal{H}_F^{-1}\{\breve{\Psi}_i\}$:

$$\breve{\Psi}_i(f_0) = \frac{1}{\pi}\mathcal{P}\int_{-\infty}^{+\infty} \frac{\breve{\Psi}(f)}{f - f_0}\,\mathrm{d}f, \qquad \breve{\Psi}(f_0) = -\frac{1}{\pi}\mathcal{P}\int_{-\infty}^{+\infty} \frac{\breve{\Psi}_i(f)}{f - f_0}\,\mathrm{d}f$$

Cauchy's principle value integral ($\mathcal{P}$ means 'valor principalis', Latin for principle value) is defined for a general function $f(x)$ by:

$$\mathcal{P}\int_{-\infty}^{+\infty} \frac{f(x)}{x - x_0}\,\mathrm{d}x = \lim_{\varepsilon \to 0}\left(\int_{-\infty}^{x_0-\varepsilon} \frac{f(x)}{x - x_0}\,\mathrm{d}x + \int_{x_0+\varepsilon}^{+\infty} \frac{f(x)}{x - x_0}\,\mathrm{d}x \right)$$

Kramers-Kronig Relation

$$\underbrace{-\epsilon_{ri}(f)}_{\Im\{\underline{\chi}(f)\}} = \frac{1}{\pi}\mathcal{P}\int_{-\infty}^{+\infty} \frac{\epsilon_r(f') - 1}{f' - f}\,\mathrm{d}f', \qquad \underbrace{\epsilon_r(f) - 1}_{\Re\{\underline{\chi}(f)\}} = \frac{1}{\pi}\mathcal{P}\int_{-\infty}^{+\infty} \frac{\epsilon_{ri}(f')}{f' - f}\,\mathrm{d}f'$$

For $\chi(f) = \epsilon_r(f) - 1 = \mathrm{const}_f$: $\epsilon_{ri}(f) = 0$ (anti-symmetric denominator in RHS integral) and therefore $\epsilon_r(f) = 1$ and $\chi(t) = 0$, i. e., no memory, no medium, no polarization. Real media with memory, so χ, χ_i are always frequency dependent.

In certain frequency ranges possible: $\chi = \mathrm{const}$ and $\chi_i = 0$. Then: Medium with real and constant refractive index. That this holds true for all frequencies (valid only for vacuum!) is implicitly assumed in the usual ansatz for $\vec{D}(t)$,

$$\vec{D} = \epsilon_0 \epsilon_r \vec{E}, \qquad n = \sqrt{\epsilon_r}$$

Free and Bound Charge Carriers

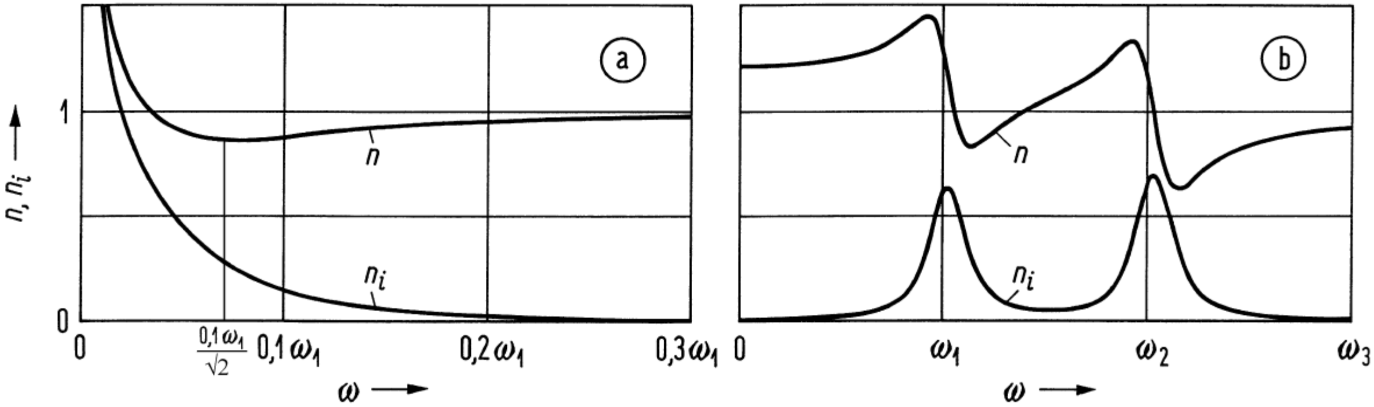

Fig. 2.1. Real part n und negative imaginary part (n_i) of complex refractive index $\bar{n} = n - \mathrm{j}\, n_i$: Frequency dependence (a) Free carriers only (b) Two collectives of bound charges with high mass (ions, low angular resonance frequency ω_1) and low mass (electrons, high angular resonance frequency ω_2)

$\vec{E}$-field forces atoms of molecules and bound electrons to vibrate. Force $\vec{F}$ exerted on charge q is $\vec{F} = q\vec{E}$. Assuming $\vec{E} = E_x\,\vec{e}_x$ and neglecting losses $\rightarrow$ Newton's second law: sum of forces (driving plus restoring force, proportionality constant ω_r^2) equals mass m_r times acceleration $\rightarrow$ electric dipole moment $P_x = qN\,x$, $a = \hat{a}\,\mathrm{e}^{\mathrm{j}\,\omega t}$:

$$qE_x(t) - m_r\omega_r^2 x(t) = m_r\frac{\mathrm{d}^2\,x(t)}{\mathrm{d}t^2}\,, \qquad \hat{x}(f) = \frac{q/m_r}{\omega_r^2 - \omega^2}\hat{E}_x(f) = \frac{\hat{P}_x(f)}{qN}$$

Free and Bound Charge Carriers

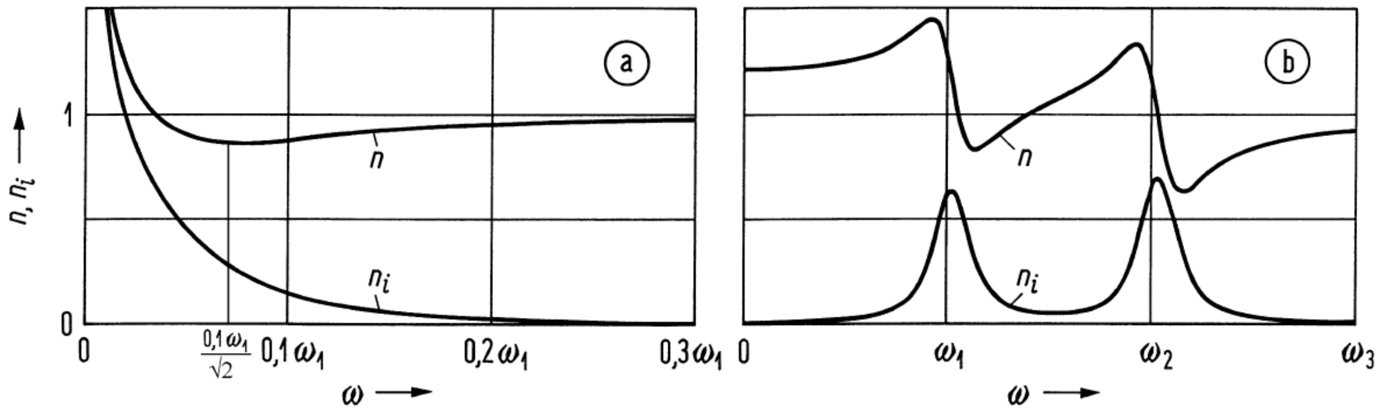

Fig. 2.1. Real part n und negative imaginary part (n_i) of complex refractive index $\bar{n} = n - \mathrm{j}\, n_i$: Frequency dependence (a) Free carriers only (b) Two collectives of bound charges with high mass (ions, low angular resonance frequency ω_1) and low mass (electrons, high angular resonance frequency ω_2)

$\vec{E}$-field forces atoms of molecules and bound electrons to vibrate. Force $\vec{F}$ exerted on charge q is $\vec{F} = q\vec{E}$. Assuming $\vec{E} = E_x\,\vec{e}_x$ and neglecting losses $\rightarrow$ Newton's second law: sum of forces (driving plus restoring force, proportionality constant ω_r^2) equals mass m_r times acceleration $\rightarrow$ electric dipole moment $P_x = qN\,x$, $a = \hat{a}\,\mathrm{e}^{\mathrm{j}\,\omega t}$:

$$\widehat{P}_x(f) = \frac{q^2 N/m_r}{\omega_r^2 - \omega^2}\widehat{E}_x(f),\ \vec{D} = \epsilon_0\epsilon_r\vec{E} = \epsilon_0\vec{E} + \vec{P} = \epsilon_0\left(1 + \frac{q^2 N/(\epsilon_0 m_r)}{\omega_r^2 - \omega^2}\right)\vec{E}$$

Plasma Oscillation

$\vec{E}$-field forces free electrons to vibrate, no restoring force, $\omega_r = 0$. Electron displacement $\vec{x} \sim -q\vec{E}$ opposite to driving force $\vec{F} = q\vec{E}$ (no loss: 180° out of phase *at all frequencies* $\omega \neq 0$).

Free electrons oscillating out of phase with incident light re-radiate wavelets that tend to cancel the incoming disturbance $\rightarrow$ rapidly decaying refracted wave.

Spatially fixed positive ions with concentration N providing f_e free electrons each, which produce polarization (relative diel. const. ϵ_r, refract. index n, imag. part $-n_i$, real $\bar{\epsilon}_r = n^2 - n_i^2$, $\epsilon_{ri} = 2nn_i = 0$):

if $\bar{\epsilon}_r > 0$: $n_i = 0$
if $\bar{\epsilon}_r < 0$: $n = 0$

$$\vec{P} = -eN f_e \frac{-e/m_e}{-\omega^2}\vec{E} = -\frac{N f_e e^2}{m_e\omega^2}\vec{E}, \qquad \vec{D} = \epsilon_0\epsilon_r\vec{E} = \epsilon_0\vec{E} + \vec{P},$$

$$\bar{\epsilon}_r = \bar{n}^2 = 1 - \frac{N f_e e^2}{\epsilon_0 m_e \omega^2} = 1 - \frac{\omega_p^2}{\omega^2}, \qquad \omega_p^2 = \frac{N f_e e^2}{\epsilon_0 m_e}$$

Fig. 2.1a: Plasma (ang.) frequency $\omega_p = \frac{0.1\omega_1}{\sqrt{2}} \approx 0.7071 \times (0.1\omega_1)$

Free and Bound Charge Carriers

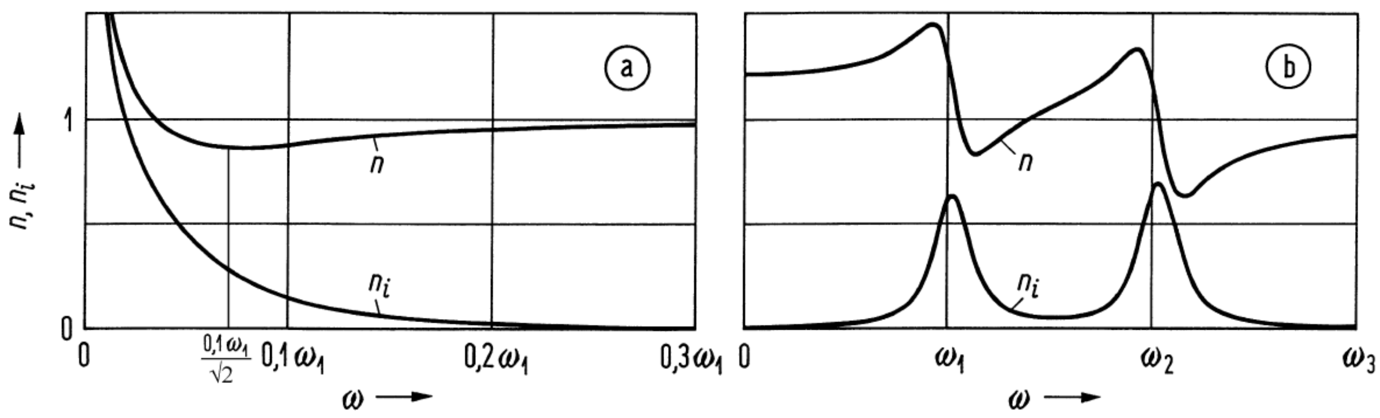

Fig. 2.1. Real part n und negative imaginary part (n_i) of complex refractive index $\bar{n} = n - \mathrm{j}\, n_i$: Frequency dependence (a) Free carriers only (b) Two collectives of bound charges with high mass (ions, low angular resonance frequency ω_1) and low mass (electrons, high angular resonance frequency ω_2)

$$\frac{\mathrm{d}n}{\mathrm{d}\omega} > 0\,, \qquad \frac{\mathrm{d}n}{\mathrm{d}\lambda} < 0 \qquad \text{normal dispersion}$$

$$\frac{\mathrm{d}n}{\mathrm{d}\omega} < 0\,, \qquad \frac{\mathrm{d}n}{\mathrm{d}\lambda} > 0 \qquad \text{anomalous dispersion}$$

Homogeneous Medium — Monochromatic Waves

Maxwell's Equations

$$\operatorname{curl}\vec{H} = \frac{\partial\vec{D}}{\partial t}, \qquad \operatorname{curl}\vec{E} = -\frac{\partial\vec{B}}{\partial t},$$

$$\operatorname{div}\vec{D} = 0, \qquad \operatorname{div}\vec{B} = 0,$$

$$\vec{D} = \epsilon_0\epsilon_r\vec{E}, \qquad \vec{B} = \mu_0\vec{H}$$

For Cartesian coordinates only:

$$\Psi(t,x,y,z) = E_q(t,x,y,z), H_q(t,x,y,z), \qquad q = x,y,z,$$

$$\Psi(t,r,\varphi,z) = E_z(t,r,\varphi,z), H_z(t,r,\varphi,z),$$

$$\nabla^2\Psi(t,\vec{r}) = \frac{n^2}{c^2}\frac{\partial^2}{\partial t^2}\Psi(t,\vec{r})$$

Decoupled versions of Maxwell's equations, starting with:

$$\operatorname{curl}\vec{H} = \epsilon_0\epsilon_r \frac{\partial}{\partial t}\vec{E}\,, \qquad \operatorname{curl}\vec{E} = -\mu_0\frac{\partial}{\partial t}\vec{H}\,,$$

$$\operatorname{curl}\operatorname{curl}\vec{H} = \epsilon_0\epsilon_r \frac{\partial}{\partial t}\operatorname{curl}\ \vec{E} + \operatorname{grad}(\epsilon_0\epsilon_r)\times\frac{\partial}{\partial t}\vec{E}, \qquad \operatorname{curl}\operatorname{curl}\vec{E} = -\mu_0\frac{\partial}{\partial t}\operatorname{curl}\vec{H}$$

Further:

$$\operatorname{div}\vec{H} = 0\,,$$

$$\operatorname{div}\left(\epsilon_0\epsilon_r\vec{E}\right) = \epsilon_0\epsilon_r\operatorname{div}\vec{E} + \operatorname{grad}(\epsilon_0\epsilon_r)\cdot\vec{E} = 0\,,$$

$$\operatorname{div}\vec{E} = -\frac{\operatorname{grad}(\epsilon_0\epsilon_r)}{\epsilon_0\epsilon_r}\cdot\vec{E} = -\operatorname{grad}\ln(\epsilon_r)\cdot\vec{E}$$

With the help of the vector identity:

$$\nabla^2\vec{E} = \operatorname{grad}\operatorname{div}\vec{E} - \operatorname{curl}\operatorname{curl}\vec{E}, \qquad \triangle\Psi = \operatorname{div}\operatorname{grad}\Psi$$

(differential operator ∇^2 operates on vector $\vec{E}$, not identical with Laplace operator $\triangle$ as applied to scalar function Ψ) → Decoupled relations:

$$\nabla^2\vec{H} = \operatorname{grad}\operatorname{div}\vec{H} - \operatorname{curl}\operatorname{curl}\vec{H} = -\epsilon_0\epsilon_r\frac{\partial}{\partial t}\operatorname{curl}\vec{E} - \operatorname{grad}(\epsilon_0\epsilon_r)\times\frac{\partial}{\partial t}\vec{E}$$

$$= -\epsilon_0\epsilon_r\frac{\partial}{\partial t}\left(-\mu_0\frac{\partial}{\partial t}\vec{H}\right) - \operatorname{grad}(\epsilon_0\epsilon_r)\times\frac{1}{\epsilon_0\epsilon_r}\operatorname{curl}\vec{H}\,,$$

$$\nabla^2\vec{E} = \operatorname{grad}\operatorname{div}\vec{E} - \operatorname{curl}\operatorname{curl}\vec{E} = \operatorname{grad}\left(-\operatorname{grad}\ln(\epsilon_r)\cdot\vec{E}\right) - \left(-\mu_0\frac{\partial}{\partial t}\operatorname{curl}\vec{H}\right)$$

$$= \operatorname{grad}\left(-\operatorname{grad}\ln(\epsilon_r)\cdot\vec{E}\right) - \left(-\mu_0\frac{\partial}{\partial t}\left(\epsilon_0\epsilon_r\frac{\partial}{\partial t}\vec{E}\right)\right)$$

Decoupled Versions of Maxwell's Equations (2)

Decoupled relations:

$$\nabla^2 \vec{H} = \operatorname{grad}\operatorname{div}\vec{H} - \operatorname{curl}\operatorname{curl}\vec{H} = -\epsilon_0\epsilon_r \frac{\partial}{\partial t}\operatorname{curl}\vec{E} - \operatorname{grad}(\epsilon_0\epsilon_r) \times \frac{\partial}{\partial t}\vec{E}$$

$$= -\epsilon_0\epsilon_r \frac{\partial}{\partial t}\left(-\mu_0 \frac{\partial}{\partial t}\vec{H}\right) - \operatorname{grad}(\epsilon_0\epsilon_r) \times \frac{1}{\epsilon_0\epsilon_r}\operatorname{curl}\vec{H},$$

$$\nabla^2 \vec{E} = \operatorname{grad}\operatorname{div}\vec{E} - \operatorname{curl}\operatorname{curl}\vec{E} = \operatorname{grad}\left(-\operatorname{grad}\ln(\epsilon_r)\cdot\vec{E}\right) - \left(-\mu_0\frac{\partial}{\partial t}\operatorname{curl}\vec{H}\right)$$

$$= \operatorname{grad}\left(-\operatorname{grad}\ln(\epsilon_r)\cdot\vec{E}\right) - \left(-\mu_0\frac{\partial}{\partial t}\left(\epsilon_0\epsilon_r\frac{\partial}{\partial t}\vec{E}\right)\right)$$

Simplification yields ($c^2 = (\mu_0\epsilon_0)^{-1}$):

$$\nabla^2\vec{H} + \operatorname{grad}\ln(\epsilon_r) \times \operatorname{curl}\vec{H} = \frac{\epsilon_r}{c^2}\frac{\partial^2\vec{H}}{\partial t^2},$$

$$\nabla^2\vec{E} + \operatorname{grad}\left(\operatorname{grad}\ln(\epsilon_r)\cdot\vec{E}\right) = \frac{\epsilon_r}{c^2}\frac{\partial^2\vec{E}}{\partial t^2} \quad \blacksquare$$

Homogeneous Medium — Monochromatic Waves

$$\nabla^2\vec{E} + \operatorname{grad}\left(\left(\cancel{\operatorname{grad}\ln n^2}\right)\cdot\vec{E}\right) = \frac{n^2}{c^2}\frac{\partial^2\vec{E}}{\partial t^2},$$

$$\nabla^2\vec{H} + \left(\cancel{\operatorname{grad}\ln n^2}\right)\times\operatorname{curl}\vec{H} = \frac{n^2}{c^2}\frac{\partial^2\vec{H}}{\partial t^2}$$

$$\nabla^2\vec{E} = \operatorname{grad}\operatorname{div}\vec{E} - \operatorname{curl}\operatorname{curl}\vec{E} =$$
$$= \vec{e}_x\operatorname{div}\operatorname{grad}E_x + \vec{e}_y\operatorname{div}\operatorname{grad}E_y + \vec{e}_z\operatorname{div}\operatorname{grad}E_z =$$
$$= \vec{e}_x\nabla^2E_x + \vec{e}_y\nabla^2E_y + \vec{e}_z\nabla^2E_z = \vec{e}_x\triangle E_x + \vec{e}_y\triangle E_y + \vec{e}_z\triangle E_z$$

For Cartesian coordinates only:

$$\Psi(t,x,y,z) = E_q(t,x,y,z),\, H_q(t,x,y,z), \qquad q = x,y,z\,,$$

$$\Psi(t,r,\varphi,z) = E_z(t,r,\varphi,z),\, H_z(t,r,\varphi,z),$$

$$\nabla^2\Psi(t,\vec{r}) = \frac{n^2}{c^2}\frac{\partial^2}{\partial t^2}\Psi(t,\vec{r})$$

Amplitude and Phase Surfaces

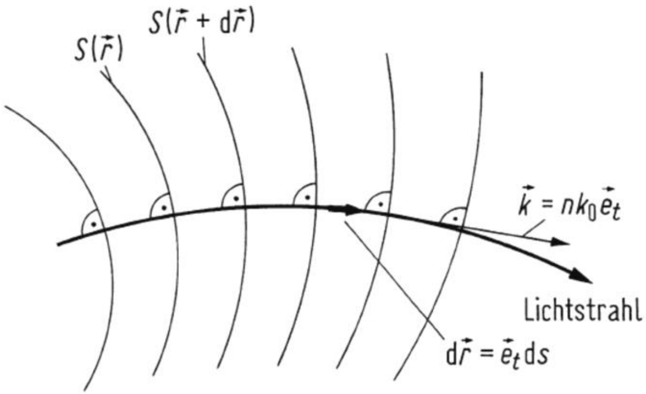

Monochromatic wave (A, φ, φ_i real):

$$\Psi(t,\vec{r}) = A(\vec{r})\,\mathrm{e}^{\mathrm{j}[\omega t - \varphi(\vec{r})]} = \mathrm{e}^{\mathrm{j}\,\omega t}\,\mathrm{e}^{-\mathrm{j}\,\bar{\varphi}(\vec{r})},$$

$$\bar{\varphi}(\vec{r}) = \varphi(\vec{r}) + \mathrm{j}\,\varphi_i(\vec{r})$$

$A(\vec{r})$ and $\varphi(\vec{r})$: Amplitude and phase of wave

$A(\vec{r}) = \text{const}$: Ampl. surface ($\varphi_i(\vec{r}) = \text{const}$)

$\varphi(\vec{r}) = \text{const}$: Phase surface

Amplitude vector: $\vec{a} = -\,\mathrm{grad}\,\varphi_i$

Phase vector: $\vec{b} = \mathrm{grad}\,\varphi$

Propagation vector: $\mathrm{grad}\,\bar{\varphi}$ (real $\vec{a}$, $\vec{b}$)

$$\mathrm{grad}\,\bar{\varphi} = \mathrm{grad}\,\varphi + \mathrm{j}\,\mathrm{grad}\,\varphi_i = \vec{b} - \mathrm{j}\,\vec{a}$$

Plane Waves in a Homogeneous Medium

Wave equation in homogeneous medium:

$$\nabla^2 \Psi(t,\vec{r}) \equiv \left(\frac{\partial^2}{\partial x^2} + \frac{\partial^2}{\partial y^2} + \frac{\partial^2}{\partial z^2}\right)\Psi(t,\vec{r}) = \frac{n^2}{c^2}\frac{\partial^2}{\partial t^2}\Psi(t,\vec{r})$$

With separation ansatz for plane phase fronts:

$$\begin{aligned}\Psi(t,\vec{r}) &= \exp(\mathrm{j}\,\omega t)\exp\left[-\mathrm{j}\,\bar{\varphi}(\vec{r})\right] \\ &= \exp(\mathrm{j}\,\omega t)\exp\left(-\mathrm{j}\,\vec{k}\cdot\vec{r}\right) = \exp(\mathrm{j}\,\omega t)\exp\left[-\mathrm{j}(k_x x + k_y y + k_z z)\right]\end{aligned}$$

Valid for separation condition:

$$(-k_x^2 - k_y^2 - k_z^2)\,\Psi(t,\vec{r}) = -\omega^2\frac{n^2}{c^2}\Psi(t,\vec{r}),$$

$$k_x^2 + k_y^2 + k_z^2 \stackrel{!}{=} n^2\left(\frac{\omega}{c}\right)^2 = n^2 k_0^2$$

Separation condition leads to separation constant nk_0, thus:

$$\bar{\varphi}(\vec{r}) = \vec{k}\cdot\vec{r}, \qquad \vec{k}^2 = \vec{k}\cdot\vec{k} = n^2 k_0^2 \quad \text{(real!)}, \qquad k_0 = \frac{\omega}{c} = 2\pi\frac{f}{c} = \frac{2\pi}{\lambda}$$

Phase Velocity and Plane Waves

Velocity of phase surface (phase front) in direction of propagation defines phase velocity v of wave. In 1D version, $\exp\left[\mathrm{j}\left(\omega t - kz\right)\right]$ with total phase $\phi = \omega t - kz$ and $\mathrm{d}\phi = 0$:

$$\mathrm{d}\phi = \mathrm{d}(\omega t) - \mathrm{d}(kz) = \frac{\partial\left(\omega t\right)}{\partial t}\mathrm{d}t - \frac{\partial\left(kz\right)}{\partial z}\mathrm{d}z = \omega\,\mathrm{d}t - k\,\mathrm{d}z = 0 \;\rightarrow\; v = \frac{\mathrm{d}z}{\mathrm{d}t} = \frac{\omega}{k}$$

Vectorial notation, $\exp\left[\mathrm{j}\left(\omega t - \varphi(\vec{r}\,)\right)\right]$:

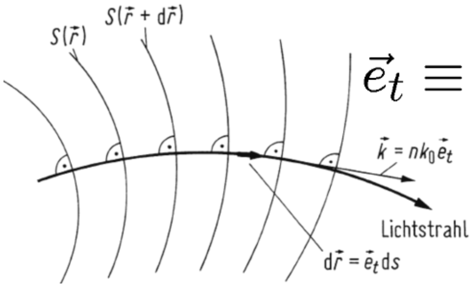

$$\vec{e}_t \equiv \vec{e}_b$$

$$\omega\,\mathrm{d}t - \mathrm{d}\varphi(\vec{r}\,) = \omega\,\mathrm{d}t - \frac{\partial\,\varphi(\vec{r}\,)}{\partial\,\vec{r}}\cdot\mathrm{d}\vec{r}$$

$$= \omega\,\mathrm{d}t - \operatorname{grad}\varphi\cdot\mathrm{d}\,\vec{r} = 0\,, \qquad \mathrm{d}\,\vec{r} = \vec{e}_b\,\mathrm{d}\,s = \frac{\operatorname{grad}\varphi}{|\operatorname{grad}\varphi|}\mathrm{d}s\,,$$

$$\omega\,\mathrm{d}t = \frac{(\operatorname{grad}\varphi)\cdot(\operatorname{grad}\varphi)}{|\operatorname{grad}\varphi|}\mathrm{d}s = \frac{|\operatorname{grad}\varphi|^2}{|\operatorname{grad}\varphi|}\mathrm{d}s \;\rightarrow\; v = \frac{\mathrm{d}s}{\mathrm{d}t} = \frac{\omega}{|\operatorname{grad}\varphi|} = \frac{\omega}{|\vec{b}|}$$

Propagation along $\vec{b}$ normal to phase surfaces. Unit vector $\vec{e}_b = \vec{b}/|\vec{b}| = \operatorname{grad}\varphi/|\operatorname{grad}\varphi|$ ($\equiv \vec{e}_t$ tangential to $\vec{r}\,$) with phase velocity v.

Waves named after shape of phase surfaces.

Homogeneous Plane Waves — Phase and Group Velocity

Phase velocity v for homogeneous plane waves defined formerly. Additionally: Group velocity v_g, group delay t_g for geometrical propagation length L, propagation constant k:

$$v = \frac{\omega}{k} = \frac{c}{n}, \qquad v_g = \frac{\mathrm{d}\omega}{\mathrm{d}k} = \frac{c}{n_g}, \qquad n_g = n + f\frac{\mathrm{d}n}{\mathrm{d}f} = n - \lambda\frac{\mathrm{d}n}{\mathrm{d}\lambda},$$

$$k = n\frac{\omega}{c}, \qquad \frac{t_g}{L} = \frac{\mathrm{d}k}{\mathrm{d}\omega} = \frac{n_g}{c}, \qquad \frac{\mathrm{d}n_g}{\mathrm{d}\lambda} = -\lambda\frac{\mathrm{d}^2 n}{\mathrm{d}\lambda^2}.$$

The group refractive index n_g represents an effective refractive index for the propagation of a wave group in a dispersive medium, its derivative measures the group delay difference.

LECTURE 4

Group Velocity — Physical Meaning

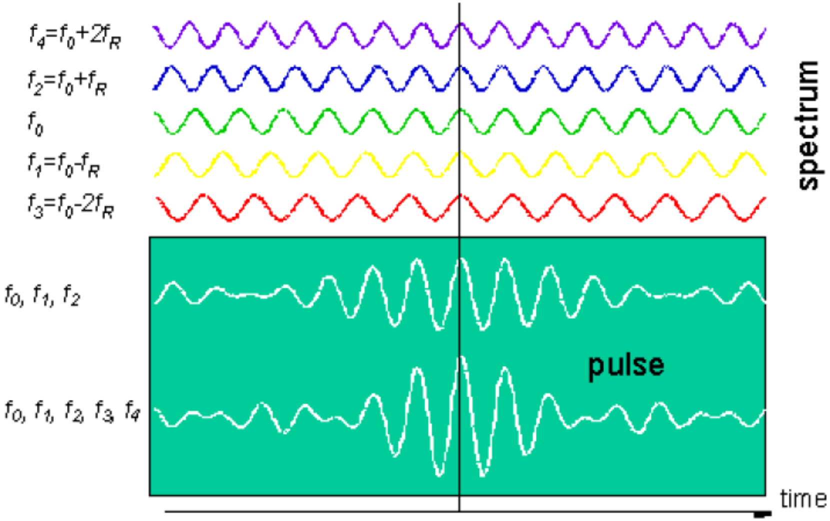

(a) Superposition of three and five sinusoidals

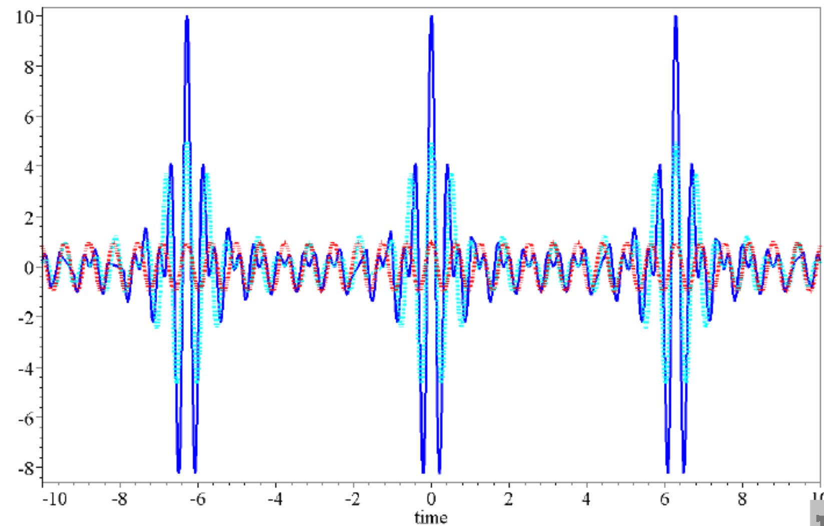

(b) Superposition of one, five and ten sinusoidals

Signal localized in time, superposition of n sinusoidals with equidistant frequencies. (a) $N = 3, 5$ for a limited time span (b) $N = 1, 5, 10$ for a more extended time span. If the frequency increment $f_R \to 0$ decreases and the number of sinusoidal $N \to \infty$ increases, the peaks become narrower and their time distance in (b) approaches infinity, so that a single Dirac impulse $\delta(t)$ remains.

How do we transport information? The answer is, by signals localized in time. Why so? We need to be taken by surprise. Information theory says that the less predictable an event is, the more information it carries.

Localization in Time

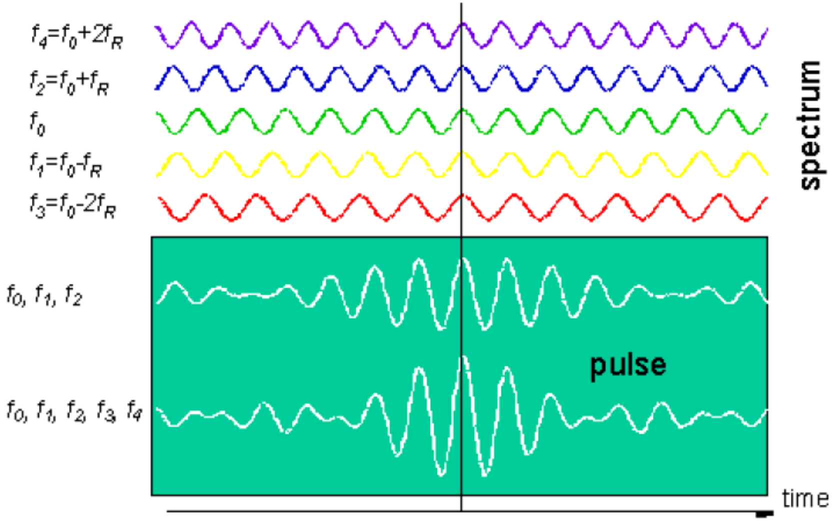

(a) Superposition of three and five sinusoidals

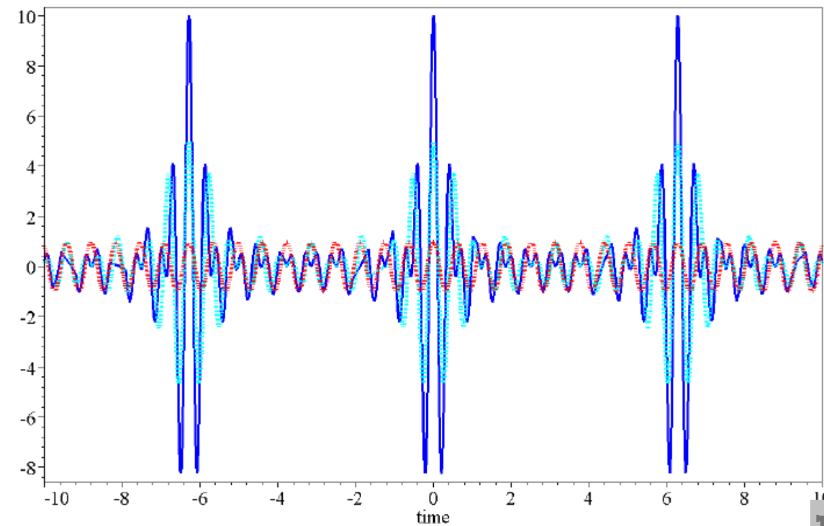

(b) Superposition of one, five and ten sinusoidals

But: A superposition of sinusoidals with different frequencies is localized in time! $N = 2$ homogeneous plane waves,

$$\psi(t,z) = \cos(\omega_1 t - k_1 z) + \cos(\omega_2 t - k_2 z)$$
$$= 2\cos\left(\frac{\omega_1 - \omega_2}{2} t - \frac{k_1 - k_2}{2} z\right)\cos\left(\frac{\omega_1 + \omega_2}{2} t - \frac{k_1 + k_2}{2} z\right)$$
$$v_g = \frac{\Delta\omega}{\Delta k} = \frac{c}{n_g}, \qquad v = \frac{\omega}{k} = \frac{c}{n}$$

More on Adding Phasors with Equidistant Frequencies

Sum of periodic functions is periodic:

$$\sum_{i=0}^{N-1} \cos\left(\omega_0 + i\omega_R\right) t = \frac{\sin\left(N\omega_R t/2\right)}{\sin\left(\omega_R t/2\right)} \cos\left(\omega_0 + \tfrac{N-1}{2}\omega_R\right) t$$

For $\omega_0 = 0$, $\omega_R \to 0$, $N \to \infty$, $N\omega_R = \text{const}$,

$\cos(x-y) = \cos x \cos y + \sin x \sin y$, $\sin x \cos x = \frac{1}{2}\sin(2x)$, and

$$\cos\left(\omega t\right) = \exp\left(-\mathrm{j}\,2\pi f t\right) + \mathrm{j}\sin\left(\omega t\right),$$

$$\int_{-Nf_R}^{+Nf_R} \sin\left(\omega t\right) \mathrm{d}f = 0 \;:$$

$$\lim_{\substack{\omega_R \to 0 \\ N \to \infty \\ N\omega_R = \text{const}}} \frac{\omega_R}{\pi} \sum_{i=0}^{N-1} \cos\left(i\omega_R t\right) = \frac{N\omega_R}{\pi} \frac{\sin(N\omega_R t)}{N\omega_R t} \quad \text{non-per./periodic!}$$

$$\lim_{N\omega_R \to \infty} \frac{N\omega_R}{\pi} \frac{\sin(N\omega_R t)}{N\omega_R t} = \lim_{Nf_R \to \infty} \int_{-Nf_R}^{+Nf_R} \cos\left(\omega t\right) \mathrm{d}f$$

$$\text{non-periodic!} \qquad = \lim_{Nf_R \to \infty} \int_{-Nf_R}^{+Nf_R} \mathrm{e}^{-\mathrm{j}\,2\pi f t}\, \mathrm{d}f = \delta(t)$$

Properties of Silica Glass — Attenuation

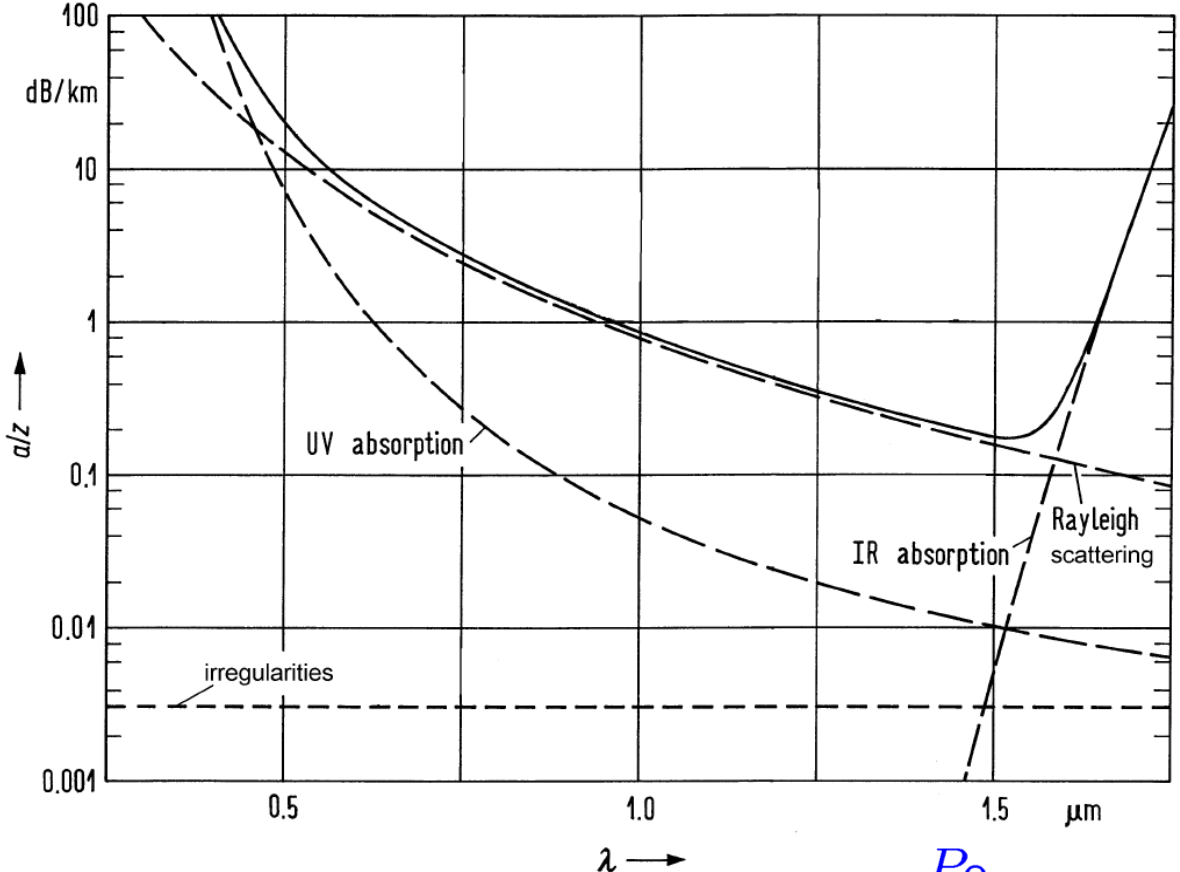

Losses through scattering and absorption.

Power attenuation constant α (unit km^{-1}) expressed by attenuation a (unit dB).

$$P(z) = P_0\,\mathrm{e}^{-\alpha z}, \qquad a = 10\,\lg\frac{P_0}{P(z)} = \alpha z\, 10\,\lg\mathrm{e} = 4.34\,\alpha z$$

Fig. 2.3. Attenuation of Ge-doped ($\Delta = 0.25\,\%$) singlemode fibre. VAD: produced with VAD-technology MCVD: produced with MCVD-technology. Unregelmäßigkeiten des Wellenleiters = irregularities of waveguide, berechnete Gesamtdämpfung = calculated total attenuation, gemessene Gesamtdämpfung = measured total attenuation, Rayleigh-Streuung = Rayleigh scattering

Properties of Silica Glass — History

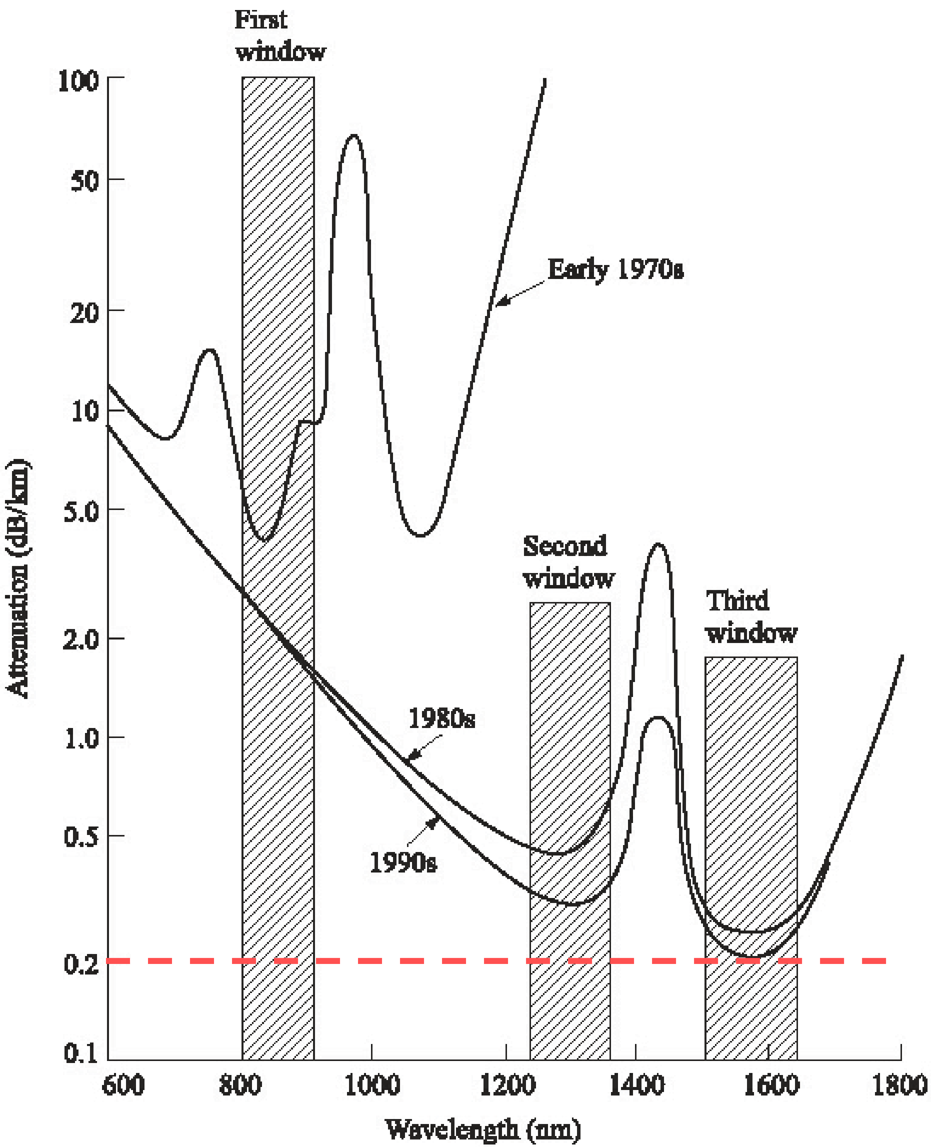

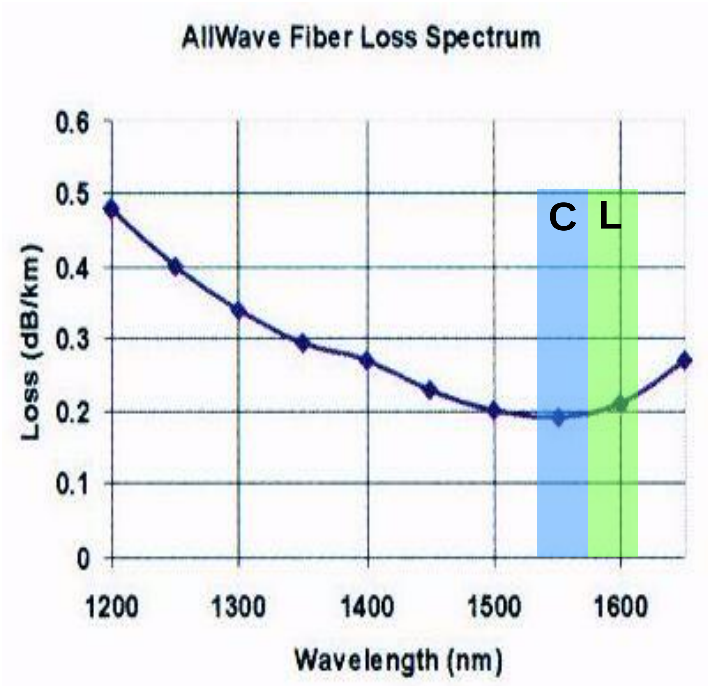

Modern communication fibre

Gerd Keiser: Optical Fiber Communications, 3rd ed. McGraw-Hill 2000

Properties of Silica Glass — Absorption by (OH^-) Bonds

(OH^-)-bond absorption is most important. Fundamental resonance $\lambda_{\mathrm{OH}} = 2.72\,\mu\mathrm{m}$ (110 THz). Harmonics and combinations: $\lambda_{\mathrm{OH}} = 2.22,\ 1.90,\ 1.38,\ 1.24,\ 1.13,\ 0.945,\ 0.88\,\mu\mathrm{m}$. With MCVD technology (modified chemical vapour deposition), relative (OH^-)-weights of 0.1 ppm (1 ppm $\widehat{=}\ 10^{-6}$) possible. VAD (vapour axial deposition) with dehydrated preform sets a lower limit of 1 ppb. Typical loss peaks at $\lambda_{\mathrm{OH}} = 1.38,\ 1.24,\ 0.945\,\mu\mathrm{m}$ are $a/z = 5.4$, 0.23, 0.083 dB / km (MCVD) and $a/z = 0.054$, 0.0023, 0.00083 dB / km (VAD).

At $\lambda = 0.85,\ 1.3,\ 1.55\,\mu\mathrm{m}$ an attenuation of $a/z = 2.2$, 0.35, 0.2 dB / km is feasible. Top results (undoped SiO_2-core with minimum Rayleigh scattering, matched F-SiO_2-cladding, $\Delta = 0.3\,\%$) for $\lambda = 1.3,\ 1.55\,\mu\mathrm{m}$ are $a/z = 0.291$, 0.154 dB / km. The basic attenuation limit of quartz glass can be reached routinely at

$$\lambda_\alpha = 1.55\,\mu\mathrm{m} \qquad \text{with} \qquad a/z|_{\lambda_\alpha} = 0.154\,\mathrm{dB}\,/\,\mathrm{km}\,.$$

Fibre Fabrication — Overview

MCVD+Variations
- Solution Method
- Metalorg.Compounds

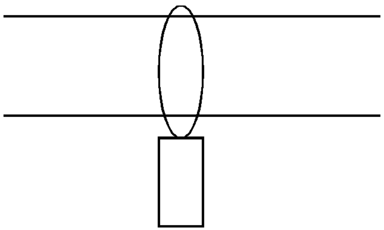

1800°C

2200°C

Glass Melting

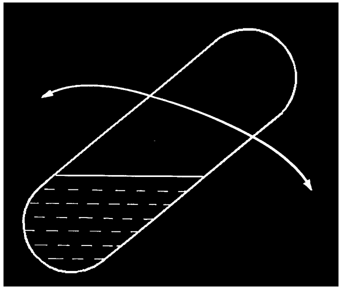

200...1000°C

Preform Drawing

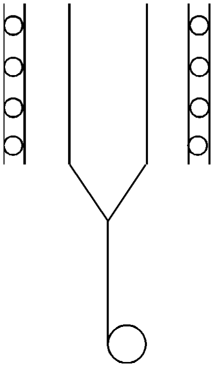

2000°C

Crucible Drawing

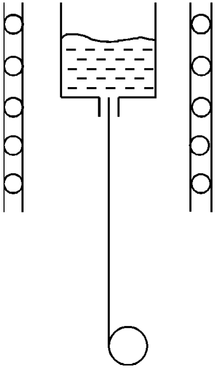

200...1000°C

Quartz Glass
"high-silica glasses"

Chalcogenide Glass

Jens Kobelke, Institut für Physikalische Hochtechnologie e.V. Jena, Bereich Optik, Abteilung Optische Fasern (2002)

Fibre Fabrication — PCVD/MCVD and VAD Method

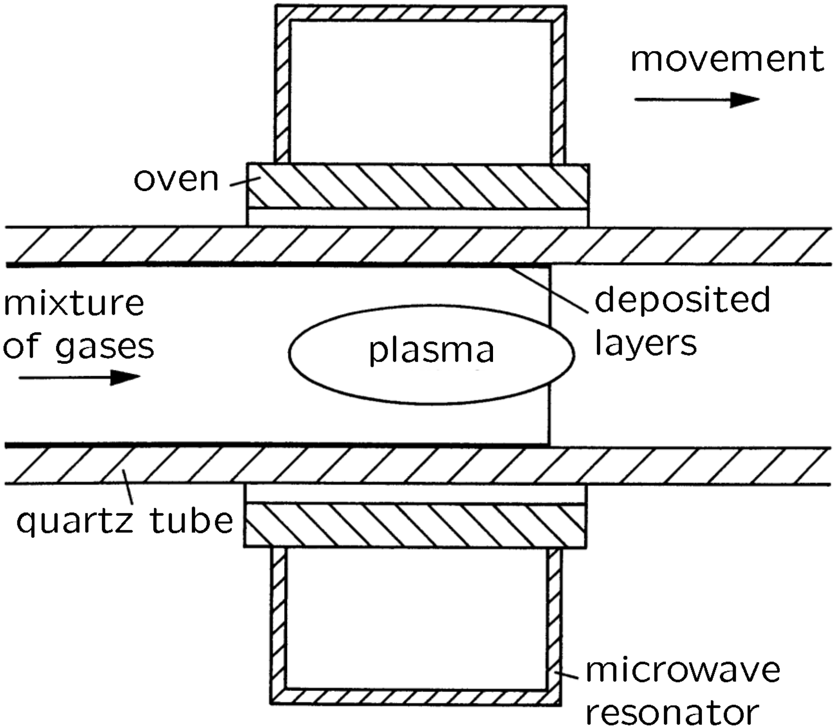

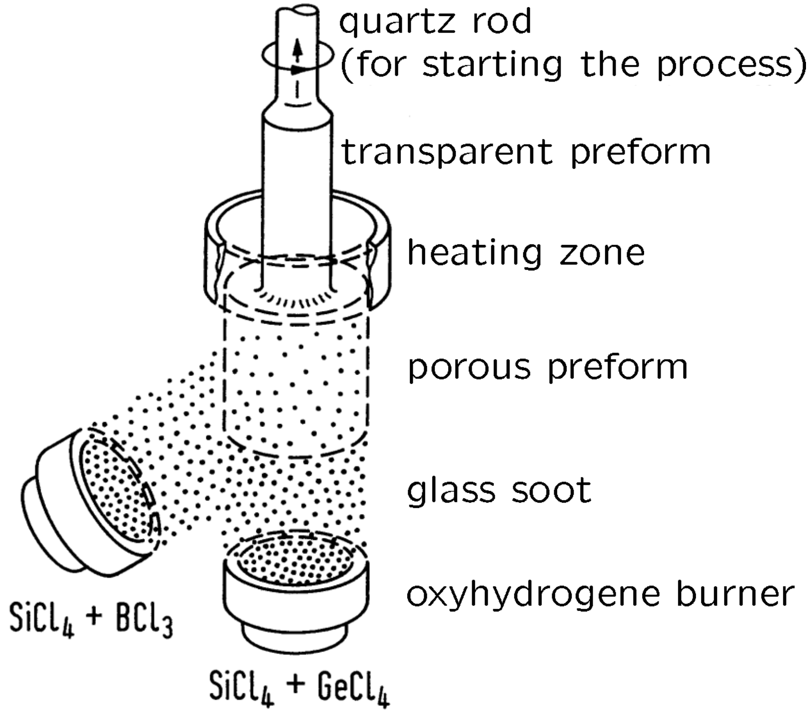

Plasma activated chemical vapour deposition (PCVD, Niederdruck-Plasma)

Similar: Modified chemical vapour deposition (MCVD)

Vapour axial deposition (VAD, deposition of glass soot by flame hydrolysis)

Fibre Fabrication — MCVD Method

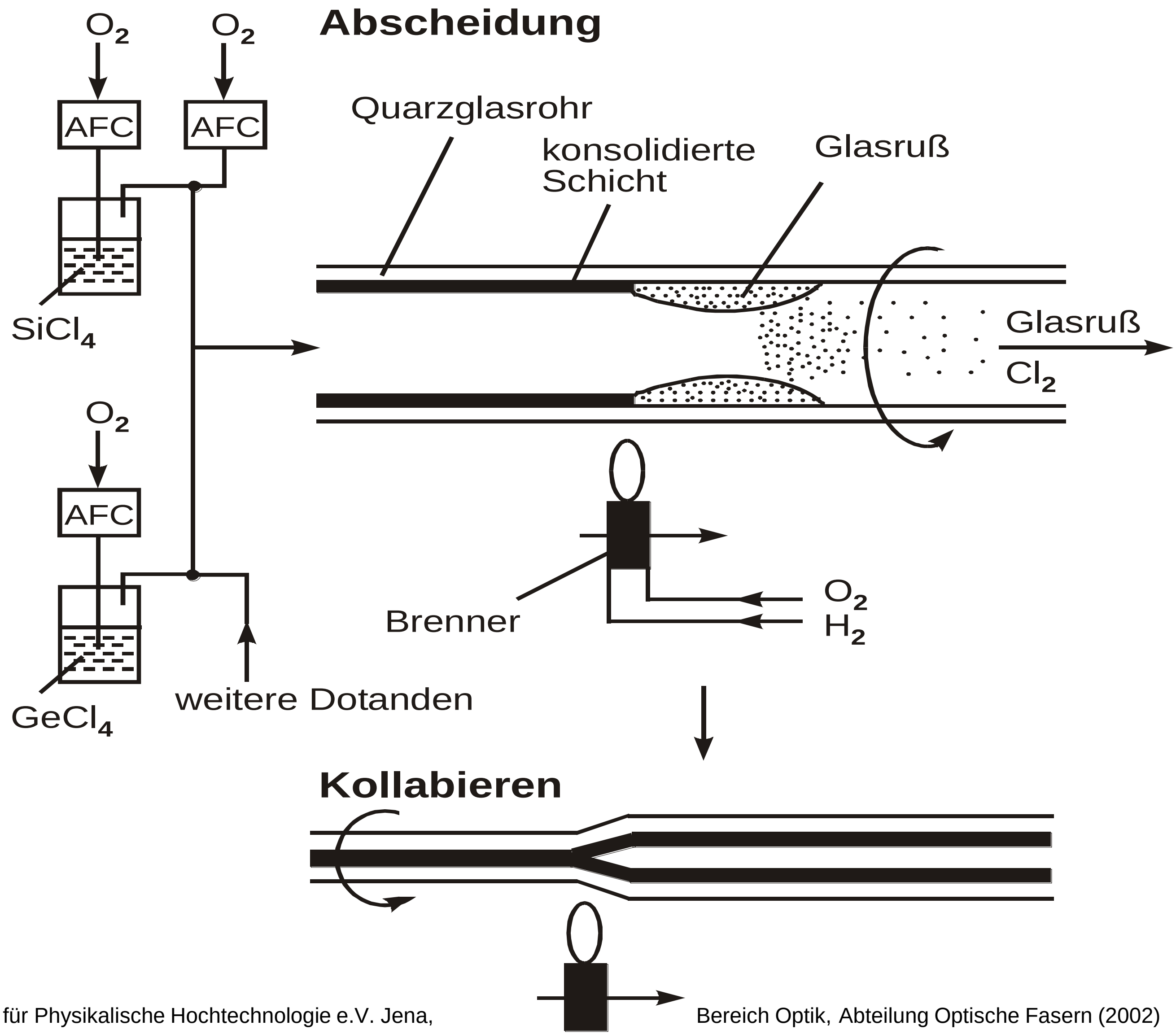

Jens Kobelke, Institut für Physikalische Hochtechnologie e.V. Jena, Bereich Optik, Abteilung Optische Fasern (2002)

Fibre Fabrication — MCVD Apparatus

$$SiCl_4(g) + O_2 \longrightarrow SiO_2\,(s) + 2Cl_2(g)$$

$$GeCl_4(g) + O_2 \longrightarrow GeO_2(s) + 2Cl_2(g)$$

Evaporation of $SiCl_4$, $GeCl_4$, $POCl_3$, CCl_4, $C_2Cl_3F_3$

Quartz glass tube

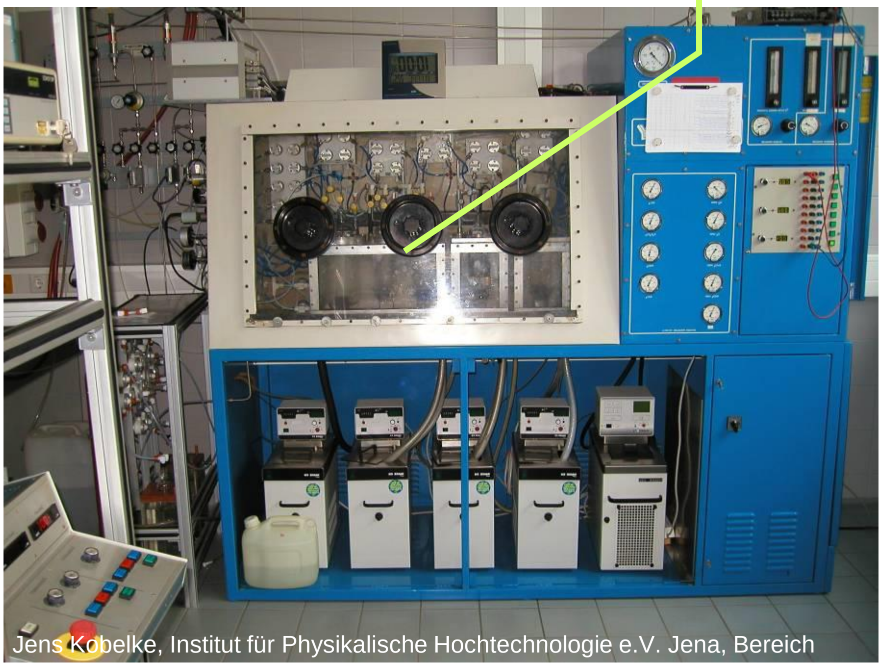

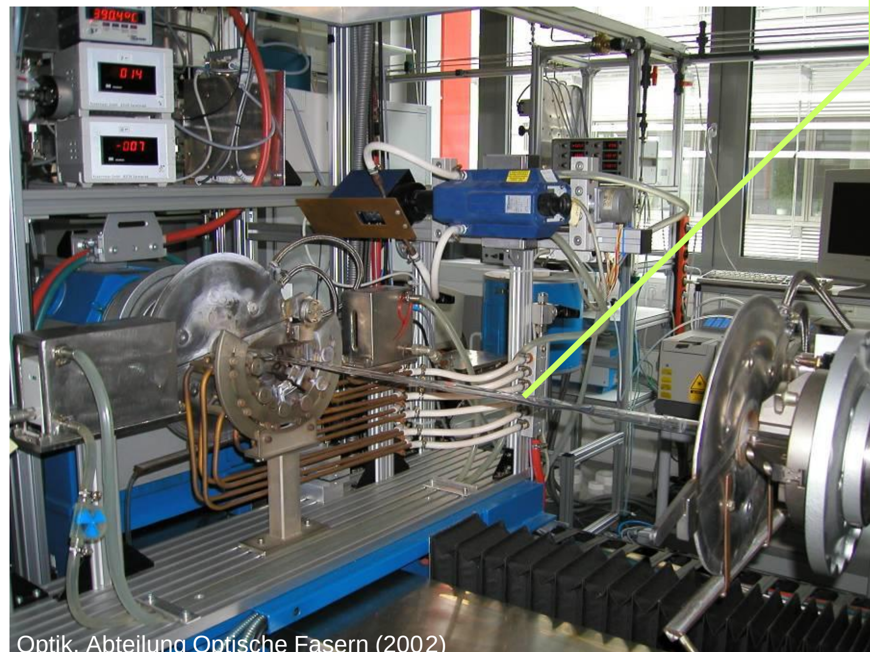

Jens Kobelke, Institut für Physikalische Hochtechnologie e.V. Jena, Bereich Optik, Abteilung Optische Fasern (2002)

Fibre Fabrication — Drawing Apparatus (1)

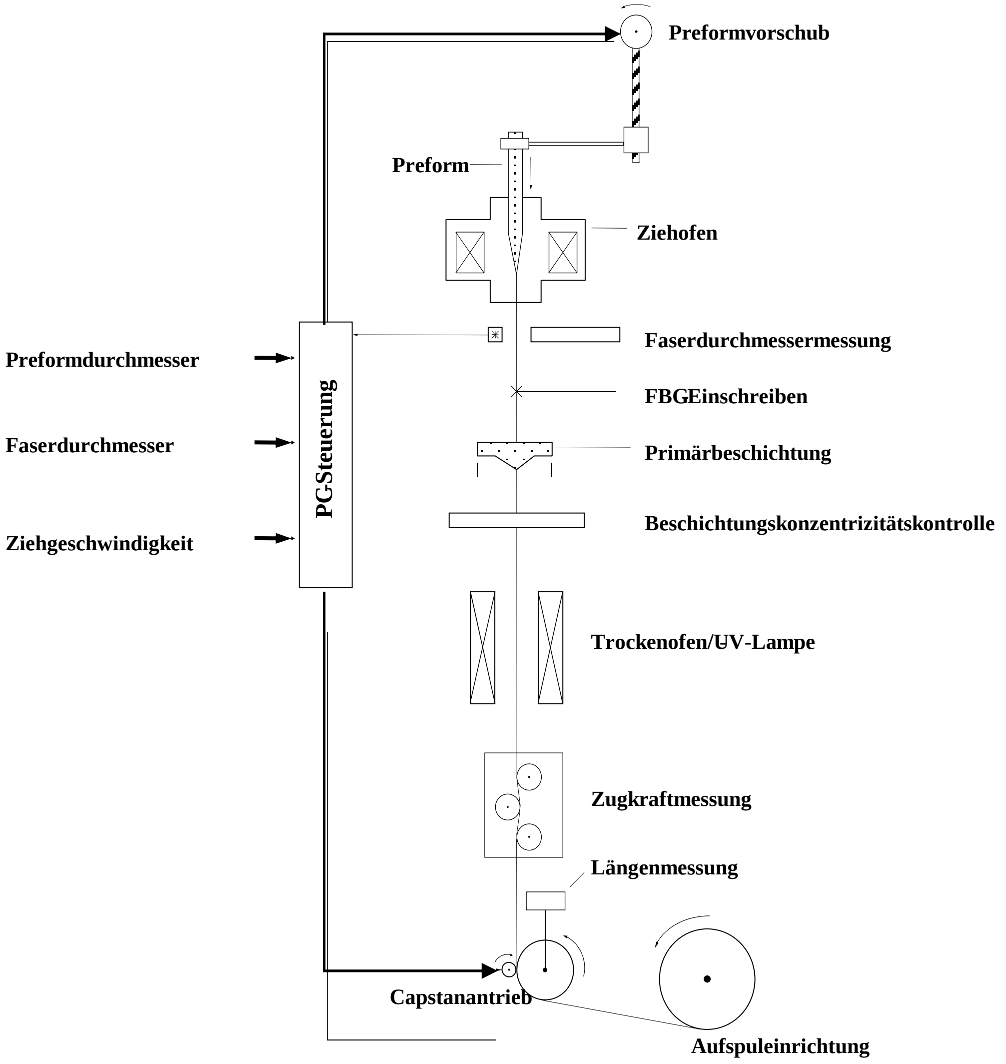

Jens Kobelke, Institut für Physikalische Hochtechnologie e.V. Jena, Bereich Optik, Abteilung Optische Fasern (2002)

Fibre Fabrication — Drawing Apparatus (2)

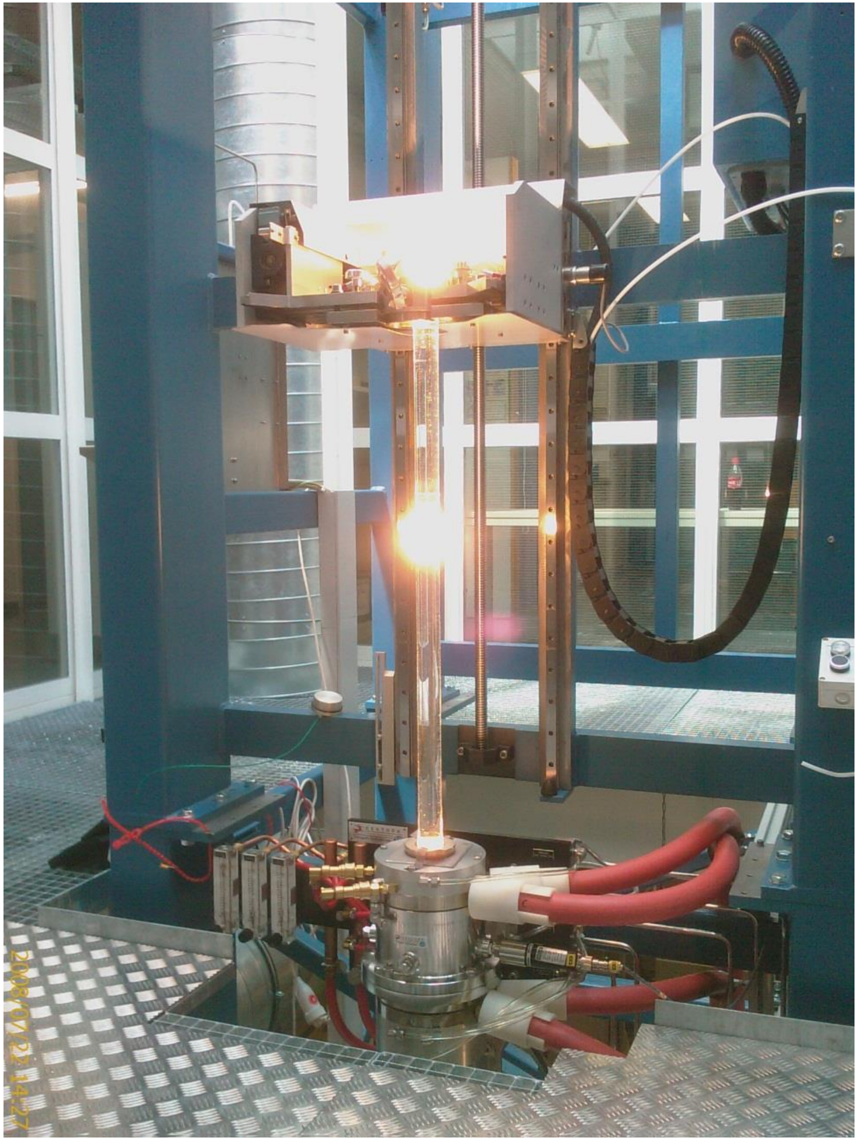

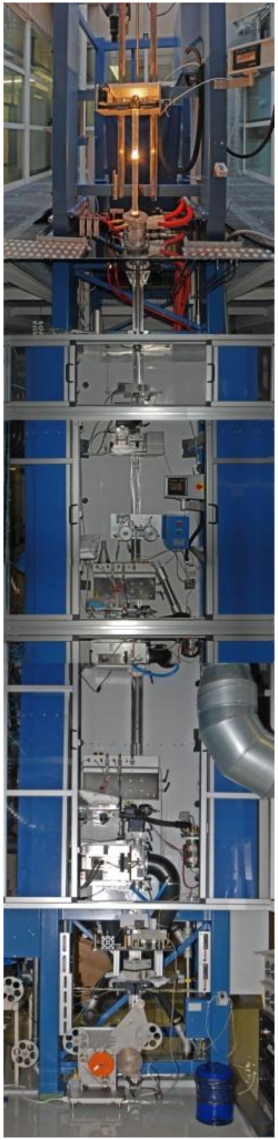

Armin Austerschulte, Institut für Strahlwerkzeuge; Universität Stuttgart (2008)

Dispersion — Definition

Real media have losses (or possibly gain), leads to $n(f)$, $v(f)$, and $v(f) \neq v_g(f) \rightarrow$ "dispersion". Different frequency components of a signal have different group delays t_g or group velocities v_g, signal becomes distorted after some length L.

Waveguiding properties $\rightarrow$ More influences on group delay which spread the signal delay times. In optical communications, the notion "dispersion" embraces all effects, which lead to a group delay time (or group velocity) spread.

If changes of the group delay with varying f are regarded, it is called "chromatic dispersion", sometimes also group velocity dispersion (GVD).

Dispersion — Material

Group delay difference of two plane waves (non-guided!) at optical carriers differing in λ by $\Delta\lambda = \lambda - \lambda_1$:

$$t_g(\lambda) = t_g(\lambda_1) + \frac{\mathrm{d}t_g}{\mathrm{d}\lambda}(\lambda - \lambda_1) + \frac{1}{2!}\frac{\mathrm{d}^2 t_g}{\mathrm{d}\lambda^2}(\lambda - \lambda_1)^2 + \ldots,$$

$$\Delta t_g = t_g(\lambda) - t_g(\lambda_1) = \frac{\mathrm{d}t_g}{\mathrm{d}\lambda}\Delta\lambda + \frac{1}{2!}\frac{\mathrm{d}^2 t_g}{\mathrm{d}\lambda^2}(\Delta\lambda)^2 + \ldots$$

"Material dispersion". Length related group delay difference:

$$\frac{\Delta t_g}{L} = M\,\Delta\lambda + N\,(\Delta\lambda)^2 + \ldots, \quad \frac{t_g}{L} = \frac{\mathrm{d}k}{\mathrm{d}\omega} = \frac{n_g}{c}, \quad M = \frac{1}{c}\frac{\mathrm{d}n_g}{\mathrm{d}\lambda}, \quad N = \frac{1}{2c}\frac{\mathrm{d}^2 n_g}{\mathrm{d}\lambda^2}$$

First-order material dispersion M dominates if $M(\lambda_0) \neq 0$. Condition $M(\lambda_0) = 0$ is (inaccurately) called "zero material dispersion wavelength". Material dispersion does <u>not</u> disappear, second-order material dispersion N takes over. Fused silica:

$$N_0 \approx 5.3\times 10^{-2}\,\mathrm{ps}/(\mathrm{km\,nm}^2), \qquad 2N_0\lambda_0 \approx 135\,\mathrm{ps}/(\mathrm{km\,nm})$$

Dispersion — Data

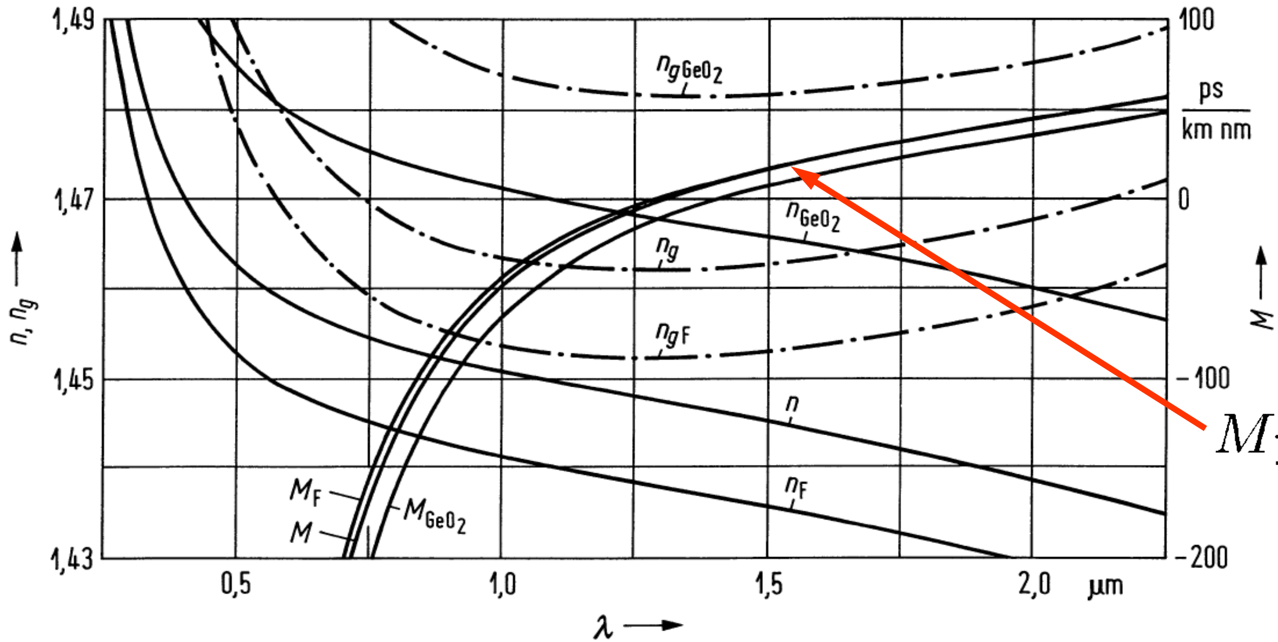

$$M_{1.55\,\mu\mathrm{m}} = \frac{16\,\mathrm{ps}}{\mathrm{km\ nm}}$$

Fig. 2.4. Refractive index n, group index n_g and material dispersion coefficient M, computed using the so-called Sellmeier coefficients for pure SiO_2 and (appropriately subscripted) for SiO_2 with dopings of 2 mol % F, 13.3 mol % GeO_2. Zeros of M are at $\lambda_{0F} = 1.2649\,\mu$m, $\lambda_0 = 1.2758\,\mu$m, $\lambda_{0GeO_2} = 1.3722\,\mu$m

$$\frac{\Delta t_g}{L} = M\,\Delta\lambda + N\,(\Delta\lambda)^2 + \ldots, \quad \frac{t_g}{L} = \frac{\mathrm{d}k}{\mathrm{d}\omega} = \frac{n_g}{c}, \quad M = \frac{1}{c}\frac{\mathrm{d}n_g}{\mathrm{d}\lambda}, \quad N = \frac{1}{2c}\frac{\mathrm{d}^2 n_g}{\mathrm{d}\lambda^2}$$

Dispersion — Physical Meaning

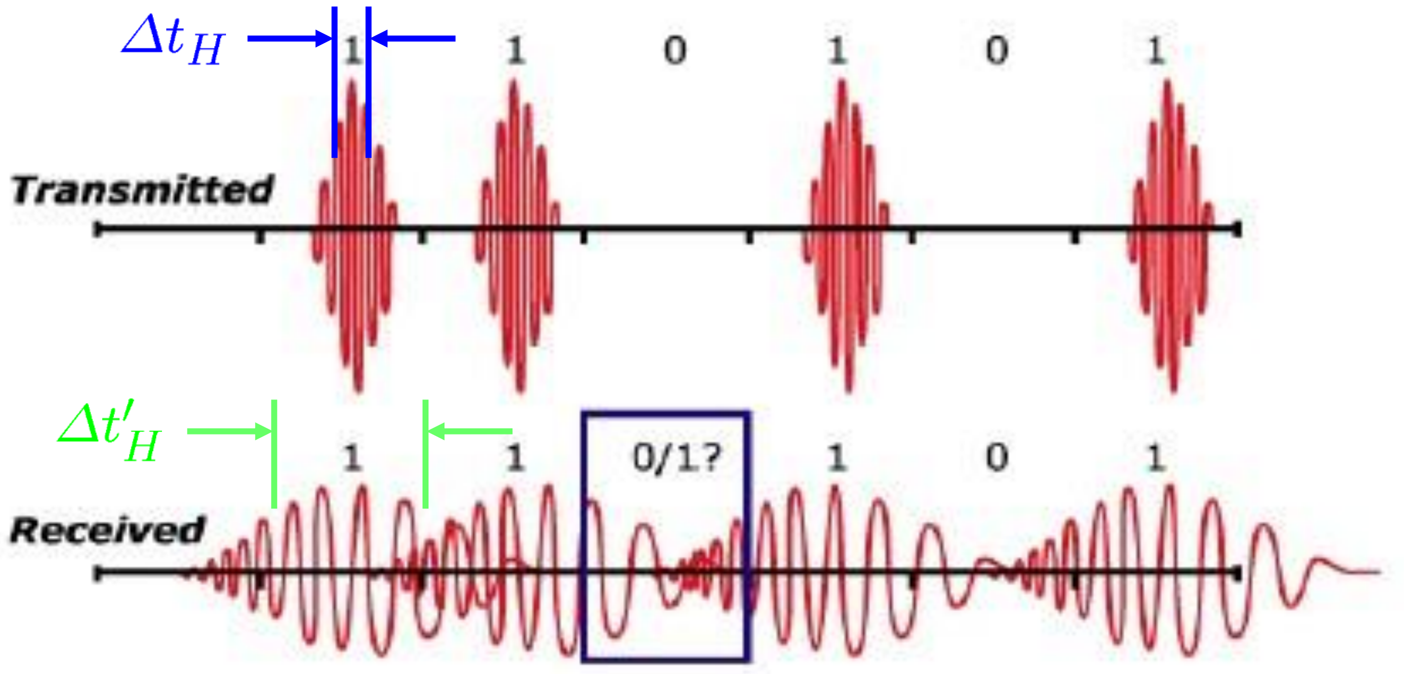

$M(1.55\,\mu\text{m}) = 16\,\text{ps}\,/(\text{km nm})$: Homogeneous medium. Gaussian impulse, half-power width Δt_H, propagates $L = 1\,\text{km}$. Gaussian spectrum of modulated source, width $\Delta\lambda = 1\,\text{nm}$

$\Rightarrow$ Impulse broadened by $\Delta t_g = ML\Delta\lambda = 16\,\text{ps}$. Total width:

$$\Delta t'_H \approx \sqrt{(\Delta t_g)^2 + (\Delta t_H)^2}$$

Christopher R. Moylan, University of California, Santa Cruz. http://www.soe.ucsc.edu/classes/ee230/Spring04

Inhomogeneous Medium — Plane Waves

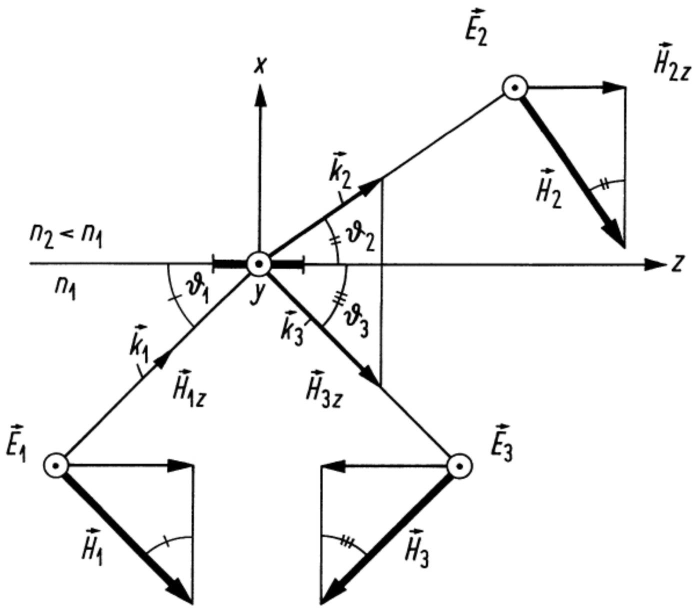

Fig. 2.5. Reflection and refraction of E-polarized (H-polarized) waves at a plane boundary; the subscripts 1, 2 and 3 designate the incident, transmitted and reflected waves, respectively. $\odot$-vectors point to the observer (perpendicularly out of the drawing area). (a) Reflection und refraction at the transition to the denser medium

Regions n_1, n_2, boundary plane $x = 0$. Wanted: Solutions for incident plane wave ($n_1 > n_2$). Ansatz: Three superimposed monochromatic plane waves:

$$\vec{\Psi}(t, \vec{r}\,) = \vec{\Psi} \exp(\mathrm{j}\,\omega t - \mathrm{j}\,\vec{k}_s \cdot \vec{r}\,), \qquad \vec{\Psi}_s = \vec{E}_s, \vec{H}_s\,, \qquad s = 1, 2, 3$$

Inhomogeneous Medium — Plane Waves

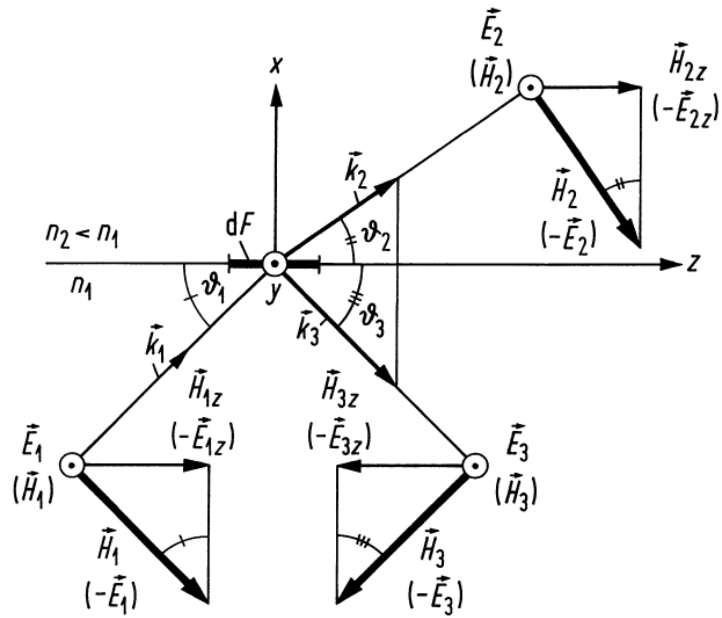

Fig. 2.5. Reflection and refraction of E-polarized (H-polarized) waves at a plane boundary; the subscripts 1, 2 and 3 designate the incident, transmitted and reflected waves, respectively. $\odot$-vectors point to the observer (perpendicularly out of the drawing area). (a) Reflection und refraction at the transition to the denser medium

Regions n_1, n_2, boundary plane $x = 0$. Wanted: Solutions for incident plane wave ($n_1 > n_2$). Ansatz: Three superimposed monochromatic plane waves:

$$\vec{\Psi}(t, \vec{r}\,) = \vec{\Psi} \exp(\mathrm{j}\,\omega t - \mathrm{j}\,\vec{k}_s \cdot \vec{r}\,), \qquad \vec{\Psi}_s = \vec{E}_s, \vec{H}_s\,, \qquad s = 1, 2, 3$$

Inhomogeneous Medium — Boundary Conditions

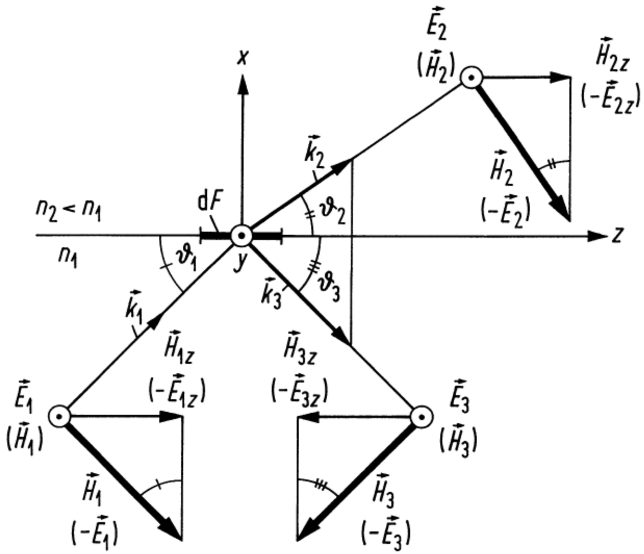

$$\vec{\Psi}(t,\vec{r}) = \vec{\Psi}\exp(\mathrm{j}\,\omega t - \mathrm{j}\,\vec{k}_s\cdot\vec{r}),$$
$$\vec{\Psi}_s = \vec{E}_s, \vec{H}_s\,, \qquad s = 1,2,3\,.$$

Subscripts 1, 2, 3: Incident, transmitted and reflected waves. Only the total of <u>three</u> solve the problem. Vector component subscripts are coordinates $q = x, y, z$. For the incident wave we assume $k_{1y} = 0$.

E-pol. ($\vec{E}_s = E_s\vec{e}_y \parallel$ boundary plane, $E_{sz} = 0$, TE- or H-wave), or
H-pol. ($\vec{H}_s = H_s\vec{e}_y \parallel$ boundary plane, $H_{sz} = 0$, TM- or E-wave).
Example for transverse E- and H-components in boundary $x = 0$:

$$E_{2y}\exp[-\mathrm{j}(\overbrace{k_{2x}x}^{x=0} + \overbrace{k_{2y}y}^{\to 0} + k_{2z}z)] = E_{1y}\exp[-\mathrm{j}(\underbrace{k_{1x}x}_{x=0} + \underbrace{k_{1y}y}_{=0} + k_{1z}z)]$$
$$+\, E_{3y}\exp[-\mathrm{j}(\underbrace{k_{3x}x}_{x=0} + \underbrace{k_{3y}y}_{\to 0} + k_{3z}z)]$$

Inhomogeneous Medium — Snell´s Formula

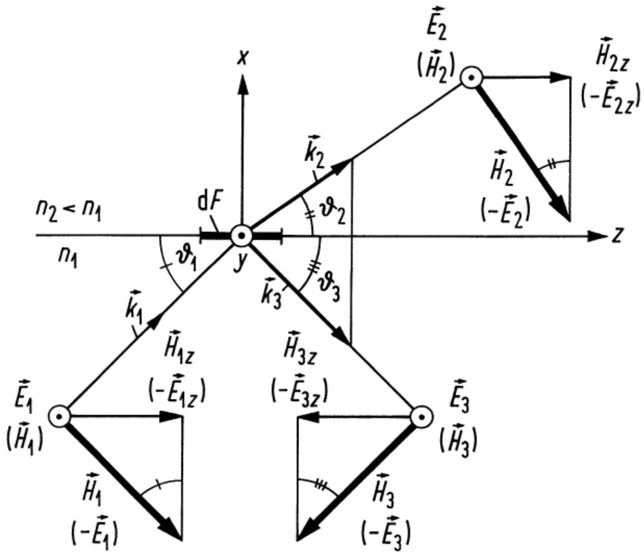

$$k_{1y} = k_{2y} = k_{3y} = 0,$$
$$k_{1z} = k_{2z} = k_{3z}\,;$$

E-polarization:

$$E_{2y} = E_{1y} + E_{3y},$$
$$H_{2z} = H_{1z} + H_{3z},$$
$$|H_{sz}| = H_s \sin\vartheta_s, \qquad (H_{3z} < 0),$$
$$Z_s = E_{sy}/H_{sz} = \frac{Z_0}{n_s} k_s/k_{sx},$$
$$Y_s = -H_{sy}/E_{sz} = \frac{n_s}{Z_0} k_s/k_{sx}.$$

The z-components of $\vec{k}_s$ and the amplitudes at both sides of $x = 0$ must be identical, so that the fields propagate in synchronism along the z-axis. Snell's law and the limiting angle ϑ_{1T} of total internal reflection (TIR) follow:

$$\vartheta_1 = \vartheta_3, \qquad n_1 \cos\vartheta_1 = n_2 \cos\vartheta_2, \qquad \cos\vartheta_{1T} = \frac{n_2}{n_1}$$

LECTURE 5

Demonstration of Total Internal Reflection (1)

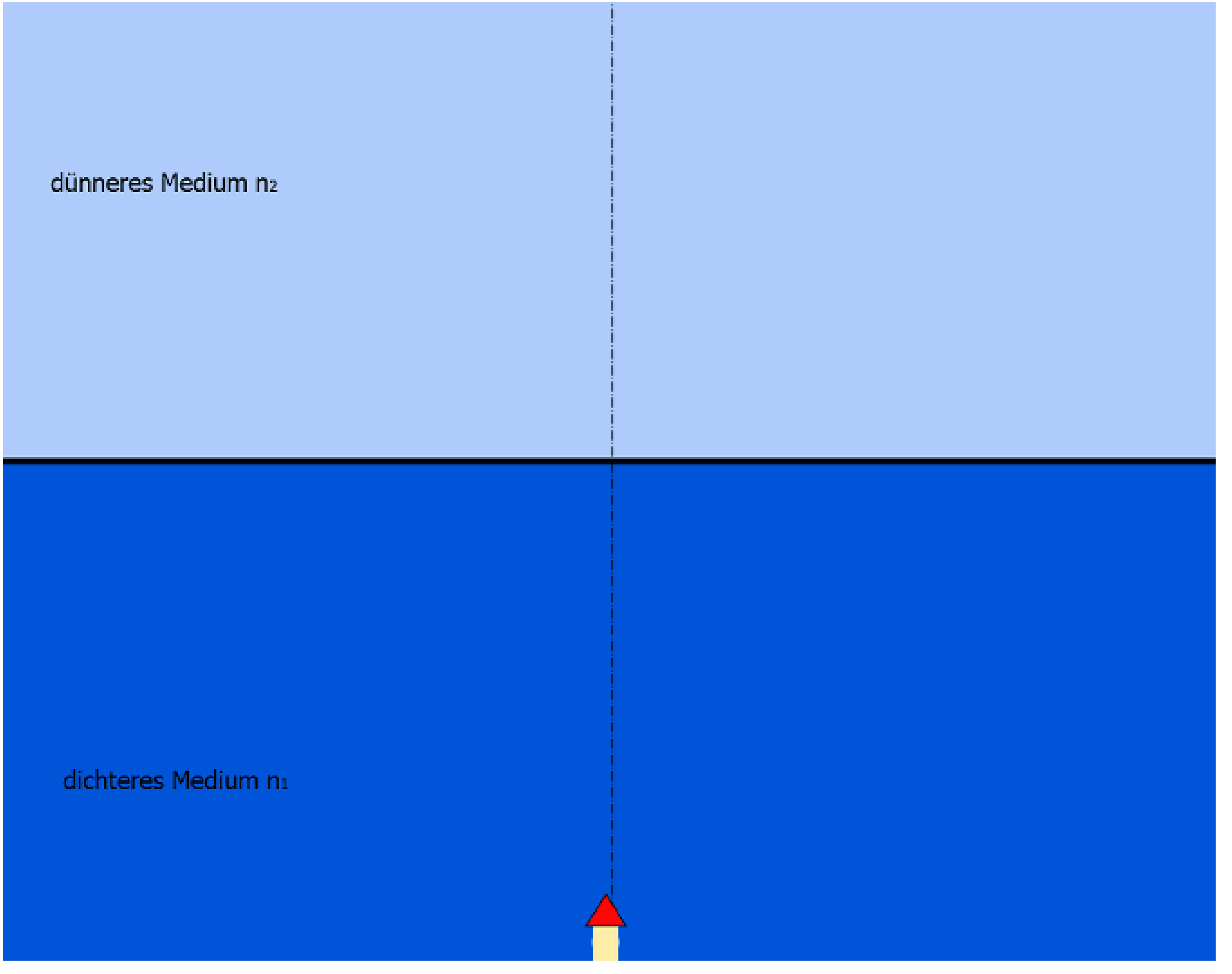

http://upload.wikimedia.org/wikipedia/commons/f/f4/Totalreflexion_%C3%9Cberarbeitet.gif

Demonstration of Total Internal Reflection (2)

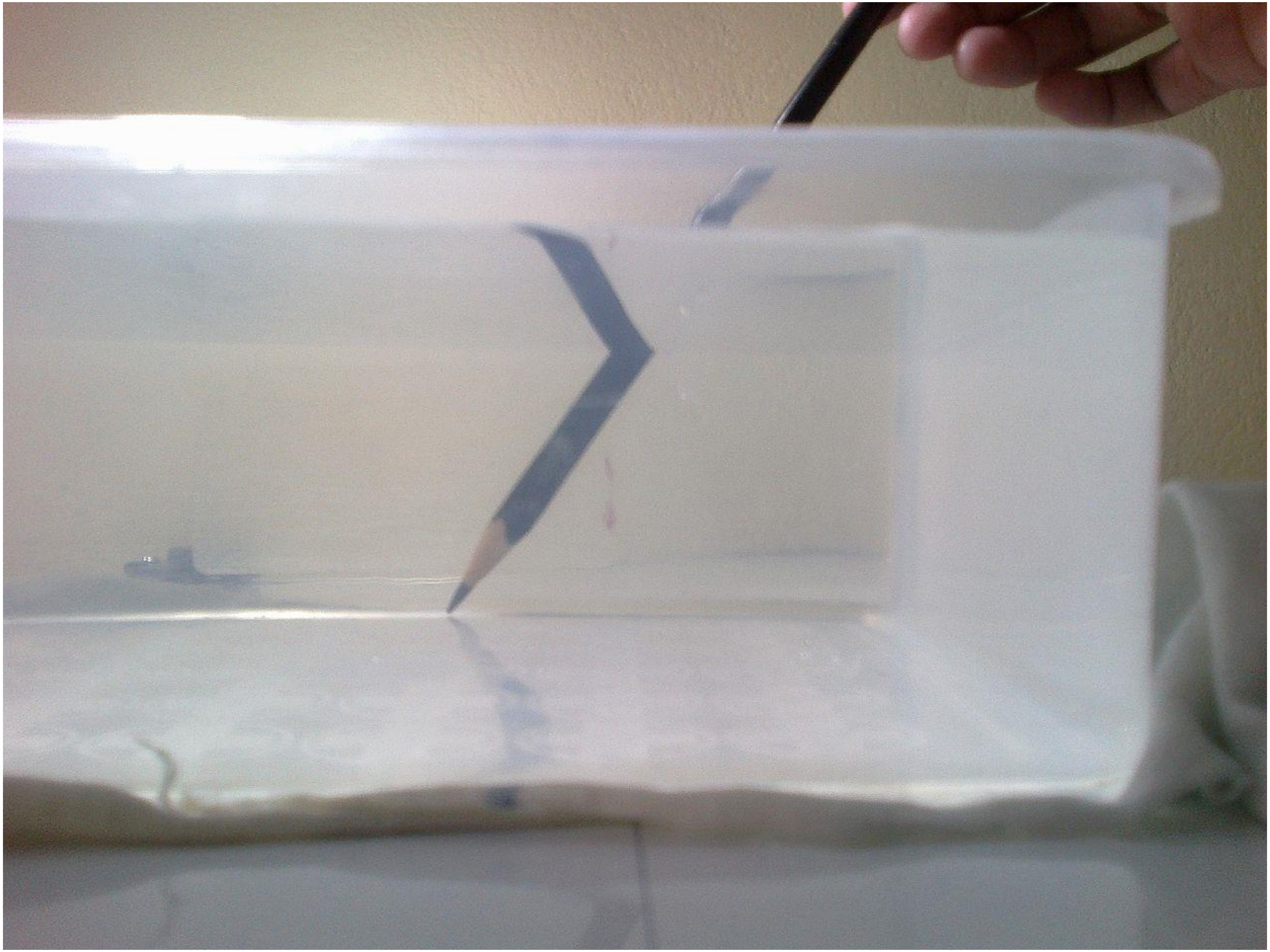

http://upload.wikimedia.org/wikipedia/commons/thumb/3/36/Mirror_like_effect.jpg/1280px-Mirror_like_effect.jpg

Inhomogeneous Medium — Fresnel´s Formula Derived

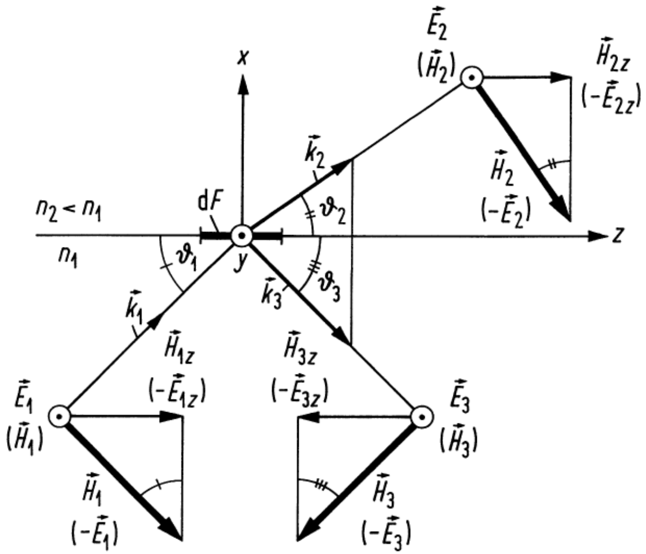

$$k_{1y} = k_{2y} = k_{3y} = 0,$$
$$k_{1z} = k_{2z} = k_{3z}\,;$$

E-polarization:

$$E_{2y} = E_{1y} + E_{3y},$$
$$H_{2z} = H_{1z} + H_{3z},$$
$$|H_{sz}| = H_s \sin\vartheta_s, \qquad (H_{3z} < 0),$$
$$Z_s = E_{sy}/H_{sz} = \frac{Z_0}{n_s} k_s/k_{sx},$$
$$Y_s = -H_{sy}/E_{sz} = \frac{n_s}{Z_0} k_s/k_{sx}.$$

Amplitude reflection coefficient r_E in E-polarization:

$$r_E = \frac{E_3}{E_1} = \frac{E_{3y}}{E_{1y}} = \frac{E_{2y}}{E_{1y}} - 1$$
$$\frac{E_{2y}}{E_{1y}} = \frac{Z_2}{Z_1}\frac{H_{2z}}{H_{1z}}$$
$$\frac{H_{2z}}{H_{1z}} = 1 + \frac{H_{3z}}{H_{1z}}$$
$$\frac{H_{3z}}{H_{1z}} = \frac{-E_{3y}}{Z_1 H_{1z}} = \frac{-E_{3y}}{E_{1y}}$$

$$r_E = \frac{E_3}{E_1} = \frac{E_{3y}}{E_{1y}} = \frac{Z_2}{Z_1}\left(1 - \frac{E_{3y}}{E_{1y}}\right) - 1 \;\Rightarrow\; \frac{E_{3y}}{E_{1y}}\left(\frac{Z_2}{Z_1} + 1\right) = \frac{Z_2}{Z_1} - 1 \;\Rightarrow\; r_E = \frac{Z_2 - Z_1}{Z_2 + Z_1}$$

Inhomogeneous Medium — Below and at the TIR Angle

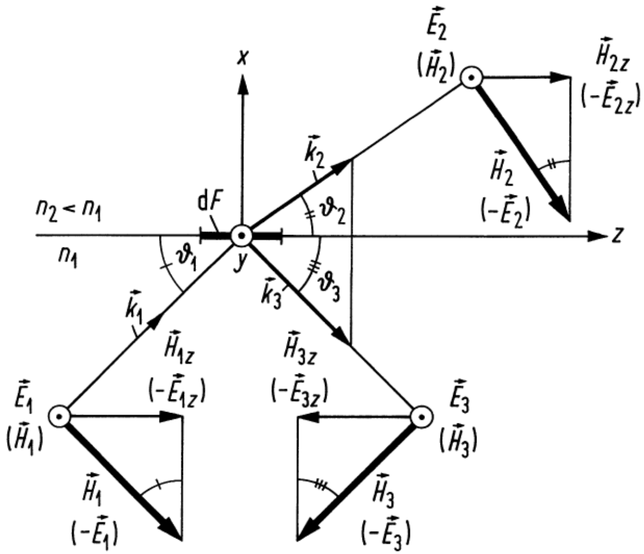

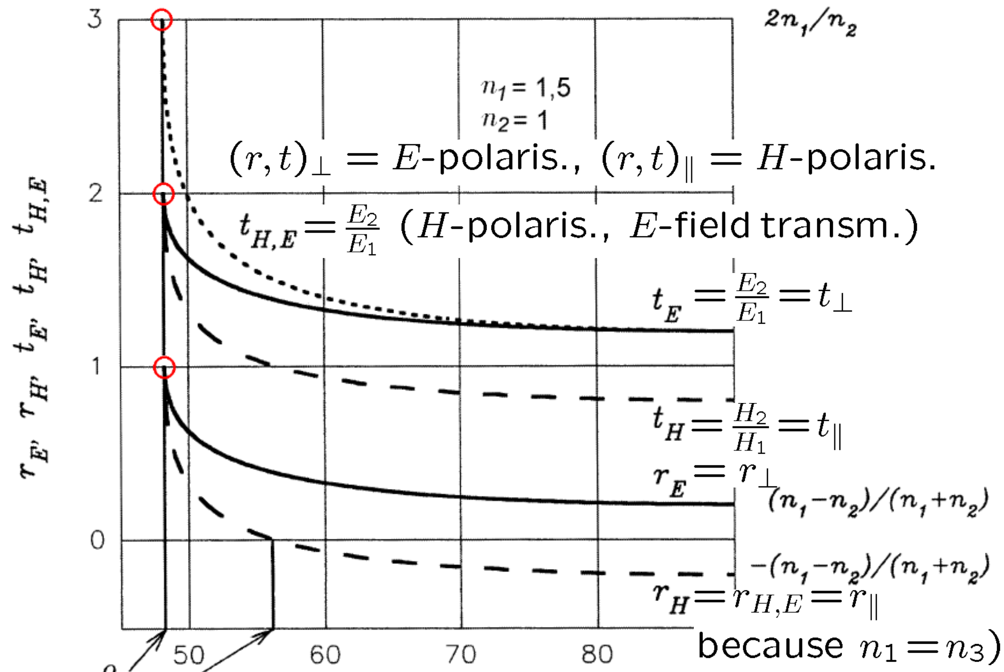

Always $\vartheta_1 > \vartheta_2$ if $n_2 < n_1$.

At $\vartheta_1 = \vartheta_{1T} \rightarrow \vartheta_2 = 0$.

incident angle ϑ_1 in degree

Fresnel's formulae:

Brewster: $\vartheta_{1B} + \vartheta_{2B} = \pi/2$

Fig. 2.6. Amplitude reflection and transmission coefficients as a function of incident angle ϑ_1 for $n_1 = 1.5$, $n_2 = 1$. (glass-air interface). Einfallswinkel ϑ_1 in Grad = incident angle ϑ_1 in degree

$$r_E = \frac{E_3}{E_1} = \frac{Z_2 - Z_1}{Z_2 + Z_1} = \frac{k_{1x} - k_{2x}}{k_{1x} + k_{2x}} = \frac{n_1 \sin\vartheta_1 - n_2 \sin\vartheta_2}{n_1 \sin\vartheta_1 + n_2 \sin\vartheta_2},$$

$$r_H = \frac{H_3}{H_1} = \frac{Y_2 - Y_1}{Y_2 + Y_1} = \frac{n_2^2 k_{1x} - n_1^2 k_{2x}}{n_2^2 k_{1x} + n_1^2 k_{2x}} = \frac{n_2 \sin\vartheta_1 - n_1 \sin\vartheta_2}{n_2 \sin\vartheta_1 + n_1 \sin\vartheta_2}$$

The Different Signs of r_E and r_H — Perpendicular Incidence, $k_z = 0$

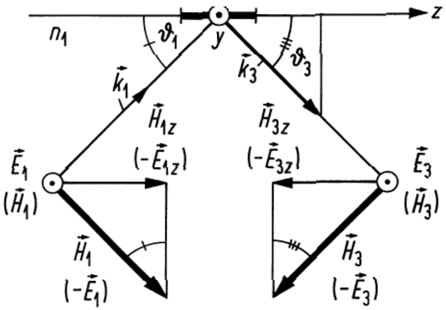

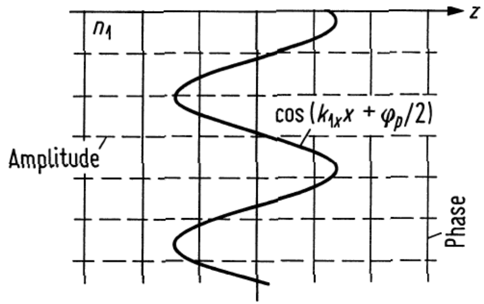

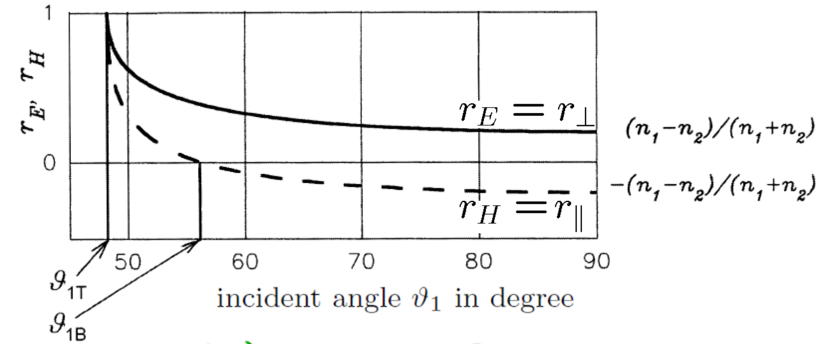

Incident (upwards) and reflected (downwards) waves form standing wave. Reflection coefficients $-r_E = r_H$, $|r_E| = r_H = r_\parallel = 1$, $\varphi_p = \pi$ for "short circuit" $n_1 \ll n_2$, i. e., E ($\widehat{=}$ voltage) is zero, H ($\widehat{=}$ current) doubles at $x = 0$). TE and TM waves indiscriminate. No energy transport along x-direction, E and H out of phase by $\pi/2$:

TE wave: $$E_{1y}(t, \vec{r}\,) = E_{1y}\,\mathrm{e}^{\mathrm{j}\,\omega t}\left(\underbrace{\mathrm{e}^{-\mathrm{j}\,k_{1x}x} - \mathrm{e}^{+\mathrm{j}\,k_{1x}x}}_{=-\mathrm{j}\,2\sin(k_{1x}x)}\right)$$

Impedance Z $(x \leq 0)$:

$$\frac{E_{1y}(t, \vec{r}\,)}{H_{1z}(t, \vec{r}\,)} = -\mathrm{j}\,\frac{Z_0}{n_1}\tan(k_{1x}x) \qquad H_{1z}(t, \vec{r}\,) = H_{1z}\,\mathrm{e}^{\mathrm{j}\,\omega t}\left(\underbrace{\mathrm{e}^{-\mathrm{j}\,k_{1x}x} + \mathrm{e}^{+\mathrm{j}\,k_{1x}x}}_{=2\cos(k_{1x}x)}\right),$$

identical to TM wave: $$H_{1y}(t, \vec{r}\,) = H_{1y}\,\mathrm{e}^{\mathrm{j}\,\omega t}\left(\underbrace{\mathrm{e}^{-\mathrm{j}\,k_{1x}x} + \mathrm{e}^{+\mathrm{j}\,k_{1x}x}}_{=2\cos(k_{1x}x)}\right)$$

http://upload.wikimedia.org/wikipedia/commons/7/7d/Standing_wave_2.gif

The Different Signs of r_E and r_H — Perpendicular Incidence, $k_z\!=\!0$

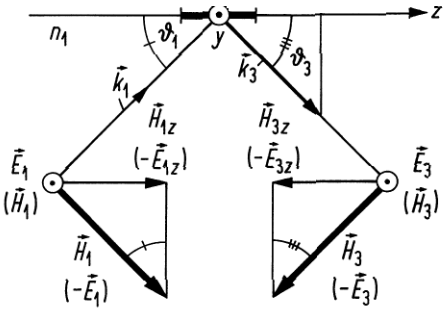

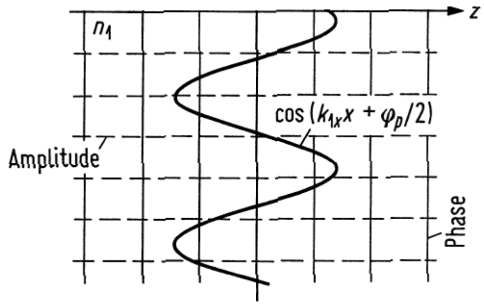

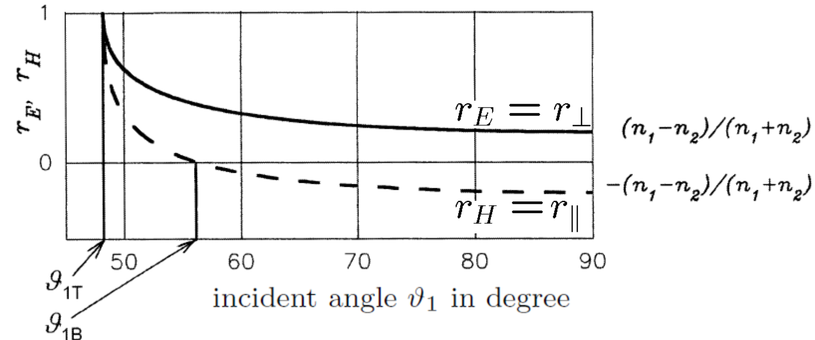

Incident (upwards) and reflected (downwards) waves form standing wave. Reflection coefficients $r_E = -r_H$, $r_E = |r_H| = r_\perp = 1$, $\varphi_p = 0$ for "open circuit" $n_1 \gg n_2$, i. e., E ($\widehat{=}$ voltage) doubles, H ($\widehat{=}$ current) is zero at $x = 0$). TE and TM waves indiscriminate. No energy transport along x-direction, E and H out of phase by $\pi/2$:

$$\text{TE wave:}\quad E_{1y}(t,\vec{r}\,) = E_{1y}\,\mathrm{e}^{\mathrm{j}\,\omega t}\Big(\underbrace{\mathrm{e}^{-\mathrm{j}\,k_{1x}x} + \mathrm{e}^{+\mathrm{j}\,k_{1x}x}}_{=2\cos(k_{1x}x)}\Big)$$

Impedance $Z\,(x \le 0)$:

$$\frac{E_{1y}(t,\vec{r}\,)}{H_{1z}(t,\vec{r}\,)} = \mathrm{j}\,\frac{Z_0}{n_1}\cot(k_{1x}x) \qquad H_{1z}(t,\vec{r}\,) = H_{1z}\,\mathrm{e}^{\mathrm{j}\,\omega t}\Big(\underbrace{\mathrm{e}^{-\mathrm{j}\,k_{1x}x} - \mathrm{e}^{+\mathrm{j}\,k_{1x}x}}_{=-\mathrm{j}\,2\sin(k_{1x}x)}\Big),$$

$$\text{identical to TM wave:}\quad H_{1y}(t,\vec{r}\,) = H_{1y}\,\mathrm{e}^{\mathrm{j}\,\omega t}\Big(\underbrace{\mathrm{e}^{-\mathrm{j}\,k_{1x}x} - \mathrm{e}^{+\mathrm{j}\,k_{1x}x}}_{=-\mathrm{j}\,2\sin(k_{1x}x)}\Big)$$

http://www.youtube.com/watch?feature=player_detailpage&v=kJn_a9flKGk

Inhomogeneous Medium — Below and at the TIR Angle

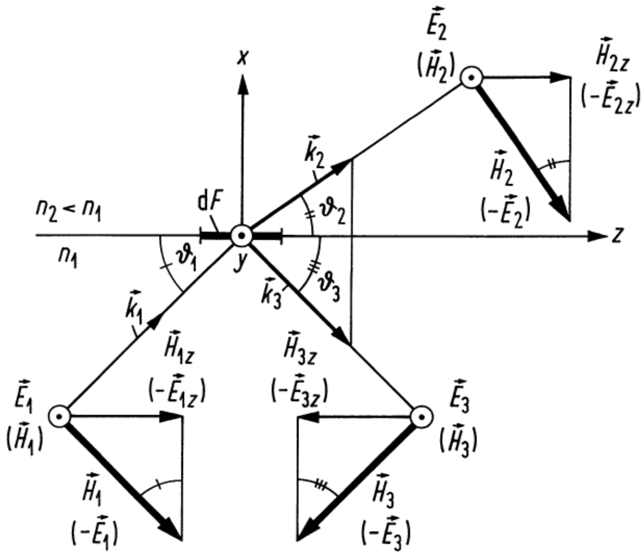

Always $\vartheta_1 > \vartheta_2$ if $n_2 < n_1$.

At $\vartheta_1 = \vartheta_{1T} \rightarrow \vartheta_2 = 0$.

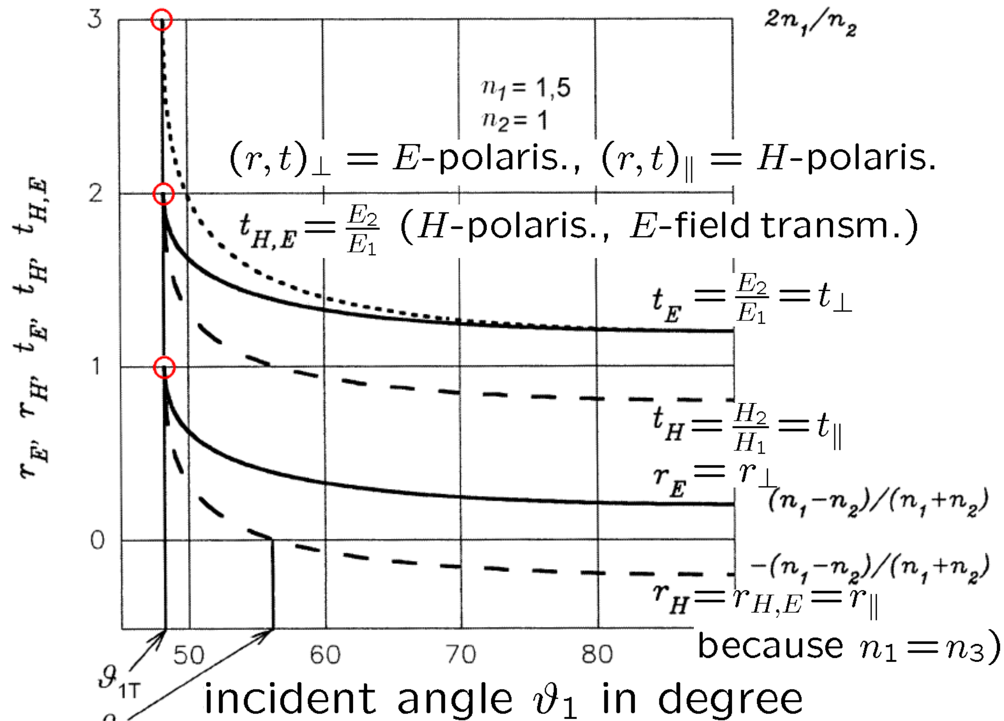

Fresnel's formulae:

Brewster: $\vartheta_{1B} + \vartheta_{2B} = \pi/2$

Fig. 2.6. Amplitude reflection and transmission coefficients as a function of incident angle ϑ_1 for $n_1 = 1.5$, $n_2 = 1$. (glass-air interface). Einfallswinkel ϑ_1 in Grad = incident angle ϑ_1 in degree

$$r_E = \frac{E_3}{E_1} = \frac{Z_2 - Z_1}{Z_2 + Z_1} = \frac{k_{1x} - k_{2x}}{k_{1x} + k_{2x}} = \frac{n_1 \sin\vartheta_1 - n_2 \sin\vartheta_2}{n_1 \sin\vartheta_1 + n_2 \sin\vartheta_2},$$

$$r_H = \frac{H_3}{H_1} = \frac{Y_2 - Y_1}{Y_2 + Y_1} = \frac{n_2^2 k_{1x} - n_1^2 k_{2x}}{n_2^2 k_{1x} + n_1^2 k_{2x}} = \frac{n_2 \sin\vartheta_1 - n_1 \sin\vartheta_2}{n_2 \sin\vartheta_1 + n_1 \sin\vartheta_2}$$

Inhomogeneous Medium — Below and at the TIR Angle

For TIR $\vartheta_1 \leq \vartheta_{1T}$, $k_{2z} > k_2 \rightarrow k_{2x}$ negative imaginary $\rightarrow$ spatial contraction of $\Psi_{2q}(t, \vec{r}\,) = E_{2q}, H_{2q}$,

$$k_{2x} = -\sqrt{k_2^2 - k_{2z}^2} = -\mathrm{j}\, k_0 \sqrt{n_1^2 \cos^2\vartheta_1 - n_2^2} = -\mathrm{j}\, |k_{2x}^{(i)}|\,,$$

$$\Psi_{2q}(t, \vec{r}\,) = \Psi_{2q}\, \mathrm{e}^{\mathrm{j}\,\omega t}\, \mathrm{e}^{-\mathrm{j}\, k_{2x} x}\, \mathrm{e}^{-\mathrm{j}\, k_{2z} z} = \Psi_{2q}\, \mathrm{e}^{-|k_{2x}^{(i)}| x}\, \mathrm{e}^{\mathrm{j}(\omega t - k_{2z} z)}$$

Field evanescent in $+x$-direction, $\vec{k}_2 = -\mathrm{j}\, |k_{2x}^{(i)}|\, \vec{e}_x + k_{1z}\, \vec{e}_z$. For E-polarization:

$$r_E = \frac{k_{1x} - k_{2x}}{k_{1x} + k_{2x}} = \frac{\overbrace{k_{1x} + \mathrm{j}\, |k_{2x}^{(i)}|}^{A \exp\left[\mathrm{j} \arctan\left(|k_{2x}^{(i)}|/k_{1x}\right)\right]}}{\underbrace{k_{1x} - \mathrm{j}\, |k_{2x}^{(i)}|}_{A \exp\left[\mathrm{j} \arctan\left(-|k_{2x}^{(i)}|/k_{1x}\right)\right]}} = \frac{A}{A}\, \mathrm{e}^{\mathrm{j}\, 2 \arctan\left(|k_{2x}^{(i)}|/k_{1x}\right)}$$

$$\varphi_E = 2 \arctan \frac{|k_{2x}^{(i)}|}{k_{1x}}\,, \qquad \varphi_H = 2 \arctan \frac{n_1^2 |k_{2x}^{(i)}|}{n_2^2 k_{1x}}$$

Inhomogeneous Medium — TIR Summary

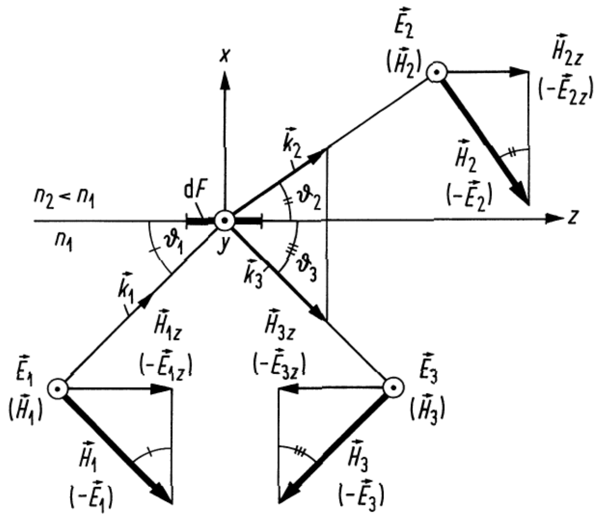

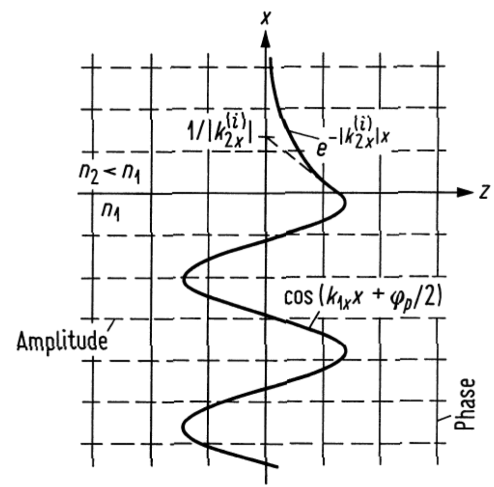

Incident & reflected waves form standing wave (φ_E of r_E ignored):

$$\Psi_{1q}(t,\vec{r}) = \Psi_{1q}\,\mathrm{e}^{\mathrm{j}\,\omega t}\left(\underbrace{\mathrm{e}^{-\mathrm{j}\,k_{1x}x} + \mathrm{e}^{+\mathrm{j}\,k_{1x}x}}_{=2\cos(k_{1x}x)}\right)\mathrm{e}^{-\mathrm{j}\,k_{1z}z}$$

In cladding decay as $\exp(-|k_{2x}^{(i)}|x)$. Power reflection factors:

$$\tfrac{1}{2}n_2|E_2|^2\,\mathrm{d}F\sin\vartheta_2 = \tfrac{1}{2}n_1|E_1|^2\,\mathrm{d}F\sin\vartheta_1 - \tfrac{1}{2}n_1|E_3|^2\,\mathrm{d}F\sin\vartheta_1\,,$$

$$\frac{\tfrac{1}{2}n_2|E_2|^2\,\mathrm{d}F\sin\vartheta_2}{\tfrac{1}{2}n_1|E_1|^2\,\mathrm{d}F\sin\vartheta_1} = T_p = 1 - R_p, \qquad R_p = |r_p|^2, \qquad p = E, H$$

$\perp$ glass-air: $R_E = R_H = 4\,\%$; $\perp$ GaAs-air: $R_E = R_H = 32\,\%$

Waveguiding — Requirements

Waveguiding achieved by surrounding a core along z-axis with lower density cladding, i. e., refractive index decreases away from axis, core-cladding or graded-index waveguide.

Light waveguides made from transparent dielectrics like glass or semiconductors based on Si, GaAs or InP. Symmetric slabs and strips particularly important: Simple models for waveguiding in, e. g., semiconductor lasers (laser diodes).

All essential light waveguide properties studied at little mathematical cost. Physical insight can then be transferred to more complex waveguiding structures.

play

Slab Waveguide — Eigenfields

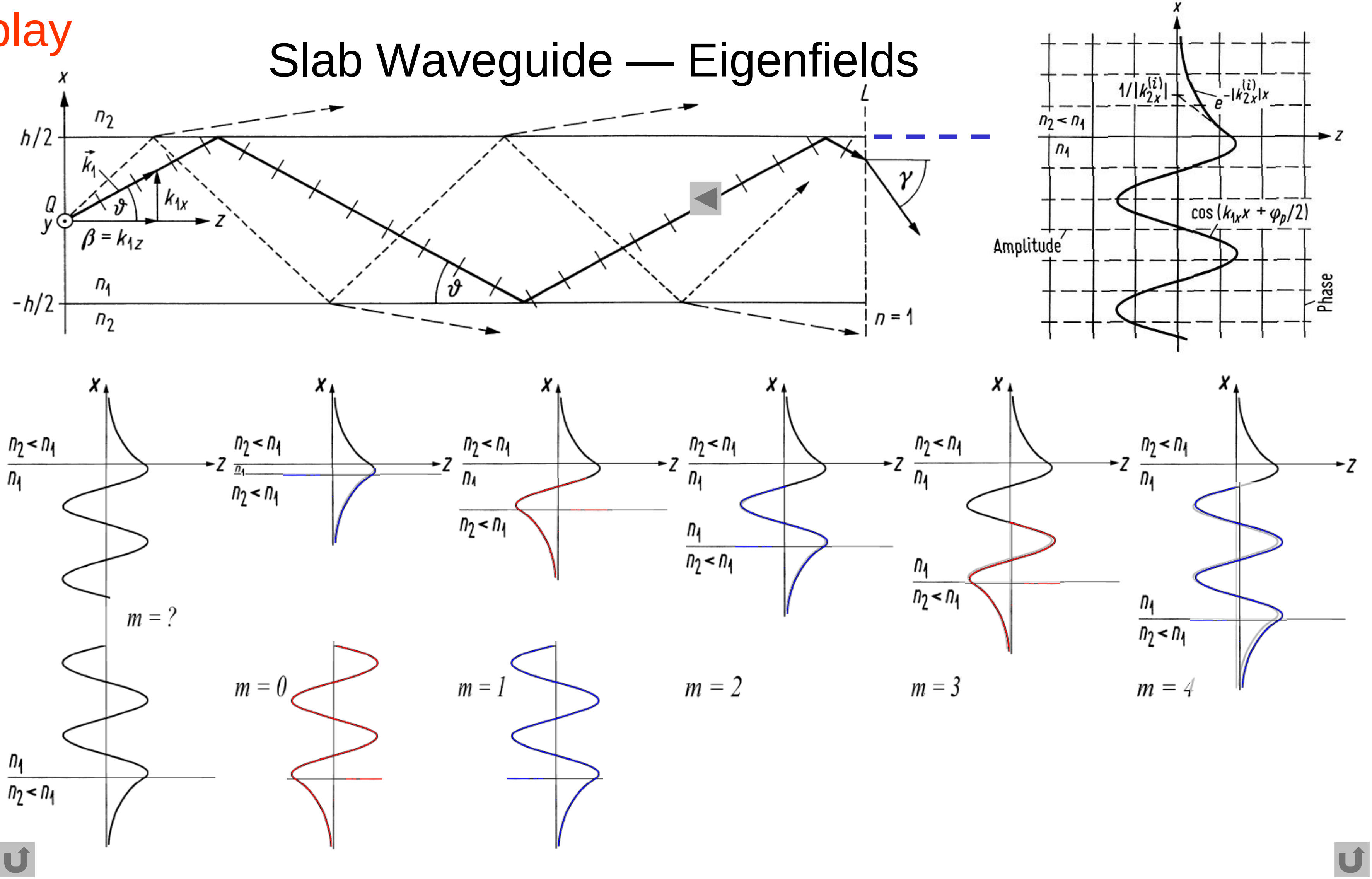

Fig. 2.8. Modes in a slab waveguide according to the results of Fig. 2.5(b). The upper boundary (UB) remains spatially fixed. The lower boundary (LB) is shifted to a distance $x_{\mathrm{UB}} - x_{\mathrm{LB}} = h$ such that the standing waves originating from the reflections at the UB and LB are in phase. From left to right: UB and LB at arbitrary distance, no phase match ($m = ?$). LB at minimum distance (fundamental mode $m = 0$). LB moved to the next possible phase match positions ($m = 1, 2, 3, 4, \ldots$)

Slab Waveguide — Num. Aperture and Propag. Constant

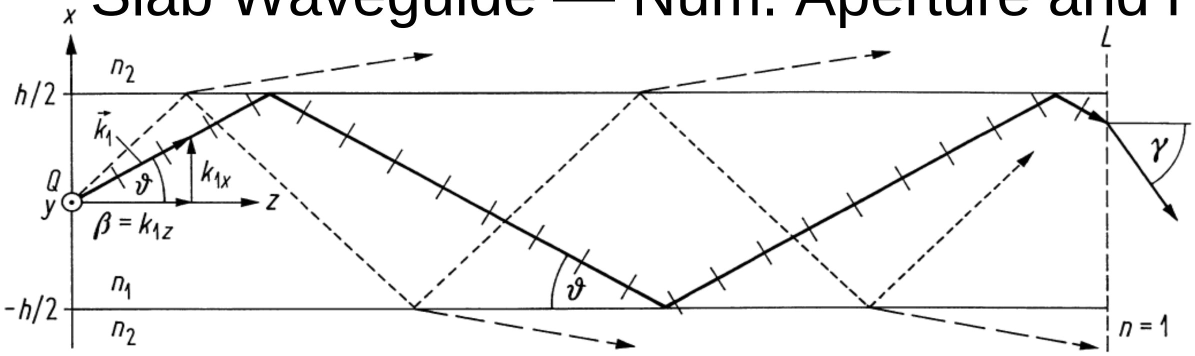

Fig. 2.7. Slab waveguide. Guided (——) and radiated waves (– – –)

Angle γ_N defines light-shadow boundary in far-field, may be measured outside and is preferred to ϑ_T. With Snell's law:

$$\sin\gamma_N = n_1 \sin\vartheta_T = \sqrt{n_1^2 - n_2^2},$$

$$A_N = \sqrt{n_1^2 - n_2^2} = n_1\sqrt{2\Delta}, \qquad \Delta = \frac{n_1^2 - n_2^2}{2n_1^2} \approx \{n_1 \approx n_2\} \approx \frac{n_1 - n_2}{n_1}$$

Propag. const. (phase veloc. $\frac{\omega}{\beta} > \frac{c}{n_1}$ larger than speed of light in core!)

$$\beta = k_{1z} = k_1 \cos\vartheta = k_{2z} \;\; (k_2 < \beta < k_1), \qquad n_e = \frac{\beta}{k_0} \;\; (n_2 < n_e < n_1),$$

$$k_{1x} = k_1 \sin\vartheta = \sqrt{k_1^2 - \beta^2}, \qquad\qquad k_{2x} = \pm\mathrm{j}\sqrt{\beta^2 - k_2^2}$$

Slab Waveguide — Notation and Eigenvalue Condition

Transverse core phase constant (core parameter "transversales Phasenmaß") u, transverse cladding attenuation (cladding parameter "transversales Dämpfungsmaß") w, normalized frequency (waveguide parameter) V, relative refractive index difference Δ, normalized propagation constants B, δ,

$$u = k_{1x}\frac{h}{2} = \frac{h}{2}\sqrt{k_1^2 - \beta^2}, \qquad w = |k_{2x}|\frac{h}{2} = \frac{h}{2}\sqrt{\beta^2 - k_2^2},$$

$$V = \frac{h}{2}k_0 A_N = \sqrt{u^2 + w^2}, \qquad \Delta = \frac{n_1^2 - n_2^2}{2n_1^2} \approx \{n_1 \approx n_2\} \approx \frac{n_1 - n_2}{n_1},$$

$$B = \frac{\beta^2 - k_2^2}{k_1^2 - k_2^2} = \frac{w^2}{V^2} = 1 - \frac{u^2}{V^2} = 1 - \frac{\delta}{\Delta} \approx \{\Delta \ll 1\} \approx \frac{\beta - k_2}{k_1 - k_2}.$$

Not all β allowed for guided waves $k_2 < \beta < k_1$. Transversely consistent field at boundary planes $x = \pm h/2$: Matching standing waves from top and bottom:

$$\cos(k_{1x}x) = \cos\left(\frac{2u}{h}x\right), \qquad \sin(k_{1x}x) = \sin\left(\frac{2u}{h}x\right)$$

Slab Waveguide — Matching the Fields

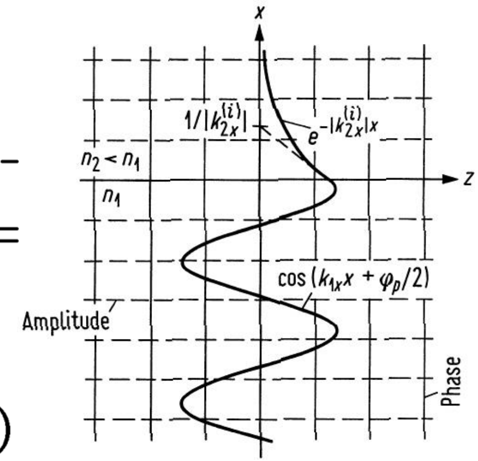

Incident (amplitude $\Psi_{1q} e^{-j k_{1x} x} e^{-j k_{1z} z}$) and reflected wave (amplitude $\Psi_{1q} r_p e^{+j k_{1x} x} e^{-j k_{1z} z} = \Psi_{1q} e^{j \varphi_p} e^{+j k_{1x} x} e^{-j k_{1z} z}$) superimposed:

$$e^{-j k_{1x} x} + e^{j \varphi_p} e^{j k_{1x} x} = e^{j \varphi_p/2}\, 2 \cos(k_{1x} x + \varphi_p/2)$$

Coordinate shift from boundary to WG centre, $x' = x + h/2$:

$$\cos[k_{1x} x + \varphi_p/2] = \cos\left[k_{1x}\left(x' - h/2\right) + \varphi_p/2\right]$$

For a consistent mode which does not change its field when propagating along z, $x' = 0$ <u>must</u> be a symmetry plane:

$$\cos\left[k_{1x}\left(x' - h/2\right) + \varphi_p/2\right] = \pm\cos\left[k_{1x}\left(-x' - h/2\right) + \varphi_p/2\right]$$

Symmetric (extremum, cos) and antisymmetric modes (node, sin):

$$\cos(-k_{1x} h/2 + \varphi_p/2) = \pm 1\,, \qquad \cos(-k_{1x} h/2 + \varphi_p/2) = 0$$

Slab Waveguide — Eigenvalue Equation

Symmetric and antisymmetric modes:

$$\cos\left(-k_{1x}h/2+\varphi_p/2\right)=\pm 1\,,\qquad \cos\left(-k_{1x}h/2+\varphi_p/2\right)=0$$

Transverse phase difference after two total internal reflections:

$$-k_{1x}\frac{h}{2}+\frac{\varphi_p}{2}=-m\frac{\pi}{2},\quad -2k_{1x}h+2\varphi_p=-2m\pi\,,\quad -u+\frac{\varphi_p}{2}=-m\frac{\pi}{2},$$

$$\varphi_p=2\arctan\left(\sigma_p\frac{|k_{2x}^{(i)}|}{k_{1x}}\right),$$

$$u=\frac{\varphi_p}{2}+m\frac{\pi}{2}=\arctan\left(\sigma_p\frac{w}{u}\right)+m\frac{\pi}{2},$$

$$\tan\left(u-m\tfrac{\pi}{2}\right)=\sigma_p\frac{w}{u}$$

For even and odd TE- and TM-waves, we find the result:

$$\sigma_p w_{pm}=\sigma_p\sqrt{V^2-u_{pm}^2}=\begin{cases} u_{pm}\tan u_{pm} & m=0,2,4,\dots \\ -u_{pm}\cot u_{pm} & m=1,3,5,\dots \end{cases}$$

TE-wave (H-wave): $p=E,\qquad \sigma_E=1$

TM-wave (E-wave): $p=H,\qquad \sigma_H=n_1^2/n_2^2$

LECTURE 6

Slab Waveguide — Eigenvalues

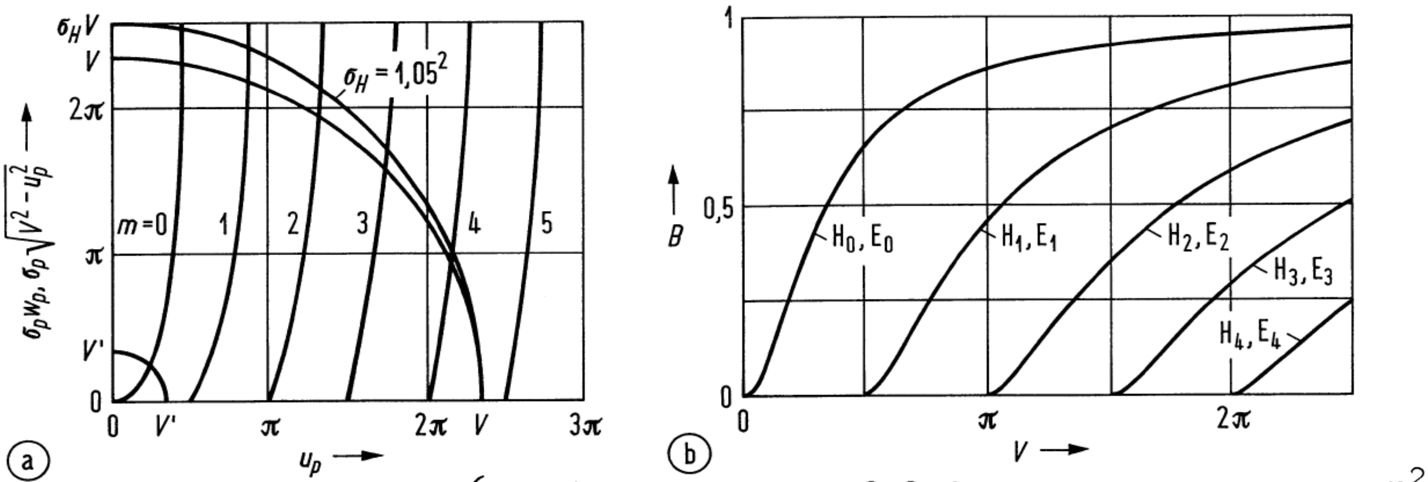

$\sigma_E = 1\,,$
$\sigma_H = n_1^2/n_2^2$

$$\sigma_p w_p = \sigma_p\sqrt{V^2-u_p^2} = \begin{cases} u_p \tan u_p & m = 0,2,4,\ldots \\ -u_p \cot u_p & m = 1,3,5,\ldots \end{cases} \qquad \sigma_E = 1, \qquad \sigma_H = \frac{n_1^2}{n_2^2}$$

Eigenvalues of the propagation constant β or the core parameter u. (a) Graphical solution of the eigenvalue equation for TE-modes (H-waves, $\sigma_E = 1$) and TM-modes (E-waves $\sigma_H = 1.05^2$), $V = 7.33$. $u_E \le u_H$, $\beta_E \ge \beta_H$, $B_E \ge B_H$ (b) Normalized propagation constant for $\boxed{\text{weakly guiding LWG}}$

Characteristic equation (eigenvalue or dispersion equation, mathematical formulation of the graphical procedure above) defines allowed angles ϑ_m or so-called eigenvalues β_m.
Waves $\vec{\Psi}_m(\vec{r}) = \vec{\Psi}_m(x)\exp(-\mathrm{j}\,\beta_m z)$ are eigenwaves or *modes* of waveguide. Fields with other propagation constants cannot propagate, are either evanescent along z, or radiate into cladding.

Slab Waveguide — Synopsis

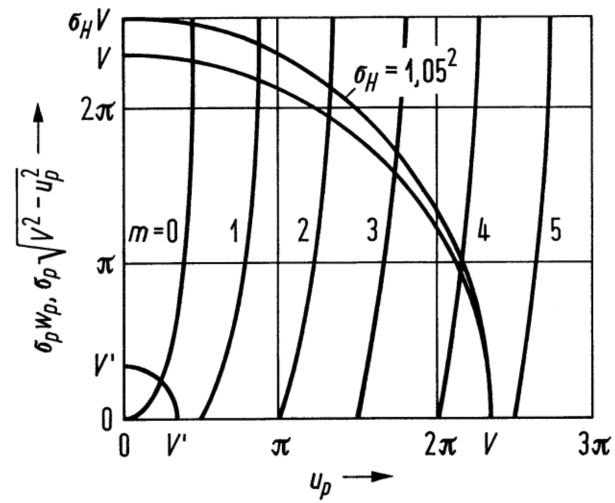

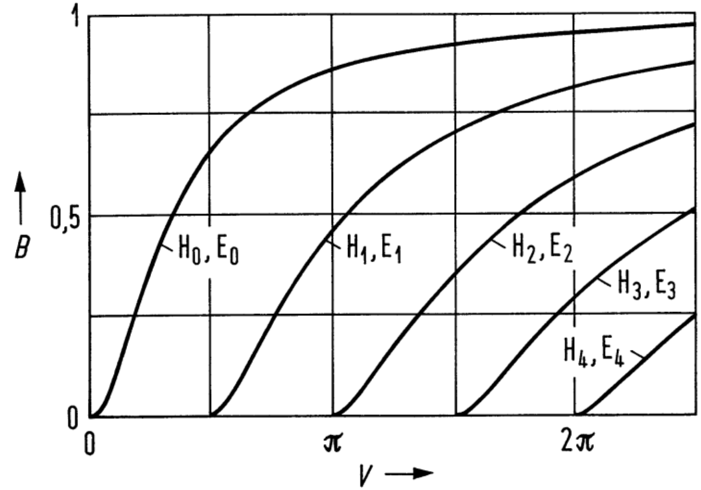

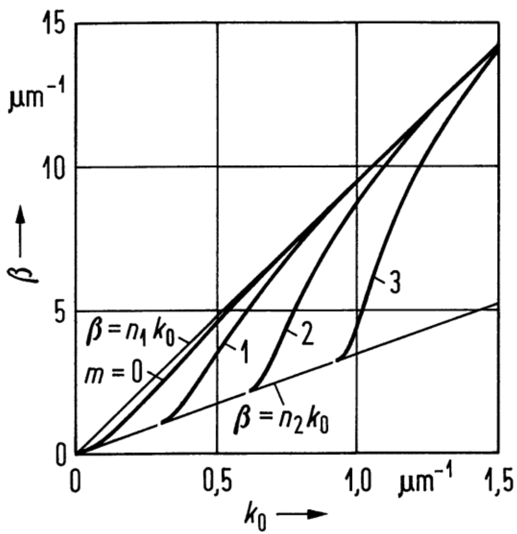

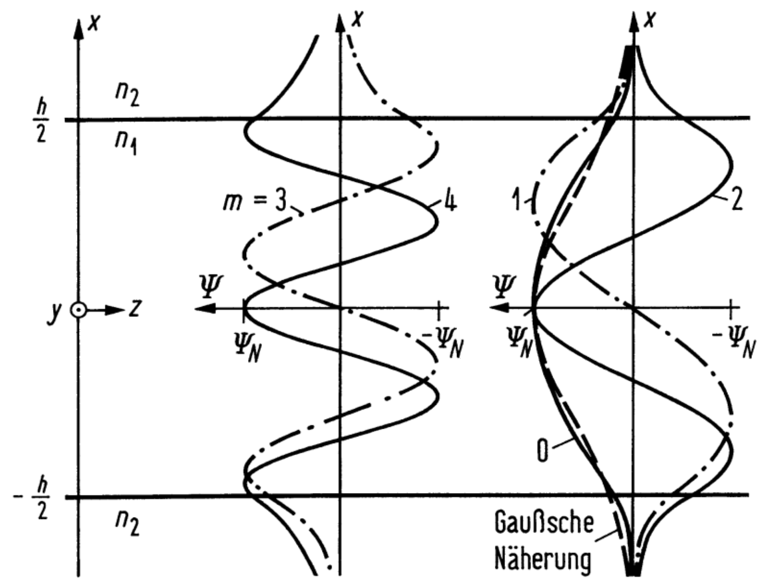

Slab Waveguide — Group Delay Dispersion (1)

Weakly guiding slab, scalar approximation. Group delay t_g after L:

$$t_g/L = \mathrm{d}\beta/\,\mathrm{d}\omega = n_{eg}/c\,, \qquad B \approx \frac{\beta - k_2}{k_1 - k_2}\,, \qquad \beta = k_2 + (k_1 - k_2)\,B\,,$$

$$\frac{t_g}{L} = \frac{\mathrm{d}\beta}{\mathrm{d}\,\omega} = \frac{1}{c}\frac{\mathrm{d}\beta}{\mathrm{d}k_0} \approx \left\{ \begin{array}{l} \qquad \Delta \ll 1 \\ \dfrac{\mathrm{d}V}{\mathrm{d}k_0} \approx \dfrac{V}{k_0}\,, \qquad V = \frac{h}{2} k_0 n_1 \sqrt{2\Delta} \\ n_{1g} - n_{2g} \approx n_1 - n_2 \end{array} \right\} \approx$$

$$\approx \frac{n_{2g}}{c} + \frac{n_{1g} - n_{2g}}{c} B + (k_1 - k_2)\,\frac{\mathrm{d}B}{\mathrm{d}\omega} \approx \frac{n_{2g}}{c} + \frac{n_{1g} - n_{2g}}{c}\left(B + k_0\frac{\mathrm{d}B}{\mathrm{d}k_0}\right)$$

$$\approx \frac{n_{2g}}{c} + \frac{n_{1g} - n_{2g}}{c}\left(B + k_0\frac{\mathrm{d}B}{\mathrm{d}V}\frac{\mathrm{d}V}{\mathrm{d}k_0}\right) \approx \frac{n_{2g}}{c} + \frac{n_{1g} - n_{2g}}{c}\left(B + k_0\frac{\mathrm{d}B}{\mathrm{d}V}\frac{V}{k_0}\right)$$

$$\approx \frac{n_{2g}}{c} + \frac{n_{1g} - n_{2g}}{c}\left(B + V\frac{\mathrm{d}B}{\mathrm{d}V}\right) = \underbrace{\frac{n_{2g}}{c}}_{\text{mat. disp.}} + \underbrace{\frac{n_{1g} - n_{2g}}{c}\,\overbrace{\frac{\mathrm{d}(VB)}{\mathrm{d}V}}^{\text{gr. delay fctr}}}_{\text{waveguide dispersion}}$$

Slab Waveguide — Group Delay Dispersion (2)

Length-related group delay difference $\Delta t_g/L$, two signals in same mode m at optical carriers differing by $\Delta\lambda$:

$$\Delta t_g/L = [t_g(\lambda + \Delta\lambda, m) - t_g(\lambda, m)]\,/L = C\Delta\lambda = (M + W)\Delta\lambda\,,$$

$$M = M_s = \underbrace{\frac{1}{c}\frac{\mathrm{d}n_{sg}}{\mathrm{d}\lambda}}_{\substack{\text{material}\\\text{dispersion}}} \quad (s = 1 \text{ or } 2), \qquad W = -\frac{n_{1g} - n_{2g}}{c\lambda}\, \underbrace{V\,\frac{\mathrm{d}^2(VB)}{\mathrm{d}V^2}}_{\substack{\text{dispersion}\\\text{factor}}}$$

In core (M_1) and cladding ($M_2 \approx M_1$) assumed to be similar.

Chromatic dispersion first-order C (unit ps / (km nm)). Second-order dispersion coefficient D (unit ps / (km nm)^2),

$$\Delta t_g/L = C\,\Delta\lambda + D\,(\Delta\lambda)^2 + \ldots, \qquad C = \frac{1}{L}\frac{\mathrm{d}t_{gm}}{\mathrm{d}\lambda}, \qquad D = \frac{1}{2L}\frac{\mathrm{d}^2 t_{gm}}{\mathrm{d}\lambda^2}$$

$C(\lambda_C) = 0\,,\quad \lambda_C$ is zero of $C(\lambda_C)$ for mode m.

$$\Delta t_g/L = C_\lambda(\lambda)\,\Delta\lambda = (C + D\,\Delta\lambda)\,\Delta\lambda, \qquad D = \frac{\mathrm{d}C_\lambda(\lambda)}{\mathrm{d}\lambda}$$

Dispersion slope: D

Slab Waveguide — Dispersion Types

Intramodal dispersion Group delay dispersion (or group velocity dispersion, GVD) for a fixed mode m. Parameters: Chromatic dispersion coefficient $C = M + W$, material dispersion coefficient M, waveguide dispersion coefficient W, dispersion factor $V\,\mathrm{d}^2(VB)/\,\mathrm{d}V^2$, dispersion slope D.

Intermodal dispersion (or simply modal dispersion) For V fixed, the slopes of $B(V) \mathrel{\widehat{=}} \beta(\omega)$ corresponding to group delay vary between different modes (see zigzag rays ◀). Short impulse at $z = 0$ generates series of impulses at $z = L$. Spread of group delays between different modes m and $m + \Delta m$,

$$\Delta t_g/L = \left[t_g(\lambda, m + \Delta m) - t_g(\lambda, m)\right]/L = G\Delta m$$

G is modal dispersion coefficient. For $\Delta \ll 1$, maximum spread of allowed zig-zag path angles diminished, and so is the modal dispersion.

Slab Waveguide — Bend

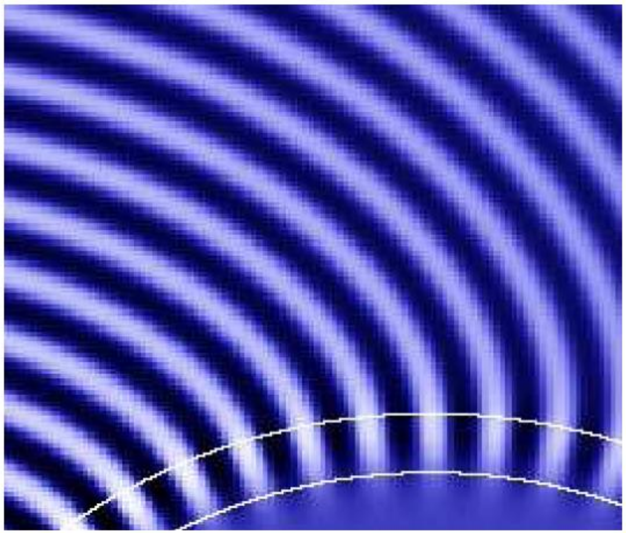

(a) Phase fronts for a bent waveguide

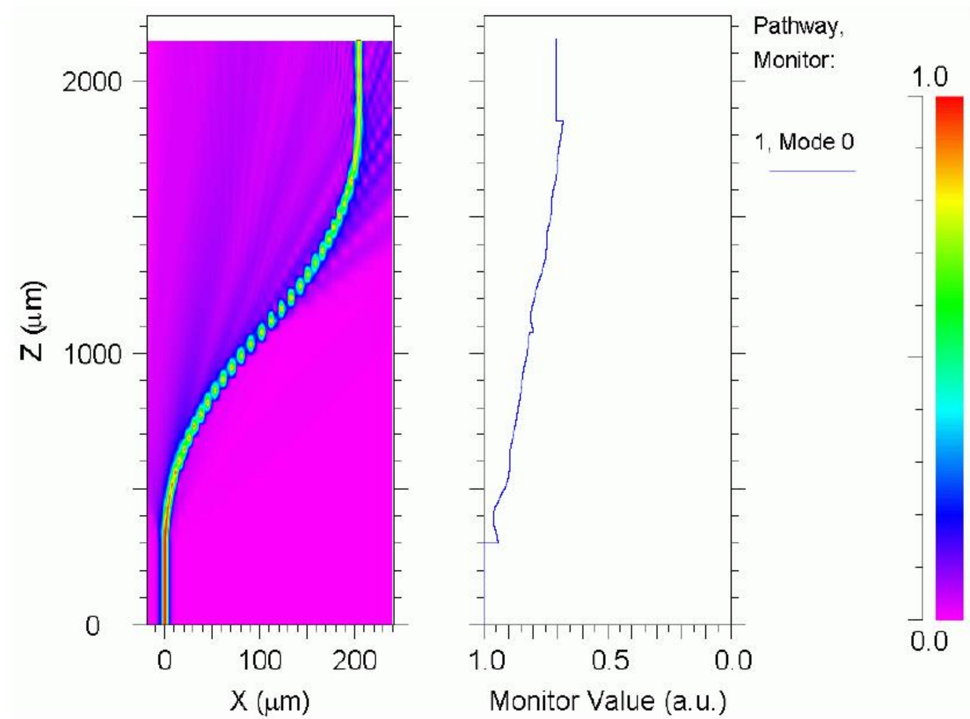

(b) Electric field magnitude and waveguide power for an S-bend

Fig. 2.10. Slab waveguide bends in scalar approximation. (a) Phase surfaces for a circular waveguide bend[20] (b) Waveguide height $h = 5\,\mu$m, initial and ending straight section lengths $300\,\mu$m, bend radii 3 mm, angle of oblique section $15\,°$, refractive index difference $n_1 - n_2 = 0.007$, cladding refractive index $n_2 = 1.5$, vacuum wavelength $\lambda = 1.55\,\mu$m. Excitation of fundamental guided mode $m = 0$ (Fig. 2.8) in straight waveguide at $z = 0$. (left) Contour plot of electric field magnitude with colour scale at rightmost side (right) Total power in waveguide cross-section along the waveguide axis (1, Mode 0, blue)

LECTURE 7

Slab Waveguide — Directional Coupler

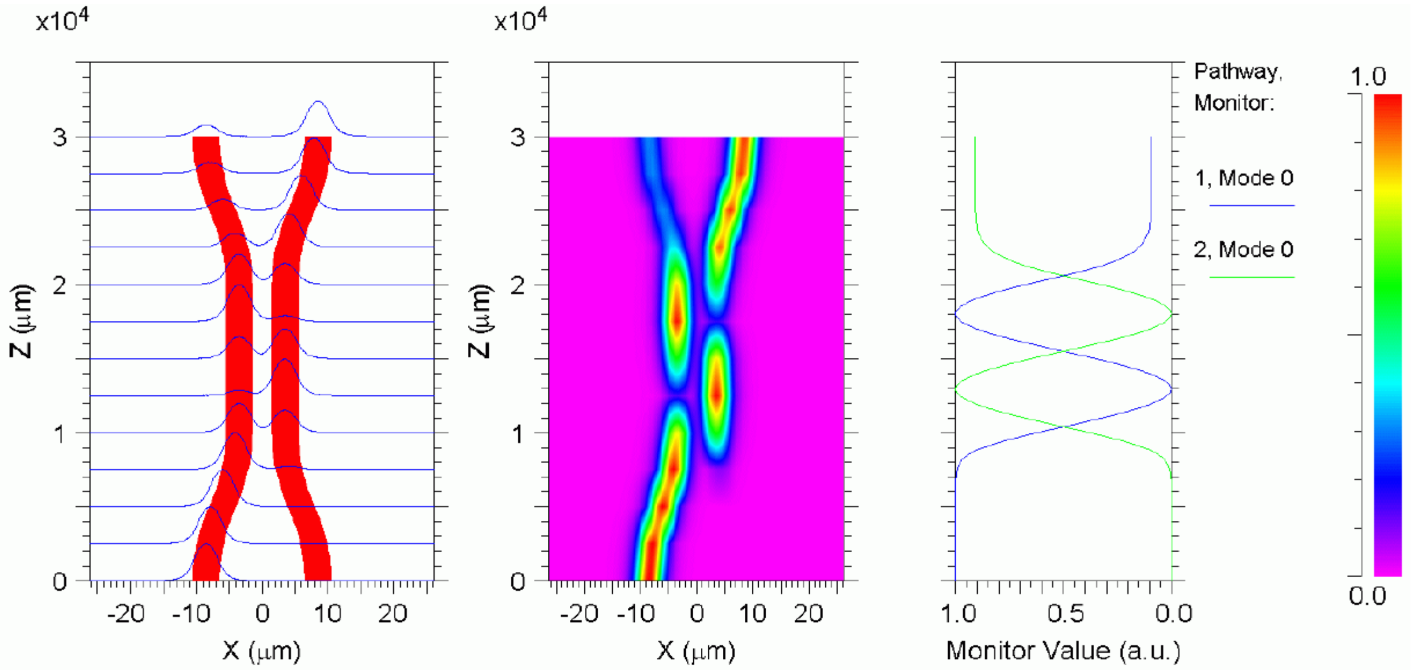

Fig. 2.11. Slab waveguide directional coupler in scalar approximation. Waveguide height $h = 4\,\mu\text{m}$, separation of inner core-cladding boundaries $3\,\mu\text{m}$, refractive index difference $n_1 - n_2 = 0.0067$, cladding refractive index $n_2 = 3.378$, vacuum wavelength $\lambda = 1.3\,\mu\text{m}$. Excitation of fundamental guided mode $m = 0$ (Fig. 2.8) in straight waveguide at lower left coupler input. Mind the vast scale differences for the x- and the z-directions; the curved section is angled only at about $6°$. (left) Slice plot of electric field magnitude (middle) Contour plot of electric field magnitude with colour scale at rightmost side (right) Total power in waveguide cross-sections along the axes of left-hand side waveguide (1, Mode 0, blue) and of right-hand side waveguide (2, Mode 0, green)

Analogy: Double pendulum ($\omega_0 = \sqrt{K/m}$, elong. x, rest. force Kx, mass m)

Java control panel (javacpl.exe): Sicherheit, Hoch (Mindestempfehlung) → Mittel, Anwenden. **Run Java.** Then return to original setting: Mittel → Hoch (Mindestempfehlung), OK

Slab Waveguide — Directional Coupler. Supermodes (1)

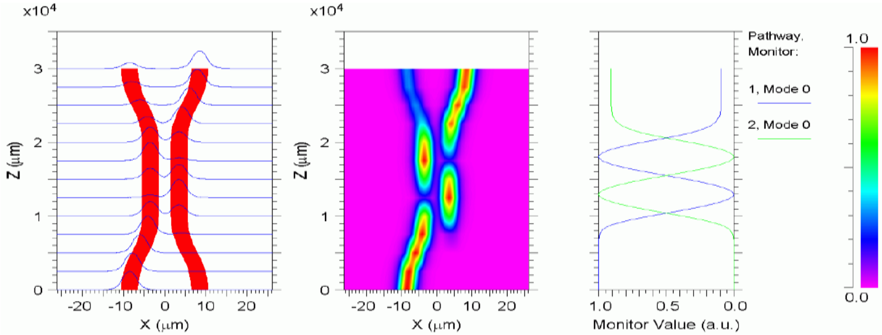

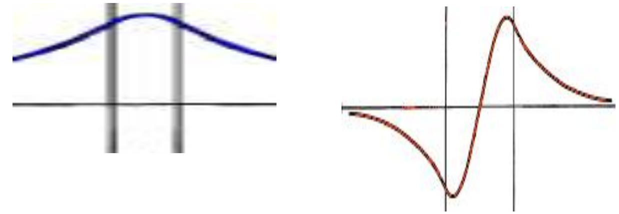

Spatial period symmetric mode: $z_s = \frac{2\pi}{\beta_s} \leq z_a$

Spatial period antisymmetric mode: $z_a = \frac{2\pi}{\beta_a} \geq z_s$

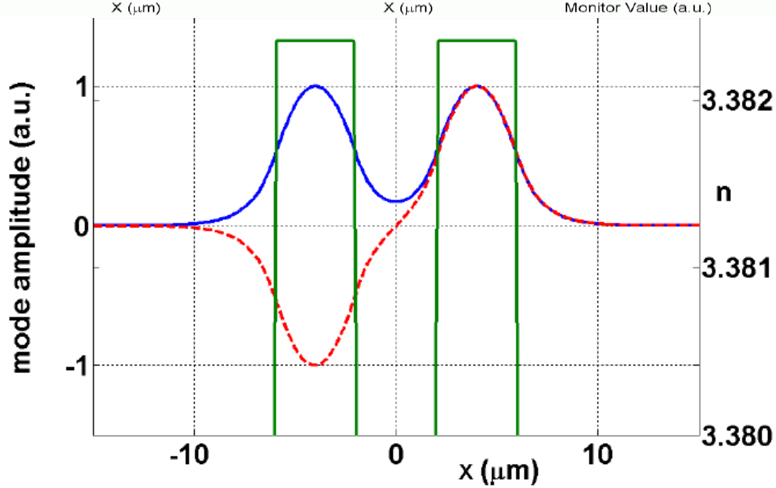

(a) Electric field magnitudes and refractive index

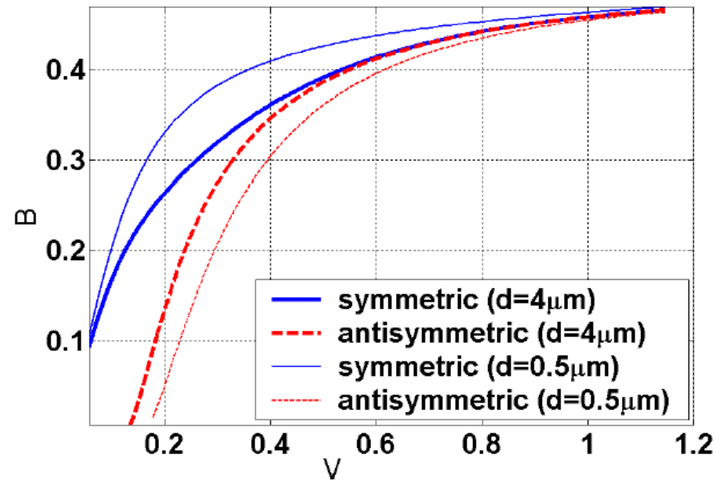

(b) Dispersion diagrams

Fig. 2.12. Directional coupler with two infinitely long parallel slabs. Waveguide height $h = 4\,\mu$m, separation of inner core-cladding boundaries $d = 4\,\mu$m, refractive index difference $n_1 - n_2 = 0.0067$, cladding refractive index $n_2 = 3.378$, vacuum wavelength $\lambda = 1.3\,\mu$m. Fundamental symmetric (blue, ——) and next higher-order antisymmetric supermode (red, – – –) (a) Electric field magnitudes, and refractive index profile $n(x)$ (rectangular shapes, green, right-hand side axis) (b) Dispersion diagrams for wider ($d = 4\,\mu$m, thick lines) and narrower separated waveguides ($d = 0.5\,\mu$m, thin lines). Normalized frequency $V = \frac{h}{2} k_0 (n_1^2 - n_2^2)^{1/2}$

Slab Waveguide — Directional Coupler. Supermodes (2)

Symmetric and antisymmetric mode excited with transverse electric field magnitudes $E_s(x)$ and $E_a(x)$. Superposition:

$$E_-(x,z) = E_s(x)\,\mathrm{e}^{-\mathrm{j}\,\beta_s z} - E_a(x)\,\mathrm{e}^{-\mathrm{j}\,\beta_a z},$$

$$E_+(x,z) = E_s(x)\,\mathrm{e}^{-\mathrm{j}\,\beta_s z} + E_a(x)\,\mathrm{e}^{-\mathrm{j}\,\beta_a z}$$

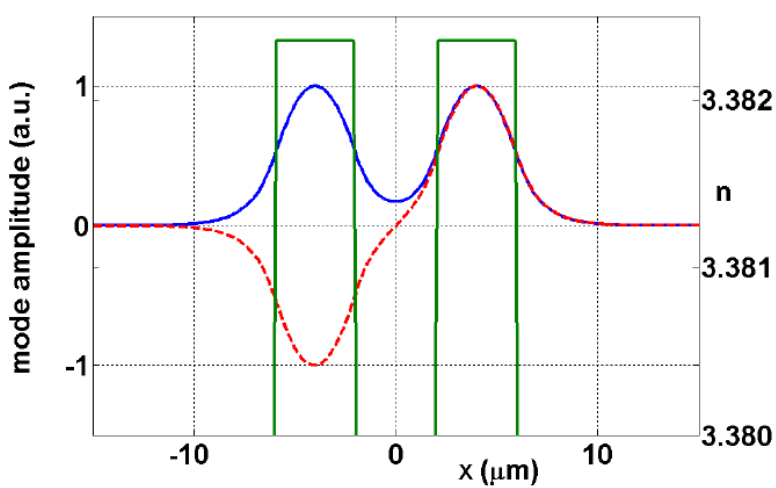

Electric field magnitudes and refractive index

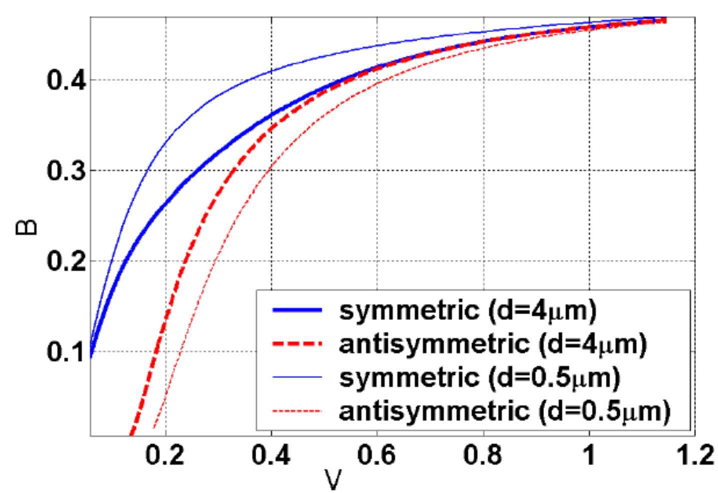

Dispersion diagrams

Slab Waveguide — Directional Coupler. Beat Length (1)

Mode profiles $E_{s,a}(x)$ very similar. Superposition $E_-(x,z)$ concentrates virtually all power in left slab. $E_+(x,z)$ has all power in right slab. Supermodes propagate with different $v_{s,a} = \omega/\beta_{s,a} \rightarrow$ transverse field shapes $E_\mp(x,z)$ change with z. If phase difference 2π, constellation at $z=0$ repeats after beat length ($n_{e\,s,a} = \beta_{s,a}/k_0$):

$$|\beta_s - \beta_a|\,\Lambda = 2\pi\,, \qquad \Lambda = \frac{2\pi}{|\beta_s - \beta_a|} = \frac{\lambda}{|n_{e\,s} - n_{e\,a}|}$$

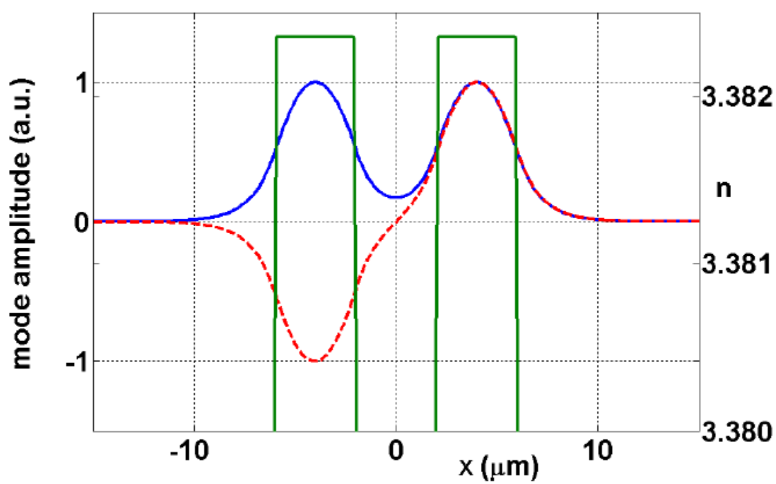

Electric field magnitudes and refractive index

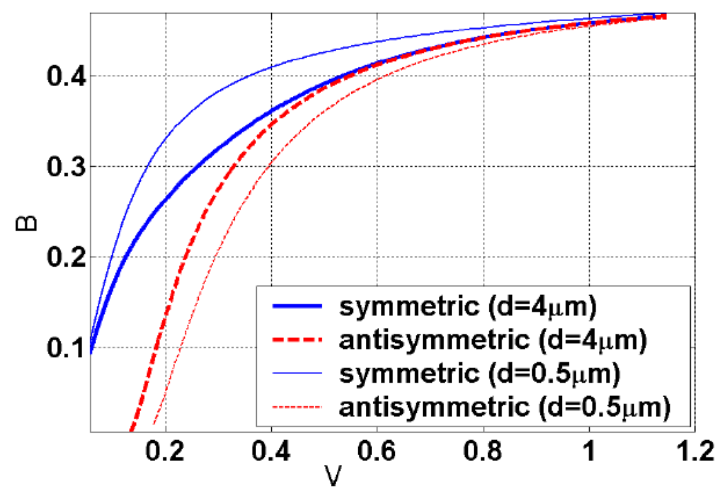

Dispersion diagrams

Slab Waveguide — Directional Coupler. Beat Length (2)

At $z = \Lambda/2$, phase shift is π, superposition $E_{-}(x, z) \leftrightarrow E_{+}(x, z)$. Virtually all power transferred from one waveguide to the other one. The longer Λ, i. e., the longer the interaction between both WG needs to be, the weaker the coupling. Explanation:

If waveguide separation reduced from $h = 4\,\mu$m to $h = 0.5\,\mu$m, propagation constants $\beta_{s,a}$ differ more $\rightarrow \Lambda = 2\pi\,/|\beta_s - \beta_a|$ reduced.

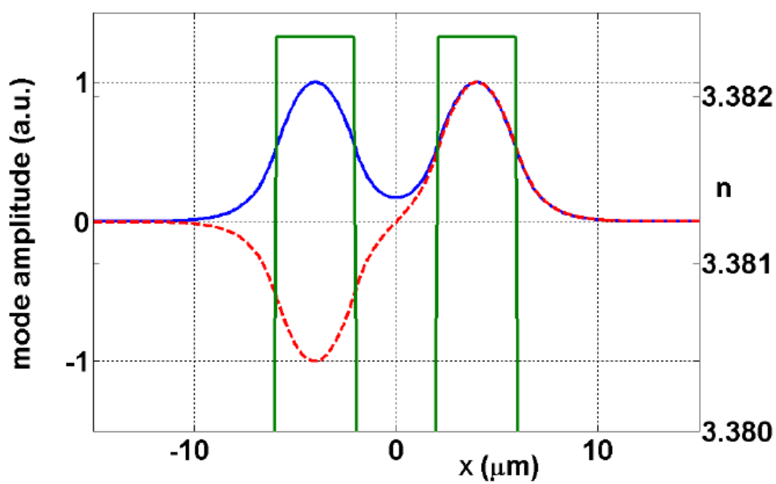

Electric field magnitudes and refractive index

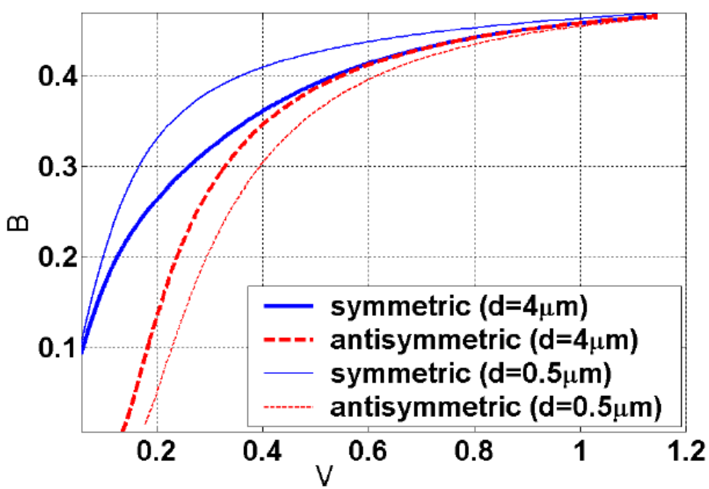

Dispersion diagrams

Directional Coupler — Fused Fibres. 2 × 2 / 4 × 4

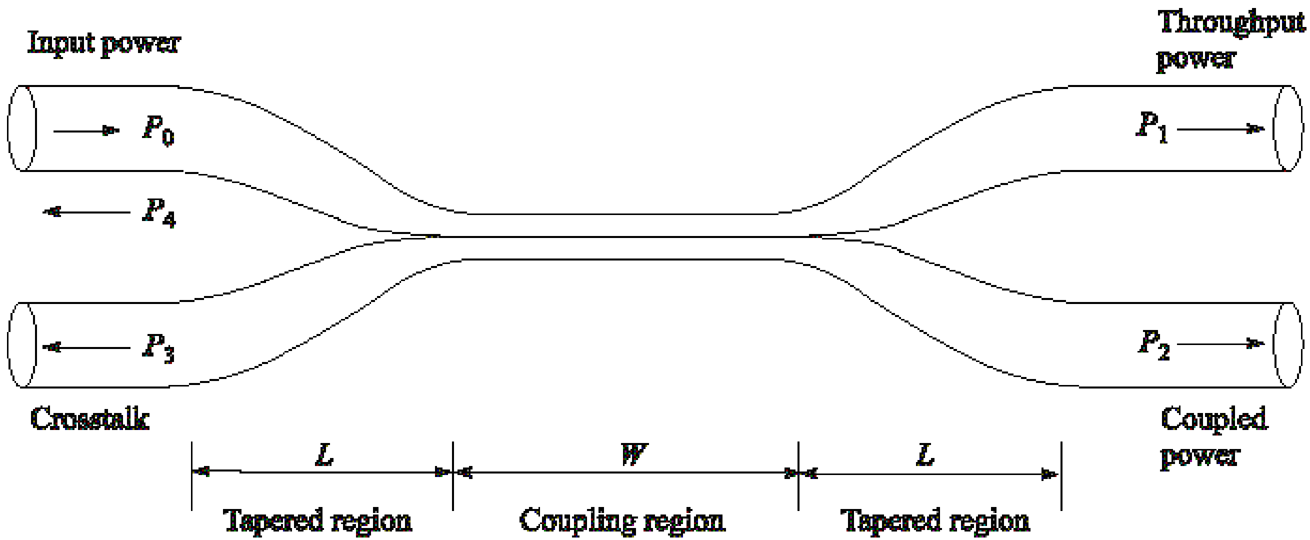

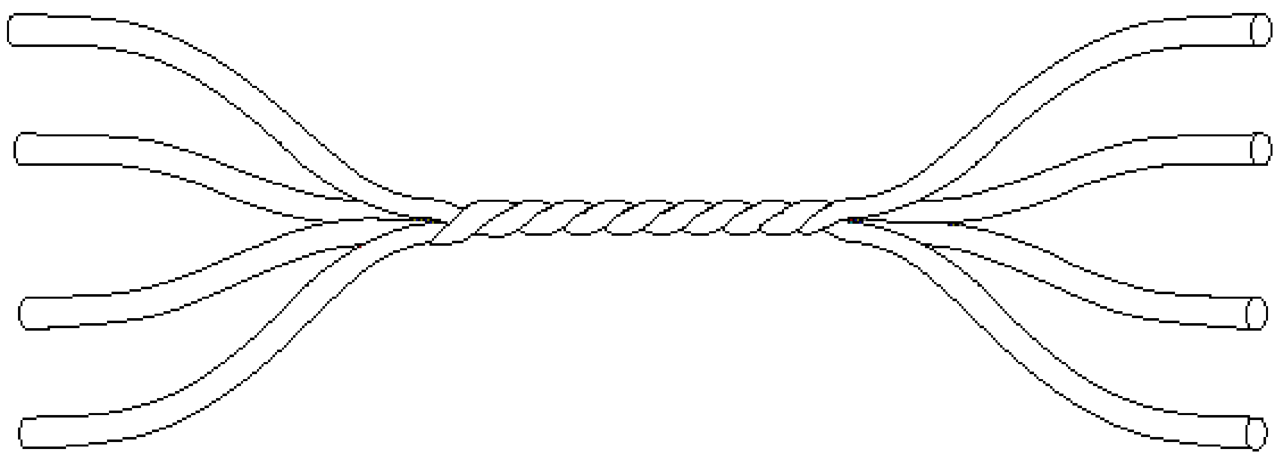

Directional Coupler — Manufacturing Machinery

Corner Stone's Fiber Coupler Manufacturing Workstation FCMW-2100. http://www.cornerstone.com.tw (2005)

Slab Waveguide — Y-Branch

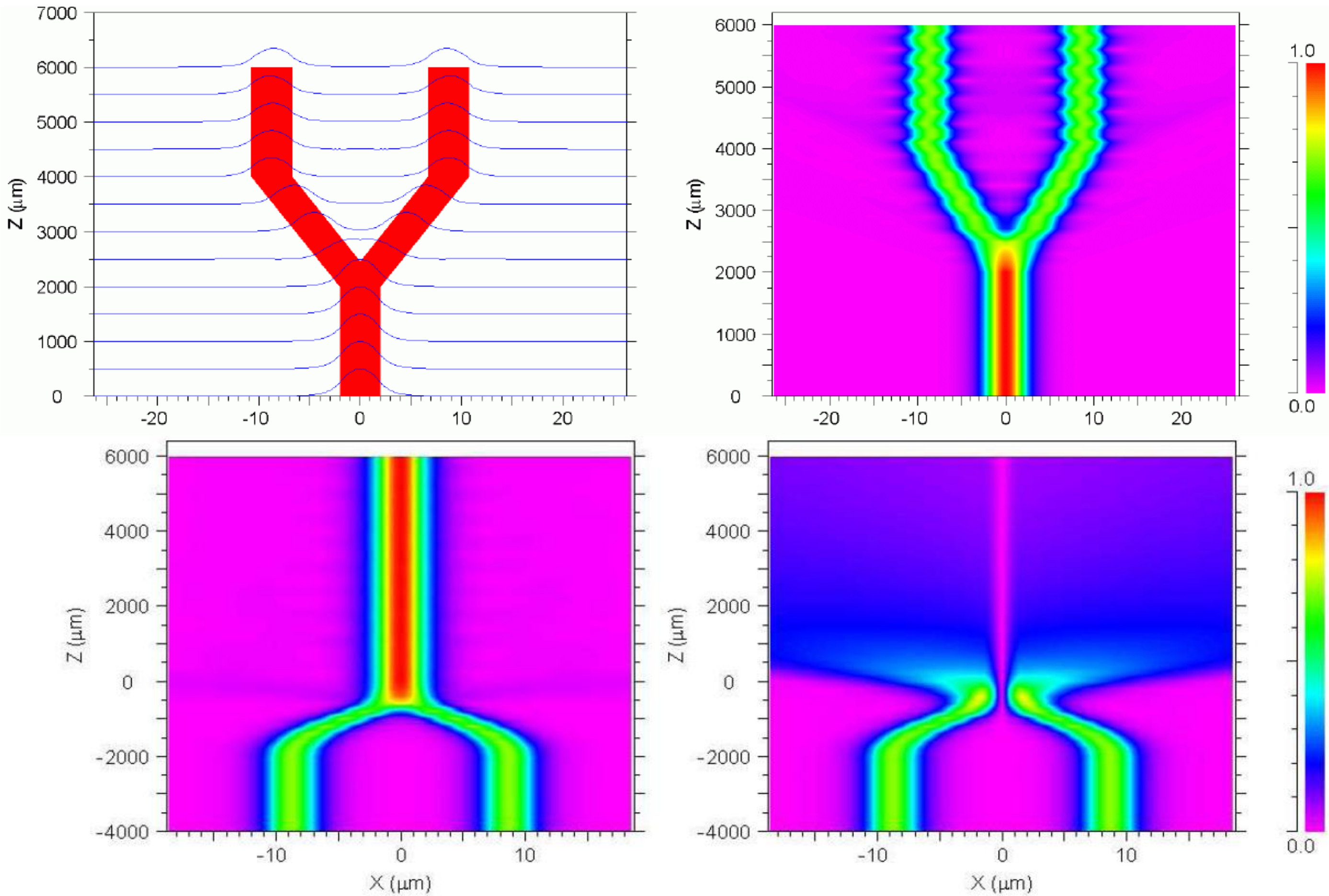

Fig. 2.14. Slab waveguide Y-branch in scalar approximation. Waveguide height $h = 3\,\mu$m, refractive index difference $n_1 - n_2 = 0.0067$, cladding refractive index $n_2 = 3.378$, vacuum wavelength $\lambda = 1.3\,\mu$m. Mind the vast scale differences for the x- and the z-directions; the branch section is angled at only 0.25°. Contour plot of electric field magnitude with colour scale at rightmost side. (left) Symmetric-mode excitation (right) Antisymmetric-mode excitation

Strip Waveguide — Symmetric

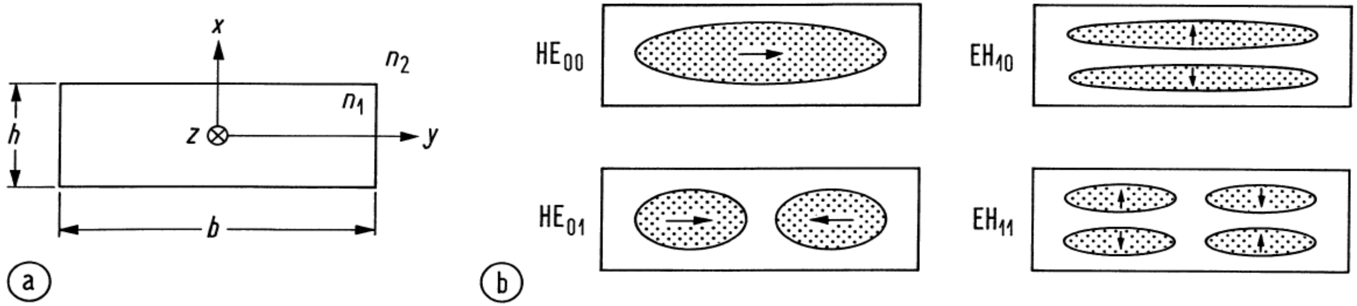

Cross-section of a buried strip waveguide (a) geometric arrangement (b) transverse electric field and near-field intensity (dotted areas correspond to high intensity)

A lateral phase condition equivalent to the previous vertical phase condition holds. A dispersion equation for u_S and w_S (subscript S like strip) similar to $w = u \tan u$, $w = -u \cot u$ may be calculated. A second, lateral mode index $n = 0, 1, 2, \ldots$ counts the $n + 1$ intensity maxima inside the strip along the y-direction. Slight tilt of E_m-waves generates H-component in z-direction in addition to the already existing E-component. Modes with longitudinal E- and H-components are called hybrid modes or EH_{mn}-modes. Analogously: Hybrid HE_{mn}-modes from H_m-waves of the slab waveguide.

Strip Waveguide — Asymmetric, Pedestal

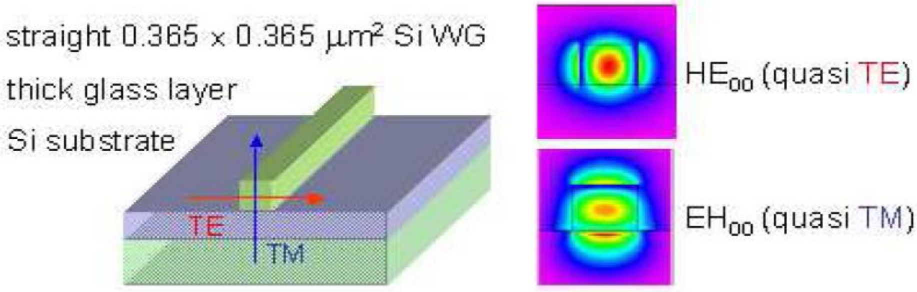

(a) SOI strip waveguide with fundamental mode field magnitudes

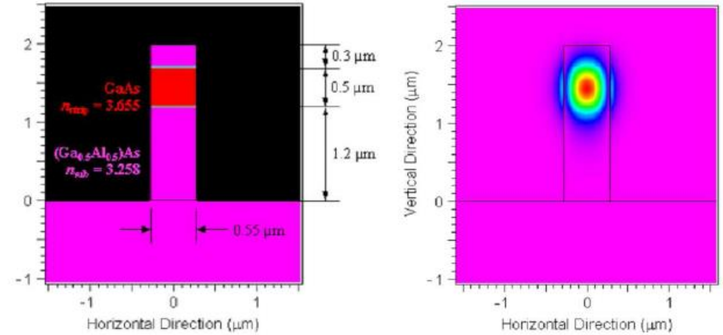

(b) GaAs/GaAlAs pedestal waveguide. Left: index profile. Right: quasi-TE field magnitude

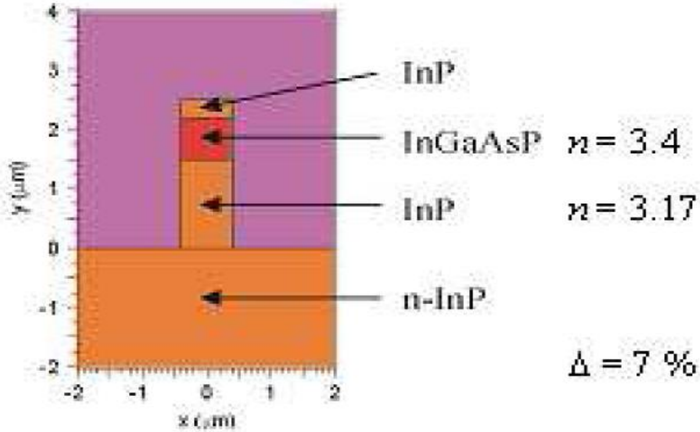

(a) InGaAsP/InP pedestal waveguide, refractive index profile

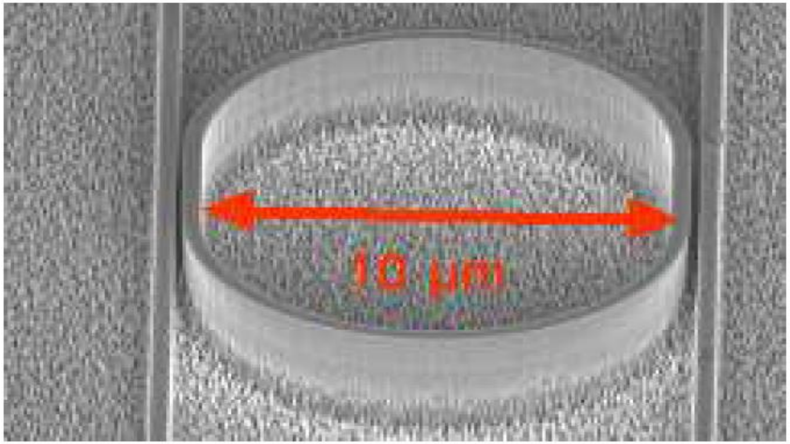

(b) InGaAsP/InP pedestal waveguide, race-track ring filter

Fig. 2.17. InGaAsP/InP pedestal waveguide structure (a) Refractive index profile (b) Scanning electron microscope (SEM) picture of race-track ring resonator with two straight bus waveguides. Waveguide widths 400 nm, coupling gaps 100 nm (left) and 200 nm (right). At ring resonances, all power is transfered from one bus to the other. Signals at other frequencies pass unaffected

Strip Waveguide — High-Index Contrast

Straight 550 × 400 nm^2 Si WG $n_1 = 3.5$

thick glass layer $n_2 = 1.4$

Si substrate $n_3 = 3.5$

contrast $\Delta = 60\ \%$

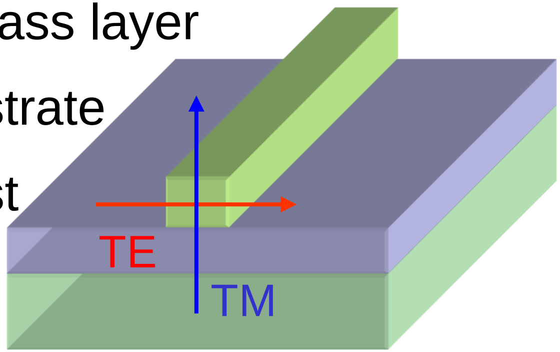

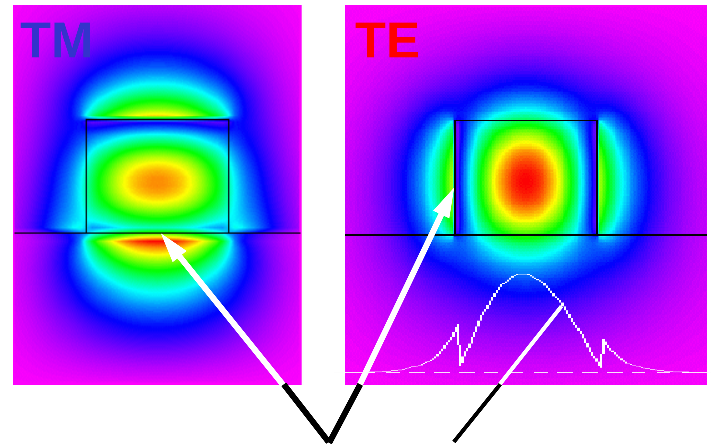

Normal component D_n of $\vec{D}(\vec{r})$ continuous: $D_n = \varepsilon_0 \varepsilon_r(\vec{r}) E_n(\vec{r})$

Single-moded for width $w \approx \lambda / n_1$, i,.e., ultra-compact nanostrips, couplers, bends. Spectral (e.g., resonator) accuracy $\delta\lambda \sim 1.4$ nm $\rightarrow$ **$\delta w \sim 1$ nm**

Usual conventional waveguides are weakly guiding:

$\Delta = (n_1 - n_2) / n_1 = 0.1 \ldots 5\ \%$

single-moded for width $w \approx 10\lambda / n_1 = 10 \frac{1.5\ \mu\text{m}}{1.5} = 10\ \mu\text{m}$

bends and couplers need long, adiabatic transitions

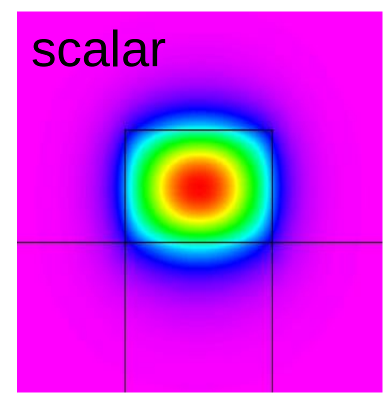

Only for weak guiding, a scalar approximation suffices.

Silicon-Organic Hybrid Slot Waveguide

Field enhancement in low-index cladding:

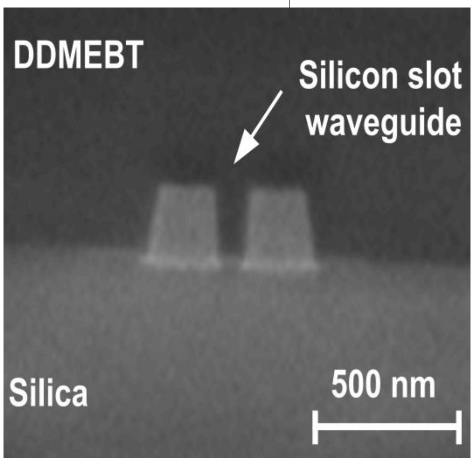

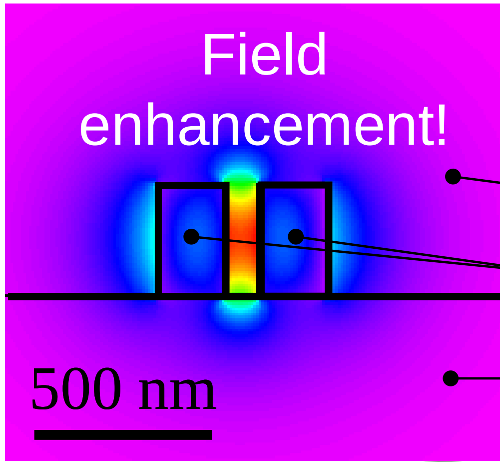

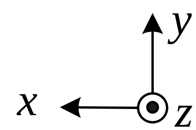

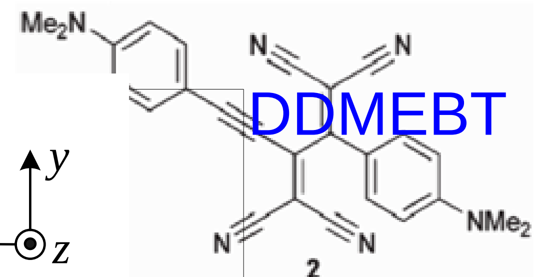

DDMEBT

NL, $n \approx 1.8$ $n_2 = 2\times 10^{-17}\,\mathrm{m^2/W}$

Si, $n = 3.48$

SiO_2, $n = 1.44$

Field confinement due to slot geometry:

$A_{\mathrm{eff}}^{(3)} \approx 0.1\,\mu\mathrm{m}^2$ for slot width of 100 nm

Maximum nonlinearity depends on organic material. Measured:

$$\gamma = \frac{n_2 k_0}{A_{\mathrm{eff}}^{(3)}} \approx 10^5/(\mathrm{W\,km}), \qquad \text{negligible FCA}$$

Koos, C.; Vorreau, P.; Vallaitis, T.; Dumon, P.; Bogaerts, W.; Baets, R.; Esembeson, B.; Biaggio, I.; Michinobu, T.; Diederich, F.; Freude, W.; Leuthold, J.: 'All-optical high-speed signal processing with silicon–organic hybrid slot waveguides,' Nature Photon. 3 (2009) 216–219. Published online: 15 March 2009

Pedestal Nanostrip — Rough Sidewalls

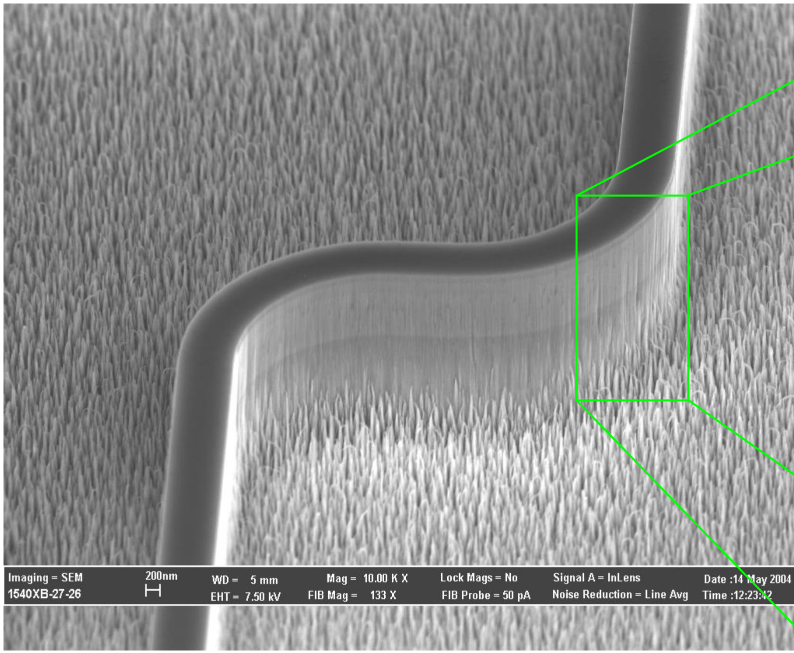

InGaAsP/InP pedestal (1.55 µm) WG
h = 700 nm, *w* = 600 nm (CAIBE, SiN_x)

Meas. attenution: 7 dB/mm (TE)
4 dB/mm (TM)

Cooperation with R. Steingrüber, Fraunhofer Heinrich Hertz Institut, Berlin

Measurement of Surface Roughness

Roughness is vertically chiselled, and so can be described by the parameters σ and D:

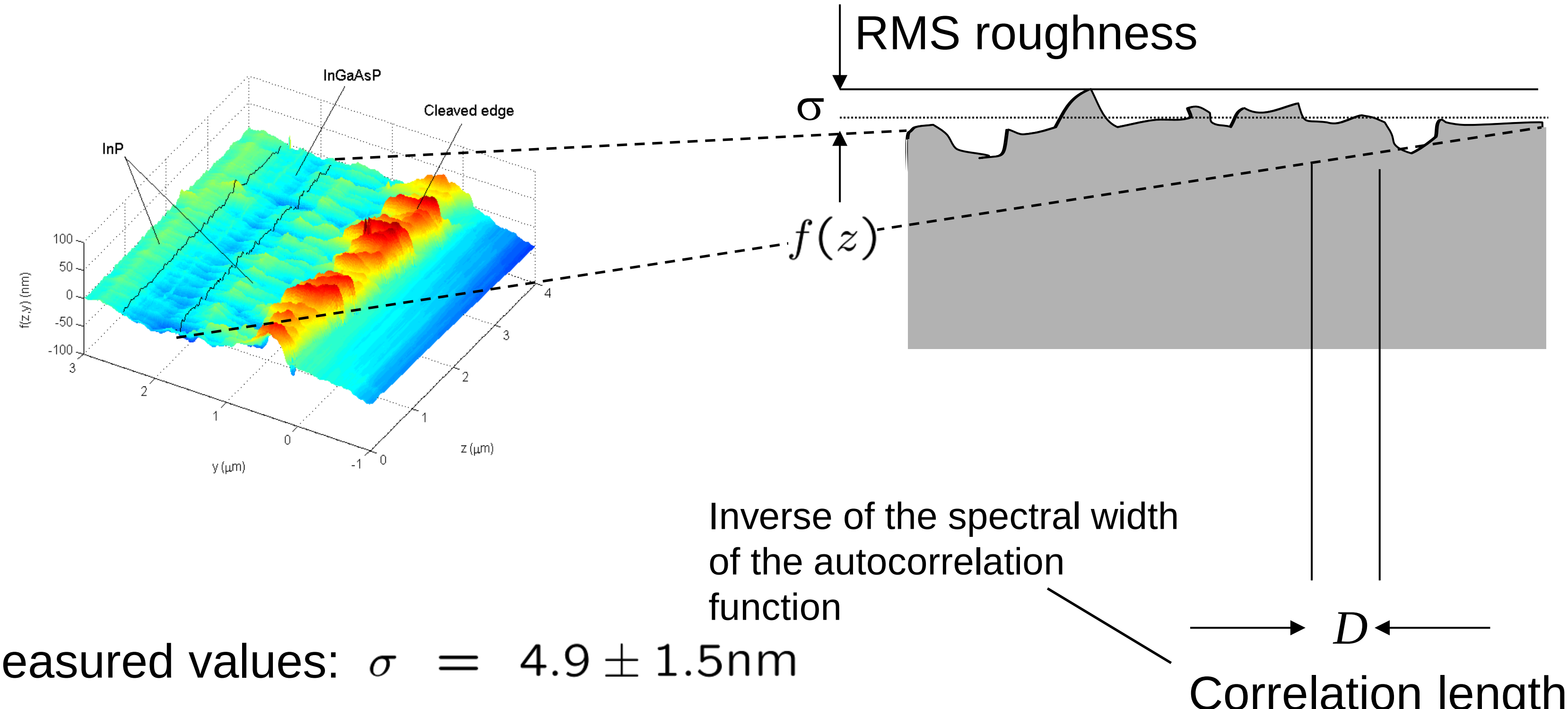

Measured values: $$\sigma = 4.9 \pm 1.5\text{nm}$$ $$D = 54 \pm 21\text{nm}$$

How does the attenuation of the waveguide depend on the RMS roughness and on the correlation length?

Strip Waveguide — Nanostrips. Versatile Ring Resonator

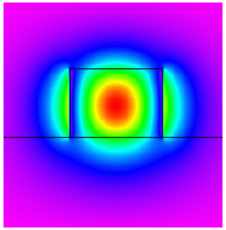

HE$_{00}$ (quasi TE)

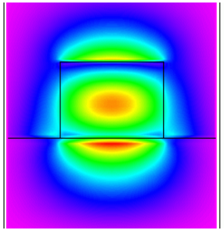

EH$_{00}$ (quasi TM)

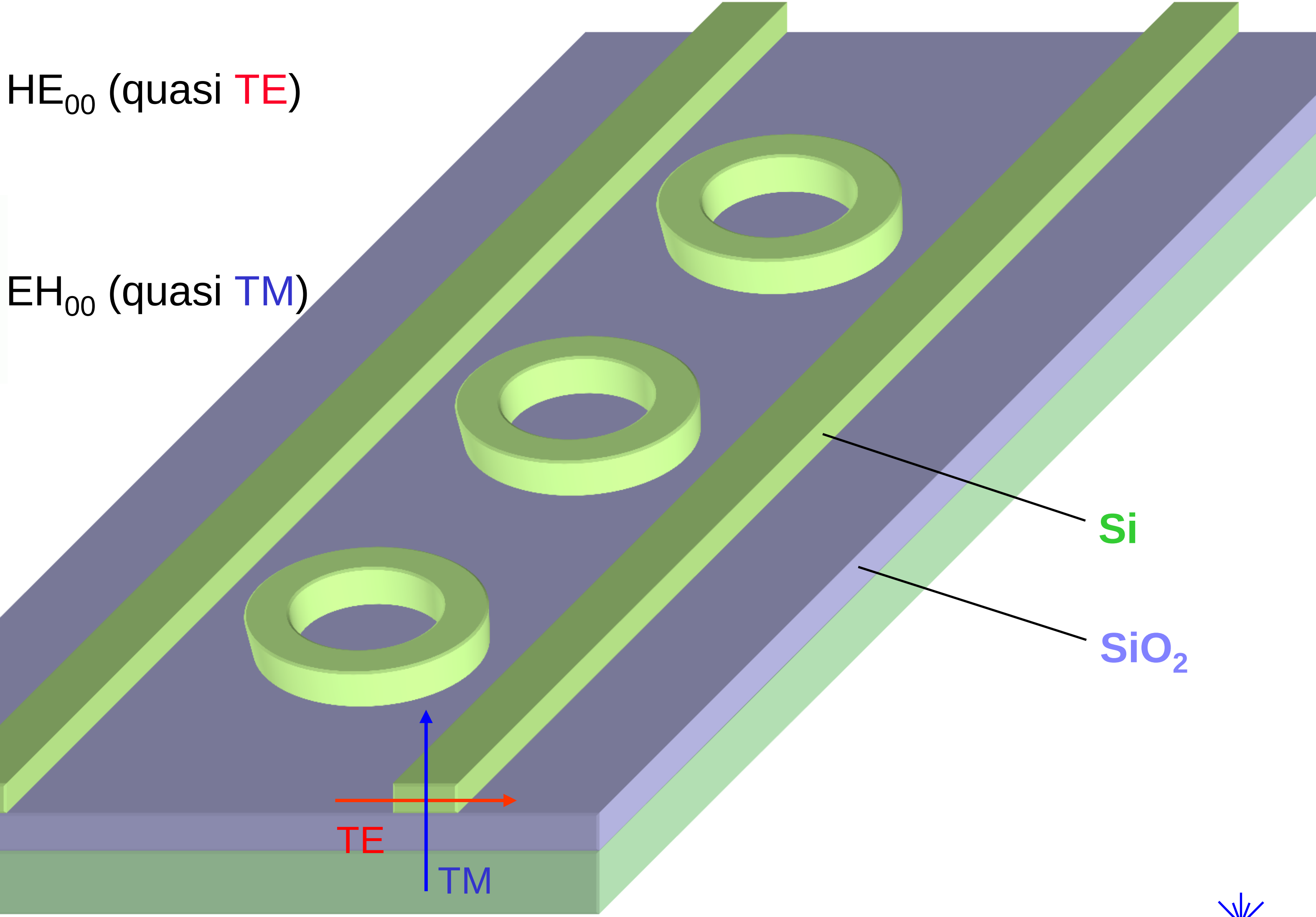

Fibre Waveguide — Refractive Index Profile

Transmission lengths in the 100 ... 1 000 km range, low production cost, low attenuation (0.2 dB / km), and low group delay dispersion important → quartz glass fibres. For 100 m LAN very inexpensive plastic optical fibres (POF) preferable.

Isotropic, cylindersymmetric core (n_1) / cladding ($n_2 < n_1$), $2a = 10 \ldots 100\,\mu$m / $2b = 125\,\mu$m $\to \infty$. Cylindrical coordinates r, φ, z.

Refractive index profile, relative refractive index difference:

$$n^2(r) = \begin{cases} n_1^2\,[1 - 2\Delta g(r/a)]\,, & 0 \leq r < a, \\ n_1^2\,[1 - 2\Delta] = n_2^2, & a \leq r < \infty, \end{cases} \qquad g(r/a) = \begin{cases} 0, & r = 0 \\ 1, & r \geq a \end{cases}$$

Profile function $g(r/a)$ for power low profiles:

$$g(r/a) = (r/a)^q, \qquad 0 \leq q < \infty$$

Step-index profile ($q \to \infty$, $n = n_1$ for $0 \leq r < a$, $n = n_2$ for $r \geq a$).

Parabolic profile $q = 2$. Graded-index profile with q for minimum intermodal dispersion.

LECTURE 8

Step-Index Fibre — Vector Fields (1)

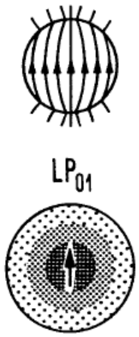

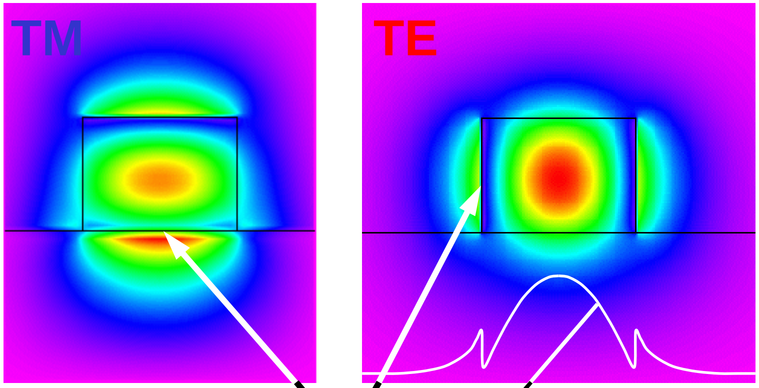

$$D_n = \varepsilon_0 \varepsilon_r(\vec{r}) E_n(\vec{r})$$

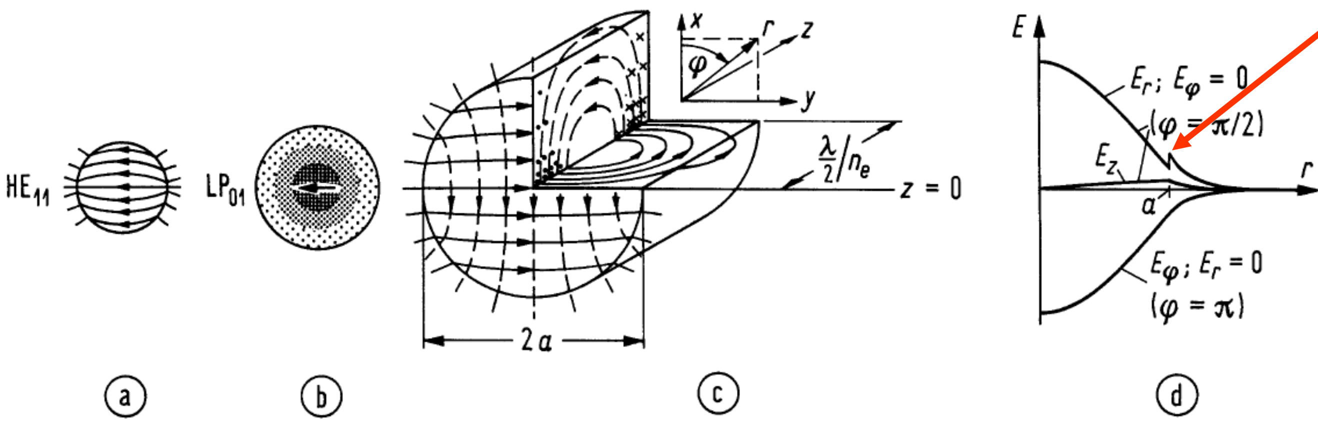

Fig. 2.19. Fields in a step-index fibre. Electric field strength (——); magnetic field strength (– – –); intensity (shaded). (a) electric field of vector modes and (b) electric field and intensity of vector and LP–modes, viewed in $-z$–direction (c) graphs of electric and magnetic fields, $B = 0.9$ (d) radial dependency of electric field strength, $V = 4.75$, $\Delta = 4\,\%$; E_r, E_φ (depicted in plane $z = 0$) are cophasal to each other and in quadrature to E_z (depicted in plane $z = \lambda/(4n_e)$)

Step-Index Fibre Fields (2)

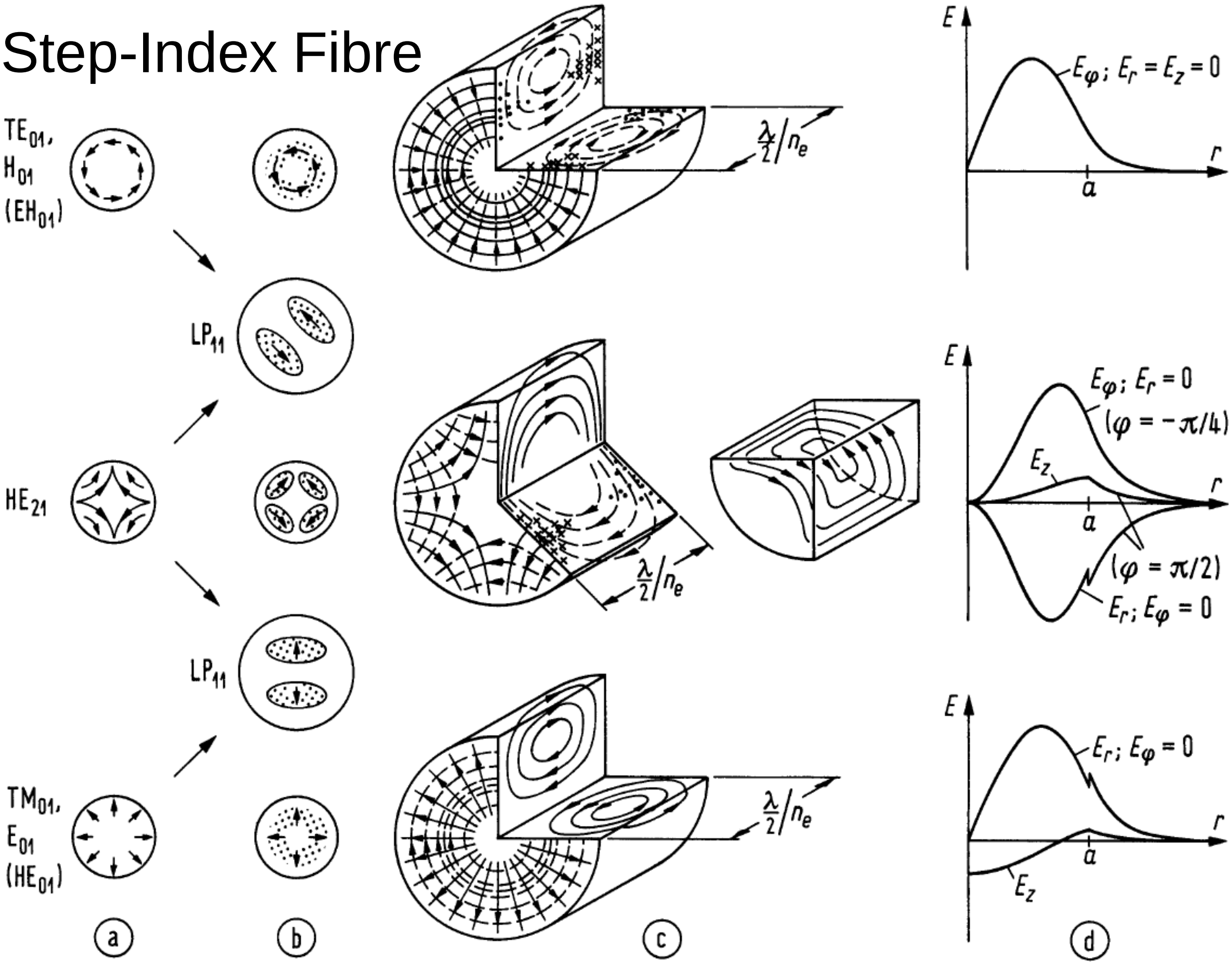

Prop. const. $\mathrm{HE}_{\nu+1,\mu}$-$\mathrm{H}_{0\mu}$, $\mathrm{E}_{0\mu}$-$\mathrm{EH}_{\nu-1,\mu}$ differ by $\Delta\beta$, beat length Λ, LP-modes rotate: ◀

$$\Lambda = \frac{2\pi}{\Delta\beta} = \frac{\lambda}{n_e}\frac{\beta}{\Delta\beta}$$

If $V \gg V_{\nu\mu G}$, $\Delta\beta$ de-, Λ increases, see slab. ◀

Fig. 2.19. Fields in a step-index fibre. Electric field strength (——); magnetic field strength (– – –); intensity (shaded). (a) electric field of vector modes and (b) electric field and intensity of vector and LP–modes, viewed in $-z$–direction (c) graphs of electric and magnetic fields, $B = 0.9$ (d) radial dependency of electric field strength, $V = 4.75$, $\Delta = 4\,\%$; E_r, E_φ (depicted in plane $z = 0$) are cophasal to each other and in quadrature to E_z (depicted in plane $z = \lambda/(4n_e)$)

$\mathrm{LP}_{\nu\mu}$ Modes (1)

Weak guidance $\Delta \ll 1 \rightarrow \mathrm{LP}_{\nu\mu}$, scalar Helmholtz equation, cylindrical coordinates $\vec{r} = (r, \varphi, z)$:

$$\Psi(t, \vec{r}) = \Psi(\vec{r})\, \mathrm{e}^{\mathrm{j}\,\omega t}, \qquad \left(\nabla^2 + k_0^2 n^2(\vec{r})\right) \Psi(\vec{r}) = 0$$

Separation ansatz, $\Psi(\vec{r}) = \Psi(r, \varphi, z) = \Psi(r)\,\Psi(\varphi)\exp(-\mathrm{j}\,\beta z)$:

$$\left(\frac{1}{r}\frac{\partial}{\partial r}\left(r\frac{\partial}{\partial r}\right) + \frac{1}{r^2}\frac{\partial^2}{\partial\varphi^2} + (-\mathrm{j}\,\beta)^2 + k_0^2 n^2(r)\right)\Psi(r)\,\Psi(\varphi) = 0\,,$$

$$\frac{1}{r}\frac{\partial}{\partial r}\left(r\frac{\partial\Psi(r)}{\partial r}\right)\Psi(\varphi) + \frac{1}{r^2}\frac{\partial^2\Psi(\varphi)}{\partial\varphi^2}\Psi(r) + \left(k_0^2 n^2(r) - \beta^2\right)\Psi(r)\,\Psi(\varphi) = 0, \qquad \Big| \cdot \frac{r^2}{\Psi(r)\,\Psi(\varphi)}$$

$$r\left(1 \cdot \frac{\partial\Psi(r)}{\partial r} + r\frac{\partial^2\Psi(r)}{\partial r^2}\right)\frac{1}{\Psi(r)} + r^2\left(k_0^2 n^2(r) - \beta^2\right) = C_r^2(r)\,, \qquad \Big| \cdot \frac{\Psi(r)}{r^2}$$

$$\frac{\partial^2\Psi(\varphi)}{\partial\varphi^2}\frac{1}{\Psi(\varphi)} = C_\varphi^2(\varphi)\,, \qquad C_r^2(r) = -C_\varphi^2(\varphi) = C^2 = \mathrm{const}_{r,\varphi} \qquad \Big| \cdot \Psi(\varphi)$$

LP$_{\nu\mu}$ Modes (2)

Separation constant $C^2 = \text{const}_{r,\varphi}$:

$$\frac{\partial^2 \Psi(r)}{\partial r^2} + \frac{1}{r}\frac{\partial \Psi(r)}{\partial r} + \left(k_0^2 n^2(r) - \beta^2\right)\Psi(r) = \frac{\overbrace{C^2}^{k_\varphi^2(r)}}{r^2}\,\Psi(r),$$

$$\frac{\partial^2 \Psi(\varphi)}{\partial \varphi^2} + \overbrace{C^2}^{r^2 k_\varphi^2(r)}\,\Psi(\varphi) = 0\,, \qquad \Psi(\varphi) = \begin{cases}\cos\,(C\,\varphi)\\ \sin\,(C\,\varphi)\end{cases}$$

$$\frac{\partial \Psi(\varphi)}{\partial \varphi} = C\begin{cases}-\sin\,(C\,\varphi)\\ \cos\,(C\,\varphi)\end{cases}, \qquad \frac{\partial^2 \Psi(\varphi)}{\partial \varphi^2} = C^2\begin{cases}-\cos\,(C\,\varphi)\\ -\sin\,(C\,\varphi)\end{cases},$$

Azimuthal resonance: $C = \nu$, $\nu = 0, 1, 2, \ldots,\ -2\pi r|k_\varphi| = -\nu \cdot 2\pi$

Propagation vector of locally plane wave in weakly inhomogeneous medium:

$$\vec{k} = k_r\vec{e}_r + k_\varphi\vec{e}_\varphi + k_z\vec{e}_z, \qquad |k_\varphi(r)| = \frac{\nu}{r}, \quad k_z = \beta,$$

$$|\vec{k}|^2 = k^2 = k_0^2 n^2(r) = k_r^2 + k_\varphi^2 + \beta^2$$

Weakly Guiding Fibre — Orthonormality and Radial Equation

Radial differential equation (primes on functions mean derivatives wrt argument):

$$\Psi''(r) + \frac{1}{r}\Psi'(r) + k_r^2(r)\,\Psi(r) = 0, \qquad \Psi(r) \equiv \Psi_\mu^{(\nu)}(r),$$
$$k_r^2(r) = k_0^2 n^2(r) - k_\varphi^2 - \beta^2, \qquad |k_\varphi| = \nu/r$$

Longitudinal and azimuthal solution, orthonormality:

$$\Psi_{\nu\mu}(r,\varphi,z) = \Psi_{\nu\mu}(r,\varphi)\,\mathrm{e}^{-\mathrm{j}\,\beta_{\nu\mu}z}, \quad \nu,\nu' = 0,1,\ldots, \quad \mu,\mu' = 1,2,\ldots,$$
$$\Psi_{\nu\mu}(r,\varphi) = \Psi_\mu^{(\nu)}(r)\Psi^{(\nu)}(\varphi), \qquad \Psi^{(\nu)}(\varphi) = \frac{1}{\sqrt{1+\delta_{\nu 0}}}\left\{\begin{matrix}\cos\nu\varphi\\ \text{or}\\ \sin\nu\varphi\end{matrix}\right\},$$
$$n_1\int_{\varphi=0}^{2\pi}\int_{r=0}^{\infty}\Psi_{\nu\mu}(r,\varphi)\,\Psi_{\nu'\mu'}(r,\varphi)\,r\,\mathrm{d}r\,\mathrm{d}\varphi = \delta_{\nu\nu'}\delta_{\mu\mu'},$$

Intensity: $\quad I_{\nu\mu}(r,\varphi) = \frac{1}{2}n_1|\Psi_{\nu\mu}(r,\varphi)|^2$

$LP_{\nu\mu}$ Modes — Step-index Profile. (Modified) Bessel Functions

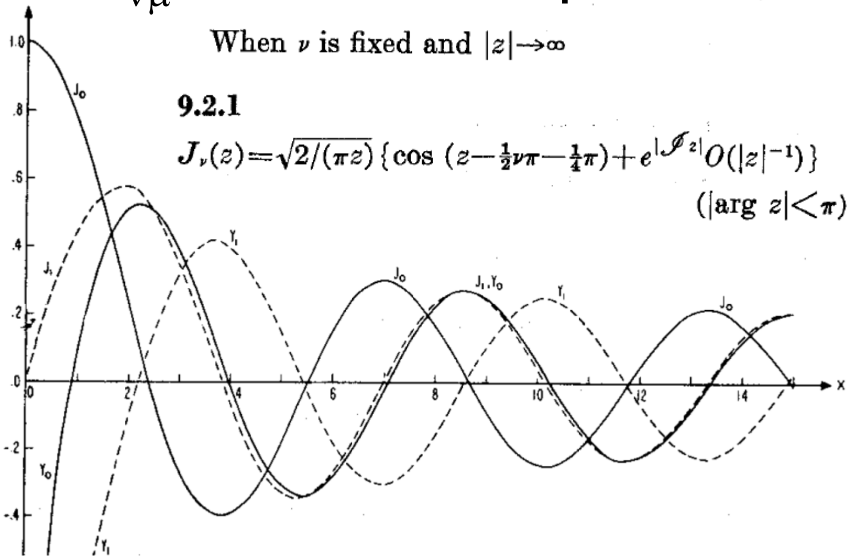

When ν is fixed and $|z|\to\infty$

9.2.1

$$J_\nu(z)=\sqrt{2/(\pi z)}\left\{\cos\left(z-\tfrac{1}{2}\nu\pi-\tfrac{1}{4}\pi\right)+e^{|\mathscr{I}z|}O(|z|^{-1})\right\}$$

$$(|\arg z|<\pi)$$

ZEROS AND ASSOCIATED VALUES OF BESSEL FUNCTIONS AND THEIR DERIVAT

s	$j_{0,s}$	$J'_0(j_{0,s})$	$j_{1,s}$	$J'_1(j_{1,s})$	$j_{2,s}$	$J'_2(j_{2,s})$
1	2.40482 55577	−0.51914 74973	3.83171	−0.40276	5.13562	−0.33967
2	5.52007 81103	+0.34026 48065	7.01559	+0.30012	8.41724	+0.27138
3	8.65372 79129	−0.27145 22999	10.17347	−0.24970	11.61984	−0.23244
4	11.79153 44391	+0.23245 98314	13.32369	+0.21836	14.79595	+0.20654
5	14.93091 77086	−0.20654 64331	16.47063	−0.19647	17.95982	−0.18773
6	18.07106 39679	+0.18772 88030	19.61586	+0.18006	21.11700	+0.17326
7	21.21163 66299	−0.17326 58942	22.76008	−0.16718	24.27011	−0.16170
8	24.35247 15308	+0.16170 15507	25.90367	+0.15672	27.42057	+0.15218
9	27.49347 91320	−0.15218 12138	29.04683	−0.14801	30.56920	−0.14417
10	30.63460 64684	+0.14416 59777	32.18968	+0.14061	33.71652	+0.13730
11	33.77582 02136	−0.13729 69434	35.33231	−0.13421	36.86286	−0.13132
12	36.91709 83537	+0.13132 46267	38.47477	+0.12862	40.00845	+0.12607
13	40.05842 57646	−0.12606 94971	41.61709	−0.12367	43.15345	−0.12140
14	43.19979 17132	+0.12139 86248	44.75932	+0.11925	46.29800	+0.11721
15	46.34118 83717	−0.11721 11989	47.90146	−0.11527	49.44216	−0.11343
16	49.48260 98974	+0.11342 91926	51.04354	+0.11167	52.58602	+0.10999
17	52.62405 18411	−0.10999 11430	54.18555	−0.10839	55.72963	−0.10685
18	55.76551 07550	+0.10684 78883	57.32753	+0.10537	58.87302	+0.10396
19	58.90698 39261	−0.10395 95729	60.46946	−0.10260	62.01622	−0.10129
20	62.04846 91902	+0.10129 34989	63.61136	+0.10004	65.15927	+0.09882

Radially standing wave in core $J_\nu\left(u_{\nu\mu}\frac{r}{a}\right)$

Exponentially decaying wave in cladding $K_\nu\left(w_{\nu\mu}\frac{r}{a}\right)$

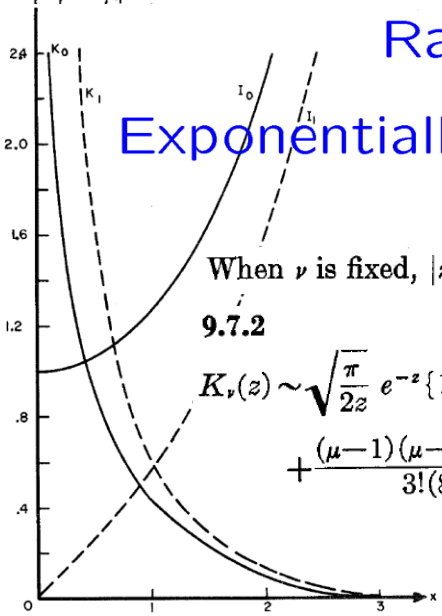

When ν is fixed, $|z|$ is large and $\mu=4\nu^2$

9.7.2

$$K_\nu(z)\sim\sqrt{\frac{\pi}{2z}}\,e^{-z}\left\{1+\frac{\mu-1}{8z}+\frac{(\mu-1)(\mu-9)}{2!(8z)^2}+\frac{(\mu-1)(\mu-9)(\mu-25)}{3!(8z)^3}+\ldots\right\}\quad(|\arg z|<\tfrac{3}{2}\pi)$$

Abramowitz, M.; Stegun, I. A. (Eds.): Handbook of mathematical functions, 9. Ed.. New York: Dover Publications 1970

Here for Gauss-Laguerre modes in parabolic-index fibre. However, structure for step-index fibre (but not size!) is essentially the same.

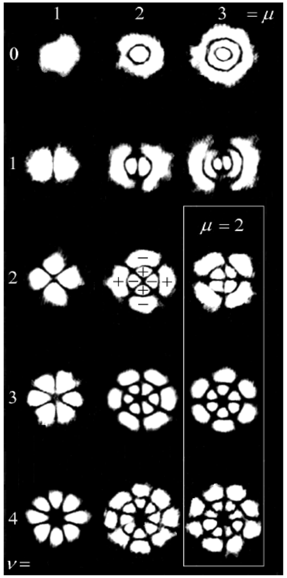

Fig. 2.22. Gauss-Laguerre

Weakly Guiding Fibre — Notation

In analogy to slab waveguide, define core parameter u, cladding parameter w (also expressed by cladding penetration depth r_w), normalized frequency V, relative refractive index difference Δ, κ (an abbreviation for a combination of modified Bessel functions K_ν of order ν), normalized propagation constants B, δ:

$$u = a\sqrt{k_1^2 - \beta^2}, \qquad w = a\sqrt{\beta^2 - k_2^2} = 2a/r_w,$$

$$V = ak_0 A_N = \sqrt{u^2 + w^2}, \qquad A_N = \sqrt{n_1^2 - n_2^2} = n_1\sqrt{2\Delta},$$

$$\kappa(w) = \mathrm{K}_\nu^2(w)/[\mathrm{K}_{\nu-1}(w)\ \mathrm{K}_{\nu+1}(w)], \qquad \beta^2 = k_1^2(1 - 2\delta),$$

$$B = \frac{\beta^2 - k_2^2}{k_1^2 - k_2^2} = \frac{w^2}{V^2} = 1 - \frac{u^2}{V^2} = 1 - \frac{\delta}{\Delta} \approx \{\Delta \ll 1\} \approx \frac{\beta - k_2}{k_1 - k_2}$$

Weakly Guiding Fibre — Step-Index Profile (1)

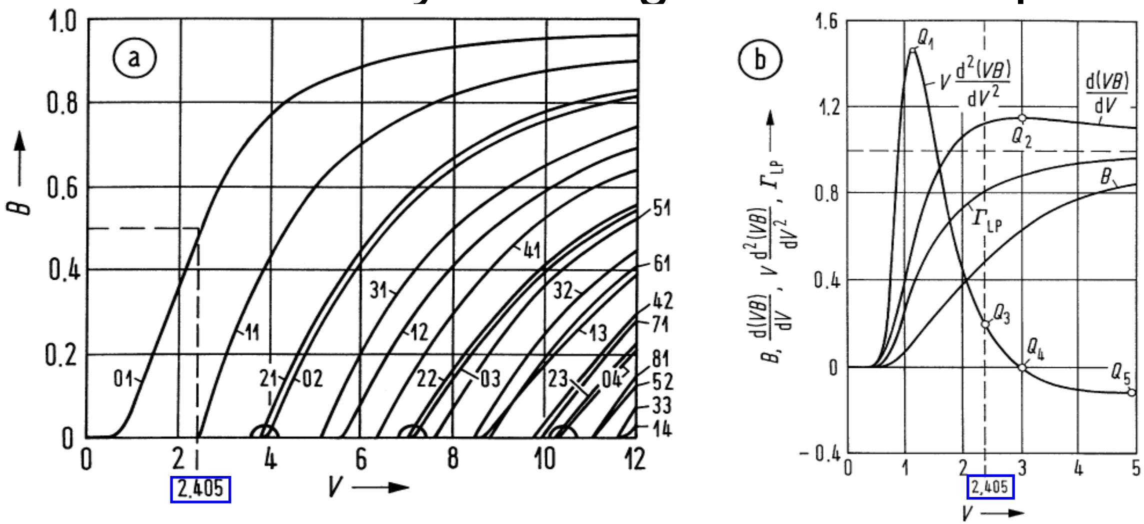

Propagation of LP$_{\nu\mu}$–modes in a step-index fibre. (a) Normalized proagation constant B; cutoff frequencies $V_{0\mu G} = V_{2,\mu-1,G}$ for $\mu \geq 2$ marked by semicircles, $\boxed{V_{11G} = 2.405}$, $V_{21G} = V_{01G} = 3.832$ (b) fundamental mode mode LP$_{01}$: normalized propagation constant B, group delay factor $\mathrm{d}(VB)/\,\mathrm{d}V$, dispersion factor $V\,\mathrm{d}^2(VB)/\,\mathrm{d}V^2$, and field confinement factor Γ_{LP}. $Q_1 = (1.15, 1.46)$, $Q_2 = (3, 1.14)$, $Q_3 = (2.405, 0.2)$, $Q_4 = (3.04, 0)$, $Q_5 = (4.95, -0.113)$

$$\frac{t_g}{L} = \underbrace{\frac{n_{2g}}{c}}_{\text{mat. disp.}} + \underbrace{\frac{n_{1g} - n_{2g}}{c} \overbrace{\frac{\mathrm{d}(VB)}{\mathrm{d}V}}^{\text{gr. delay fctr}}}_{\text{waveguide dispersion}}, \quad \frac{\Delta t_g}{L} = \frac{t_{g,\lambda+\Delta\lambda} - t_{g,\lambda}}{L} = C\Delta\lambda = (M + W)\Delta\lambda,$$

$$M = M_s = \underbrace{\frac{1}{c}\frac{\mathrm{d}n_{sg}}{\mathrm{d}\lambda}}_{\substack{\text{material}\\ \text{dispersion}}} \quad (s = 1 \text{ or } 2), \qquad W = -\frac{n_{1g} - n_{2g}}{c\lambda} \underbrace{V \frac{\mathrm{d}^2(VB)}{\mathrm{d}V^2}}_{\substack{\text{dispersion}\\ \text{factor}}}$$

Weakly Guiding Fibre — Step-Index Profile (2)

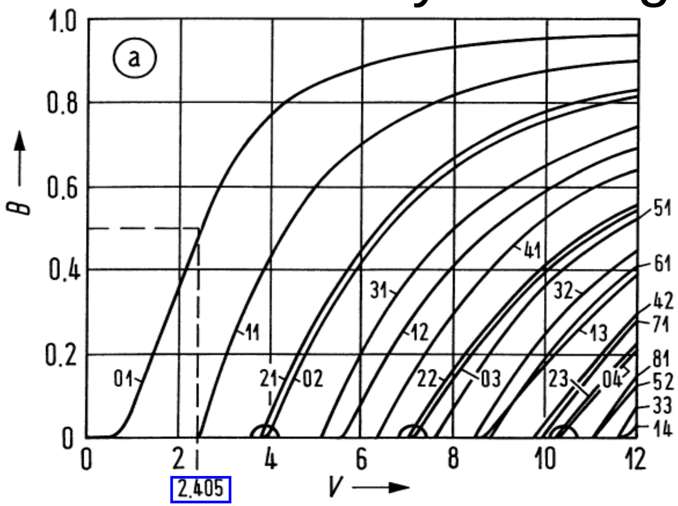

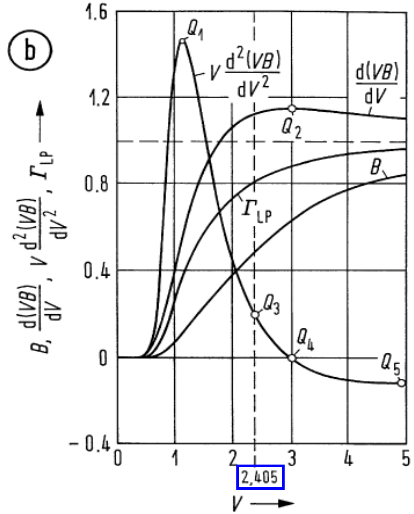

Each pair (ν, μ) stands for 4 LP$_{\nu\mu}$-modes or 4 guided vector modes:

$$M_g \approx \frac{V^2}{2}, \qquad V \gg 1$$

Sign. near-field ext.:

$$r_M \geq 1.6\, a$$

$$\frac{\Delta t_{g\,\max}}{L} \approx \frac{n_1 - n_2}{c} = \frac{n_1}{c}\Delta$$

$$\frac{t_g}{L} = \underbrace{\frac{n_{2g}}{c}}_{\text{mat. disp.}} + \underbrace{\frac{n_{1g} - n_{2g}}{c}\overbrace{\frac{\mathrm{d}(VB)}{\mathrm{d}V}}^{\text{gr. delay fctr}}}_{\text{waveguide dispersion}}, \quad \frac{\Delta t_g}{L} = \frac{t_{g,\lambda+\Delta\lambda} - t_{g,\lambda}}{L} = C\Delta\lambda = (M + W)\Delta\lambda,$$

$$M = M_s = \underbrace{\frac{1}{c}\frac{\mathrm{d}n_{sg}}{\mathrm{d}\lambda}}_{\substack{\text{material}\\ \text{dispersion}}} \quad (s = 1 \text{ or } 2), \qquad W = -\frac{n_{1g} - n_{2g}}{c\lambda}\underbrace{V\frac{\mathrm{d}^2(VB)}{\mathrm{d}V^2}}_{\substack{\text{dispersion}\\ \text{factor}}}$$

Step-Index Fibre — Conventional and Dispersion Shifted

$\lambda/\,\mu\mathrm{m}$	1.1	1.3	1.56
$V = a k_0 A_N$	2.497	2.113	1.761
$V\,\mathrm{d}^2(VB)/\,\mathrm{d}V^2$	0.150	0.370	0.710
$M\,/\,\frac{\mathrm{ps}}{\mathrm{km\,nm}}$	−23.18	+1.58	+21.93
$W\,/\,\frac{\mathrm{ps}}{\mathrm{km\,nm}}$	−1.78	−3.72	−5.94
$C\,/\,\frac{\mathrm{ps}}{\mathrm{km\,nm}}$	−24.96	−2.14	+15.99
$D(\lambda_C = 1.325\,\mu\mathrm{m}) = 0.0415\,\mathrm{ps}\,/\,\left(\mathrm{km\,nm}^2\right)$			

Table 2.1. Dispersion characteristics[25] of a step-index CSF with $n_1 = 1.450840$, $n_2 = 1.446918$, $\boxed{a = 4.1\,\mu\mathrm{m}}$ and $\boxed{\Delta = 0.27\,\%}$. Wavelength of zero chromatic dispersion $C(\lambda_C) = 0$ is $\lambda_C = 1.325\,\mu\mathrm{m}$, cutoff at $\lambda_{11G} = 1.142\,\mu\mathrm{m}$

$\lambda/\,\mu\mathrm{m}$	1.1	1.3	1.56
$V = a k_0 n_1 \sqrt{2\Delta}$	2.346	1.985	1.654
$V\,\mathrm{d}^2(VB)/\,\mathrm{d}V^2$	0.223	0.476	0.845
$M\,/\,\frac{\mathrm{ps}}{\mathrm{km\,nm}}$	−25.04	+0.58	+21.5
$W\,/\,\frac{\mathrm{ps}}{\mathrm{km\,nm}}$	−7.33	−13.24	−19.59
$C\,/\,\frac{\mathrm{ps}}{\mathrm{km\,nm}}$	−32.37	−12.65	+1.94
$D(\lambda_C = 1.523\,\mu\mathrm{m}) = 0.024\,\mathrm{ps}\,/\,\left(\mathrm{km\,nm}^2\right)$			

$$-\frac{n_{1g} - n_{2g}}{c\lambda}\,\underbrace{V\,\frac{\mathrm{d}^2(VB)}{\mathrm{d}V^2}}_{\text{dispersion factor}} =$$

Table 2.2. Dispersion characteristics[26] of a step-index DSF with $n_1 = 1.457893$, $n_2 = 1.446918$, $\boxed{a = 2.3\,\mu\mathrm{m}}$ and $\boxed{\Delta = 0.75\,\%}$. Wavelength of zero chromatic dispersion $C(\lambda_C) = 0$ is $\lambda_C = 1.523\,\mu\mathrm{m}$, cutoff at $\lambda_{11G} = 1.073\,\mu\mathrm{m}$

Step-Index Fibre — Dispersion-Compensating and -Flattened

$\lambda / \mu\mathrm{m}$	**1.1**	**1.3**	**1.56**
V	2.531	2.141	1.784
$C \,/\, \frac{\mathrm{ps}}{\mathrm{km\,nm}}$	-97.0	-67.0	-50.0

Table 2.3. Dispersion characteristics[28] of a step-index DCF with $n_1 = 1.476754$, $n_2 = 1.446918$, $a = 1.5\,\mu\mathrm{m}$ and $\Delta = 2\,\%$, cutoff at $\lambda_{11G} = 1.158\,\mu\mathrm{m}$

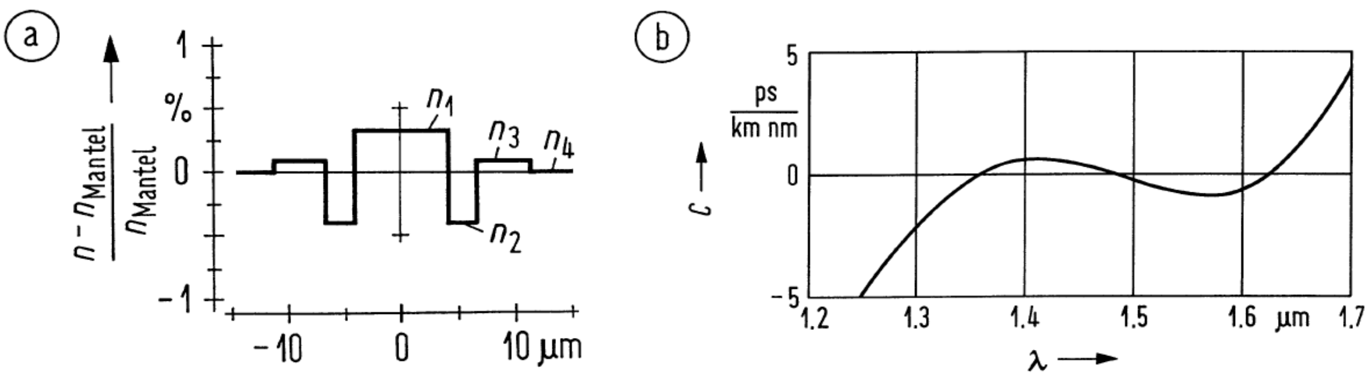

Dispersion characteristics of a triple-clad step-index DFF. (a) Refractive index profile (b) Chromatic dispersion. Quartz glass core with F-doped claddings (computed) $a_1 = 3.8\,\mu\mathrm{m}$, $a_2 = 7\,\mu\mathrm{m}$, $a_3 = 12.95\,\mu\mathrm{m}$. Refractive indices at $\lambda = 1.064\,\mu\mathrm{m}$ are $n_1 = 1.45$, $n_2 = 1.4383$, $n_3 = 1.4471$, $n_4 = 1.4442$. Three zeros $C(\lambda_{C\,1,2,3}) = 0$ at $\lambda_{C\,1} = 1.36$, $\lambda_{C\,2} = 1.48$, $\lambda_{C\,3} = 1.625\,\mu\mathrm{m}$. (Mantel = cladding)

Dispersion Characteristics of Step-Index Fibres

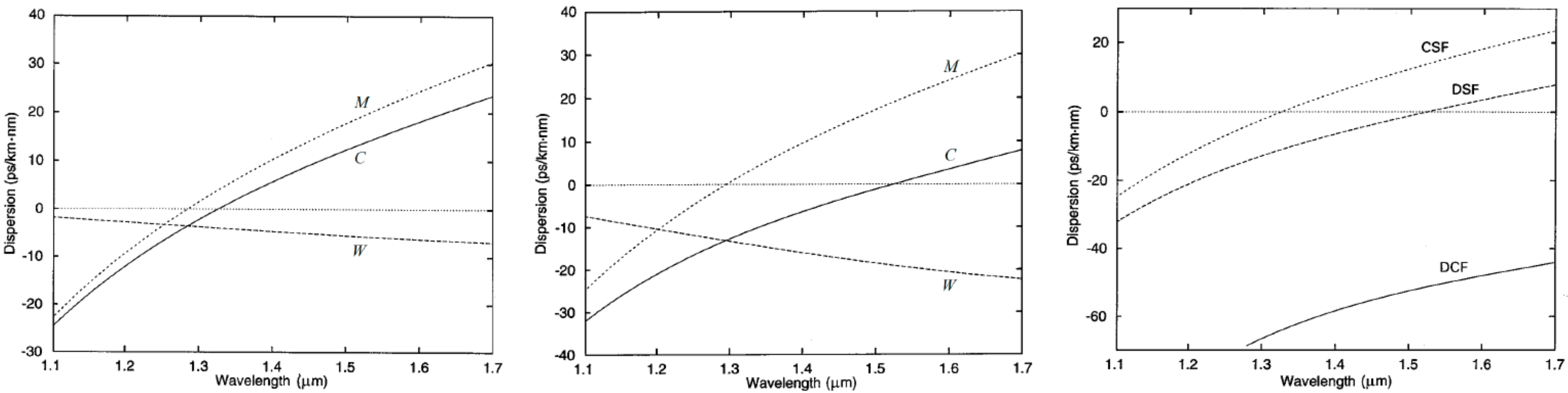

(a) CSF: $\Delta = 0.27\,\%$, $a = 4.1\,\mu$m, $\lambda_C = 1.325\,\mu$m, $\lambda_{11G} = 1.142\,\mu$m (Table 2.1)

(b) DSF: $\Delta = 0.75\,\%$, $a = 2.3\,\mu$m, $\lambda_C = 1.523\,\mu$m, $\lambda_{11G} = 1.073\,\mu$m (Table 2.2)

(c) DCF: $\Delta = 2\,\%$, $a = 1.5\,\mu$m, $\lambda_{11G} = 1.158\,\mu$m (Table 2.3). Comparison of CSF, DCF and DCF

Fig. 2.21. Dispersion characteristics of basic step-index fibre types with cladding index $n_2 = 1.446918$ as described in Tables 2.1–2.3. (a), (b) Upper curves: Material dispersion M. Lower curves: Waveguide dispersion W. Middle curves: Total chromatic dispersion C (all in units of ps/(km nm)), see Eq. (2.55) on Page 27. (c) Comparison of CSF (upper curve), DSF (middle curve) and DCF (lower curve) [adapted from Figs. 10.2–10.4 in reference Footnote 25 on Page 39]

$$\Delta t_g/L = C\,\Delta\lambda + D\,(\Delta\lambda)^2 + \ldots, \qquad C = \frac{1}{L}\frac{\mathrm{d}t_{gm}}{\mathrm{d}\lambda}, \qquad D = \frac{1}{2L}\frac{\mathrm{d}^2 t_{gm}}{\mathrm{d}\lambda^2}$$

$C(\lambda_C) = 0$, $\quad \lambda_C$ is zero of $C(\lambda_C)$ for mode m.

$$\Delta t_g/L = C_\lambda(\lambda)\,\Delta\lambda = (C + D\,\Delta\lambda)\,\Delta\lambda, \qquad \text{slope } D = \frac{\mathrm{d}C_\lambda(\lambda)}{\mathrm{d}\lambda}$$

Singlemode Impulse Response

Analytic transfer function $\breve{h}_m(f)$, causal real impulse response $h_m(t)$ in mode m, $\beta_m(\omega) = -\beta_m(-\omega)$:

$$\breve{h}_m(f) = \mathrm{e}^{-\mathrm{j}\,\beta_m(\omega)L}, \qquad h_m(t) = \int_{-\infty}^{+\infty} \breve{h}_m(f)\,\mathrm{e}^{\mathrm{j}\,2\pi f t}\,\mathrm{d}f$$

Distortion-less transmission in vacuum:

$$\beta_m(\omega) = k_0 = \frac{\omega}{c}, \quad h_m(t) = \delta\left(t - \frac{L}{c}\right), \quad u(t) \to w(t) = u\left(t - \frac{L}{c}\right)$$

Signal spectra concentrated near f_0, $\beta_m^{(i)} = \mathrm{d}^i \beta_m(\omega) / \mathrm{d}\omega^i|_{\omega=\omega_0}$:

$$\beta_m(\omega) \approx \beta_m^{(0)} + (\omega-\omega_0)\beta_m^{(1)} + \frac{(\omega-\omega_0)^2}{2!}\beta_m^{(2)} + \frac{(\omega-\omega_0)^3}{3!}\beta_m^{(3)}$$

Phase delay $L\beta_m^{(0)}/\omega_0 = t_{p\,m}$ and group delayay $L\beta_m^{(1)} = t_{gm}$.

Terms up to $\beta_m^{(1)}$: $A_0(t - t_{gm})\,\mathrm{e}^{\mathrm{j}\,\omega_0(t - t_{p\,m})}$

Envelope $A_0(t)$ unchanged, delayed by t_g, carrier phase retarded by $\omega_0 t_{p\,m}$. — Higher-order terms $\beta_m^{(i\geq 2)}$: Linear distortions

Distortion-free Transmission

Input signal: $a_0(t) = A_0(t)\exp[\mathrm{j}\,\omega_0 t] \circ\!\!-\!\!\bullet\ \breve{A}_0(f - f_0)$:

Transfer function: $\breve{h}_m(f) = \mathrm{e}^{-\mathrm{j}(\beta_m^{(0)} + (\omega-\omega_0)\beta_m^{(1)})L}$

Signal spectrum at $z = L$: $\breve{A}_0(f - f_0)\,\mathrm{e}^{-\mathrm{j}(\beta_m^{(0)} + (\omega-\omega_0)\beta_m^{(1)})L}$

Output signal:

$$
\begin{aligned}
a_L(t) &= \int_{-\infty}^{+\infty} \breve{A}_0(f - f_0)\,\mathrm{e}^{-\mathrm{j}(\beta_m^{(0)} + (\omega-\omega_0)\beta_m^{(1)})L}\,\mathrm{e}^{\mathrm{j}\,2\pi f t}\,\mathrm{d}f \\
&= \mathrm{e}^{-\mathrm{j}(\beta_m^{(0)} - \omega_0\beta_m^{(1)})L} \int_{-\infty}^{+\infty} \breve{A}_0(f - f_0)\,\mathrm{e}^{-\mathrm{j}\,\omega\beta_m^{(1)}L}\,\mathrm{e}^{\mathrm{j}\,2\pi f t}\,\mathrm{d}f \\
&= \mathrm{e}^{-\mathrm{j}(\beta_m^{(0)} - \omega_0\beta_m^{(1)})L} \int_{-\infty}^{+\infty} \breve{A}_0(f - f_0)\,\mathrm{e}^{\mathrm{j}\,2\pi f(t-\beta_m^{(1)}L)}\,\mathrm{d}f \\
&= \mathrm{e}^{-\mathrm{j}(\beta_m^{(0)} - \omega_0\beta_m^{(1)})L} \int_{-\infty}^{+\infty} \breve{A}_0(f')\,\mathrm{e}^{\mathrm{j}\,2\pi(f'+f_0)(t-\beta_m^{(1)}L)}\,\mathrm{d}f' \\
&= \mathrm{e}^{\mathrm{j}\,\omega_0\left(t-\frac{\beta_m^{(0)}}{\omega_0}L\right)} \int_{-\infty}^{+\infty} \breve{A}_0(f')\,\mathrm{e}^{\mathrm{j}\,2\pi f'(t-\beta_m^{(1)}L)}\,\mathrm{d}f'
\end{aligned}
$$

$$
a_L(t) = A_0(t - \beta_m^{(1)}L)\exp\left[\mathrm{j}\,\omega_0\left(t - \frac{\beta_m^{(0)}}{\omega_0}L\right)\right]
$$

LECTURE 9

Gaussian Impulse — Visualized

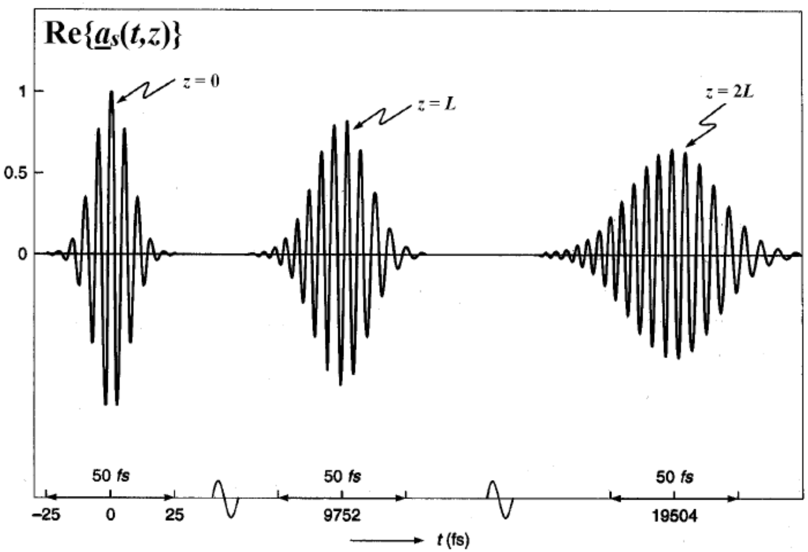

(a) CSF: $C_{\mathrm{CSF}} = 16\,\mathrm{ps/(km\,nm)}$ (Table 2.1)

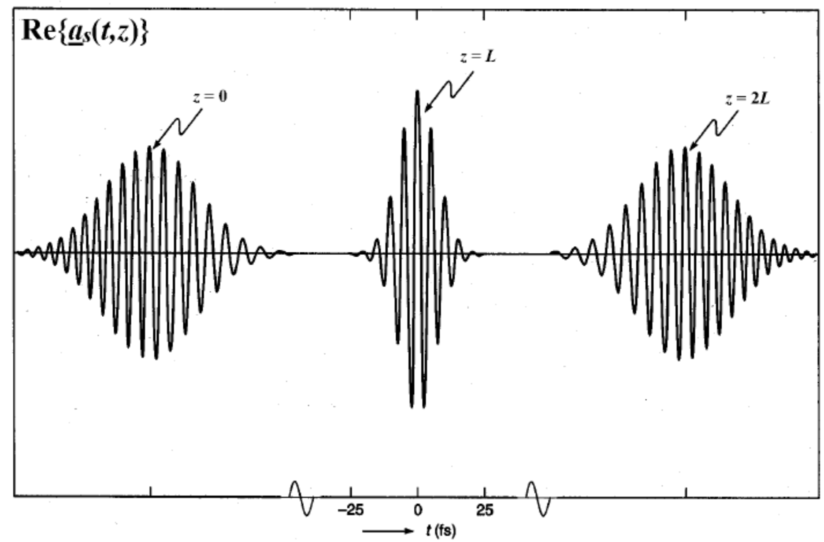

(b) DCF: $C_{\mathrm{DCF}} = -32\,\mathrm{ps/(km\,nm)}$ (Table 2.3)

Propagation of a light impulse with a Gaussian envelope. Displayed is the real part $a_s(t,z) = \Re\{A(t,z) \times \exp[\mathrm{j}(\omega_0 t - \beta^{(0)} z)]\}$ of the analytic signal $\underline{a}_s(t,z)$ for $\lambda_0 = 1.55\,\mu\mathrm{m}$, $z_0 = 0$, $z \geq 0$, Eq. (2.123) on Page 56. For the chromatic dispersion, see Table 2.1 on Page 47 (CSF), and compare to Table 2.3 on Page 49 (DCF) [adapted from reference Footnote 37 on Page 62].

Commercial Singlemode Fibre Data

Fiber Type	Attenuation	Chromatic Dispersion		MFD	Polarization
	α_0 [dB/km]	D [ps/nm/km]	D' slope [ps/nm^2/km]	A_{eff} [μm^2]	PMD [ps/√km]
PirelliWIDELIGHT_1550	0.24	-6.85	0.157	51	≤ 0.1
PirelliWIDELIGHT_1625	0.25	-0.1	0.107	51	≤ 0.1
PirelliFREELIGHT_1550	0.23	4.3	0.114	72	≤ 0.1
PirelliFREELIGHT_1625	0.25	11.2	0.11	72	≤ 0.1
PirelliDEEPLIGHT_1550	0.23@1560nm	-2.2 @1560nm	0.12	70	≤ 0.1
CorningSMF28_1310	0.34	0 @1313nm	0.086	66.5	≤ 0.1
CorningSMF28_1550	0.19	16	0.086	85	≤ 0.1
CorningSMF28e_1310	0.34	0 @1313nm	0.086	66.5	≤ 0.1
CorningSMF28e_1550	0.19	16		85	≤ 0.1
CorningLEAF	0.2 @1550nm	4 @1550nm	0.1 @1550nm	72	≤ 0.1
CorningLEAF_submarine	0.2 @1550nm	0 @1580nm	0.11 @1580nm	71	≤ 0.1
FurukawaSMF332_1310	0.32	0	0.092	68	≤ 0.5
FurukawaSMF332_1550	0.18	18	0.092	86.5	≤ 0.5
AlcatelSMF_1310	0.3	0	0.086	63.6	≤ 0.1
AlcatelSMF_1550	0.2	16		81.67	≤ 0.1
AlcatelTERALIGHT_1550	0.205	8	0.058	65	≤ 0.1
AlcatelTERALIGHT_1620	0.22	10.9 @1600nm	0.058	65	≤ 0.1
LucentTRUEWAVE_1600	0.2	4.5	0.045	55	≤ 0.1
LucentTRUEWAVE_1550	0.2	7	0.045	59	≤ 0.1
LucentALLWAVE_1310	0.3	0 @1312nm	0.088	66	≤ 0.1
LucentALLWAVE_1550	0.2	0 @1312nm	0.088	80	≤ 0.1
SumitomoZ_1550	0.17	18.5	0.056	80	
SumitomoZPLUSa_1550	0.168	20.5	0.059	110	

OptSim 4.5 Models Reference Volume I: Sample Mode (2005). RSoft Design Group, Inc., Physical Layer Division, Ossining, NY 10562. www.rsoftdesign.com

Polarization Mode Dispersion (PMD). Signal Quality (Eye Opening)

SOP: State-of Polarization

Variation of eye diagram

First-order PMD

- $d\Delta\tau/d\omega=0$
- $d\hat{e}_{\pm}/d\omega=0$

pulse broadening (pulse splitting)

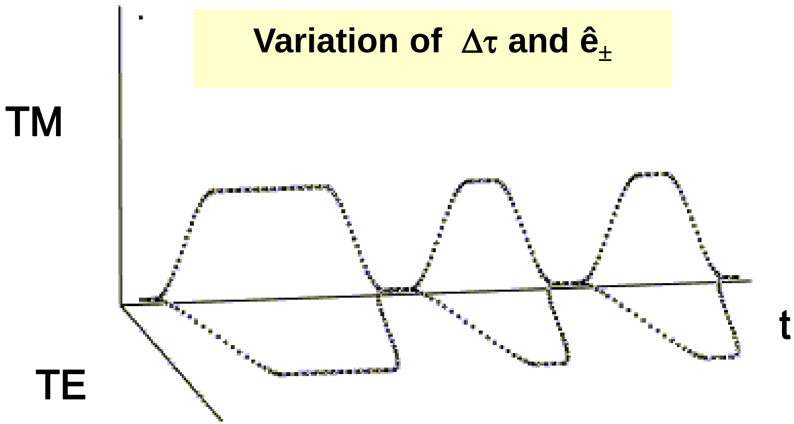

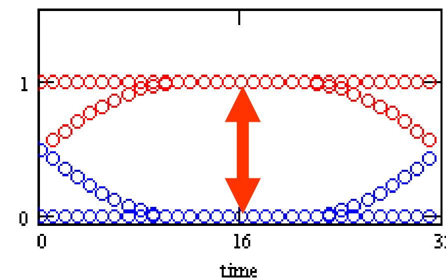

Higher-order PMD

- $d\Delta\tau/d\omega\neq0$
- $d\hat{e}_{\pm}/d\omega\neq0$

(overshoots)

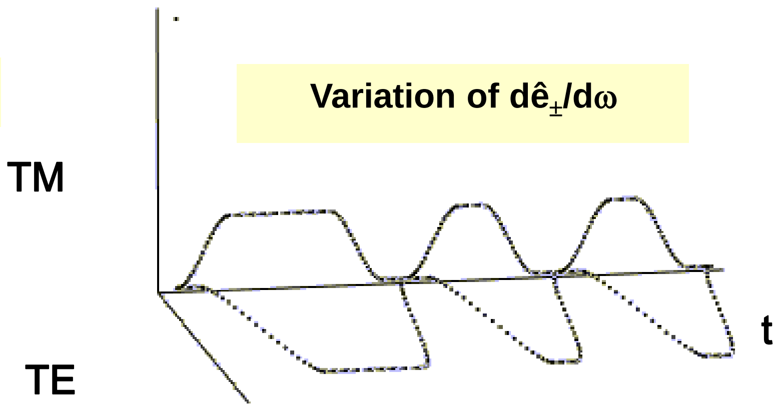

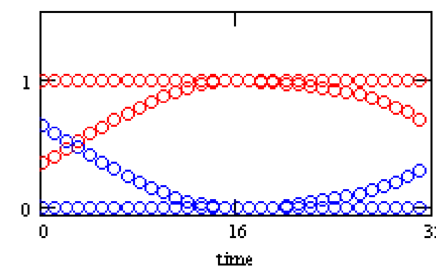

➢ PMD induces stochastic variations of fiber channel transmission paths

Courtesy H. Bülow, G. Veith (Alcatel-Lucent Deutschland, Stuttgart 2008)

Polarization Mode Dispersion (PMD)

Long term PMD measurement of installed field fibre (246 km G.652 DTAG link Stuttgart/Baden-Baden): Statistical PMD variations vs. time and vs. wavelength

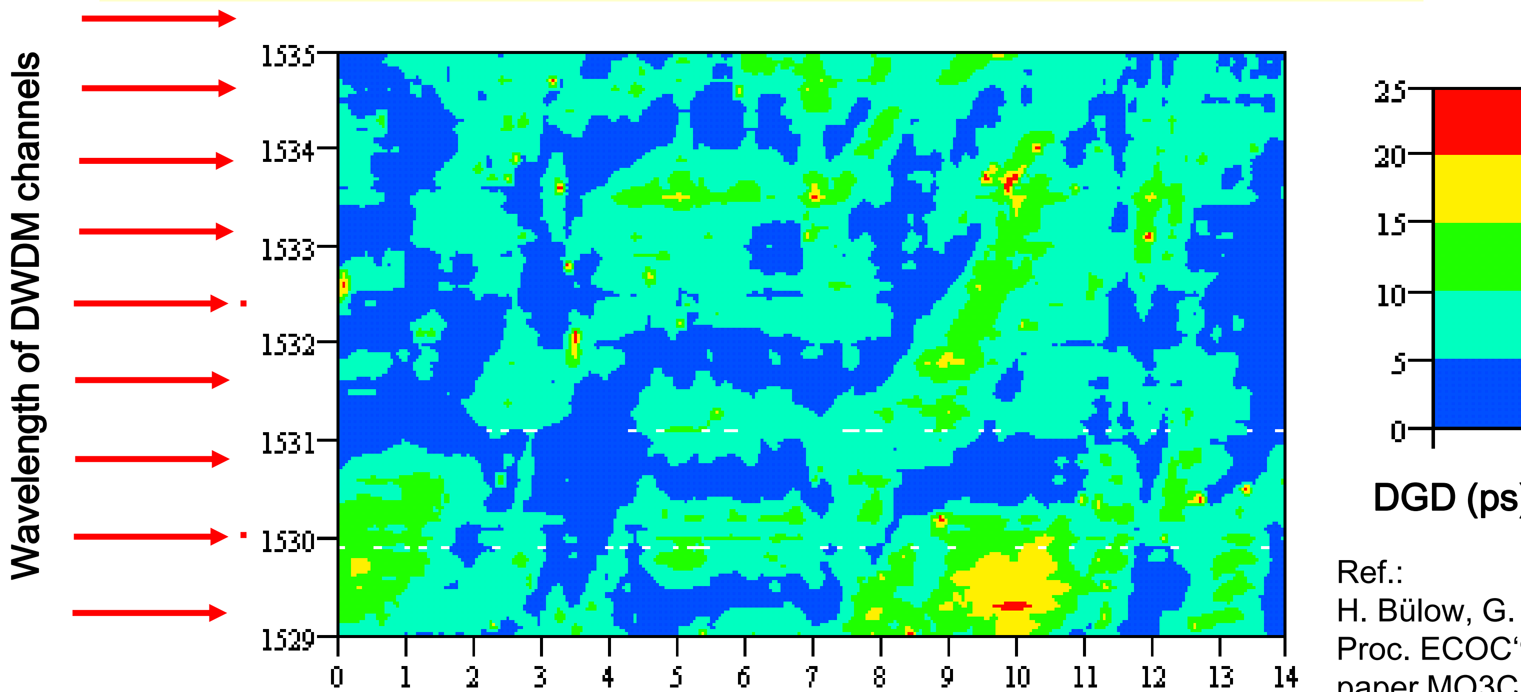

Ref.:
H. Bülow, G. Veith
Proc. ECOC'97,
paper MO3C

➢ Observed statistical PMD variations might have impact on quality of transmission at high bit rates of 10Gbit/s and beyond (40G, 100G)

Courtesy H. Bülow, G. Veith (Alcatel-Lucent Deutschland, Stuttgart 2008)

Weakly Guiding Fibre — Parabolic-Index Profile

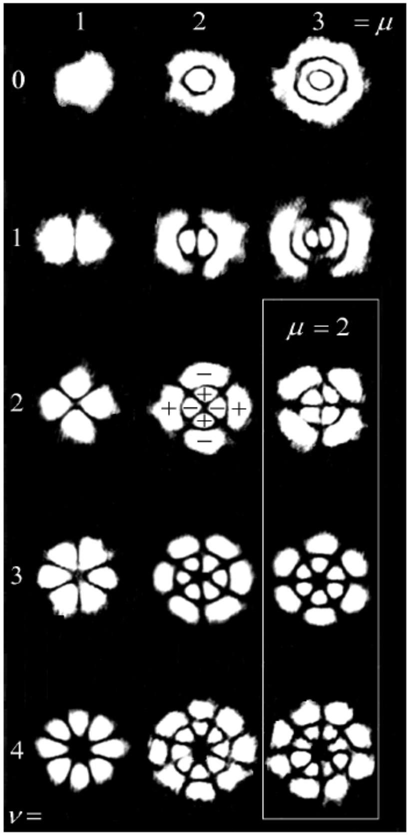

Analytical solution of scalar Helmholtz equation for (unphysically) infinitely extended parabolic refractive index profile:

$$n^2(r) = n_1^2\,[1 - 2\Delta g(r/a)]$$
$$g(r/a) = (r/a)^2 \quad \text{in } 0 \leq r < \infty$$

Gauss-Laguerre LP$_{\nu\mu}$ modes, number:

$$M_g \approx \frac{V^2}{4}, \qquad V \gg 1$$

Maximum group delay difference:

$$\frac{\Delta t_{g\,\max}}{L} \approx \frac{n_1}{c}\,\frac{\Delta^2}{2}$$

Gauss-Laguerre modes of a parabolic-index fibre with parameters $a = 23\,\mu\text{m}$, $A_N = 0.2$, $V = 46$ at $\lambda = 0.6328\,\mu\text{m}$. The beam radius of the fundamental LP$_{01}$-mode is $w_0 = 4.8\,\mu\text{m}$.

Orthogonality and Coupling Efficiency (1)

Plane $z = z'$, scalar light field $\Phi(r,\varphi,z)$, total power P_Φ. Source field $\Phi(r,\varphi,z \geq z')$ expanded into set of orthonormal guided modes $\Psi_{\nu\mu}(r,\varphi,z)$ $(n_1 \approx n_2 \approx n(r))$ and non-guided modes (NG):

$$\Phi(r,\varphi,z) = \sum_{\nu,\mu} c_{\nu\mu}(z')\,\Psi_{\nu\mu}(r,\varphi,z) + \mathrm{NG},$$

$$P_\Phi = \frac{n_1}{2}\int_0^{2\pi}\int_0^\infty |\Phi(r,\varphi,z)|^2\, r\,\mathrm{d}r\,\mathrm{d}\varphi$$

$c_{\nu\mu}$ called excitation-, coupling-, Fourier coefficients.

By multiplying with $\Psi^*_{\nu'\mu'}(r,\varphi,z')$ at $z = z'$ and integrating over cross-sectional area (disregarding for now NG):

$$\int_0^{2\pi}\int_0^\infty \Phi(r,\varphi,z')\,\Psi^*_{\nu'\mu'}(r,\varphi,z')\, r\,\mathrm{d}r\,\mathrm{d}\varphi$$

$$= \sum_{\nu,\mu} c_{\nu\mu}(z')\,\underbrace{\int_0^{2\pi}\int_0^\infty \Psi_{\nu\mu}(r,\varphi,z')\,\Psi^*_{\nu'\mu'}(r,\varphi,z')\, r\,\mathrm{d}r\,\mathrm{d}\varphi}_{\delta_{\nu\nu'}\delta_{\mu\mu'}/n_1}$$

Orthogonality and Coupling Efficiency (2)

Orthogonality of guided ◀ and non-guided modes ◀ (not proven here), sum reduces to one element:

$$\sum_{\nu,\mu} c_{\nu\mu}(z')\,\delta_{\nu\nu'}\delta_{\mu\mu'}/n_1 = c_{\nu'\mu'}(z')/n_1\,, \qquad P = \frac{1}{2}\sum_{\nu,\mu} |c_{\nu\mu}(z')|^2,$$

$$c_{\nu\mu}(z') = n_1 \int_0^{2\pi}\int_0^{\infty} \Phi(r,\varphi,z')\,\Psi^*_{\nu\mu}(r,\varphi,z')\,r\,\mathrm{d}r\,\mathrm{d}\varphi$$

Sum of modal powers $|c_{\nu\mu}|^2/2$ equals total guided power P:

$$P = \frac{1}{2}\sum_{\nu,\mu}\sum_{\nu',\mu'} c_{\nu\mu}(z')\,c^*_{\nu'\mu'}(z')\,\underbrace{n_1 \int_0^{2\pi}\int_0^{\infty} \Psi_{\nu\mu}(r,\varphi,z)\,\Psi^*_{\nu'\mu'}(r,\varphi,z)\,r\,\mathrm{d}r\,\mathrm{d}\varphi}_{\delta_{\nu\nu'}\delta_{\mu\mu'}}$$

Orthogonality and Coupling Efficiency (3)

Generally complex field $\Phi(r, \varphi, z = 0) \equiv \Phi(r, \varphi)$ launched at fibre entrance $z' = 0$. Fraction $\eta_{\nu\mu}$ of total power P_Φ coupled to guided modes $\Psi_{\nu\mu}(r, \varphi, z = 0) \equiv \Psi_{\nu\mu}(r, \varphi)$ $(c_{\nu\mu} \equiv c_{\nu\mu}(z' = 0))$:

$$\eta_{\nu\mu} = \frac{|c_{\nu\mu}|^2}{2P_\Phi} = \frac{\left| \int_0^{2\pi} \int_0^{\infty} \Phi(r, \varphi)\, \Psi_{\nu\mu}(r, \varphi)\, r\, \mathrm{d}r\, \mathrm{d}\varphi \right|^2}{\int_0^{2\pi} \int_0^{\infty} |\Phi(r, \varphi)|^2\, r\, \mathrm{d}r\, \mathrm{d}\varphi \;\; \int_0^{2\pi} \int_0^{\infty} \Psi_{\nu\mu}^2(r, \varphi)\, r\, \mathrm{d}r\, \mathrm{d}\varphi}$$

Semiconductor Laser — Counting Resonator Modes

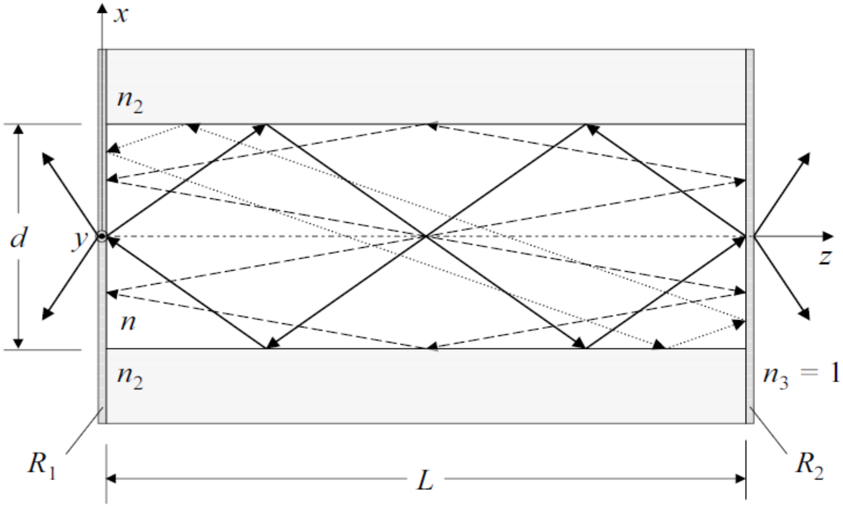

Fig. 3.1. Laser resonator modes. Resonator length L, strip waveguide height d (corresponds to h in Fig. 2.7), strip waveguide height b along y-axis, active volume $V = Lbd$, mirrors with power reflection factors $R_{1,2}$

1D WG: transv. x-resonances
2D WG: transv. (x, y)-resonances
3D resonator has in addition longitudinal z-resonances.

Vol. $V = Lbd$, or configuration-space volume $V_c = L_x L_y L_z \mathrel{\widehat{=}} L^3$

$$\text{1D}: \quad M_g^{(\mathrm{slab})} = \frac{4}{\pi} V = 2\left(2\,\frac{h}{2}\right)\frac{f}{c}\left(2\,A_N\right) \quad \left(V = \frac{h}{2}\,k_0\,A_N\right)$$

$$\text{2D}: \quad M_g^{(\mathrm{SIF})} = \frac{1}{2} V^2 = 2\left(a^2\pi\right)\frac{f^2}{c^2}\left(\pi A_N^2\right) \quad \left(V = a\,k_0\,A_N\right)$$

$$\text{3D}: \quad M_{\mathrm{tot}} = 2\,V_c\,\frac{4\pi}{3}\left(\frac{fn}{c}\right)^3 = \frac{2}{3}\left(L^3\right)\frac{f^3}{c^3}\left(4\pi\right), \qquad n = 1$$

$$\text{DOS}: \quad \varrho_{\mathrm{tot}}(f) = \frac{1}{V_c}\,\frac{\mathrm{d}M_{\mathrm{tot}}}{\mathrm{d}f} = \frac{8\pi}{c^3}(fn)^2 n_g\,, \qquad n_g = n + f\,\frac{\mathrm{d}n}{\mathrm{d}f}$$

Free Electron as a Wave Function

Electron moving in constant potential V having momentum p. De Broglie: Described by plane-wave function, angular frequency ω, wavenumber $k = p/\hbar$ (physics notation; electrical engineering: $\psi_{\mathrm{ee}}(t,x) = \exp[\mathrm{j}(\omega t - kx)] = \psi^*(x,t)$):

$$\psi(x,t) = \exp[\mathrm{j}(kx - \omega t)]$$

Electron may be excited only with energy quanta $\hbar\omega = W$ (Einstein, photoelectric effect). Result is matter wave:

$$\psi(x,t) = \exp[(\mathrm{j}/\hbar)(p\,x - W t)]$$

Derivatives of $\psi(x,t)$ wrt x and $t \rightarrow$ differential operators for conservation quantities. Eigenvalues are momentum p and energy W:

$$(-\mathrm{j}\,\hbar\,\partial/\partial x)^2\,\psi(x,t) = p^2\,\psi(x,t), \quad \mathrm{j}\,\hbar\Big(\partial/\partial t\Big)\,\psi(x,t) = W\,\psi(x,t)$$

Electron energy $W = p^2/(2m_0) + V = (\hbar k)^2/(2m_0) + V$, rest mass m_0:

$$\left[\frac{1}{2m_0}\left(\frac{\hbar}{\mathrm{j}}\frac{\partial}{\partial x}\right)^2 + V\right]\psi(x,t) = -\frac{\hbar}{\mathrm{j}}\frac{\partial}{\partial t}\,\psi(x,t)$$

Schrödinger Equation for "Bound Electron" & "Two-Level Atom"

Wave function $\psi(x,t) = \psi(x)\,\mathrm{e}^{-\mathrm{j}\,\omega t}$ and dispersion relation:

$$\left[\frac{1}{2m_0}\left(\frac{\hbar}{\mathrm{j}}\frac{\partial}{\partial x}\right)^2 + V\right]\psi(x) = W\,\psi(x)\,, \qquad W = \hbar\omega = \frac{(\hbar k)^2}{2m_0} + V$$

Potential film ($\widehat{=}$ slab waveguide) with infinitely high walls. Solutions are spatial sinusoidals or superpositions of it:

$$\psi(x,t) = \mathrm{j}(1/\sqrt{2})\,\psi_2(x)\,\mathrm{e}^{-\mathrm{j}\,\omega_2 t} + (1/\sqrt{2})\,\psi_1(x)\,\mathrm{e}^{-\mathrm{j}\,\omega_1 t},$$

$$\omega_{21} = \omega_2 - \omega_1$$

Schrödinger Equation for "Two-Level Atom"

Potential film ($\widehat{=}$ slab waveguide) with infinitely high walls. Solutions are spatial sinusoidals or superpositions of it:

$$\psi(x,t) = \mathrm{j}(1/\sqrt{2})\,\psi_2(x)\,\mathrm{e}^{-\mathrm{j}\,\omega_2 t} + (1/\sqrt{2})\,\psi_1(x)\,\mathrm{e}^{-\mathrm{j}\,\omega_1 t},$$

$$\omega_{21} = \omega_2 - \omega_1$$

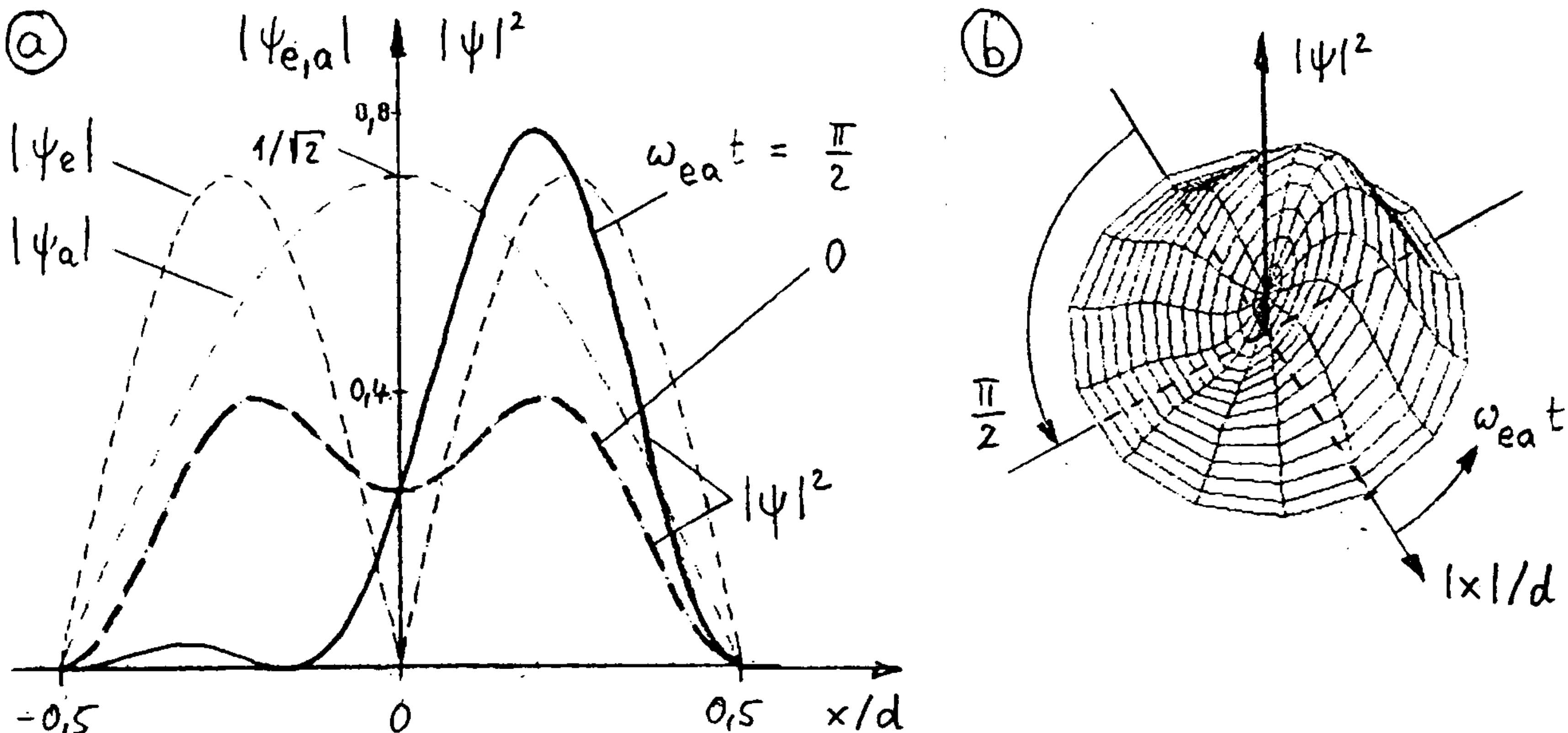

Schrödinger Equation for “Bound Electron” & “Two-Level Atom”

Wave function $\psi(x,t) = \psi(x)\ \mathrm{e}^{-\mathrm{j}\,\omega t}$ and dispersion relation:

$$\left[\frac{1}{2m_0}\left(\frac{\hbar}{\mathrm{j}}\frac{\partial}{\partial x}\right)^2 + V\right]\psi(x) = W\,\psi(x)\,, \qquad W = \hbar\omega = \frac{(\hbar k)^2}{2m_0} + V$$

Potential film ($\widehat{=}$ slab waveguide) with infinitely high walls. Solutions are spatial sinusoidals or superpositions of it:

$$\psi(x,t) = \mathrm{j}(1/\sqrt{2})\,\psi_2(x)\,\mathrm{e}^{-\mathrm{j}\,\omega_2 t} + (1/\sqrt{2})\,\psi_1(x)\,\mathrm{e}^{-\mathrm{j}\,\omega_1 t},$$

$$\omega_{21} = \omega_2 - \omega_1$$

Light-matter interaction of wave function $\psi(x,t)$ with electric field $E_0(t)$. Dipole moment $\mu = -e\,x$ leads to dipole energy $-\mu E_0(t)$:

$$\left[\frac{1}{2m_0}\left(\frac{\hbar}{\mathrm{j}}\frac{\partial}{\partial x}\right)^2 + V(x) + e\,x\,E_0(t)\right]\psi(x,t) = -\frac{\hbar}{\mathrm{j}}\frac{\partial}{\partial t}\,\psi(x,t)$$

Dipole approximation $\rightarrow$ t-dependent coefficients $c_{1,2}(t)\psi_{1,2}(x)$ $\rightarrow$ E_0-field with $\omega_0 = \omega_{21}$ $\rightarrow$ envelope with Rabi frequ. $\omega_{\mathcal{R}} = \frac{|\mu_{21}|\widehat{E}_0}{\hbar}$.

Luminescence and Laser Radiation

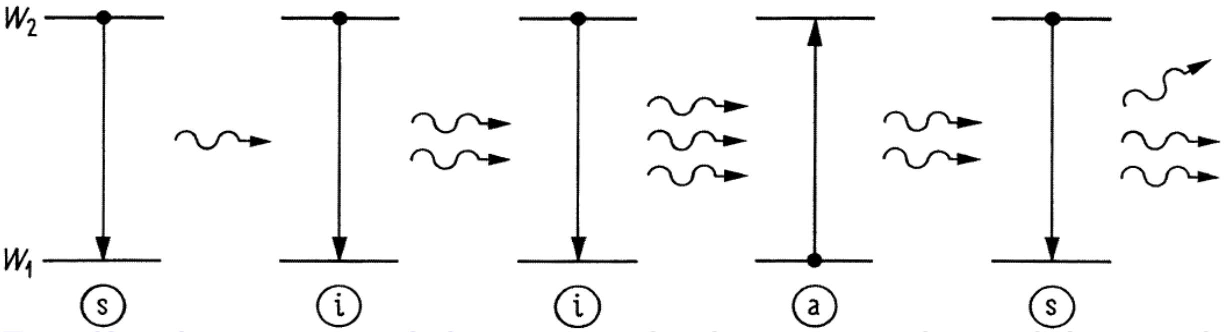

Excit. energy W_2 can be released by transition to lower-state energy W_1.

Radiative transition, emitting or absorbing photon $hf = W_2 - W_1$.

Fig. 3.2. Interaction of a two-level microsystem with electromagnetic radiation, photon energy $hf = W_2 - W_1$. (a) absorption, (s) spontaneous emission, and (i) induced (= stimulated) emission of photons

- Absorption Microsystem in ground state W_1 absorbs radiation at a frequency $f = (W_2 - W_1)/h \rightarrow$ upward transition to $W_2 \rightarrow$ induced or stimulated by an existing field.
- Spontaneous emission Excited microsystem in W_2 makes transition to ground state W_1 "spontaneously" by emitting a photon with energy $hf = W_2 - W_1$ after an average lifetime τ_{sp}.
- Induced emission $W_2 \rightarrow W_1$ induced or stimulated by radiation at $f = (W_2 - W_1)/h$. In contrast to SE: Phase coherence, same mode as stimulating radiation $\rightarrow$ amplification.

Laser Active Materials — Two-Level Systems (2)

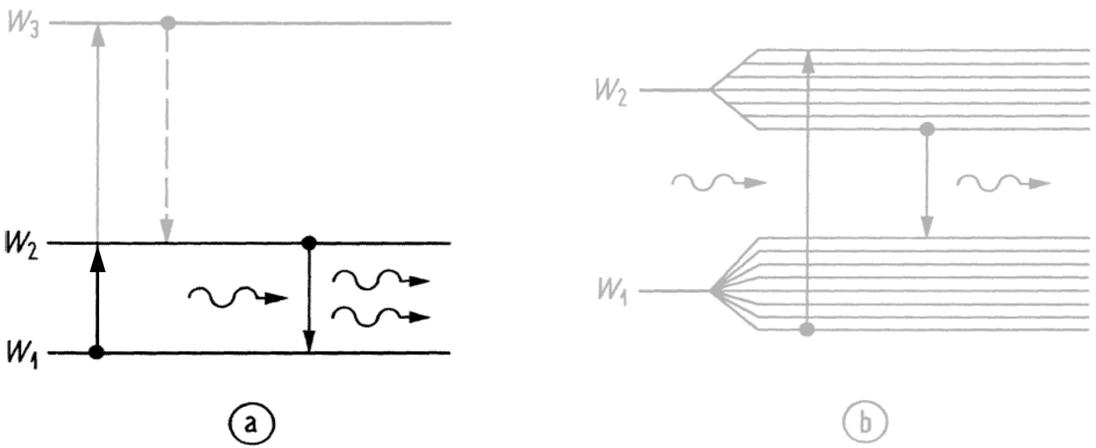

Fig. 3.3. Pump mechanism using energy levels (a) outside (three-level laser system) or (b) inside the energy level group of the laser transition (pseudo-four-level laser system)

SE reduces $N_2 \sim t$, induced emission reduces $N_2 \sim N_P t$. With elmag field of photon energy $hf \rightarrow$ dynamic equilibrium:

$$\text{(induced emissions)} = \text{(induced absorptions)}$$

For large N_P, SE is negligible $\rightarrow$ dynamic equilibrium $N_2 = N_1$ (with SE: $N_2 \leq N_1$). Medium is "transparent" in this case.

With two-level system no population inversion, no gain!

Laser Active Materials — Semiconductors

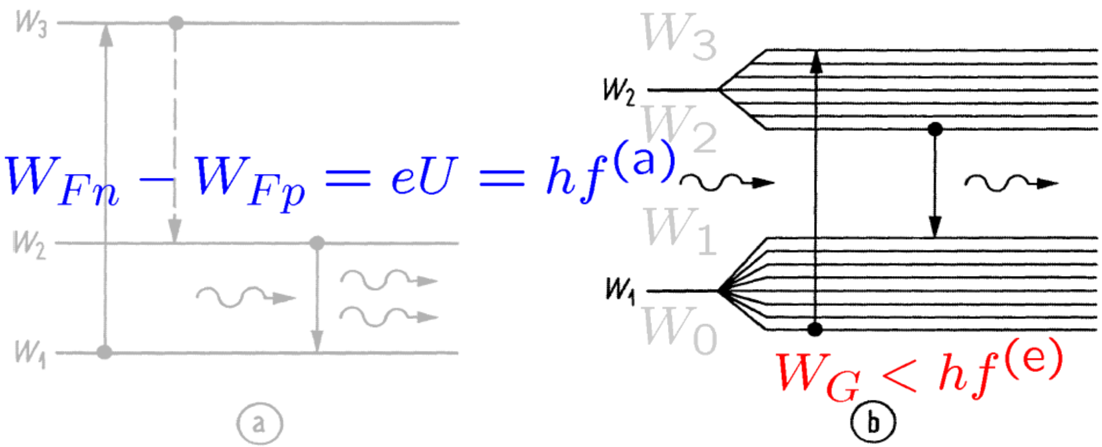

Result

$W_G < hf^{(e)} \leq hf^{(a)}$

LD acts also as PD.

Fig. 3.3. Pump mechanism using energy levels (a) outside (three-level laser system) or (b) inside the energy level group of the laser transition (pseudo-four-level laser system)

Levels W_2 and W_1 associated with conduction and valence band states. Absorbed pump $hf^{(a)}$ ($\widehat{=} W_3 - W_0$) generates electron-hole pairs. Also with forward biased pn-diode by injecting electrons and holes for a population inversion. At $T = 0$, forward voltage U defines "pump energy" $eU = hf^{(a)}$ = (energetic difference at which electrons and holes are injected) = (difference of the quasi Fermi levels).

Band Structure of Direct and Indirect Semiconductors

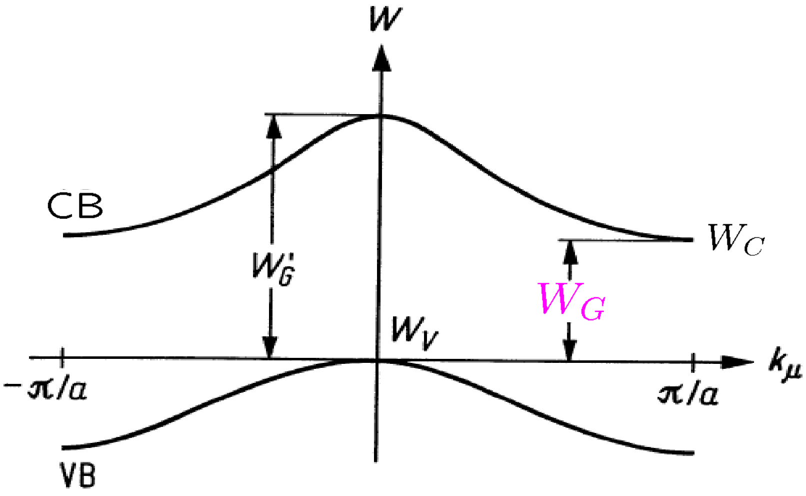

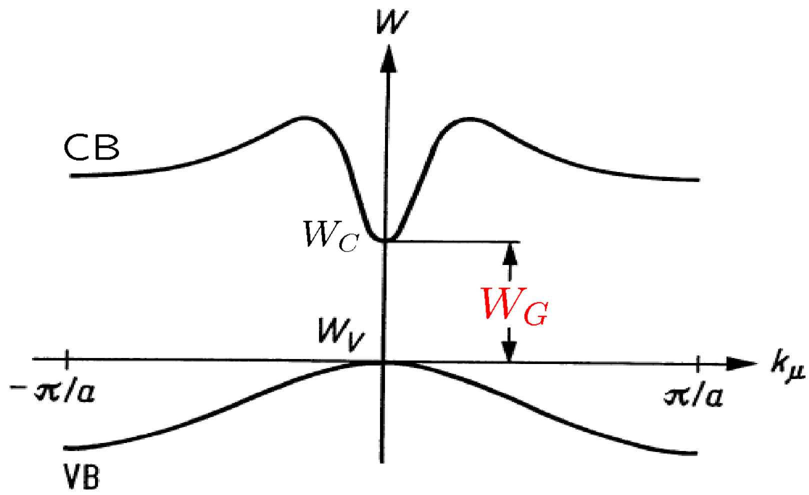

Indirect semicond. Smallest transition energy W_G for crystal momentum diff. $\Delta k_\mu = \pi/a$. Phonon required as collision partner $\rightarrow$ Radiative transition unlikely. Examples: Elemental semiconductors Si, Ge

$$W_G = \begin{cases} 0.67\,\text{eV} \,\widehat{=}\, 1.85\,\mu\text{m} & \text{(Ge)} \\ 1.13\,\text{eV} \,\widehat{=}\, 1.10\,\mu\text{m} & \text{(Si)} \end{cases}$$

$$W'_G = \begin{cases} 0.8\ \ \text{eV} \,\widehat{=}\, 1.55\,\mu\text{m} & \text{(Ge)} \\ 3.4\ \ \text{eV} \,\widehat{=}\, 0.36\,\mu\text{m} & \text{(Si)} \end{cases}$$

Direct semicond. Smallest transition energy W_G for crystal momentum difference $\Delta k_\mu = 0$. No collision partner required $\rightarrow$ Radiative transition likely. Examples: Compounds GaAs, InP, InGaAs

$$W_G = \begin{cases} 1.42\,\text{eV} \,\widehat{=}\, 0.87\,\mu\text{m} & \text{(GaAs)} \\ 1.80\,\text{eV} \,\widehat{=}\, 0.69\,\mu\text{m} & (\text{Ga}_{0.7}\text{Al}_{0.3}\text{As}) \\ 0.75\,\text{eV} \,\widehat{=}\, 1.65\,\mu\text{m} & (\text{In}_{0.53}\text{Ga}_{0.47}\text{As}) \\ 1.35\,\text{eV} \,\widehat{=}\, 0.92\,\mu\text{m} & \text{(InP)} \end{cases}$$

Radiative and Nonradiative Recombination

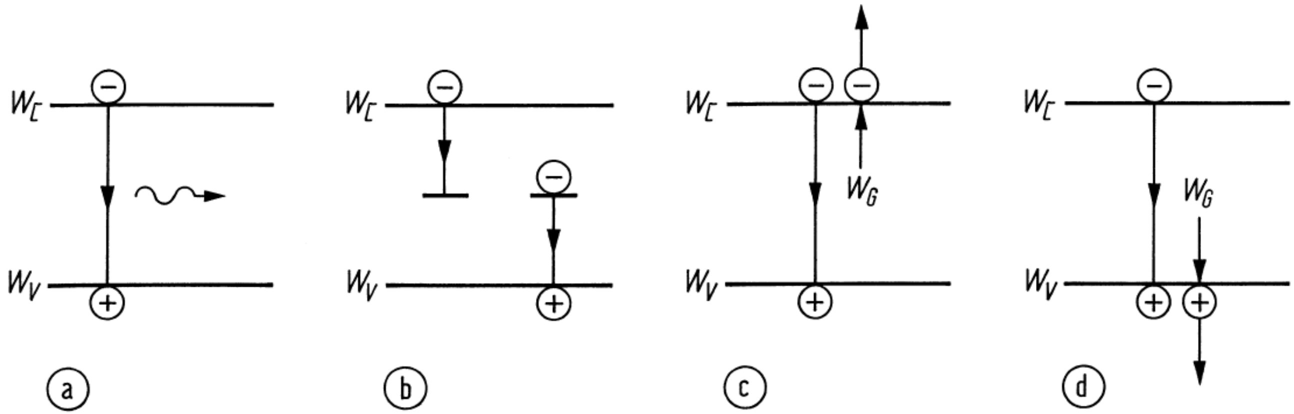

p-Si rad. lifetime $p_p = 10^{16}\,\mathrm{cm}^{-3}$:

$$\tau_{n\,\mathrm{sp}}^{-1} = \frac{\partial\, r_{\mathrm{sp}}}{\partial n_T}$$

$$\tau_{n\,\mathrm{sp}} = 33\,\mathrm{ms}$$

Radiative and nonradiative transitions. (a) Radiative band-band transition. (b) Nonradiative transition via localized states in the forbidden band. (c) (d) Nonradiative Auger recombinations (recombination energy excites excites an electron in the CB or in the VB)

Radiative recomb. (rate r_{sp}, unit $\mathrm{cm}^{-3}\,\mathrm{s}^{-1}$) of electrons and holes:

$$r_{\mathrm{sp}} = B n_T p, B = \begin{cases} 1 \quad \times 10^{-10} \ldots 7 \times 10^{-10}\,\mathrm{cm}^3\,\mathrm{s}^{-1} & \text{(Ga,Al)As} \\ 8.6 \times 10^{-11}\,\mathrm{cm}^3\,\mathrm{s}^{-1} & \text{(In,Ga)(As,P)} \\ 3 \quad \times 10^{-15}\,\mathrm{cm}^3\,\mathrm{s}^{-1} & \text{Si (indirect SC)} \end{cases}$$

Nonrad. recomb. (rate r_{ns}, unit $\mathrm{cm}^{-3}\,\mathrm{s}^{-1}$): Localized impurities, rate $r_{\ell S}$ (Shockley-Read-Hall, SRH). Recomb. energy transfered to e or h, rate r_{Au}, (Auger, in (In,Ga)(As,P) $\rightarrow$ h, not in (Ga,Al)As):

$$r_{\mathrm{ns}} = r_{\ell S} + r_{\mathrm{Au}}\,, \qquad r_{\ell S} = A n_T\,, \qquad r_{\mathrm{Au}} = C n_T p^2$$

Filling of Electronic States — Fermi Function

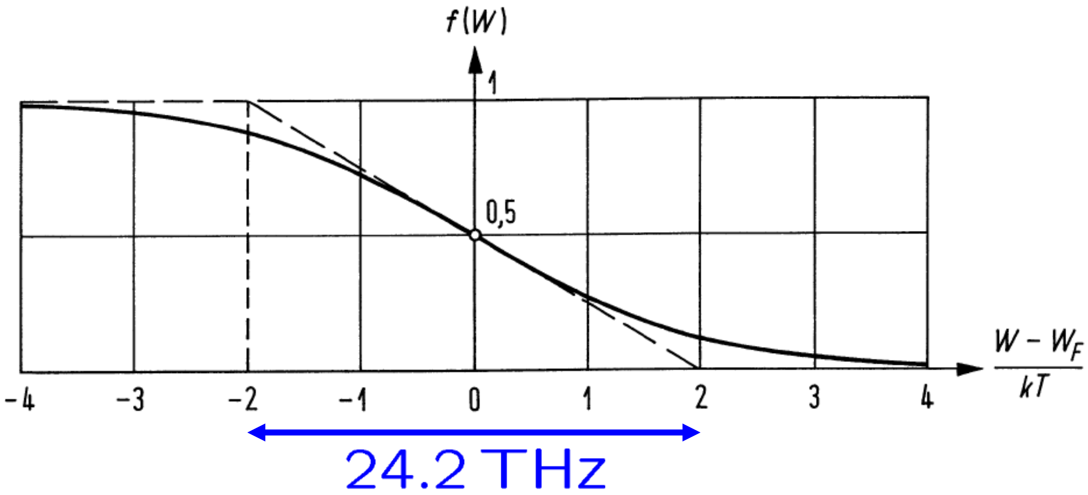

Fig. 3.8. Fermi function for band energy states ($g = 1$)

At $T = 0$ electrons fill lowest energy states. At $T > 0$ Fermi-Dirac distrib. (Fermi function):

$$f(W) = \frac{1}{1 + g \exp\left(\frac{W - W_F}{kT}\right)}$$

W_F is Fermi energy where occup. prob. $f(W) = 1/2$ at all T. Transit. "large $\to$ low": Occup. prob. $(0.88 \geq f(W) \geq 0.12)$ in region $4kT$ centred at W_F (at $T = 293\,\mathrm{K}$: $kT = 25\,\mathrm{meV}$ or $\Delta f = 2kT/h = 12.1\,\mathrm{THz}$). Boltzmann approximation:

$$f(W) \approx g \exp\left(-\frac{W - W_F}{kT}\right) \qquad \text{for } W - W_F > 3kT\,,$$

$$f(W) \approx 1 - g \exp\left(\frac{W - W_F}{kT}\right) \qquad \text{for } W - W_F < -3kT\,.$$

Density of states (parabolic bands $W_{C,V} \sim (\hbar k_\mu)^2/(2m_{n,p})$):

$$\rho_{\substack{C\\V}}(W) = \frac{1}{2\pi^2}\left(\frac{2|m_{\substack{n\\p}}|}{\hbar^2}\right)^{3/2}\sqrt{\pm(W - W_{\substack{C\\V}})}\,, \qquad N_{\substack{C\\V}} = 2\left(\frac{2\pi|m_{\substack{n\\p}}|kT}{h^2}\right)^{3/2}$$

Carrier concentrations in CB (n_T) and VB (p):

$$n_T = \int_{W_C}^{\infty} \rho_C(W)\, f(W)\, \mathrm{d}W, \qquad p = \int_{-\infty}^{W_V} \rho_V(W)\left[1 - f(W)\right]\mathrm{d}W$$

Boltzmann approximation (valid for $n_T \ll N_C$, $p \ll N_V$ only, i. e., nondegenerate doping; not true for semiconductor lasers!):

$$\left.\begin{aligned} n_T &= N_C \exp\left(-\frac{W_C - W_F}{kT}\right) \\ p &= N_V \exp\left(-\frac{W_F - W_V}{kT}\right) \end{aligned}\right\} \quad n_T p = n_i^2 = N_C N_V \exp\left(-\frac{W_G}{kT}\right)$$

Intrinsic carrier concentration n_i denotes electrons n_T (holes p) which are present pairwise in CB (VB) of pure undoped semiconductors at temperature T, independent of Fermi energy W_F.

Impurities, Doping and Carrier Concentration — Non-Equilibrium

Density of states (parabolic bands $W_{C,V} \sim (\hbar k_\mu)^2/(2m_{n,p})$):

$$\rho_{\substack{C\\V}}(W) = \frac{1}{2\pi^2}\left(\frac{2|m_{\substack{n\\p}}|}{\hbar^2}\right)^{3/2}\sqrt{\pm(W - W_{\substack{C\\V}})}\,, \qquad N_{\substack{C\\V}} = 2\left(\frac{2\pi|m_{\substack{n\\p}}|kT}{h^2}\right)^{3/2}$$

Carrier concentrations in CB (n_T) and VB (p):

$$n_T = \int_{W_C}^{\infty} \rho_C(W)\, f(W)\, \mathrm{d}W, \qquad p = \int_{-\infty}^{W_V} \rho_V(W)\left[1 - f(W)\right] \mathrm{d}W$$

Boltzmann approximation (valid for $n_T \ll N_C$, $p \ll N_V$ only, i. e., nondegenerate doping), quasi Fermi levels $W_{Fn,p}$:

$$\left.\begin{aligned} n_T &= N_C \exp\left(-\frac{W_C - W_{Fn}}{kT}\right) \\ p &= N_V \exp\left(-\frac{W_{Fp} - W_V}{kT}\right) \end{aligned}\right\} \qquad \begin{aligned} n_T p &= n_i^2 \exp\left(\frac{W_{Fn} - W_{Fp}}{kT}\right) \\ n_i^2 &= N_C N_V \exp\left(-\frac{W_G}{kT}\right) \end{aligned}$$

Intrinsic carrier concentration n_i denotes electrons n_T (holes p) which are present pairwise in CB (VB) of pure undoped semiconductors at temperature T, independent of Fermi energy W_F.

Quasi Fermi Levels in Non-Equilibrium

For laser threshold current $\rightarrow$ carrier concentrations n_T, p for shifting quasi Fermi levels W_{Fn}, W_{Fp} into bands. p-doped semiconductor with equilibrium concentration of n_{T0}, p_0 and $n_{T0}p_0 = n_i^2$. Carrier injection changes densities to $n_T = n_{T0} + \Delta n_T$, $p = p_0 + \Delta p$. Substitution into Fermi function:

$$W_{Fn} - W_F = kT \ln\left(1 + \frac{\Delta n_T}{n_{T0}}\right), \qquad W_F - W_{Fp} = kT \ln\left(1 + \frac{\Delta p}{p_0}\right)$$

Charge neutrality $\Delta p = \Delta n_T$. Carrier injection $\rightarrow$ quasi Fermi level of minority carriers shifts first (here: W_{Fn}; change of n_T by Δn_T has largest effect because n_{T0} is small). At $\Delta n_T / n_{T0} = 1$ shift amounts to $W_{Fn} - W_F = 0.7\,kT$. Because $p_0 \gg n_{T0}$ in a p-semiconductor, quasi Fermi level for majority carriers starts shifting at much higher injection current levels when $\Delta p = \Delta n_T$ reaches the order of p_0.

Abrupt pn-Homojunction in Equilibrium (Zero Bias)

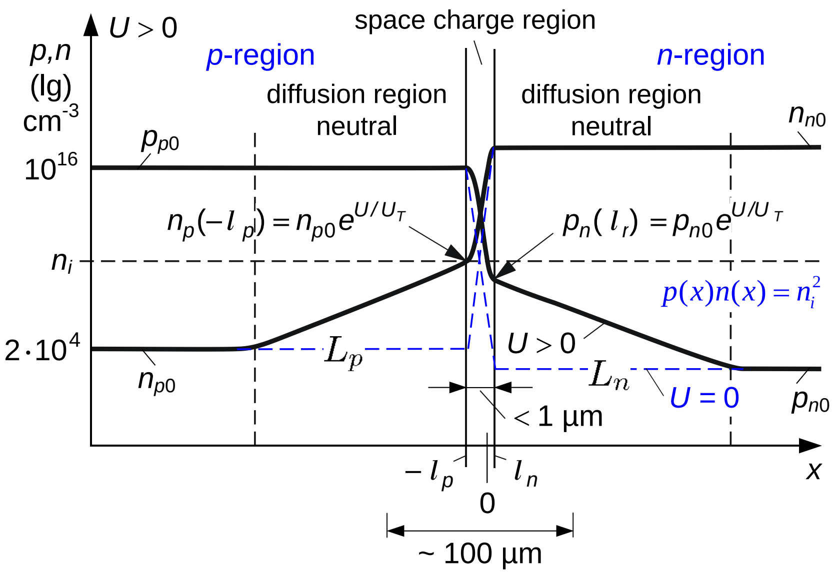

Equilibrium $U = 0$, zero current: p and n-type SC joined, majority electrons (holes) diffuse in p (n) region leaving positive (negative) donors (acceptors) in the *space charge region* → built-in potential (German: „Diffusionsspannung“):

$$U_D = U_T \ln \frac{n_D n_A}{n_i^2}, \quad U_T = \frac{kT}{e}$$

Built-in electric field draws minorities across the junction until the minority drift current compensates the majority diffusion current. For each x the mass action law holds:

(Electron concentration $n_T \widehat{=} n$) $$p(x)\, n_T(x) = n_i^2$$

Abrupt pn-Homojunction in Equilibrium (Zero Bias)

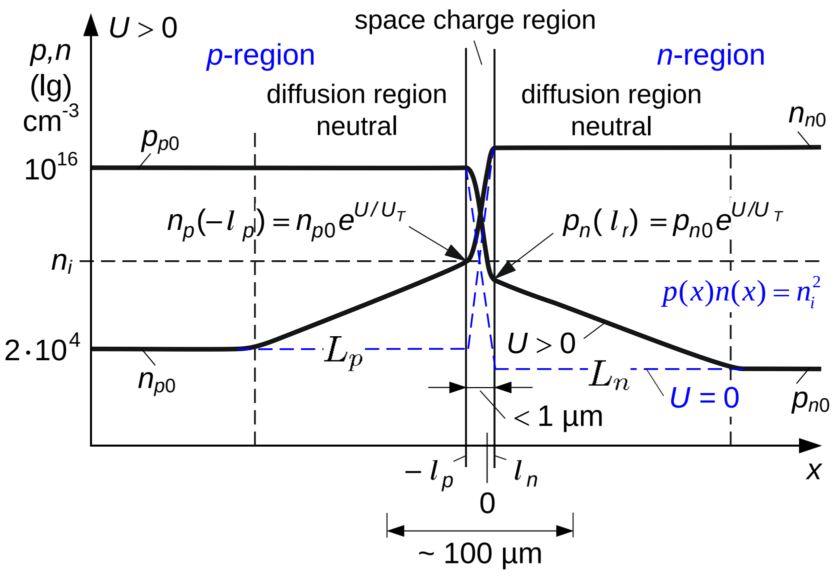

Equilibrium $U = 0$, zero current: p and n-type SC joined, majority electrons (holes) diffuse in p (n) region leaving positive (negative) donors (acceptors) in the *space charge region* $\rightarrow$ built-in potential (German: „Diffusionsspannung"):

$$U_D = U_T \ln \frac{n_D n_A}{n_i^2}, \quad U_T = \frac{kT}{e}$$

Built-in potential such that equilibrium Fermi energy is constant throughout junction:

$$eU(x) = W_{F_n}(x) - W_{F_p}(x) = 0$$

Equilibrium between carriers of conduction and valance band.

(Electron concentration $n_T \mathrel{\widehat{=}} n$)

Abrupt pn-Homojunction in Non-Equilibrium (Non-Zero Bias)

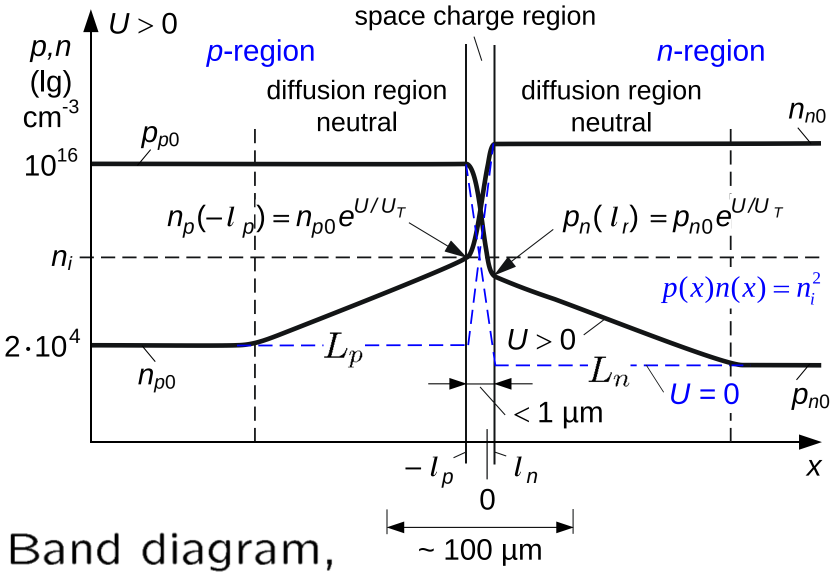

Band diagram,
quasi Fermi levels $W_{Fn,p}$

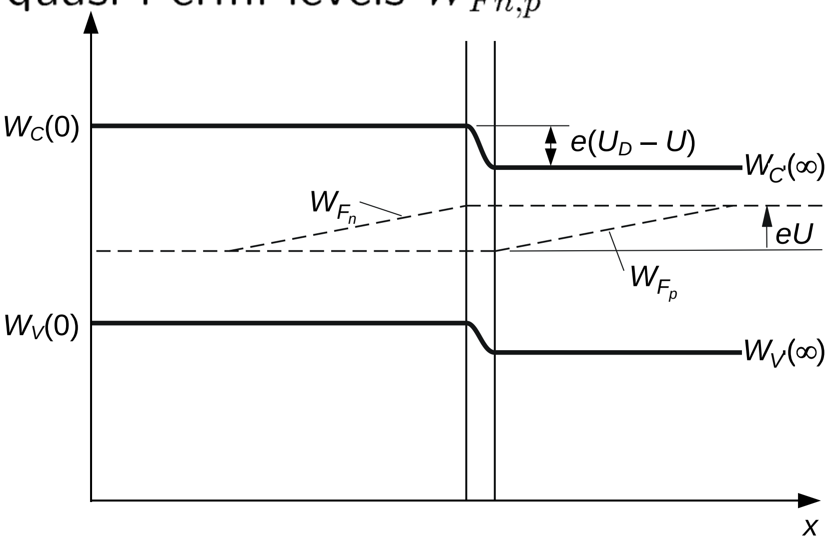

Non-equilibrium $U > 0$, forward current: Built-in potential reduced by bias U to $U_D - U$:

$$eU(x) = W_{F_n}(x) - W_{F_p}(x)$$

Increased crossing probab. for majorities → diff. current ≫ saturated minority current i_S, ext. current I:

$$I = i_S \exp\left(\frac{U}{U_T}\right) - i_S$$

Non-equilibrium $U \ll U_T$, reverse current: Built-in potential increased → diffusion current negligible wrt minority current i_S:

$$I = i_S \exp\left(\frac{-|U|}{U_T}\right) - i_S \approx -i_S$$

Abrupt pn-Homojunction in Non-Equilibrium (Non-Zero Bias)

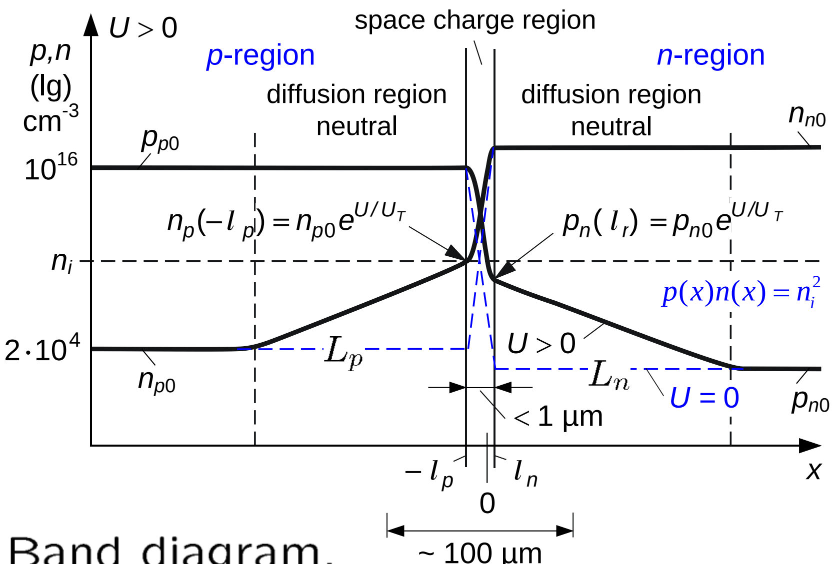

Band diagram, quasi Fermi levels $W_{Fn,p}$

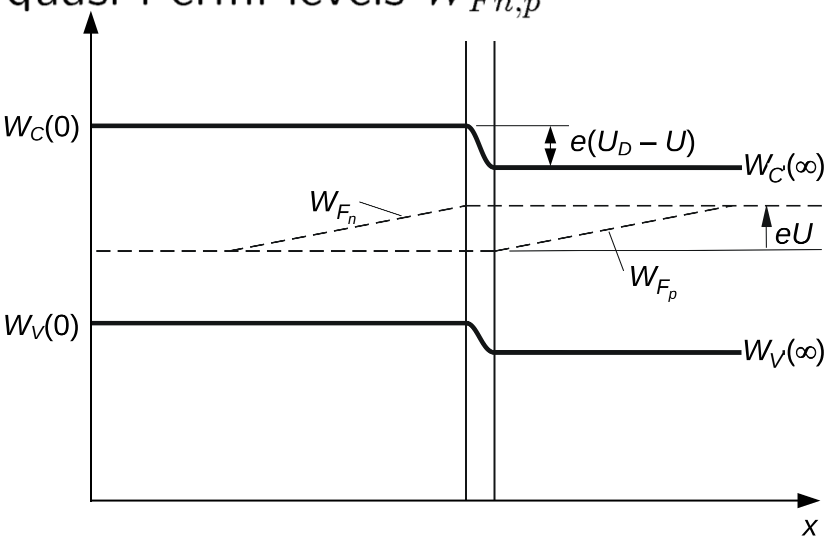

Non-equilibrium $U > 0$, forward current: Built-in potential reduced by bias U to $U_D - U$:

$$eU(x) = W_{F_n}(x) - W_{F_p}(x)$$

Increased crossing probab. for majorities $\rightarrow$ diff. current $\gg$ saturated minority current i_s, ext. current I:

$$I = i_s \exp\left(\frac{U}{U_T}\right) - i_s$$

Quasi Fermi levels $W_{Fn,p}$ result. Carriers inside respective bands still in equilibrium, but no equilibrium between carriers of conduction and valence bands.

Abrupt pn-Homojunction — Radiative / Nonradiative Recombinat.

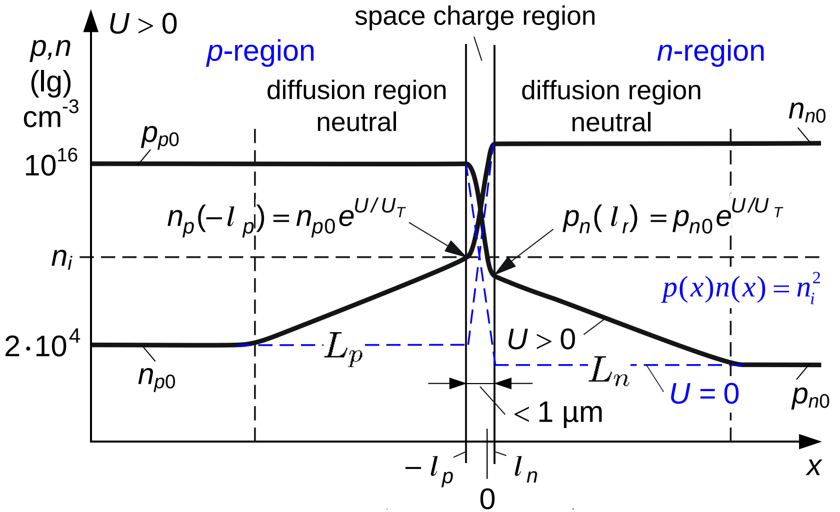

Recombination described by minorities' lifetimes $\tau_{n,p}$ in (p,n)-semiconductor (diffusion constants $D_{n,p}$, diffusion lengths $L_{n,p}$, electron n and hole concentration p):

$$\tau_{n,p}=\frac{L_{n,p}^2}{D_{n,p}}, \qquad \tau_{n\,\mathrm{sp,\,ns}}^{-1}=\frac{\partial\, r_{\mathrm{sp,\,ns}}}{\partial n_T p}$$

Radiative recomb. (rate r_{sp}, unit cm^{-3} s^{-1}) of electrons and holes:

$$r_{\mathrm{sp}}=Bn_Tp,\, B=\begin{cases}1\ \ \times 10^{-10}\ldots 7\times 10^{-10}\,\mathrm{cm^3\,s^{-1}} & \text{(Ga,Al)As}\\ 8.6\times 10^{-11}\,\mathrm{cm^3\,s^{-1}} & \text{(In,Ga)(As,P)}\\ 3\ \ \times 10^{-15}\,\mathrm{cm^3\,s^{-1}} & \text{Si (indirect SC)}\end{cases}$$

Nonrad. recomb. (rate r_{ns}, unit cm^{-3} s^{-1}): Localized impurities, rate $r_{\ell\mathrm{S}}$ (Shockley-Read-Hall, SRH). Recomb. energy transfered to e or h, rate r_{Au}, (Auger, in (In,Ga)(As,P) $\rightarrow$ h, not in (Ga,Al)As):

$$r_{\mathrm{ns}}=r_{\ell\mathrm{S}}+r_{\mathrm{Au}}\,,\qquad r_{\ell\mathrm{S}}=An_T\,,\qquad r_{\mathrm{Au}}=Cn_Tp^2$$

LECTURE 10

Radiative and Nonradiative Recombination

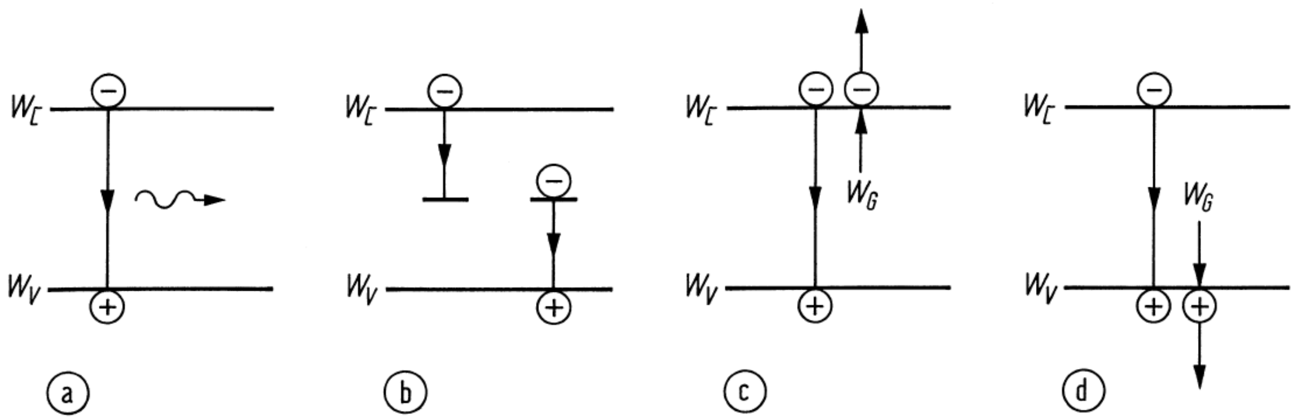

p-Si rad. lifetime
$p_p = 10^{16}\,\text{cm}^{-3}$:

$$\tau_{n\,\text{sp}}^{-1} = \frac{\partial\, r_\text{sp}}{\partial n_{Tp}}$$

$$\tau_{n\,\text{sp}} = 33\,\text{ms}$$

Radiative and nonradiative transitions. (a) Radiative band-band transition. (b) Nonradiative transition via localized states in the forbidden band. (c) (d) Nonradiative Auger recombinations (recombination energy excites excites an electron in the CB or in the VB)

oʒe

Radiative recomb. (rate r_sp, unit $\text{cm}^{-3}\,\text{s}^{-1}$) of electrons and holes:

$$r_\text{sp} = B n_T p,\; B = \begin{cases} 1 \times 10^{-10} \ldots 7 \times 10^{-10}\,\text{cm}^3\,\text{s}^{-1} & \text{(Ga,Al)As} \\ 8.6 \times 10^{-11}\,\text{cm}^3\,\text{s}^{-1} & \text{(In,Ga)(As,P)} \\ 3 \times 10^{-15}\,\text{cm}^3\,\text{s}^{-1} & \text{Si (indirect SC)} \end{cases}$$

Nonrad. recomb. (rate r_ns, unit $\text{cm}^{-3}\,\text{s}^{-1}$): Localized impurities, rate $r_{\ell\text{S}}$ (Shockley-Read-Hall, SRH). Recomb. energy transfered to e or h, rate r_Au, (Auger, in (In,Ga)(As,P) $\rightarrow$ h, not in (Ga,Al)As):

$$r_\text{ns} = r_{\ell\text{S}} + r_\text{Au}\,, \qquad r_{\ell\text{S}} = A n_T\,, \qquad r_\text{Au} = C n_T p^2$$

Compound Semiconductors (1)

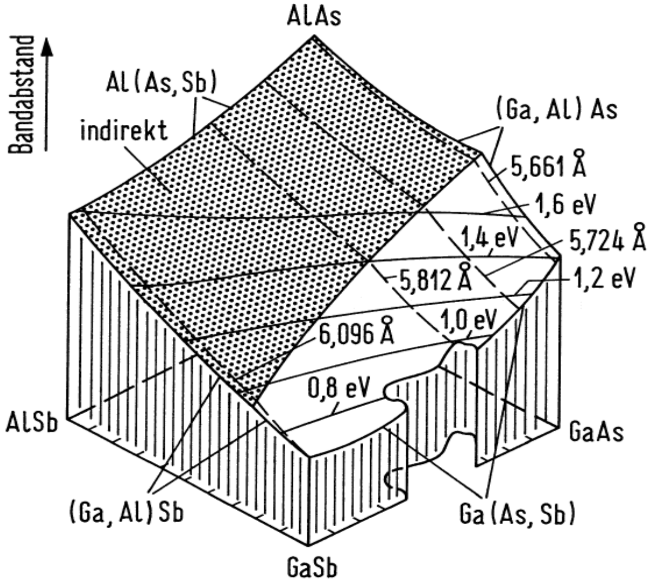

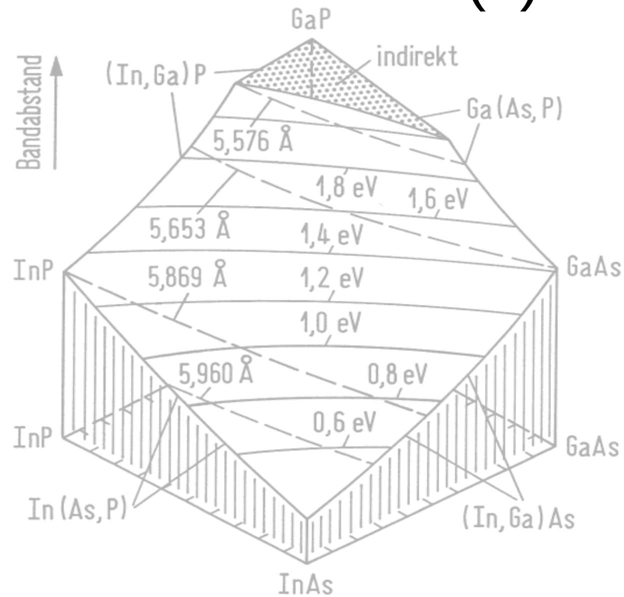

Semiconductor	$W_G/\,\mathrm{eV}$ ($\lambda_G/\,\mu\mathrm{m}$)	n at λ_G	$a/\mathrm{Å}$
GaSb, direct	0.726 (1.708)	3.82	6.096
GaAs, direct	1.424 (0.871)	3.655	5.653
AlSb, indirect	1.58 (0.785)	3.4	6.135
AlAs, indirect	2.163 (0.573)	3.178	5.660
$(\mathrm{Ga}_{1-x}\mathrm{Al}_x)\mathrm{As}$ direct: $x \leq 0.3$	$1.424 + 1.247\,x$ $1.424 \ldots 1.798$ $(0.871 \ldots 0.69)$	$3.59 - 0.71\,x +$ $+0.091\,x^2$ (at $\lambda = 0.9\,\mu\mathrm{m}$)	$5.653 + 0.027\,x$
$(\mathrm{Ga}_{1-x}\mathrm{Al}_x)(\mathrm{As}_y\mathrm{Sb}_{1-y})$ lattice-matched to GaSb direct: $x \leq 0.24$ $y = x/1.11$	$0.726 + 0.834\,x +$ $+1.134\,x^2$ $0.726 \ldots 0.991$ $(1.708 \ldots 1.25)$	?	6.096

Table 3.1. Material system $(\mathrm{Ga}_{1-x}\mathrm{Al}_x)(\mathrm{As}_y\mathrm{Sb}_{1-y})$. W_G bandgap, $\lambda_G = hc/W_G$ bandgap wavelength, n refractive index, a lattice constant

Compound Semiconductors (2)

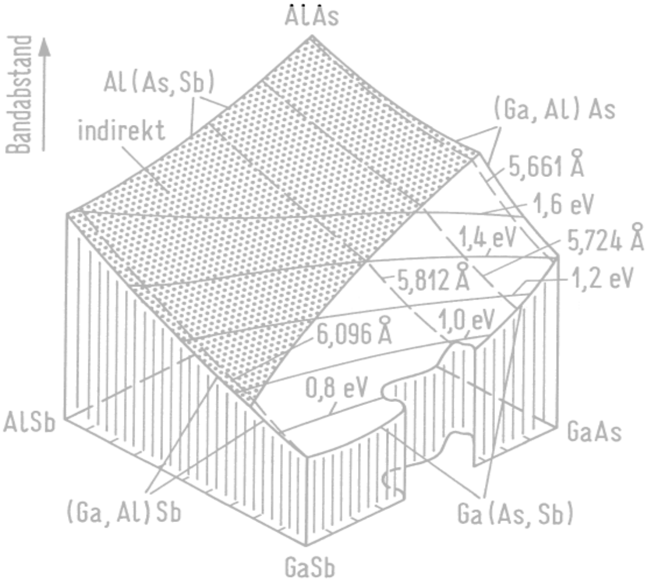

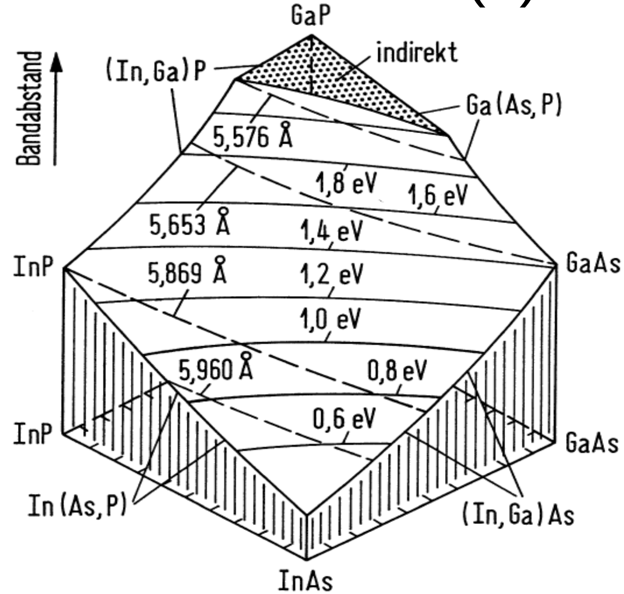

Semiconductor	W_G/ eV (λ_G/ μm)	n at λ_G	a/Å
InAs, direct	0.36 (3.444)	3.52	6.058
InP, direct	1.35 (0.918)	3.45	5.869
GaAs, direct	1.424 (0.871)	3.655	5.653
GaP, indirect	2.261 (0.548)	3.452	5.451
$(In_{0.49}Ga_{0.51})P$, direct lattice-matched to GaAs	1.833 (0.676)	3.451 ?	5.653
$(In_{0.53}Ga_{0.47})As$, direct lattice-matched to InP	0.75 (1.653)	3.61	5.869
$(In_{1-x}Ga_x)(As_yP_{1-y})$ lattice-matched to InP direct: $y \leq 1$ $x = y/(2.2091 - 0.06864\,y)$	$1.35 - 0.72\,y+$ $+0.12\,y^2$ $1.35 \ldots 0.75$ $(0.918 \ldots 1.653)$	$3.45 + 0.256\,y -$ $-0.095\,y^2$ $3.45 \ldots 3.61$	5.869

Table 3.2. Material system $(In_{1-x}Ga_x)(As_yP_{1-y})$. W_G bandgap, $\lambda_G = hc/W_G$ bandgap wavelangth, n refractive index, a lattice constant

Opto-Electronic Integrated Circuits

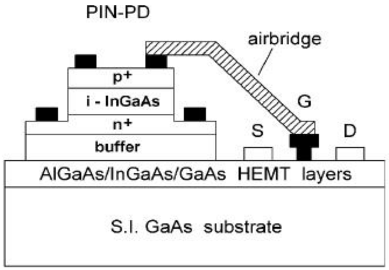

(a) InGaAs PIN photodiode on GaAs. Air bridge to HEMT amplifier[17]

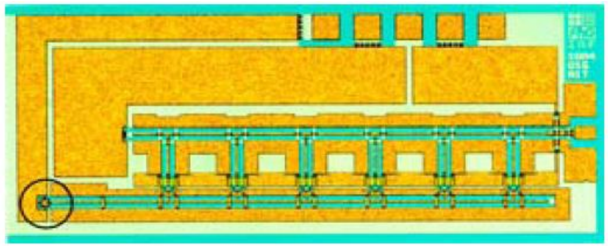

(b) Photodiode (◯) with 30 Ω coplanar transmission lines and 6 interconnecting cascoded HEMT[17]

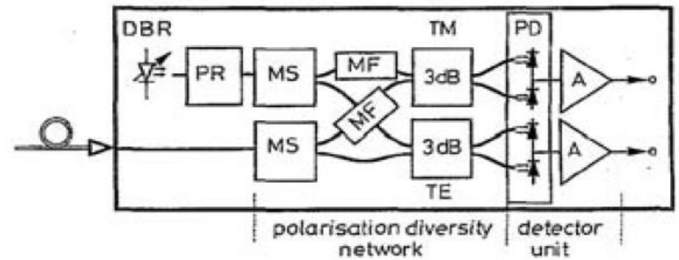

(c) Polarization diversity heterodyne receiver integrated on InP substrate with local laser, couplers, detectors, and electronics[18]

Fig. 3.5. Advanced OEIC designs. (a) Top-illuminated $(In_{0.53}Ga_{0.47})As$ pin photodiode on a semi-insulating (S.I.) GaAs substrate. Diameter of light-sensitve area $10\,\mu m$, sensitivity $S = 0.4\,A\,/\,W$, dark current 9 nA at -2 V bias (b) 40 Gbit, 6-stage travelling wave amplifier, HEMT gate length $0.15\,\mu m$. Processing time 3 months, chip size $2.5\,mm \times 1\,mm$ on a 3-in wafer (c) Optical polarization diversity heterodyne receiver with tunable local distributed Bragg reflector laser (DBR), polarization rotator (PR), mode splitters (MS), mode filters (MF), 3 dB couplers, photodiodes (PD), and electronic amplifiers (A) consisting of JFET and load resistors. Processing time 5 months, 25 mask steps, 7 epitaxy steps, 170 main processing steps, 2 in wafer, 100 receiver chips $9\,mm \times 0.6\,mm$, carrying 17 sub-components, yield $> 50\,\%$

Examples of early opto-electronic integrated circuits (OEIC):

GaAs Hybridly integrated 40 Gbit / s pin HEMT receiver (1998).

InP Monolithically integrated optical heterodyne receiver with tunable local distributed feedback (DFB) laser, polarization diversity reception and detector unit (1994).

Heterojunctions

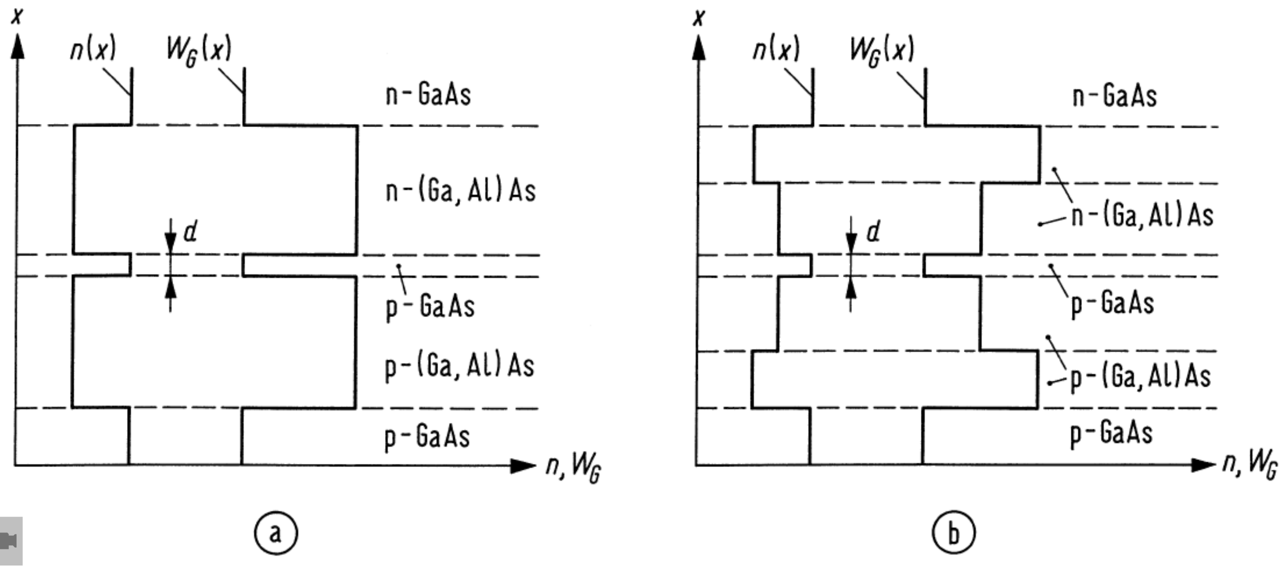

Fig. 3.11. Schematic refractive index dependence n and bandgap W_G as a function of the spatial coordinate x in a (a) 3-layer heterostructure, (b) 5-layer heterostructure

"Isotype" if semiconductors have same conduction type.

"Anisotype" if conduction type differs.

Conduction type with small letters n, i, p if semiconductor has smaller bandgap than neighbour, and with capital letters N, I, P if bandgap is larger.

Fig. 3.11(a) from top: nN, Np, pP and Pp

Band Diagram for Heterostructures

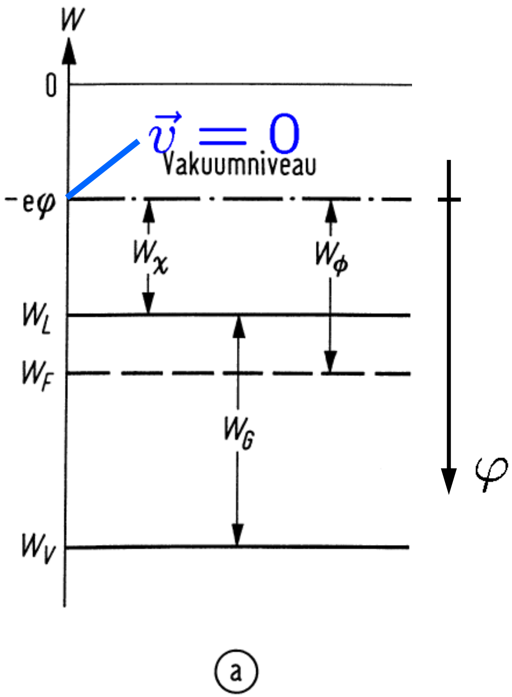

Fig. 3.12. Energy scale for electrons in a semiconductor. (a) Semiconductor at potential $\varphi \neq 0$. (b) Two independent, insulated semiconductors at potential $\varphi = 0$ with different bandgaps. W_χ electron affinity, W_ϕ work function. W_L conduction band edge ($\widehat{=} W_C$, Vacuumniveau $\widehat{=}$ vacuum level)

e leaving at $\vec{v} = 0$ are at vacuum level $W = -e\varphi$. e-affinity W_χ, work function W_ϕ. $W_G = W_C - W_V$, W_χ, W_ϕ fix distances of CB edge, Fermi level, VB edge wrt vacuum level.

Band Diagram for Heterostructures

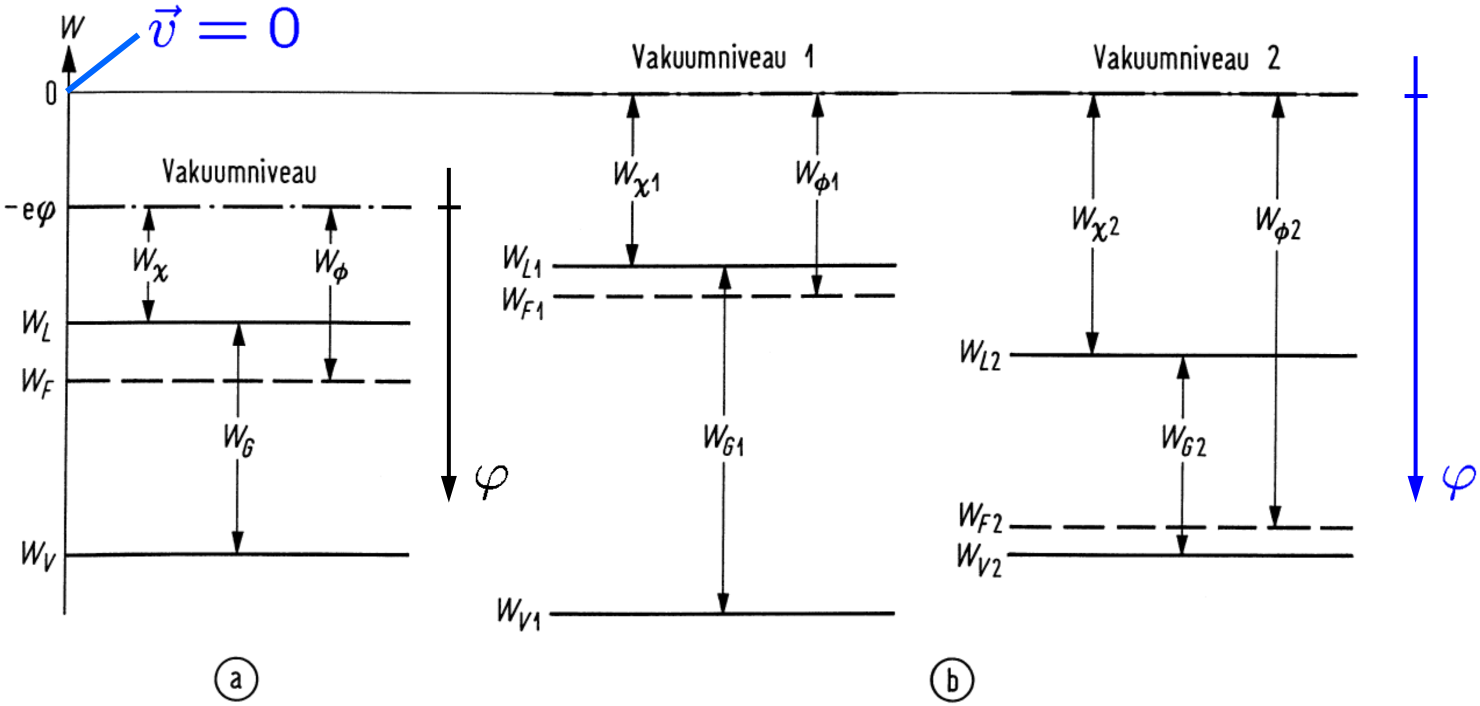

Fig. 3.12. Energy scale for electrons in a semiconductor. (a) Semiconductor at potential $\varphi \neq 0$. (b) Two independent, insulated semiconductors at potential $\varphi = 0$ with different bandgaps. W_χ electron affinity, W_ϕ work function. W_L conduction band edge ($\widehat{=}\, W_C$, Vacuumniveau $\widehat{=}$ vacuum level)

e leaving at $\vec{v} = 0$ are at vacuum level $W = -e\varphi$. e-affinity W_χ, work function W_ϕ. $W_G = W_C - W_V$, W_χ, W_ϕ fix distances of CB edge, Fermi level, VB edge wrt vacuum level.

Band Diagram of a Left-Alone NpP-Heterojunction

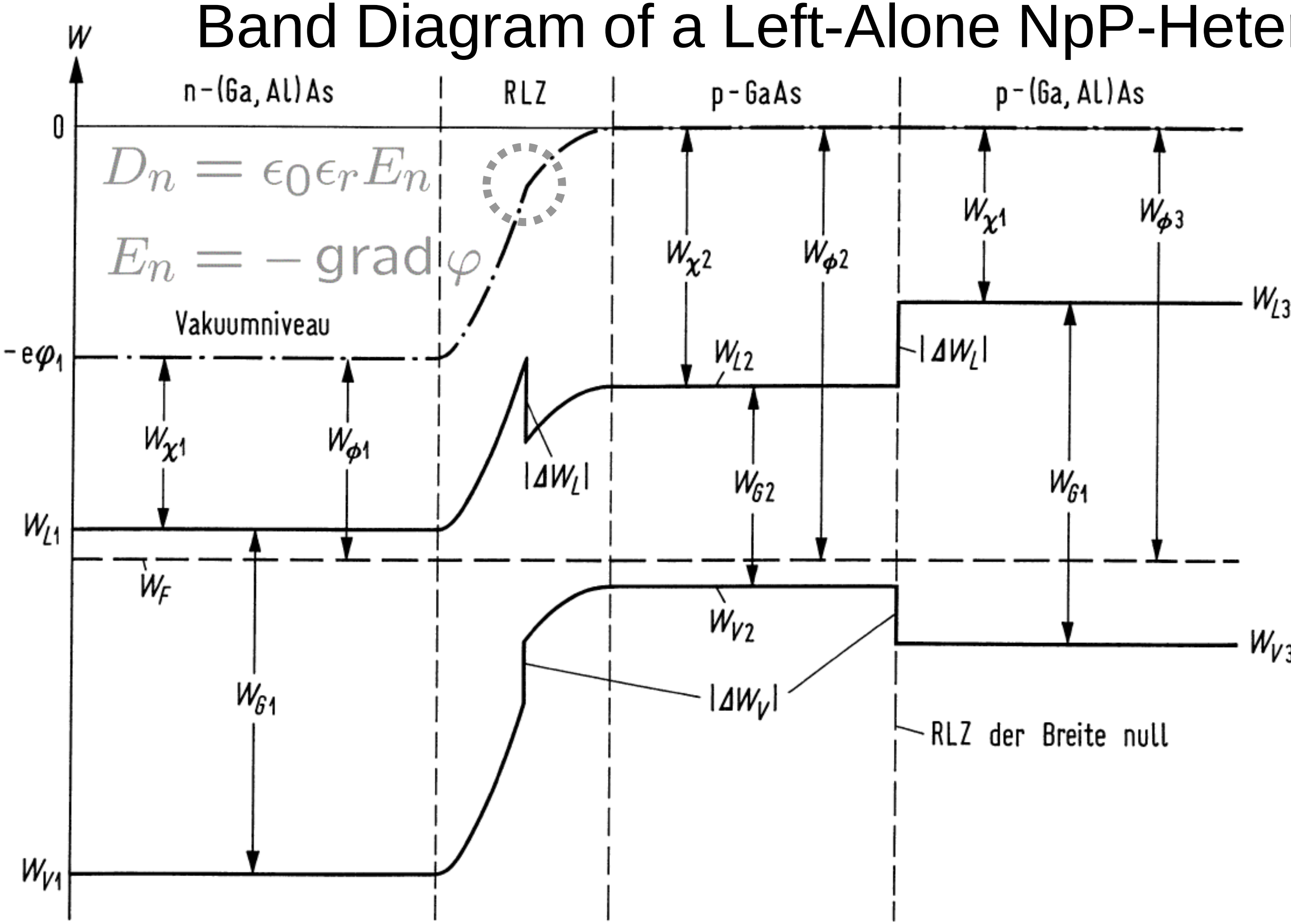

Shallow saturated impurities, $n_{T1} = n_D$, $p_2 = n_A$

Homojunction:

Diffusion voltage or built-in potential U_D (thermal voltage U_T)

Effective DOS:

$$N_B = 2\left(\frac{2\pi|m_{\text{eff}}|kT}{h^2}\right)^{\frac{3}{2}}$$

Fig. 3.13. Energy-band diagram of a double-heterostructure with anisotype Np-junction and a special isotype pP-junction with diffusion voltage zero ($W_L \mathrel{\widehat{=}} W_C$, Leitungsband $\widehat{=}$ conduction band, Vakuumniveau $\widehat{=}$ vacuum level, Raumladungszone RLZ der Breite null $\widehat{=}$ space-charge region of zero width)

$$\varphi_1 = U_D = U_T \ln\frac{n_D n_A}{n_i^2}, \qquad U_T = \frac{kT}{e}, \qquad W_G = -kT \ln\frac{n_i^2}{N_C N_V}$$

Band Diagram of a Forward-Biased NpP-Heterojunction

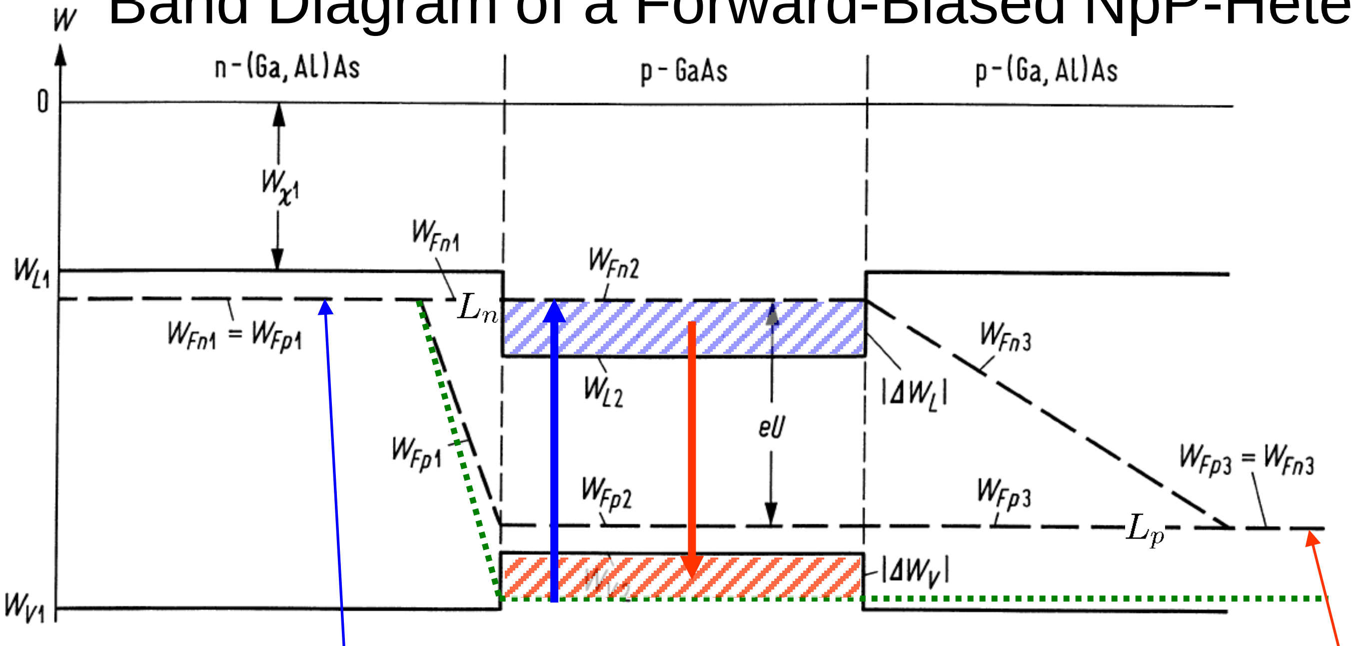

Practical for $T > 0$.
Simpler for $T = 0$:

Fig. 3.14. Energy-band diagram of a NpP-heterojunction of Fig. 3.13 with a forward bias voltage. $L_p/L_n \approx 0.2$ for GaAs ($W_L \mathrel{\hat{=}} W_C$)

Far away from junction, quasi Fermi levels of e, h unchanged. Inside thin p-GaAs layer and DZ, $W_{Fn} > W_{Fp}$ due to carrier injection. $L_n > L_p \rightarrow p$-DZ larger than n-DZ. GaAs: $L_n/L_p = 5$. e, h confined to potential well inside p-GaAs layer. Quasi Fermi level W_{Fn} moved into CB. $\rightarrow hf^{(\mathrm{a})} \geq W_{Fn} - W_{Fp} = eU \quad \rightarrow W_G < hf^{(\mathrm{e})} \leq eU$

Bulk SOA Structure for Doping Design Study at $\lambda = 1.55\,\mu\text{m}$

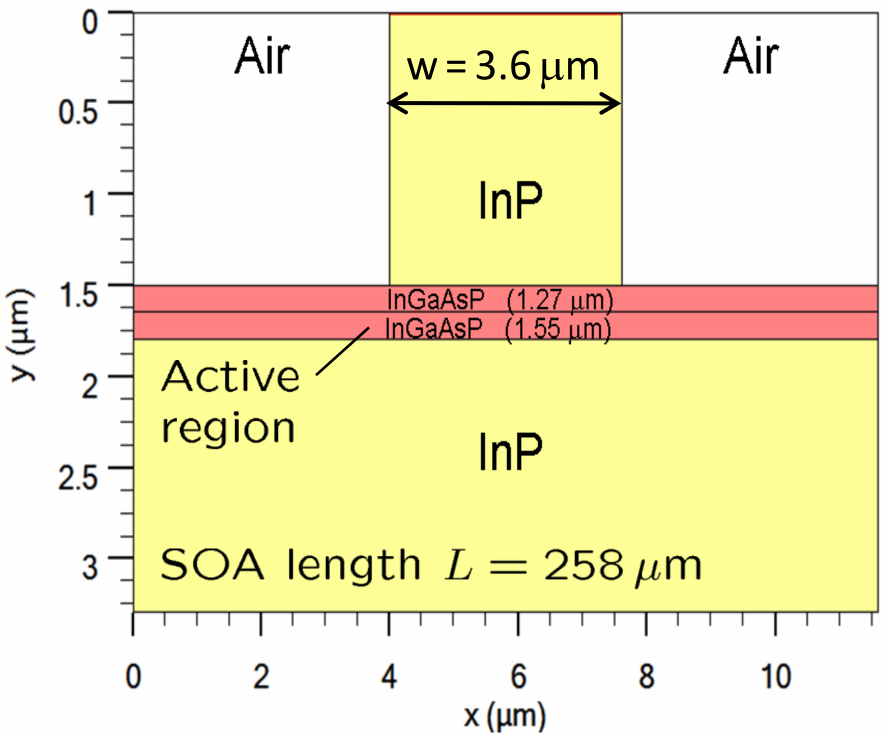

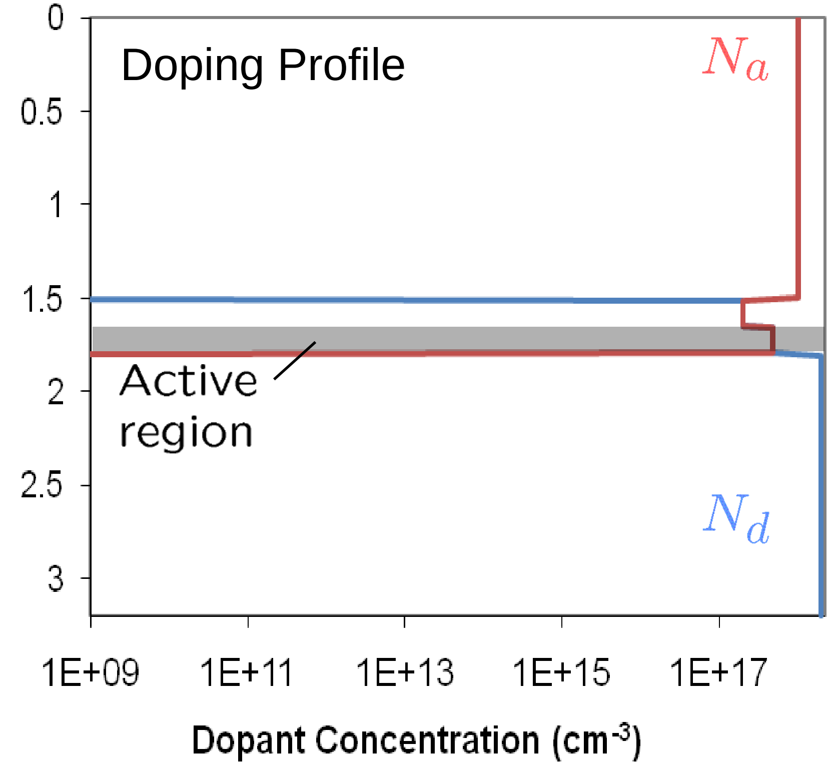

Tendencies calculated* *ab initio* with Silvaco ATLAS (modified for simulating SOA). Use of well-characterized† bulk-SOA for checking relevance of simulation results.

* Kapoor, A.; Sharma, E. K.; Freude, W.; Leuthold, J.: Investigation of the saturation characteristics of InGaAsP-InP bulk SOA. Photonics West 2010. Paper 7597-56

† Leuthold, J.: Advanced indium-phosphide waveguide Mach-Zehnder interferometer all-optical switches and wavelength converters. Konstanz: Hartung-Gorre 1999

Bulk SOA — Trends for Doping the Active Region ($\lambda = 1.55\,\mu\text{m}$)

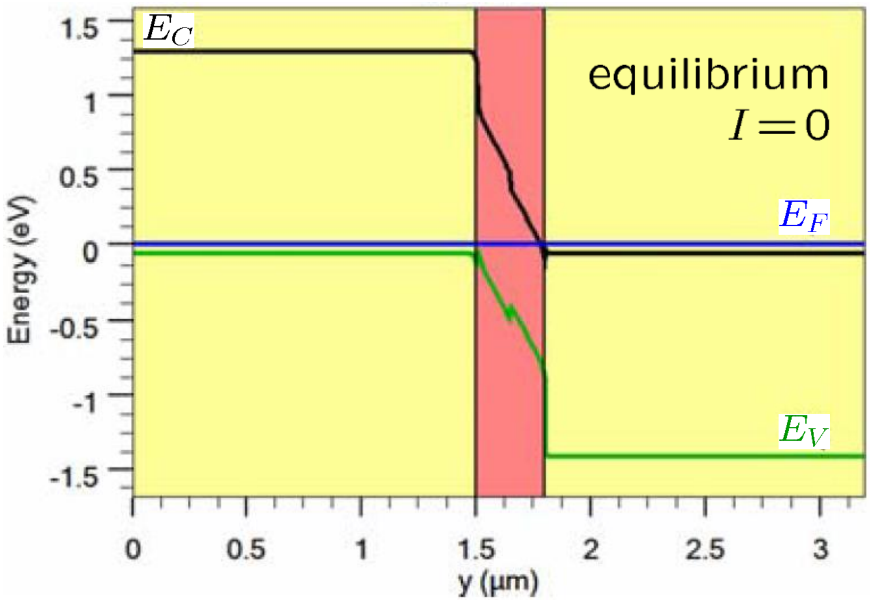

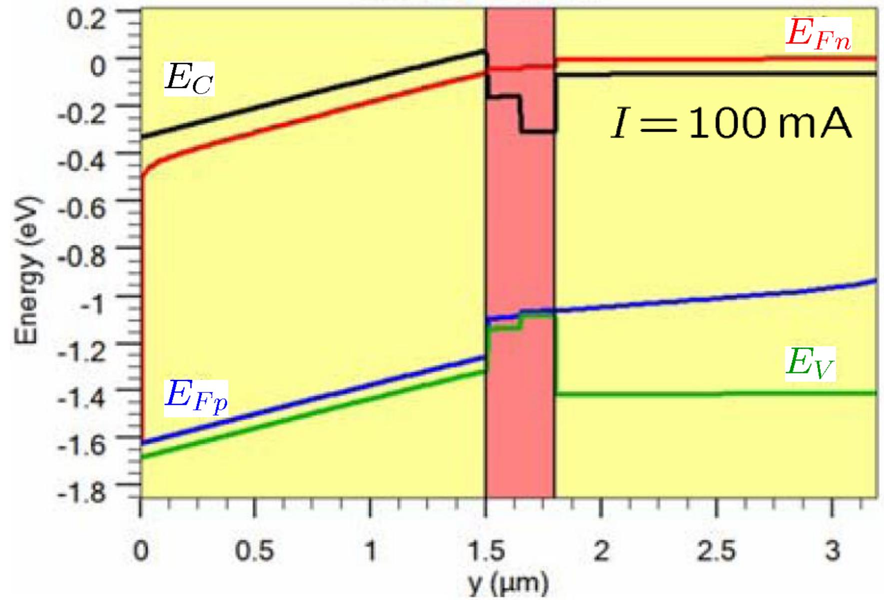

p-doping (n-doping) shifts quasi-Fermi level E_{Fp} more into (away from) the valence band → increases (decreases) small-signal gain constant g_0 and differential gain a → decreases (increases) $P_{\text{sat}}^{\text{in}}$:

$$P_{\text{in}}^{\text{sat}} = \frac{2\ln 2}{G_0 - 2} hf \frac{A/\Gamma}{a\,\tau_e}, \quad G_0 = \mathrm{e}^{\Gamma g_0 L} \qquad P_{\text{sat}}^{\text{in}} \Downarrow \qquad P_{\text{sat}}^{\text{in}} \Uparrow$$

However, there are other influences: a & τ_e (besides Γ & L)!

Emission and Absorption in a Semiconductor. Amplification

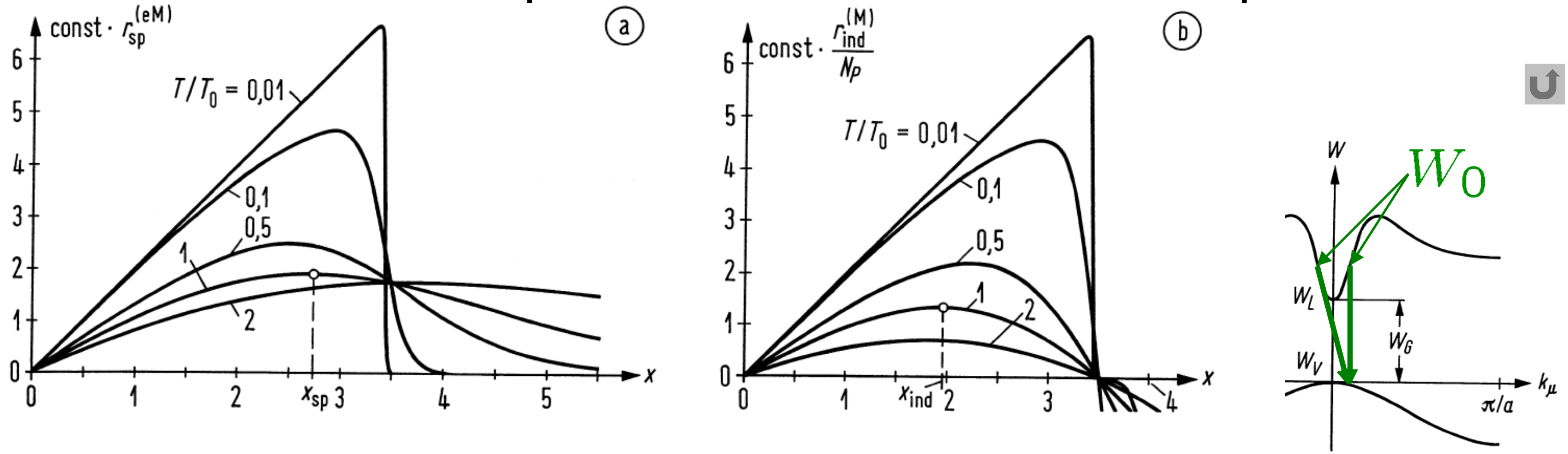

Fig. 3.15. Frequency dependence of spontaneous and induced emission for various temperatures $T/T_0 = 0.01$, 0.1, 0.5, 1, 2 (T_0 reference temperature; $W_{Fn} - W_C$ and $W_V - W_{Fp}$ are kept constant to $3\,kT_0$ and $0.5\,kT_0$, respectively; $m_n/m_p = 0.14$ as in GaAs). Normalized frequency $x = (hf - W_G)/(kT_0)$. (a) Spontaneous emission and (b) induced emission per photon, Eq. (3.44). The multiplicative constant is identical in both diagrams.

$$r_{\mathrm{ind}}^{(\mathrm{M})} = r_{\mathrm{ind}}^{(\mathrm{eM})} - r_{\mathrm{ind}}^{(\mathrm{aM})} \sim N_P\left[f_C(W_0) - f_V(W_0 - hf)\right],$$

$$r_{\mathrm{sp}}^{(\mathrm{eM})} \sim f_C(W_0)\left[1 - f_V(W_0 - hf)\right],$$

$$W_0 = W_C + \frac{\hbar^2 k_{\mu 0}^2}{2m_n}$$

Gain rate:

$$\left.\begin{aligned} r_{\mathrm{ind}}^{(\mathrm{M})} &= \frac{1}{V}\frac{\mathrm{d}N_P}{\mathrm{d}t} \\ G &= \frac{1}{N_P}\frac{\mathrm{d}N_P}{\mathrm{d}t} \end{aligned}\right\} \quad G = \frac{r_{\mathrm{ind}}^{(\mathrm{M})}}{N_P/V}$$

LECTURE 11

Emission and Absorption in a Semiconductor. Measurement

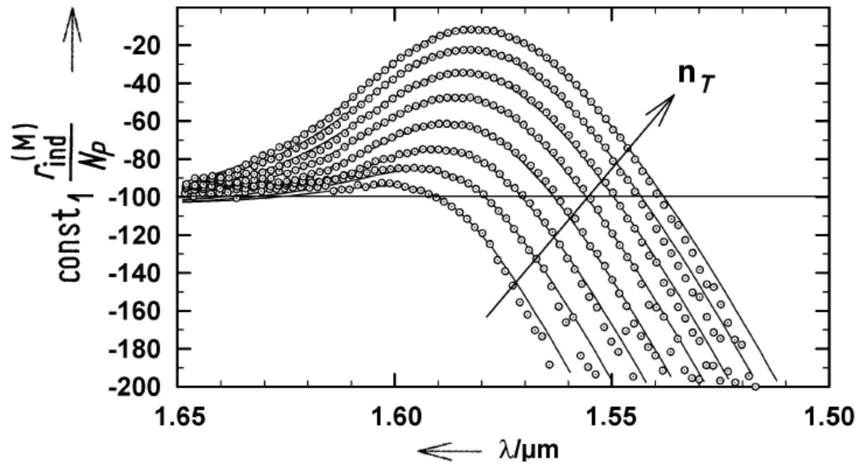

Measured wavelength dependence of induced emission per photon for various carrier densities n_T. The multiplicative constant is different from Fig. 3.15

$$r_{\mathrm{ind}}^{(\mathrm{M})} = r_{\mathrm{ind}}^{(\mathrm{eM})} - r_{\mathrm{ind}}^{(\mathrm{aM})}$$
$$\sim N_P \left[f_C(W_0) - f_V(W_0 - hf) \right],$$
$$r_{\mathrm{sp}}^{(\mathrm{eM})} \sim f_C(W_0) \left[1 - f_V(W_0 - hf) \right],$$
$$W_0 = W_C + \frac{\hbar^2 k_{\mu 0}^2}{2 m_n}$$

Gain rate:

$$\left. \begin{aligned} r_{\mathrm{ind}}^{(\mathrm{M})} &= \frac{1}{V} \frac{\mathrm{d}N_P}{\mathrm{d}t} \\ G &= \frac{1}{N_P} \frac{\mathrm{d}N_P}{\mathrm{d}t} \end{aligned} \right\} \quad G = \frac{r_{\mathrm{ind}}^{(\mathrm{M})}}{N_P / V}$$

Radiative and Nonradiative Recombination

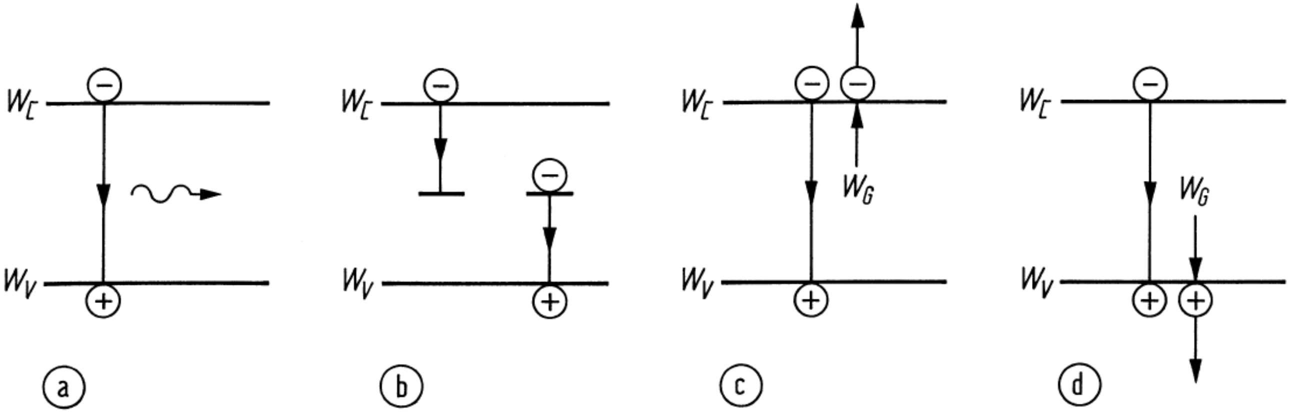

p-Si rad. lifetime
$p_p = 10^{16}\,\text{cm}^{-3}$:

$$\tau_{n\,\text{sp}}^{-1} = \frac{\partial r_\text{sp}}{\partial n_T}$$

$$\tau_{n\,\text{sp}} = 33\,\text{ms}$$

Radiative and nonradiative transitions. (a) Radiative band-band transition. (b) Nonradiative transition via localized states in the forbidden band. (c) (d) Nonradiative Auger recombinations (recombination energy excites excites an electron in the CB or in the VB)

Radiative recomb. (rate r_sp, unit $\text{cm}^{-3}\,\text{s}^{-1}$) of electrons and holes:

$$r_\text{sp} = B n_T p,\; B = \begin{cases} 1 \times 10^{-10} \ldots 7 \times 10^{-10}\,\text{cm}^3\,\text{s}^{-1} & \text{(Ga,Al)As} \\ 8.6 \times 10^{-11}\,\text{cm}^3\,\text{s}^{-1} & \text{(In,Ga)(As,P)} \\ 3 \times 10^{-15}\,\text{cm}^3\,\text{s}^{-1} & \text{Si (indirect SC)} \end{cases}$$

Nonrad. recomb. (rate r_ns, unit $\text{cm}^{-3}\,\text{s}^{-1}$): Localized impurities, rate $r_{\ell\text{S}}$ (Shockley-Read-Hall, SRH). Recomb. energy transfered to e or h, rate r_Au, (Auger, in (In,Ga)(As,P) $\rightarrow$ h, not in (Ga,Al)As):

$$r_\text{ns} = r_{\ell\text{S}} + r_\text{Au}\,, \qquad r_{\ell\text{S}} = A n_T\,, \qquad r_\text{Au} = C n_T p^2$$

Effective Carrier Recombination Lifetime. Step Response

Effective recombination rate:

$$r_{\text{eff}} = r_{\text{sp}} + r_{\text{ns}} = r_{\text{sp}} + r_{\ell\text{S}} + r_{\text{Au}}$$

In diode recombination zone (layer height d, cross-section area F) carrier density changes if injected carrier rate (injection current density J, elementary charge e) deviates from recombination rate:

$$\frac{\mathrm{d}n_T}{\mathrm{d}t} = \frac{J}{ed} - r_{\text{eff}}(n_T)$$

Strictly speaking, $r_{\text{eff}}(n_T) \to r_{\text{eff}}(n_T) - r_{\text{eff}}(n_{T\,\text{eql}})$ for correct solution at concentration $n_{T\,\text{eql}}$ for thermal equilibrium $J = 0$.
Step perturbation $J \to J_0 + J_1$. Perturbation ansatz $n_T(t) = n_{T0} + n_{T1}(t)$, series expansion $r_{\text{eff}} = r_{\text{eff}\,0} + (\partial r_{\text{eff}}/\partial n_T)n_{T1}$ at n_{T0}:

$$n_{T1}(t) = \frac{J_1 \tau_{\text{eff}}}{ed}\left(1 - \mathrm{e}^{-t/\tau_{\text{eff}}}\right), \quad \text{with} \quad \tau_{\text{eff}}^{-1} = \frac{\partial r_{\text{eff}}}{\partial n_T}$$

LED — Generated Power, Internal and Optical Efficiency

Light-emitting diodes (LED) without end mirrors, spontaneous emission rate $r_{\mathrm{sp}}^{(\mathrm{eM})}$ dominates. Double-heterostructures common. Generated light power P:

$$P = \frac{n_T F d \cdot hf}{\tau_{\mathrm{sp}}} = \eta_{\mathrm{int}}\, hf\, \frac{I}{e}, \qquad \eta_{\mathrm{int}} = \frac{\tau_{\mathrm{eff}}}{\tau_{\mathrm{sp}}} = \frac{P/(hf)}{I/e}$$

Isotropic emission into 4π. Fraction $(1 - R_P)\,\Omega_P/(4\pi)$ (TIR solid angle Ω_P, cone semi-angle $\pi/2 - \vartheta_T$) into medium $n_1 < n_2$ (GaAs):

$$n_1 \mathrel{\widehat{=}} \text{air (silica)}: \qquad \eta_{\mathrm{opt}} = \frac{\Omega_P}{4\pi}(1 - R_P) = 1.5\,\%\ (3.5\,\%)$$

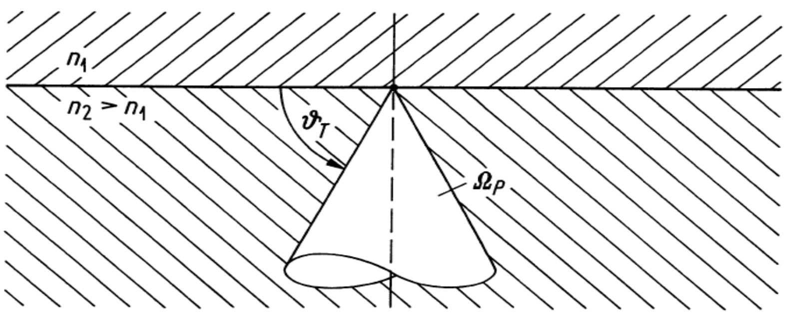

$$\left\{\begin{aligned} \Omega_P &= 2\pi(1 - \sin\vartheta_T) = 0.27\,\mathrm{sr}\ (0.54\,\mathrm{sr}) \\ \cos\vartheta_T &= n_1/n_2 \qquad = 73^\circ \quad (66^\circ) \\ R_P &= \left(\frac{n_1 - n_2}{n_1 + n_2}\right)^2 \quad = 32\,\% \quad (18\,\%) \end{aligned}\right.$$

Plane boundary between two media ($n_1, n_2 > n_1$ refractive indices, ϑ_T critical angle of total reflection, R_P power reflection factor). Only the fraction $(1 - R_P)$ of the radiation from the solid angle Ω_P is transmitted into the medium n_1.

LED — Device Structure. Surface and Edge Emitter, SLED

Small-area high-radiance (Ga,Al)As double-heterostructure surface-emitter LED with attached fibre (Burrus diode). Epoxydharz = epoxy resin, Anschlußdraht = bond wire, Metallkontakt = metal contact, Metallisierung = metallization

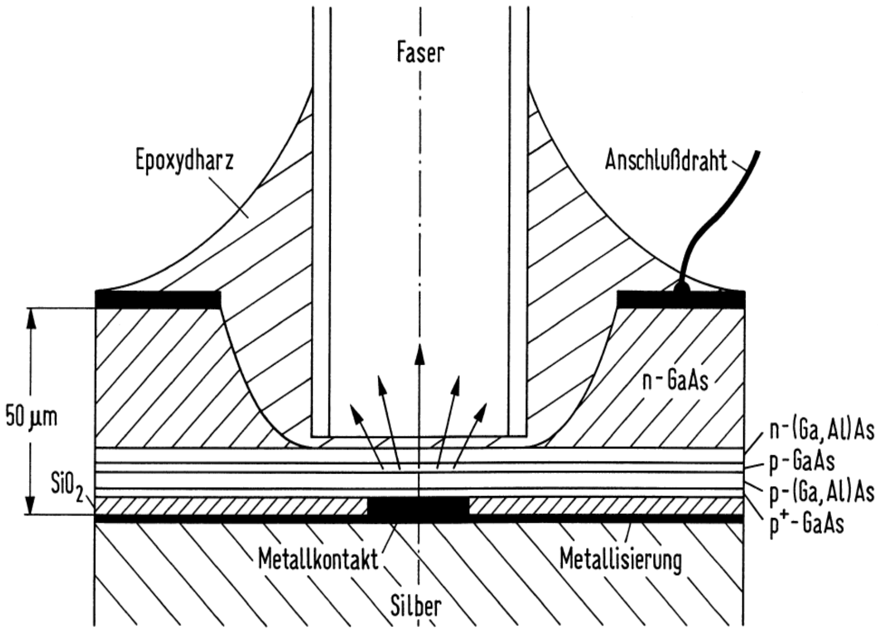

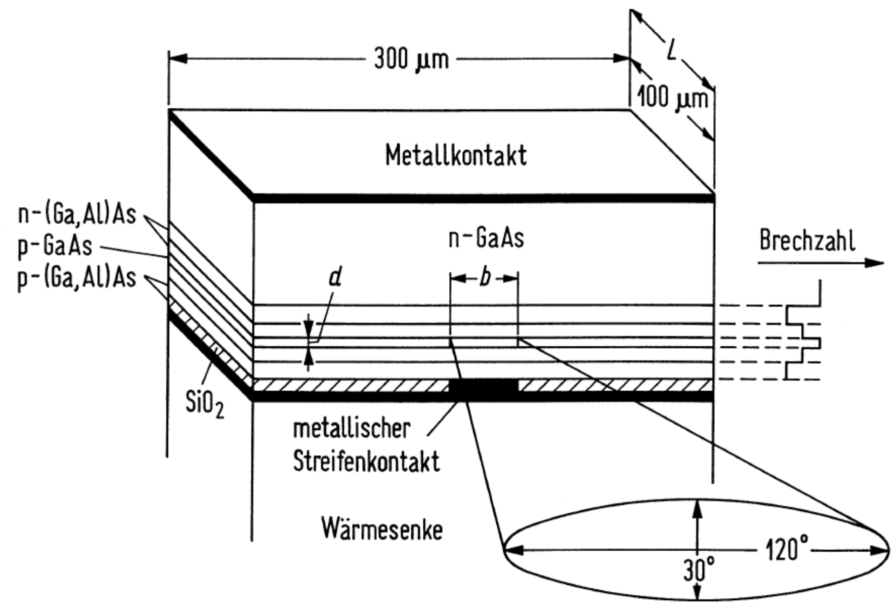

Fig. 3.20. Edge-emitting double-heterostructure LED. L, b, d are length, width and thickness of the active zone. Metallkontakt = metal contact, metallischer Streifenkontakt = metallic contact strip, Wärmesenke = heat sink, Brechzahl = refractive index

LED — Power Spectrum

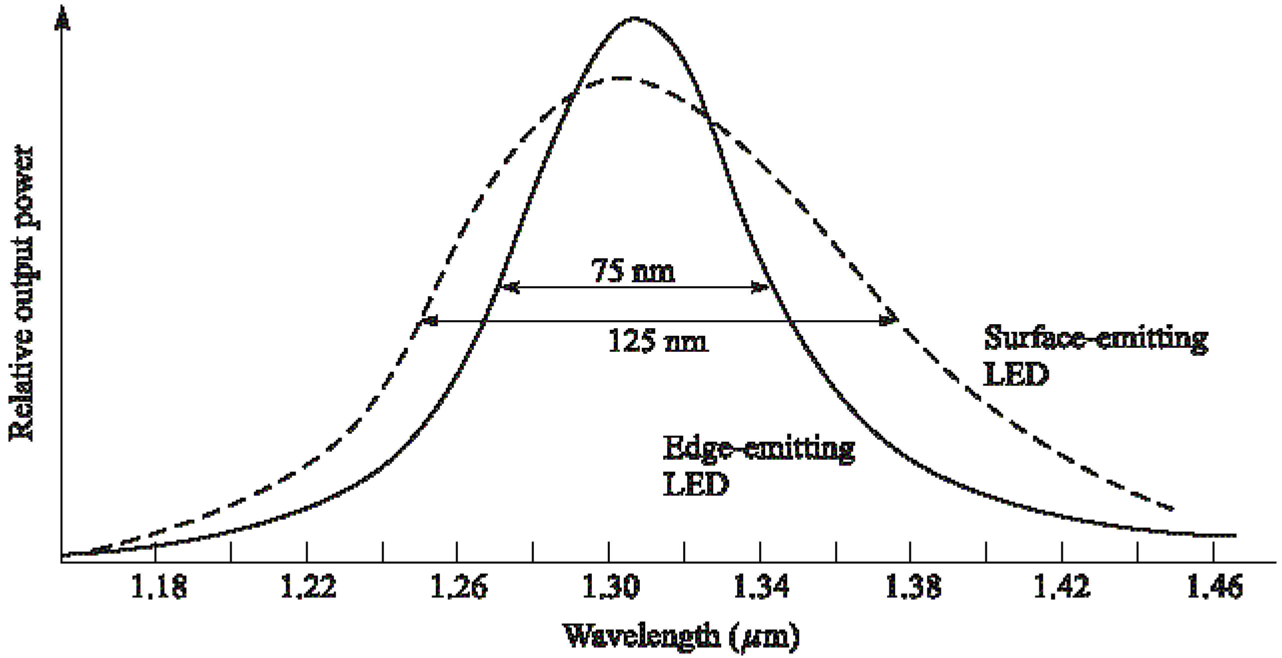

Photons emitted in spectral range $W_G \leq hf \leq (W_C + 2kT_0) - W_V$.
Total spectral emission width $h\,\Delta f_H = 2kT_0$:

$$h\,\Delta f_H = 2\,kT_0 = 50\,\text{meV}, \qquad \Delta f_H = 12.1\,\text{THz} \qquad \text{RT } T_0 = 293\,\text{K}$$

GaAs: $\Delta\lambda_H = 30\,\text{nm}$. (In,Ga)(As,P): $\Delta\lambda_H = 70\,\text{nm}$ at $\lambda = 1.3\,\mu\text{m}$.
Δf_{gain} also estimates amplification bandwidth of semiconductor laser devices. Corresponds to width Δf_H of lineshape $\rho(f)$.

LD — Cavity and Field Confinement

Conventional laser diode (LD) has rectangular cavity → Fabry-Perot (FP) resonator → Fabry-Perot laser diode (FP LD). Structure similar to LED edge-emitter.

Laser-active volume $V = dbL$ dimensions $d = 0.1 \ldots 0.2\,\mu\text{m}$ (vertical, x-axis), $b = 2 \ldots 5\,\mu\text{m}$ (lateral, y-axis), $L = 300 \ldots 1\,200\,\mu\text{m}$, (longitudinal, z-axis).

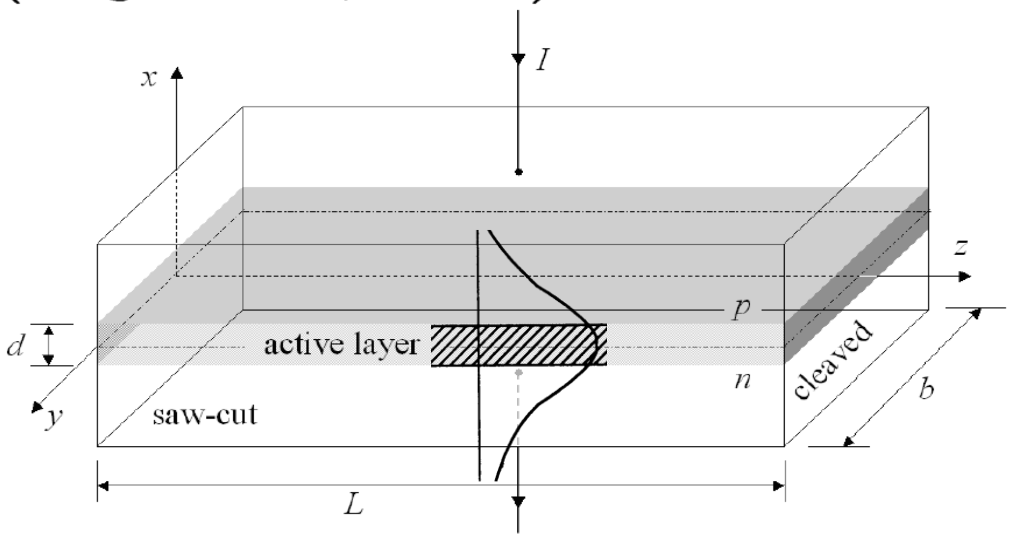

Field confinement:

$$\Gamma_{\text{TE}} = \frac{\int_{-d/2}^{+d/2} |E_y(x)|^2 \, \mathrm{d}x}{\int_{-\infty}^{+\infty} |E_y(x)|^2 \, \mathrm{d}x}$$

LD: $\Gamma_{\text{TE (TM)}} = .184\,(.145)$

SOA: $.3\,(.25)$ LD → TE

$d = .1 \rightarrow .2\,\mu\text{m}$: $\Gamma = .2 \rightarrow .6$

Fig. 3.6. Forward biased semiconductor pn-homojunction acting as a laser diode. Side-walls are saw-cut, the end facets are cleaved. Typical dimensions: $d = 0.1 \ldots 0.2\,\mu\text{m}$ (active layer), $b = 3 \ldots 6\,\mu\text{m}$, $L = 200 \ldots 600\,\mu\text{m}$

LD — Longitudinal Mode Spectrum

Transverse WG mechanism described by $\beta/k_0 = n_e < n$. Subscript e dropped.

Equivalent plane waves propagating along z-axis ($k_{x,y} = 0$, $k_z = k$):

$$k \cdot 2L = k_0 n \cdot 2L = \omega n \cdot 2L/c = m_z \cdot 2\pi\,, \qquad m_z = 1, 2, 3, \ldots$$

Regarding m_z as continuous:

$$\frac{\mathrm{d}(fn)}{\mathrm{d}m_z} = \frac{\mathrm{d}f}{\mathrm{d}m_z} n + f \frac{\mathrm{d}n}{\mathrm{d}f} \frac{\mathrm{d}f}{\mathrm{d}m_z} = \frac{\mathrm{d}f}{\mathrm{d}m_z}\left(n + f\frac{\mathrm{d}n}{\mathrm{d}f}\right) = \frac{c}{2L}$$

m_z discrete $\rightarrow$ $\mathrm{d}m_z \rightarrow 1$, $\mathrm{d}f \rightarrow \Delta f_z$.

Longitudinal mode spacing (free spectral range FSR, round-trip time τ_U):

$$\Delta f_z = \frac{c}{2 n_g L} = \frac{v_g}{2L} = \frac{1}{\tau_U}$$

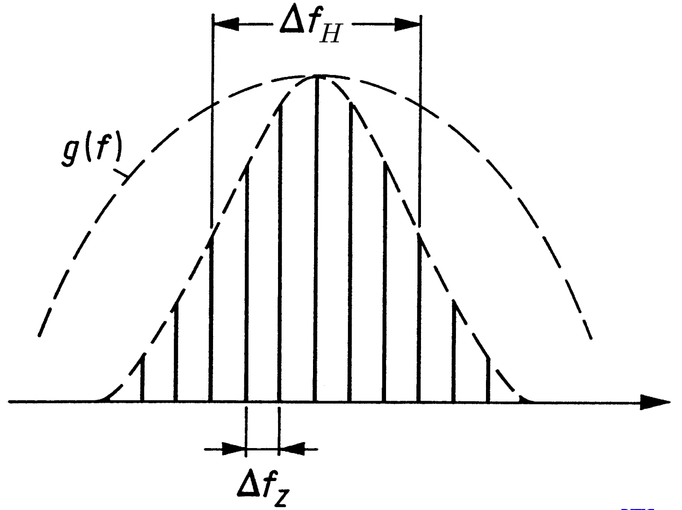

LD — Gain and Loss

Multi-moded resonator, one mode considered. Modes replaced by plane waves with effective propagation properties, complex (effective) refractive index $\bar{n} = n - \mathrm{j}\, n_i$, real part n, imaginary part $-n_i$. Subscript e dropped as before:

$$\exp(-\mathrm{j}\,\bar{k}z), \quad \left\{\begin{array}{l} \bar{k} = k_0\bar{n} = k + \mathrm{j}\,\frac{1}{2}(g - \alpha_V), \\ \bar{n} = n - \mathrm{j}\,n_i, \\ k_0 = \omega/c, \end{array}\right\}, \quad g - \alpha_V = -2\,k_0 n_i$$

Modal power gain g and loss constant α_V. Corresponds to net effective gain rate ΓG due to band-band transitions and power loss time constant $1/\tau_V$ not including band-band transitions.

Localized mirror losses $\rightarrow$ power "gain" $R_1 R_2 = \exp(-\alpha_{R1} 2L) \times \exp(-\alpha_{R2} 2L) = \exp(-\alpha_R 2L)$ distributed over round-trip time τ_U. Constant gain rate per τ_U $\rightarrow$ net N_P-increase per second:

$$G - \frac{1}{\tau_P} = \frac{1}{N_P}\frac{\mathrm{d}N_P}{\mathrm{d}t}, \quad \frac{N_P(\tau_U)}{N_P(0)} = \exp\left[\left(G - \frac{1}{\tau_P}\right)\tau_U\right], \quad \tau_U = \frac{2L}{v_g}$$

LECTURE 12

Stationary Laser Oscillation

Stationary laser oscillation with angular frequency ω_0 for $\varGamma G = 1/\tau_P$ → modal gain compensates resonator losses. A *monochromatic* light wave makes a complete round-trip during $t = \tau = 2nL/c$ without attenuation or phase shift:

$$\exp(\mathrm{j}\,\omega_0\tau)\exp\left[\frac{1}{2}\left(\varGamma G - \frac{1}{\tau_P}\right)\tau\right] = 1\,,$$

$$\omega_0\tau = m_z \cdot 2\pi\,, \quad \tau = \frac{2nL}{c}, \quad m_z = 0, 1, 2, \ldots\,, \quad \varGamma G = \frac{1}{\tau_P}$$

Condition $\omega_0\tau = m_z \cdot 2\pi$ corresponds to longitudinal mode spacing $\Delta f_z \rightarrow n_g$ is effective group refractive index.

Modal gain rate $\varGamma G = \varGamma r_{\mathrm{ind}}^{(\mathrm{M})} V/N_P$. Total resonator loss rate $1/\tau_P$ from finite mirror reflectivity $R_{1,2}$ (photon loss rate $1/\tau_{R1,2}$, total loss rate $1/\tau_R$), and from background resonator losses (photon loss rate $1/\tau_V$):

$$\tau_P^{-1} = \tau_V^{-1} + \tau_R^{-1}\,, \qquad \tau_R^{-1} = \tau_{R1}^{-1} + \tau_{R2}^{-1}\,.$$

LD — Gain and Loss Distributed

Relations between gain rate and modal power gain:

$$\begin{aligned}
\exp\left[(G-1/\tau_P)\tau_U\right] &= \exp\left[(G-1/\tau_V-1/\tau_R)\tau_U\right] \\
&= R_1R_2\exp\left[(G-1/\tau_V)\tau_U\right] \\
&= R_1R_2\exp\left[(G-1/\tau_V)2L/v_g\right] \\
&= R_1R_2\exp\left[(g-\alpha_V)2L\right] \\
&= \exp\left[(g-\alpha_V-\alpha_R)2L\right] \\
&= \exp\left[(g-\alpha_V-\alpha_{R1}-\alpha_{R2})2L\right]
\end{aligned}$$

Comparing:

$$\begin{aligned}
G &= v_g g, \\
1/\tau_V &= v_g\alpha_V, \\
1/\tau_{R1,2} &= v_g\alpha_{R1,2} = -v_g \ln R_{1,2}/(2L), \\
1/\tau_R &= v_g\alpha_R \;\; = -v_g \ln(R_1R_2)/(2L), \\
1/\tau_P &= v_g(\alpha_V+\alpha_R) = v_g[\alpha_V - \ln(R_1R_2)/(2L)]
\end{aligned}$$

LD — Gain Model and Gain Compression

Laser oscillates near f_0 (maximum spectral gain). Larger carrier number $\rightarrow$ nonlinear gain compression $\rightarrow$ energy states near hf_0 deplete (hot carrier effects, spectral hole burning). Depleted states filled only in intraband relaxation time τ_{CB} $\rightarrow$ "bottleneck" for carrier number available near hf_0.

Nonlinear gain compression modeled with gain compression factor ε_G, differential gain G_d, transparency concentration n_t:

$$G(n_T, N_P) = \frac{G(n_T)}{1 + \varepsilon_G \frac{\Gamma N_P}{V}} = G_d \frac{n_T - n_t}{1 + \varepsilon_G \frac{\Gamma N_P}{V}}$$

Empty VB (very high and constant $p = n_A$, i. e., $f_V \approx 0$ in range of interest, complete inversion $n_{\mathrm{sp}} = 1$) $\rightarrow$ (transp. concentration) $=$ $(n_t = 0)$ $\rightarrow$ slightest n_T-concentration in CB establishes some gain. Negligible gain compression $\varepsilon_G = 0$ $\rightarrow$ linear gain dependency:

$$G(n_T) = G_d n_T$$

Carrier/Gain Depletion and Recovery

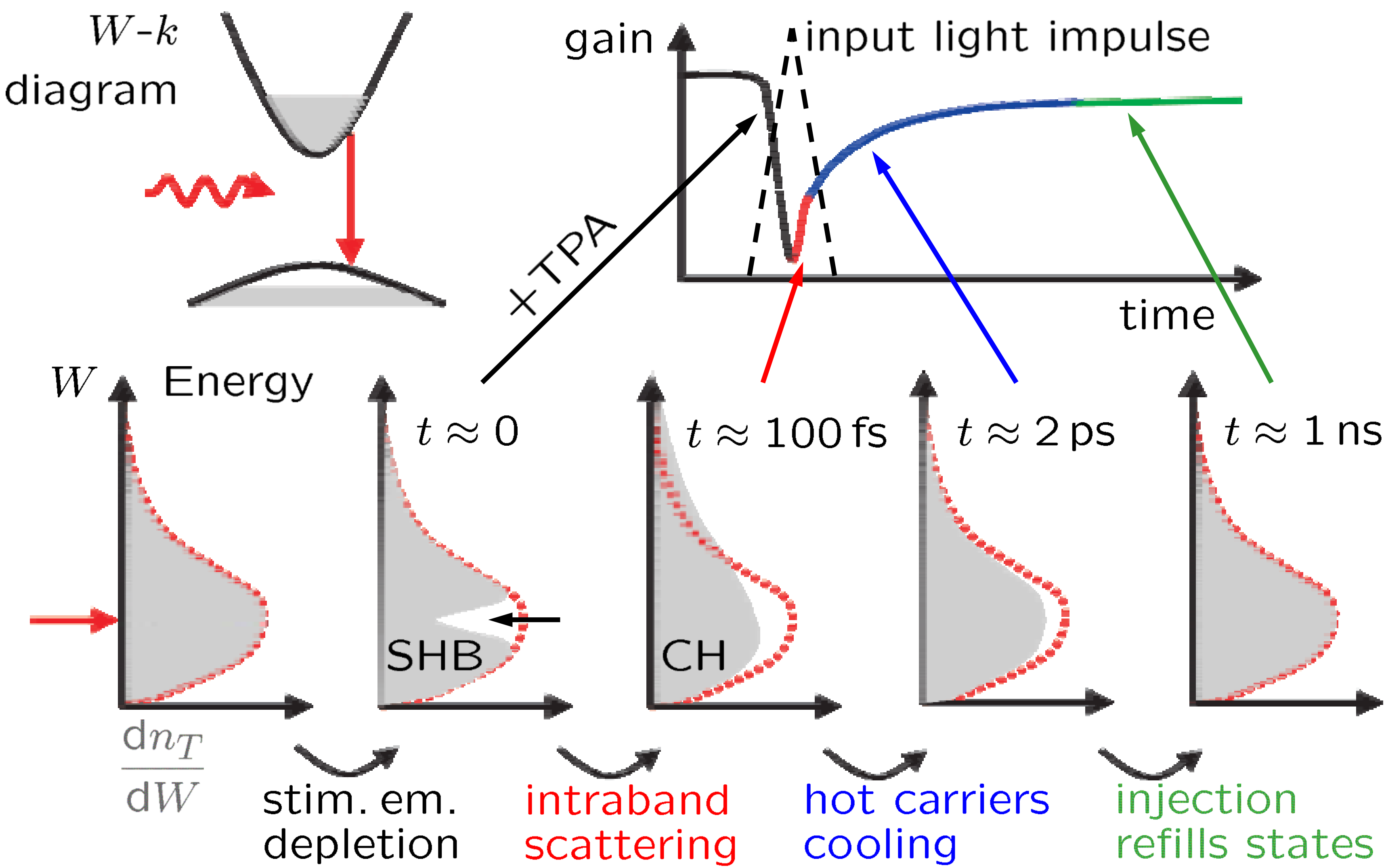

Modified from: Mørk, J. et al. IEEE LEOS Newsletter 16 (2002) 21–24. Fig. 2. — Mørk, J. et al. Optics & Photonics News July (2003) 42–48

LD — Rate Equations

Rate equations heuristically, phenomena through which N_P, $n_T V$ change in active volume V. Longitudinally and laterally single-moded laser:

$$\underbrace{\frac{\mathrm{d}N_P}{\mathrm{d}t}}_{\substack{\text{change of photon}\\ \text{number per time}}} = + \underbrace{N_P \Gamma G(n_T, N_P)}_{\substack{\text{stim. gen.}\\ \text{photons per time}}} + \underbrace{Q\frac{n_T V}{\tau_{\text{eff}}}}_{\substack{\text{spont. gen.}\\ \text{ph. p. mode, time}}} - \underbrace{\frac{N_P}{\tau_P}}_{\substack{\text{stim. depl.}\\ \text{ph. p. time}}}$$

$$\underbrace{\frac{\mathrm{d}(n_T V)}{\mathrm{d}t}}_{\substack{\text{change of electron}\\ \text{number per time}}} = - \underbrace{N_P \Gamma G(n_T, N_P)}_{\substack{\text{stim. depl.}\\ \text{electrons per time}}} - \underbrace{\frac{n_T V}{\tau_{\text{eff}}}}_{\substack{\text{spont. depl.}\\ \text{electrons per time}}} + \underbrace{\frac{I}{e}}_{\substack{\text{inj. electr.}\\ \text{per time}}}$$

Fraction of spontaneous recombinations leading to photons in oscillating mode is spontaneous emission factor Q:

$$Q = \frac{\Gamma r_{\text{sp}}^{(\text{eM})}}{r_{\text{eff}}} = \frac{\Gamma r_{\text{sp}}}{r_{\text{eff}}} \frac{\rho(f)}{\varrho_{\text{tot}}(f) V} = \Gamma \frac{\tau_{\text{eff}}}{\tau_{\text{sp}}} \frac{\rho(f)}{\varrho_{\text{tot}}(f) V}$$

LD — Rate Equations. Threshold

$Q = 0$, $N_P G \ll n_T V/\tau_\text{eff} \rightarrow$ Definition of lasing threshold (subscript S) for $\mathrm{d}/\mathrm{d}t = 0$. Above threshold: Device oscillates.

$$\Gamma G(n_{TS}, 0) = \Gamma G_S = \frac{1}{\tau_P} = v_g\left(\alpha_V - \frac{\ln(R_1 R_2)}{2L}\right),$$

$$\frac{I_S}{e} = \frac{n_{TS} V}{\tau_\text{eff}} = r_\text{eff} V$$

At threshold carrier concentration $n_T = n_{TS} \rightarrow$ net gain rate ΓG_S compensates loss rate $1/\tau_P$. $\Gamma G_S > G(n_T, N_P) = G(n_t, N_P) = 0$.

Only above threshold:

(photon number generated per t) $>$ (photon number annihilated)

Maximum τ_P for minimum mirror transmission losses.

Threshold current density $J_S = I_S/(bL)$ for 5-layer structure minimum for optimum height d of active layer:

$$J_S = \frac{I_S}{bL} = \frac{e n_t}{\tau_\text{eff}}\left[d + \frac{\Gamma \alpha_V + \alpha_R}{g_0}\,\frac{d}{\Gamma(d)}\right], \quad \Gamma(d) = \begin{cases} d^2 & \text{for } d \text{ small} \\ 1 & \text{for } d \text{ large} \end{cases}, \quad J_S = c_1 d + \frac{c_2}{d}$$

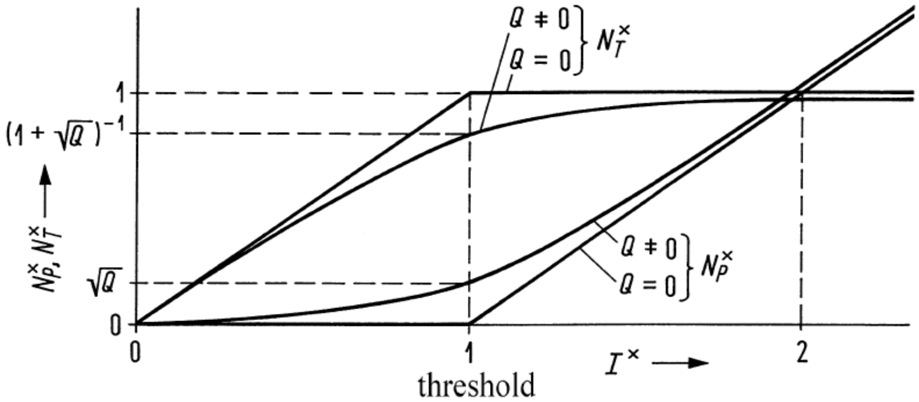

Fig. 3.21. Normalized photon number $N_P^\times$ and normalized CB carrier density $N_T^\times$ as a function of the normalized injection current $I^\times$. For $Q \neq 0$ a simplified gain dependence $G^\times = N_T^\times$

DC solution:

$$I^\times \leq 1: \quad N_T^\times = I^\times, \quad N_P^\times = 0, \quad Q = 0,$$

$$I^\times > 1: \quad N_T^\times = 1, \quad N_P^\times = I^\times - 1, \quad G^\times = 1,$$

Normalized rate equations:

$$\tau_P \frac{\mathrm{d}N_P^\times}{\mathrm{d}t} = N_P^\times (G^\times - 1) + Q N_T^\times,$$

$$\tau_{\text{eff}} \frac{\mathrm{d}N_T^\times}{\mathrm{d}t} = I^\times - N_T^\times - N_P^\times G^\times$$

LECTURE 13

LD — Small-Signal Intensity Modulation. Fourier Solution

Perturbation ansatz We assume a static operation point above threshold given by the time-independent quantities N_{P0}, n_{T0}, $G_0 = G(n_{T0}, N_{P0})$, τ_P, τ_{eff}, ε_G in Eqs. (3.83), (3.93), and small time-dependent perturbations $N_{P1}(t)$, $n_{T1}(t)$, $I_1(t)$,

$$\begin{aligned} N_P(t) &= N_{P0} + N_{P1}(t), \quad & G(t) &= G_0 + \frac{\partial G_0}{\partial n_{T0}}\, n_{T1}(t) + \frac{\partial G_0}{\partial N_{P0}}\, N_{P1}(t), \\ n_T(t) &= n_{T0} + n_{T1}(t), & G_0 &= G(n_{T0}, N_{P0}), \qquad I(t) = I_0 + I_1(t). \end{aligned} \tag{3.103}$$

The differential gain rate $\partial G_0/\partial n_{T0}$ has typical values of $1.8 \times 10^{-6} \ldots 2.9 \times 10^{-6}\,\text{cm}^3\,\text{s}^{-1}$. Substituting Eq. (3.103) into Eq. (3.83) and neglecting products of perturbation quantities, we solve the linearized rate equations with a Fourier ansatz $X_1(t) = X_1(\omega)\exp(\mathrm{j}\,\omega t)$, where $X_1(\omega)$ is the complex amplitude at the modulation frequency $f = \omega/(2\pi)$,

$$\begin{aligned} N_{P1}(\omega)\left(\mathrm{j}\,\omega + \frac{1}{\tau_P} - \frac{\Gamma G_0}{1 + \varepsilon_G \frac{\Gamma N_{P0}}{V}}\right) &= \left(\frac{Q}{\tau_{\text{eff}}} + \frac{N_{P0}}{V}\frac{\partial \Gamma G_0}{\partial n_{T0}}\right) n_{T1}(\omega) V, \\ n_{T1}(\omega) V \left(\mathrm{j}\,\omega + \frac{1}{\tau_{\text{eff}}} + \frac{N_{P0}}{V}\frac{\partial \Gamma G_0}{\partial n_{T0}}\right) &= \frac{I_1(\omega)}{e} - \frac{\Gamma G_0}{1 + \varepsilon_G \frac{\Gamma N_{P0}}{V}}\, N_{P1}(\omega)\,. \end{aligned} \tag{3.104}$$

Elimination of $n_{T1}(\omega)$ leads to the modulation transfer function

$$\frac{N_{P1}(\omega)}{I_1(\omega)} = \underbrace{\frac{\left(\frac{N_{P0}}{V}\frac{\partial \Gamma G_0}{\partial n_{T0}} + \frac{Q}{\tau_{\text{eff}}}\right)}{\omega_r^2 \tau_P}}_{\approx 1} \frac{\omega_r^2}{(\mathrm{j}\,\omega)^2 + 2\gamma_r(\mathrm{j}\,\omega) + \omega_r^2} \tag{3.105}$$

LD — Small-Signal Intensity Modulation

Static operation point above threshold at N_{P0}, n_{T0}, τ_P, τ_{eff}, $G_0 = G(n_{T0}, N_{P0})$, ε_G. Small perturbations $N_{P1}(t)$, $n_{T1}(t)$, $I_1(t)$:

$$N_P(t) = N_{P0} + N_{P1}(t), \quad G(t) = G_0 + \frac{\partial G_0}{\partial n_{T0}} n_{T1}(t) + \frac{\partial G_0}{\partial N_{P0}} N_{P1}(t),$$

$$n_T(t) = n_{T0} + n_{T1}(t), \qquad G_0 = G(n_{T0}, N_{P0}), \qquad I(t) = I_0 + I_1(t)$$

Elimination of $n_{T1}(\omega)$ leads to modulation transfer function:

$$\frac{N_{P1}(\omega)}{I_1(\omega)} \approx \frac{\omega_r^2}{(\mathrm{j}\,\omega)^2 + 2\gamma_r(\mathrm{j}\,\omega) + \omega_r^2}$$

Angular relaxation frequency ω_r, damping constant γ_r:

$$\omega_r^2 \tau_P \approx \frac{N_{P0}}{V} \frac{\partial \Gamma G_0}{\partial n_{T0}},$$

$$2\gamma_r \approx \frac{1}{\tau_{\text{eff}}} + \underbrace{\frac{N_{P0}}{V} \frac{\partial \Gamma G_0}{\partial n_{T0}} + \overbrace{\Gamma G_0\, \varepsilon_G \frac{\Gamma N_{P0}}{V}}^{\approx \tau_P^{-1} \varepsilon_G \Gamma N_{P0}/V}}_{= \omega_r^2 K_r}$$

LD — Small-Signal Intensity Modulation. Transfer Function

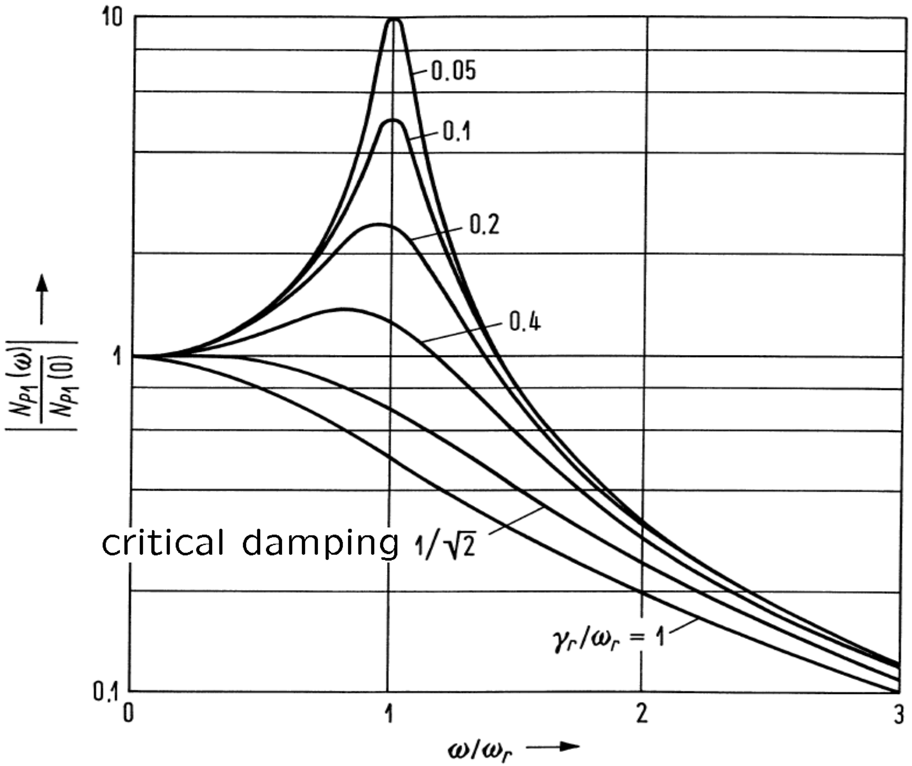

$$\left|\frac{N_{P1}(\omega)/\tau_P}{I_1/e}\right| \to \max :$$

$$\omega_R = \sqrt{\omega_r^2 - 2\gamma_r^2}$$

$$\left|\frac{N_{P1}(\omega_{3\,\mathrm{dB}})}{N_{P1}(0)}\right| = \frac{1}{\sqrt{2}},$$

$$\omega_{3\,\mathrm{dB}}^2 = (\omega_r^2 - 2\gamma_r^2) + \sqrt{(\omega_r^2 - 2\gamma_r^2)^2 + \omega_r^4}$$

Fig. 3.22. Modulus of current-light modulation transfer function as a function of normalized current modulation frequency for various values of γ_r/ω_r

$$\omega_r^2 \tau_P \approx \frac{N_{P0}}{V}\frac{\partial(\Gamma G_0)}{\partial n_{T0}}, \quad \omega_{3\,\mathrm{dB}}^{\max} = \omega_r = \gamma_r\sqrt{2}, \quad \gamma_r\sqrt{2} \approx \frac{1}{2}\omega_r^2 K_r \sqrt{2},$$

$$2\gamma_r \approx \frac{1}{\tau_{\mathrm{eff}}} + \omega_r^2 K_r \qquad \omega_{3\,\mathrm{dB}}^{\max} = \frac{\sqrt{2}}{K_r}, \qquad K_r = \tau_P + \frac{\varepsilon_G}{\partial G_0/\partial n_{T0}}$$

LD — Large-Signal Intensity Modulation

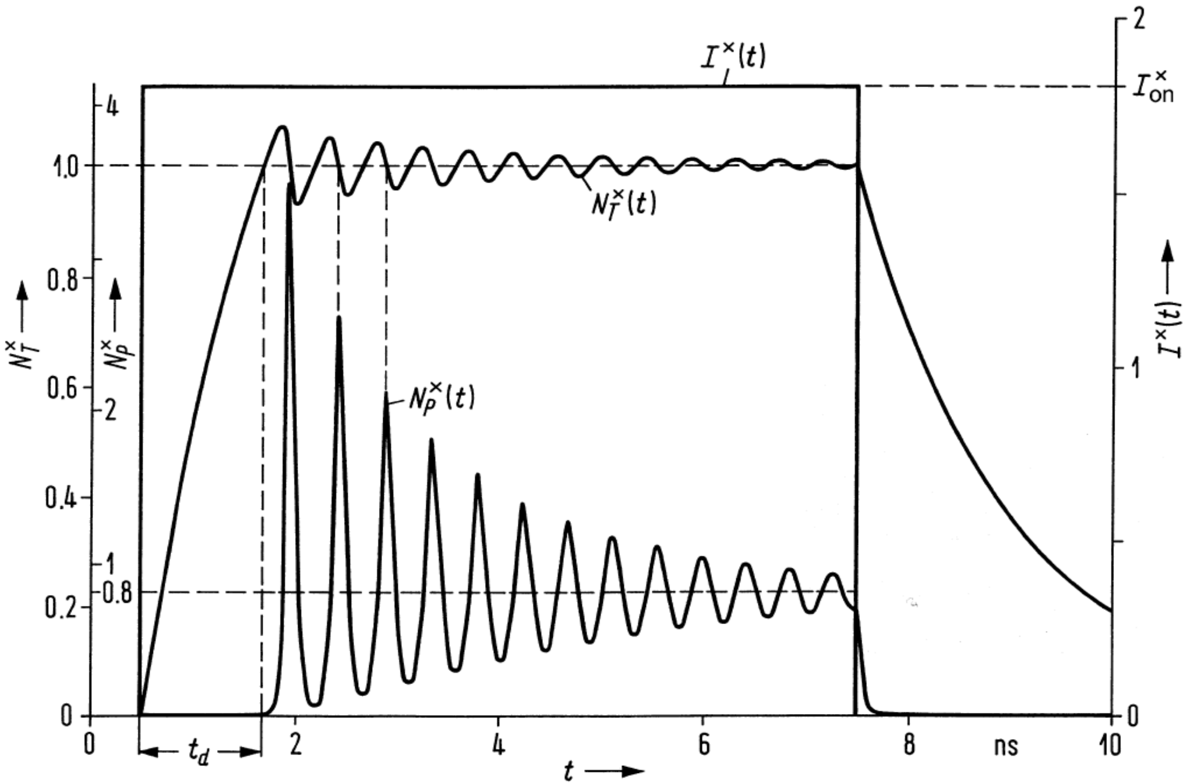

Fig. 3.24. Relaxation oscillation for a current step $I^\times = 1.8$. Parameters are $\tau_P = 2.5\,\text{ps}$, $\tau_\text{eff} = 1.5\,\text{ns}$, $Q = 5\times10^{-4}$

Normalized rate equations:

$$\tau_P \frac{\mathrm{d}N_P^\times}{\mathrm{d}t} = N_P^\times(G^\times - 1) + QN_T^\times\,, \qquad \tau_\text{eff}\frac{\mathrm{d}N_T^\times}{\mathrm{d}t} = I^\times - N_T^\times - N_P^\times G^\times$$

LD — Amplitude-Phase Coupling. Line Broadening

Depedencies of gain rate $G(f, n_T)$, modal power gain g and $-n_i$ because of emission spectrum and via quasi Fermi levels. $n(f, n_T)$ because of band filling, Coulomb interact., free-carrier absorpt.

At LD oscillation frequency $\rightarrow$ $\Delta n < 0$ and (via Kramers-Kronig) $\Delta g > 0$ for $\Delta n_T > 0$. Line broadening factor, Henry factor, α-factor:

$$\alpha = \frac{\partial n / \partial n_T}{\partial n_i / \partial n_T} = -2k_0 \frac{\partial n / \partial n_T}{\partial(\Gamma g - \alpha_V) / \partial n_T} \approx -2k_0 \frac{\partial n / \partial n_T}{\partial(\Gamma g) / \partial n_T} > 0$$

For LD oscillator: $\alpha = 2 \ldots 8$. Correlation between amplitude and phase. Spontaneous emissions $\rightarrow$ amplitude and phase changes. Amplitude change $\rightarrow$ secondary phase change $\rightarrow$ broadening of the emission line (inversion factor n_{sp}):

$$\Delta f_H \, P_a = \text{const} \cdot n_{\text{sp}} (1 + \alpha^2) h f v_g^2 (\alpha_V + \alpha_R) \alpha_R, \qquad n_{\text{sp}} = \frac{N_2}{N_2 - N_1}$$

LD — Amplitude-Phase Coupling. Chirp

Stationary laser oscillation, operating point (subscript 0) at $G(n_{T0}) = 1/\tau_P$, $G^\times = \Gamma G(n_{T0}, N_{P0})\,\tau_P = 1$. Angular optical frequency ω_0. Changing n_T differentially, $\mathrm{d}n_T \to$ gain rate $\mathrm{d}G$, and "instantaneous" (slowly varying on $(1/f_0)$-scale) optical frequency ω deviating by $\mathrm{d}\omega$. Frequency difference $\Delta\omega$ defines time derivative of optical phase, $\mathrm{d}\varphi/\mathrm{d}t = \Delta\omega$, $\omega n \cdot 2L/c = m_z \cdot 2\pi$:

$$\mathrm{d}(\omega n(\omega)) = \frac{\partial(\omega n)}{\partial\omega}\mathrm{d}\omega + \frac{\partial(\omega n)}{\partial n}\mathrm{d}n = \Bigg(\overbrace{n + \omega\frac{\partial n}{\partial\omega}}^{n_g}\Bigg)\mathrm{d}\omega + \omega\,\mathrm{d}n \stackrel{!}{=} 0\,,$$

$$\mathrm{d}\omega = -\frac{\omega}{n_g}\mathrm{d}n = -\frac{\omega}{n_g}\frac{\partial n}{\partial n_T}\mathrm{d}n_T = \frac{\alpha\omega}{2k_0 n_g}\frac{\partial(\Gamma g)}{\partial n_T}\mathrm{d}n_T$$

$$\approx \Delta\omega = \omega - \omega_0 = \frac{\mathrm{d}\varphi}{\mathrm{d}t} = \frac{\alpha}{2}v_g\frac{\partial(\Gamma g)}{\partial n_T}\Delta n_T \approx \frac{\alpha}{2}\frac{\partial(\Gamma G)}{\partial n_T}\Delta n_T$$

$$\frac{\mathrm{d}\varphi}{\mathrm{d}t} = \frac{\alpha}{2}\Bigg(\underbrace{\frac{\partial(\Gamma G)}{\partial n_T}\Delta n_T + \overbrace{\Gamma G(n_{T0}) - \frac{1}{\tau_P}}^{=0}}_{\Gamma G(n_T)}\Bigg) = \frac{\alpha}{2}\Bigg(\Gamma G - \frac{1}{\tau_P}\Bigg) \approx \frac{\alpha}{2}\frac{1}{N_P}\frac{\mathrm{d}N_P}{\mathrm{d}t}$$

LD — Amplitude-Phase Coupling. Electric Field

$$\frac{\mathrm{d}\varphi}{\mathrm{d}t} = \frac{\alpha}{2}\Bigg(\underbrace{\frac{\partial(\Gamma G)}{\partial n_T}\Delta n_T + \overbrace{\Gamma G(n_{T0}) - \frac{1}{\tau_P}}^{=0}}_{\Gamma G(n_T)} \Bigg) = \frac{\alpha}{2}\left(\Gamma G - \frac{1}{\tau_P}\right) \approx \frac{\alpha}{2}\frac{1}{N_P}\frac{\mathrm{d}N_P}{\mathrm{d}t}$$

Rate equations with optical phase change supplement, including spontaneous emission into oscillating mode ($Q \neq 0 \rightarrow \Gamma G < 1/\tau_P$):

$$\frac{\mathrm{d}N_P}{\mathrm{d}t} = N_P\left(\Gamma G - \frac{1}{\tau_P}\right) + Q\,\frac{n_T V}{\tau_{\mathrm{eff}}},$$

$$\frac{\mathrm{d}\varphi}{\mathrm{d}t} = \frac{\alpha}{2}\left(\Gamma G - \frac{1}{\tau_P}\right),$$

$$\underline{E}(t) \sim \sqrt{N_P(t)}\ \exp\Big\{\mathrm{j}\,[\omega_0 t + \varphi(t)]\Big\},$$

$$\frac{\mathrm{d}(n_T V)}{\mathrm{d}t} = -N_P \Gamma G - \frac{n_T V}{\tau_{\mathrm{eff}}} + \frac{I}{e}$$

LD — Device Structures with Gain and Index Guiding

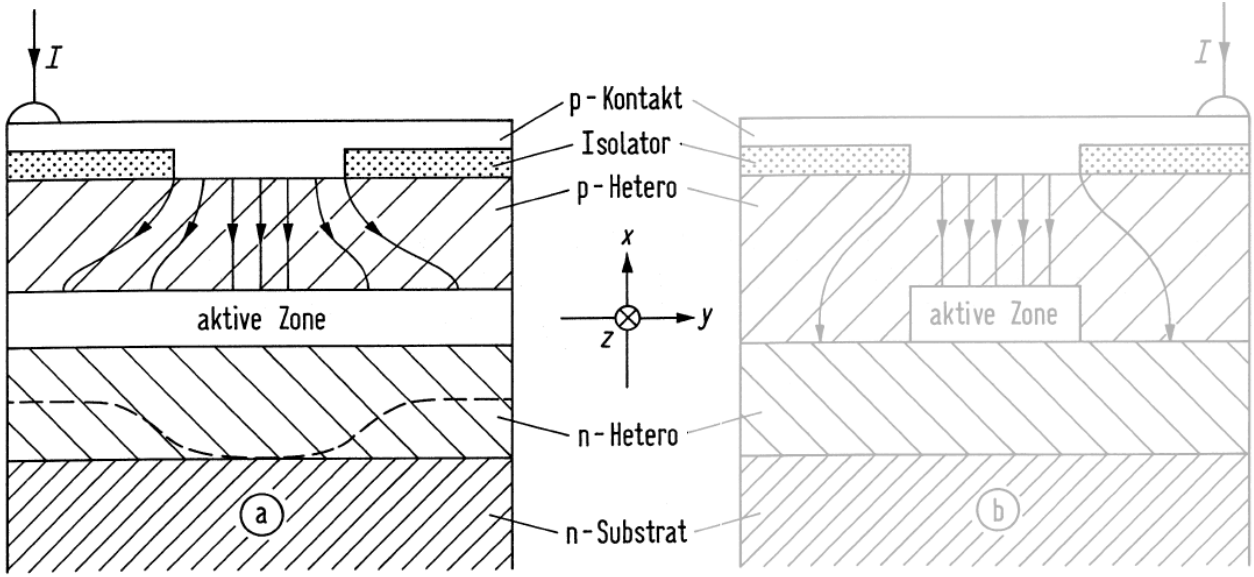

Basic laser diode structures. (a) Gain-guided laser (b) Index-guided laser. The origin of the coordinate system is located in the centre of the active zones (p-Kontakt = p-contact, Isolator = insulator, aktive Zone = active zone).

Gain guiding: Current confined $\rightarrow g - \alpha_V = -2k_0 n_i$

Effective n in high-current region lower $\rightarrow$ antiguiding

Lateral decrease of n_i dominates.

High threshold $I_S = 100\,\text{mA}$

Index guiding: Strip waveguide cavity by lateral heterojunctions.

Low threshold $I_S = 10\,\text{mA}$

Vertical Cavity Surface Emitting Laser — VCSEL

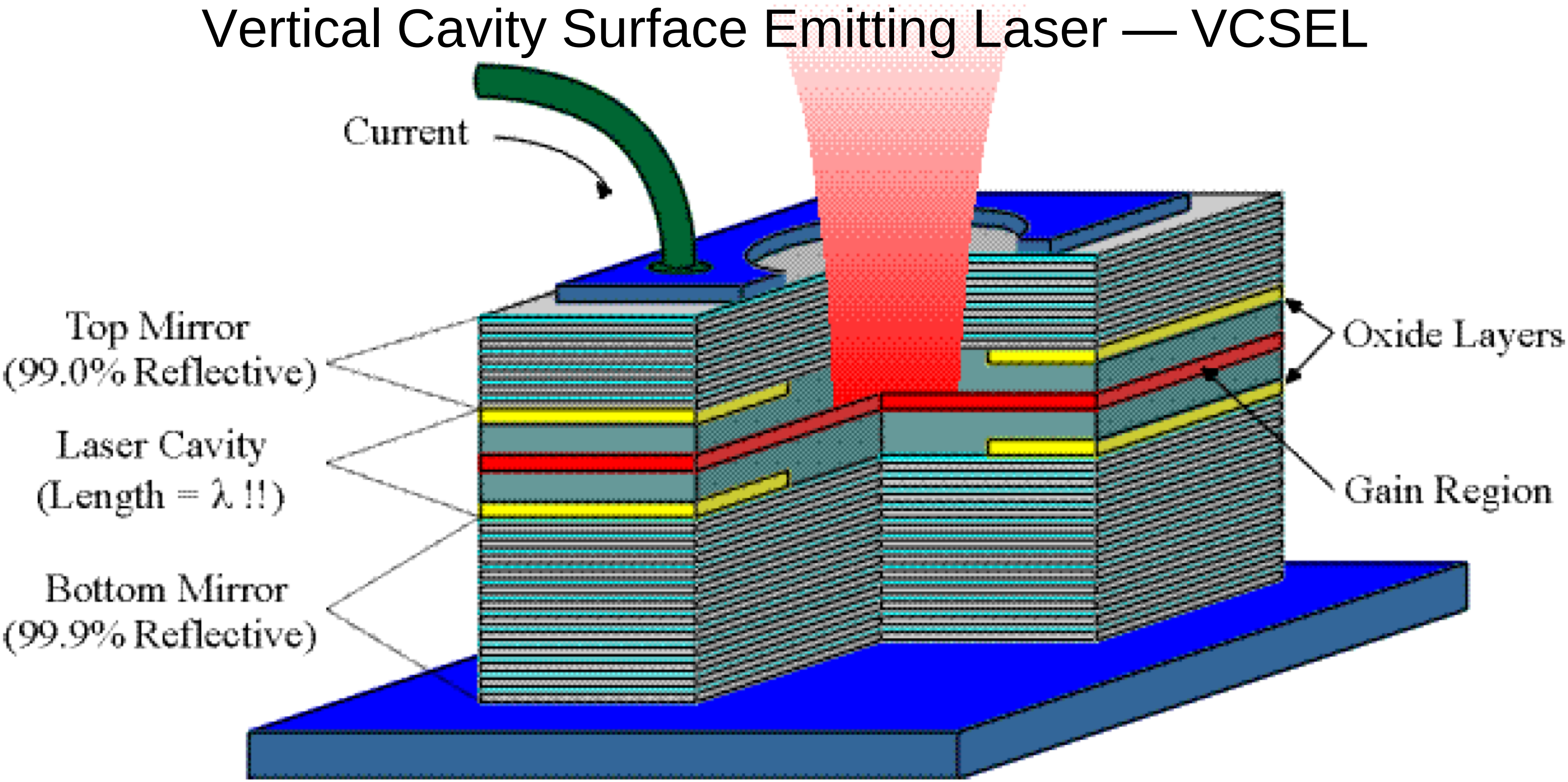

VCSEL operates in single longitudinal mode: Extremly small cavity length $L = \lambda_e/2 \approx 1\,\mu$m so that $q = 1$.

Mode spacing $\Delta f_z = c/(n_g\lambda_e) = c/\lambda \approx 300\,$THz for $\lambda = 1\,\mu$m exceeds gain bandwidth $\Delta f_H \approx 12\,$THz by far.

http://www.ino.it/~gianni Giovanni Giacomelli: Progetto INOA 4.2 : strutture spazio-temporali in laser a cavità verticale
Spatio-temporal structures in vertical cavity lasers. F:\U\Wofreu\PCTEX\SKRIPTEN\Giacomelli\INO_ Gianni Giacomelli.pdf

Vertical Cavity Surface Emitting Laser — Beam Shape and SEM

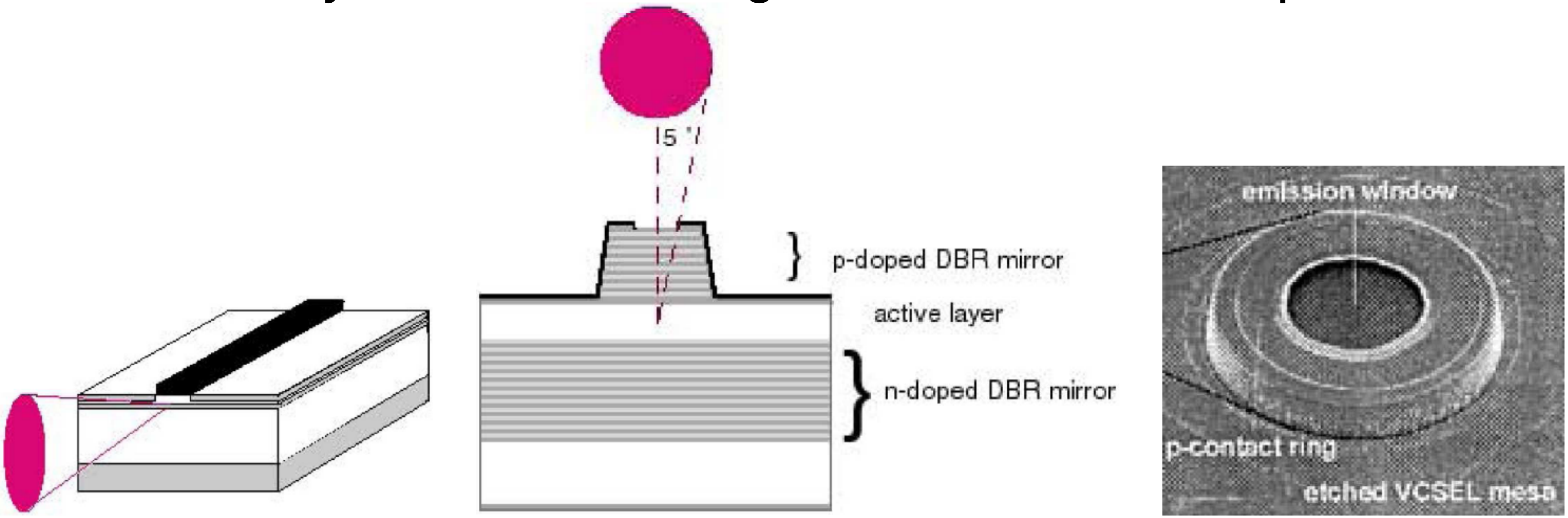

(a) (b) (c)

Edge-emitting and vertically-emitting laser diodes (a) edge-emitting laser diode and far-field radiation characteristic (b) VCSEL layer structure. p-doped DBR mirror: 25 layers $Al_{0.3}Ga_{0.7}As/AlAs$; active zone: 220 nm $Al_{0.3}Ga_{0.7}As$ with 3 $Al_{0.12}Ga_{0.88}As$ quantum films, height about 7 nm each; n-doped DBR mirror: 40 layers $Al_{0.3}Ga_{0.7}As/AlAs$ (c) microscopic image of VCSEL (all after reference Footnote 49 on Page 122)

Lower resonator mirror: 40 alternating layers of $Al_xGa_{1-x}As$ and AlAs, each layer $\lambda_e/4$ thick, power reflection factor $R_1 \geq 99.99\,\%$

Output top mirror: 25 $\lambda_e/4$ layers, reflectivity $R_2 = 99.9\,\%$

High resonator efficiency, small gain medium volume $\rightarrow I_{\text{th}} \sim \text{mA}$

LECTURE 14

Semiconductor Optical Amplifier (SOA) Gain

Gain relations of Fabry-Perot laser:

$$\exp(-\mathrm{j}\,\bar{k}z), \quad \left\{\begin{array}{l} \bar{k} = k_0\bar{n} = k + \frac{1}{2}\mathrm{j}\,(g - \alpha_V), \\ \bar{n} = n - \mathrm{j}\,n_i, \\ k_0 = \omega/c, \end{array}\right\}, \quad g - \alpha_V = -2\,k_0 n_i$$

$$G - \frac{1}{\tau_P} = \frac{1}{N_P}\frac{\mathrm{d}N_P}{\mathrm{d}t}, \qquad \frac{N_P(\tau_U)}{N_P(0)} = \exp\left[\left(G - \frac{1}{\tau_P}\right)\tau_U\right], \qquad \tau_U = \frac{2L}{v_g}$$

$$\exp\left[(G - 1/\tau_P)\tau_U\right] = R_1 R_2 \exp\left[(g - \alpha_V)2L\right]$$

SOA with distributed single-pass gain $\mathcal{G}_s$:

$$\mathcal{G}_s = \exp\left[(\mathit{\Gamma} g - \alpha_{Ve})\,L\right], \qquad \varphi = \beta L = k_0 n_e L$$

Residual mirror reflectivities $R_{1,2} \neq 0 \rightarrow$ FP amplification factor $\mathcal{G}$:

$$\mathcal{G} = \frac{\mathcal{G}_s(1 - R_1)(1 - R_2)}{\left(1 - \mathcal{G}_s\sqrt{R_1 R_2}\,\right)^2 + 4\mathcal{G}_s\sqrt{R_1 R_2}\,\sin^2\varphi},$$

$\varphi = \beta L, \qquad$ resonances: $\varphi_z = \omega_z n_e L/c = m_z \pi\,, \qquad m_z = 1, 2, 3, \ldots$

SOA Single-Pass Gain and Ripple

FP amplification factor $\mathcal{G}$:

$$\mathcal{G} = \frac{\mathcal{G}_s(1-R_1)(1-R_2)}{\left(1-\mathcal{G}_s\sqrt{R_1R_2}\,\right)^2 + 4\mathcal{G}_s\sqrt{R_1R_2}\,\sin^2\varphi},$$

$\varphi = \beta L$, res.: $\varphi_z = \omega_z n_e L/c = m_z\pi$.

Res. & anti-res.:

$$\mathcal{G}_{\max} = \frac{\mathcal{G}_s(1-R_1)(1-R_2)}{(1-\mathcal{G}_s\sqrt{R_1R_2})^2},$$

$$\mathcal{G}_{\min} = \frac{\mathcal{G}_s(1-R_1)(1-R_2)}{(1+\mathcal{G}_s\sqrt{R_1R_2})^2}$$

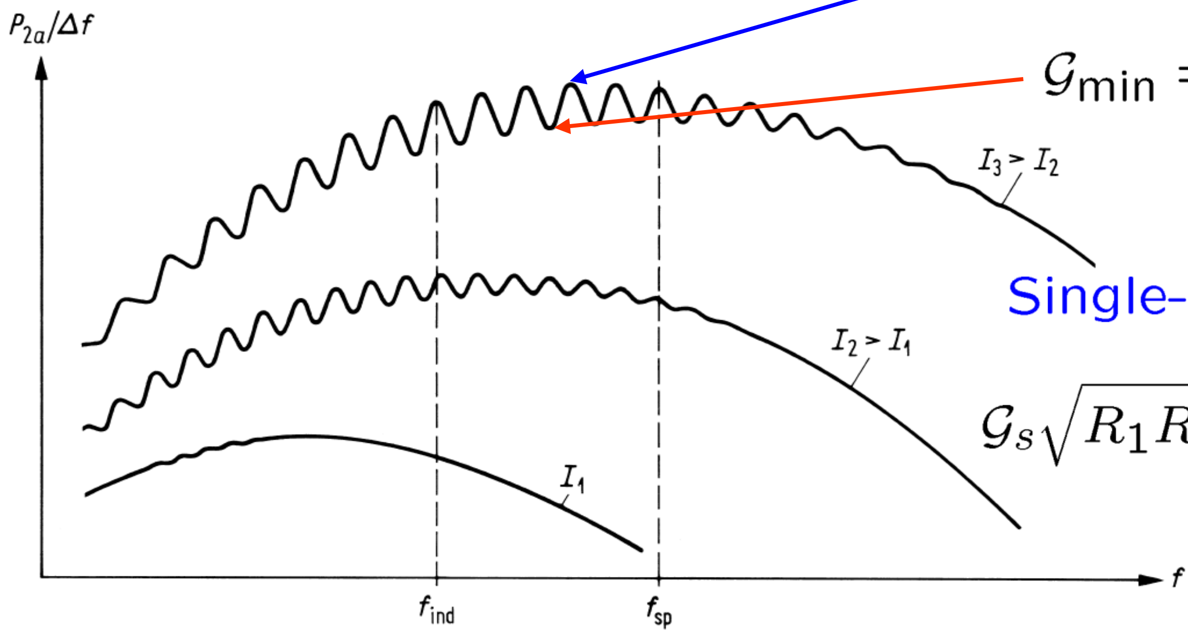

Single-pass gain from ripple:

$$\mathcal{G}_s\sqrt{R_1R_2} = \frac{\sqrt{\mathcal{G}_{\max}/\mathcal{G}_{\min}}-1}{\sqrt{\mathcal{G}_{\max}/\mathcal{G}_{\min}}+1}$$

$\mathcal{G}_{\max}/\mathcal{G}_{\min} = 2$: $\mathcal{G}_s\sqrt{R_1R_2} = 0.17$

Conv. FP: |—|. Angled: |/| $\rightarrow R_{\text{eff}\,1,2} \approx 10^{-4}$

Near-travelling-wave amplifier. Schematic of the spectral output power density $P_{2a}/\Delta F$ of amplified spontaneous emission as transmitted through mirror R_2 for varying injection currents $I_1 < I_2 < I_3$. The frequencies of maximum gain and maximum spontaneous emission are denoted as f_{ind} and f_{sp} for an operating current $I = I_3$.

SOA Chip with Angled Facets and Lensed Fibres

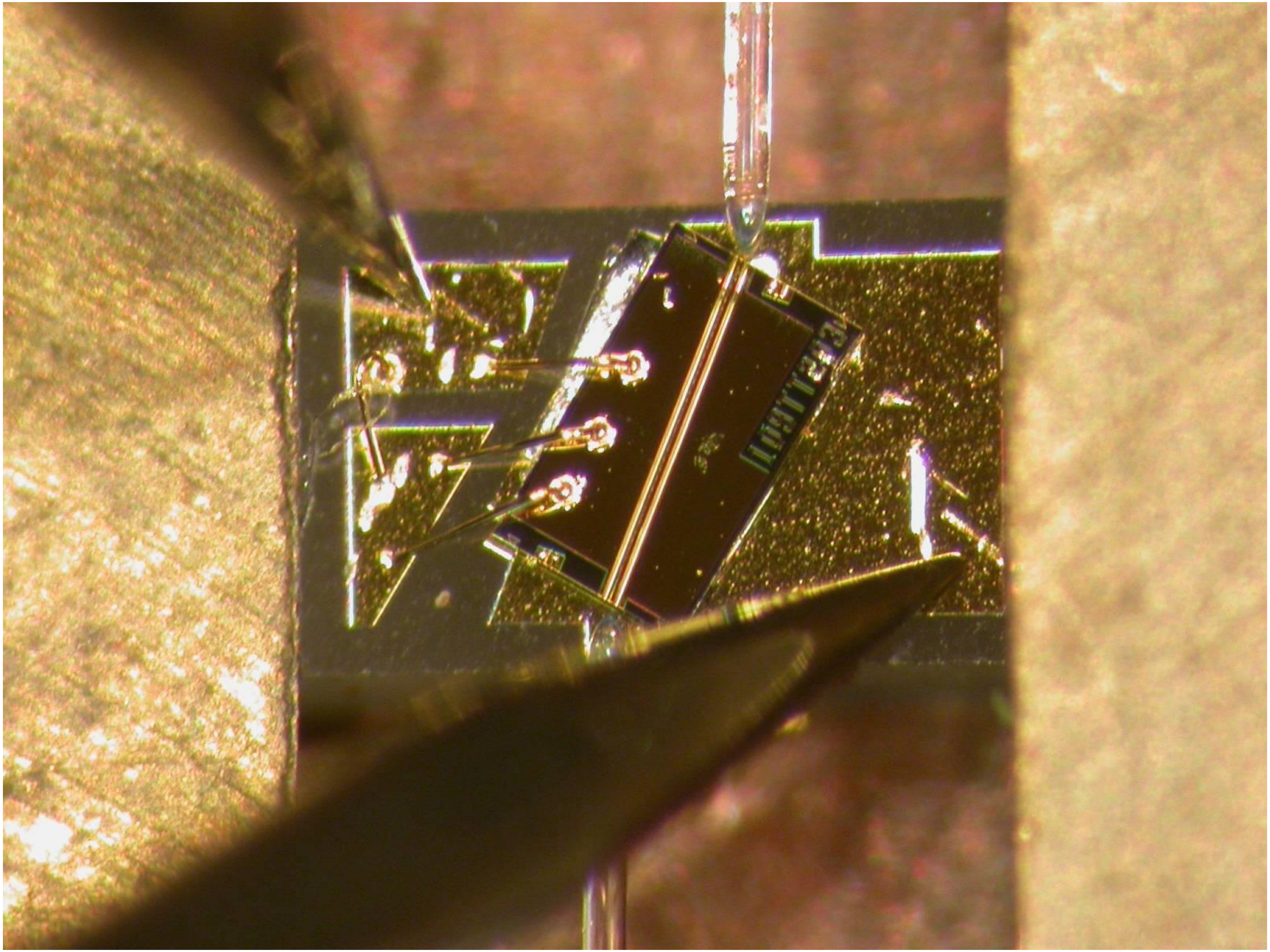

Pin Photodiode

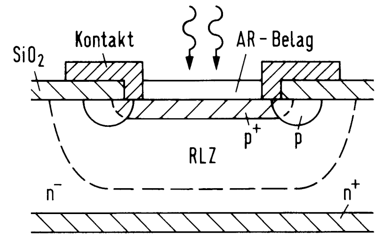

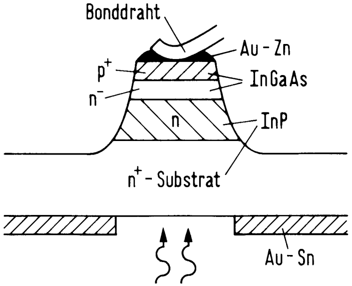

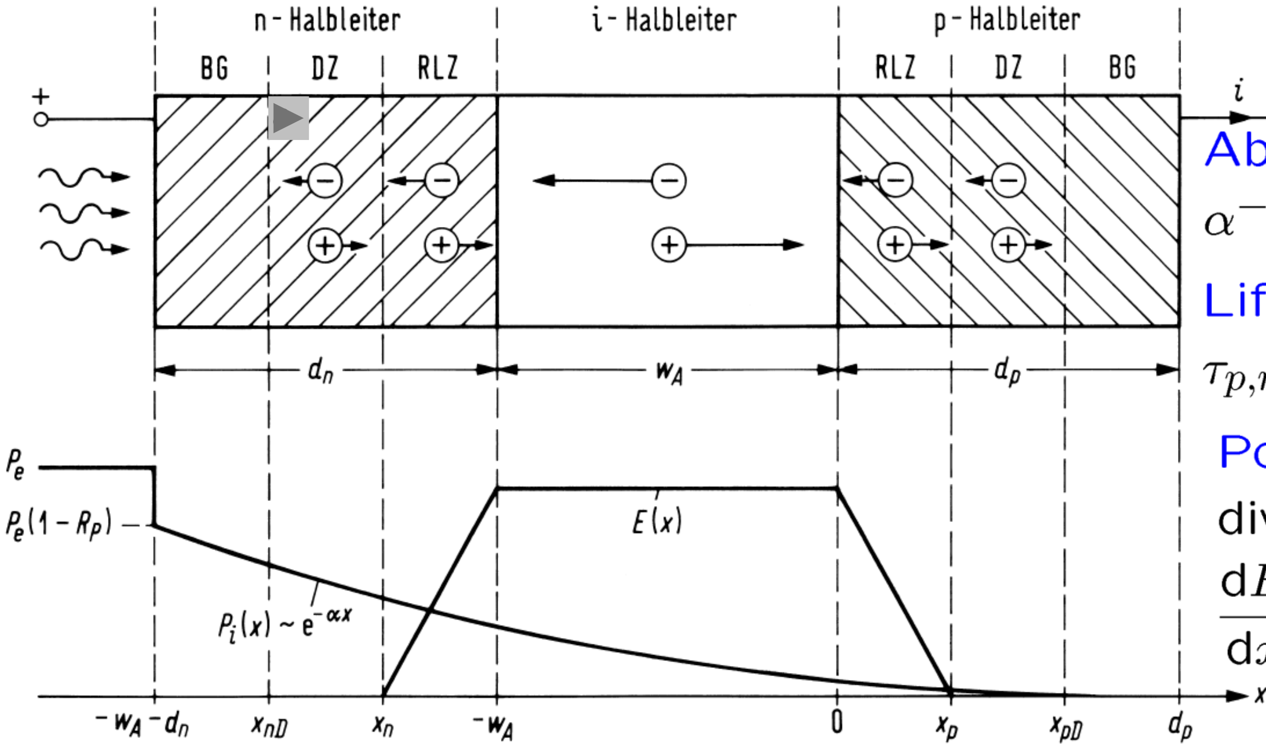

Absorption length:

$$\alpha^{-1} = 1 \ldots 10 \ldots 20\,\mu\text{m}$$

Lifetime:

$$\tau_{p,n} = L_{p,n}^2 / D_{p,n}$$

Poisson equation:

$$\text{div}\left(\epsilon_0 \epsilon_r \vec{E}\right) = \varrho$$

$$\frac{\text{d}E}{\text{d}x} = \pm \frac{e n_{D,A}}{\epsilon_0 \epsilon_r}$$

Schematic of a pin-diode. BG contact region (= *B*ahn*g*ebiet), DZ diffusion zone, RLZ space-charge (or depletion) region (= *R*aum*l*adungs*z*one). P_e light power incident from region external of semiconductor, R_P power reflection factor of the semiconductor surface, $P_i(x)$ light power inside the semiconductor, α light power attenuation constant, d_n (d_p) length of n-doped (p-doped) semiconductor, w_A length of intrinsic absorption zone, $E(x)$ x-component of electric field. Halbleiter = semiconductor

Sensitivity of a pin-Photodetector

We compute the sensitivity S (responsivity) of a pin-photodiode, which we describe by

- its technological structure, by
- a reduction to an easy-to-handle model, and by
- appropriate basic equations.

Continuity and transport equations are written

- in one-dimensional form, specified with
- quantum efficiency and generation rate, and finally
- solved for the DC case.

We find that for an external optical power P_e (photon energy hf_e)

- each absorbed photon generates one e-h pair (prob. η), which
- transports one elementary charge e in the external circuit, so
- the rate of generated charges i/e (photocurrent i) equals
- the photon absorption rate $\eta P_e/(hf_e)$ resulting in
- the sensitivity $S = \dfrac{\eta e}{hf_e}$ and a photocurrent $i = SP_e$.

Absorption Zone — Short-Circuit Current

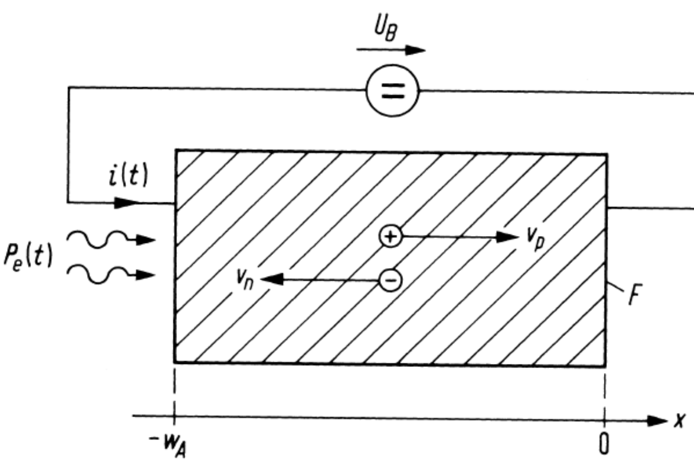

Transport equations ($\vec{v}_n$, $\vec{v}_p$ drift velocity; D_n, D_p diffusion constant; μ_n, μ_p mobility, $\vec{E}$ electric field):

$$\vec{J}_p = \quad ep\vec{v}_p \quad - eD_p \,\text{grad}\, p,$$
$$\vec{J}_n = -en_T\vec{v}_n + eD_n \,\text{grad}\, n_T$$

i-layer of a pin-photodiode (one-dimensional case, cross-section area F). Saturation drift velocities $v_n > 0$ and $v_p > 0$ for electrons and holes, incident external optical power $P_e(t)$, total conduction current $i(t)$, open-circuit voltage U_B of a battery with an internal resistance of zero

Absorption Zone — Basic 1D-Equations

Saturation velocities v_n, v_p. Recombination rates r_n, r_p neglected (carrier lifetime much larger than drift time in absorption zone $-w_A \le x \le 0$), diffusion currents neglected compared to field currents. Photo generation dominates, $g_p = g_n = g$. Currents i instead of current densities J (cross-section area F):

$$\frac{1}{v_p}\frac{\partial i_p}{\partial t} + \frac{\partial i_p}{\partial x} = eFg\,, \qquad i_p = Fepv_p\,,$$

$$\frac{1}{v_n}\frac{\partial i_n}{\partial t} - \frac{\partial i_n}{\partial x} = eFg\,, \qquad i_n = Fen_T v_n\,,$$

$$\epsilon\frac{\partial E}{\partial x} = e(p - n_T),$$

$$F\epsilon\frac{\partial}{\partial t}\left(\frac{\partial E}{\partial x}\right) = Fe\left(\frac{1}{Fev_p}\frac{\partial i_p}{\partial t} - \frac{1}{Fev_n}\frac{\partial i_n}{\partial t}\right),$$

$$\frac{\partial}{\partial x}\Bigg(\underbrace{i_n + i_p + F\epsilon\frac{\partial E}{\partial t}}_{\text{total current } i(t)}\Bigg) = 0$$

Absorption Zone — Convection Current and External Current

Total time-dependent conduction current:

$$i(t) = i_n(x,t) + i_p(x,t) + F\epsilon \frac{\partial E(x,t)}{\partial t}$$

Averaging over absorption zone $-w_A \leq x \leq 0$, observe:

$$\int_{-w_A}^{0} E(x,t)\,\mathrm{d}x = U_B \quad \rightarrow \quad \int_{-w_A}^{0} \frac{\partial E(x,t)}{\partial t}\,\mathrm{d}x = \frac{\mathrm{d}U_B}{\mathrm{d}t} = 0$$

Total conduction current found (= external short-circuit current, $\mathrm{d}U_B = 0$) by averaging the sum of carrier convection currents inside absorption region $-w_A \leq x \leq 0$:

$$i(t) = \frac{1}{w_A} \int_{-w_A}^{0} \left[\, i_n(x,t) + i_p(x,t)\,\right] \mathrm{d}x$$

Absorption Zone — Quantum Efficiency

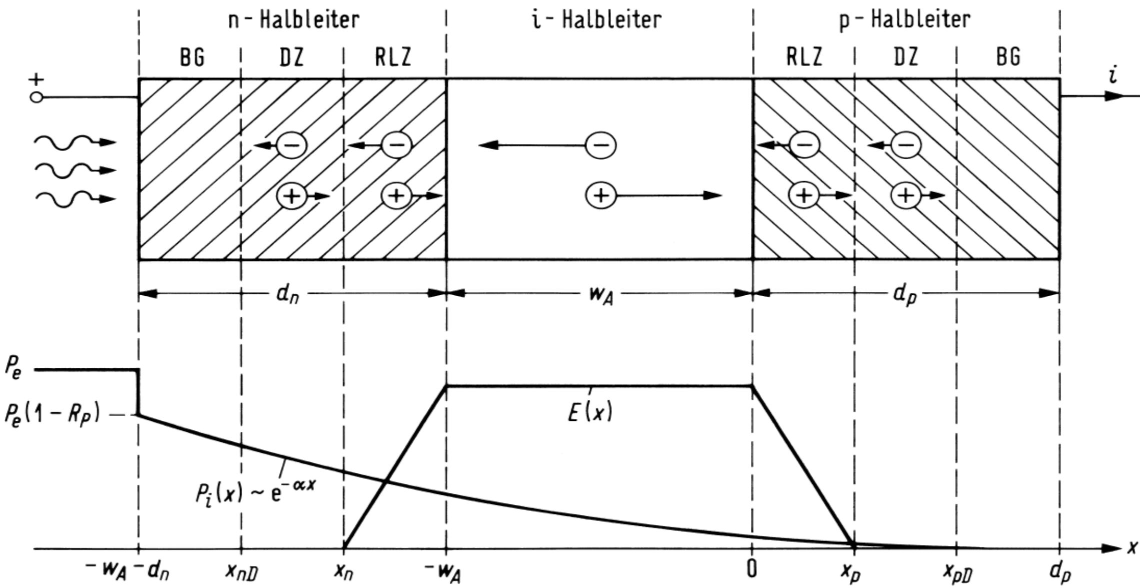

If $\alpha\, d_n \to 0$ (n-SC small comp. to abs. length), then $P_i(x,t)$ in i-region:

$$P_i(x,t) = P_e(t)\,(1 - R_P)\,\mathrm{e}^{-\alpha(x+w_A)}$$

Light transit time neglected. P_e, P_i are powers averaged over a few optical periods. Fraction of power absorbed in i-zone is quantum efficiency η:

$$\eta = \frac{P_i(-w_A,t) - P_i(0,t)}{P_e(t)} = (1 - R_P)\left(1 - \mathrm{e}^{-\alpha w_A}\right)$$

Absorption Zone — Generation Rate g (unit $\mathrm{cm}^{-3}\,\mathrm{s}^{-1}$)

No current harmonics produced by detection process:

$$i \sim \left\langle |E|^2 \cos^2(\omega_L t) \right\rangle = \frac{1}{2} |E|^2 \left\langle 1 + \cancel{\cos(2\omega_L t)} \right\rangle = \frac{1}{2} |E|^2$$

Absorption detectors of this kind are unable to emit optical photons $2hf_L$!

N_P photons, power P: $\qquad N_P\, h f_L = P \times 1\,\mathrm{s}$

$$P_i(x,t) = P_e(t)\,(1 - R_P)\,\mathrm{e}^{-\alpha(x+w_A)}$$

$$\left(\overline{\text{CP generation rate }} g\right) = \left(\overline{\text{photon absorption rate}}\right)$$

Power *gained* in ∂x:

$$\frac{\partial P_i(x,t)}{\partial x} = \frac{P_i(x+\partial x,t) - P_i(x,t)}{\partial x}$$

$$= \frac{(\text{power lost or abs. in}\,\mathrm{d}x)\,/\,(h f_L)}{(\text{differential volume})}$$

Power *lost* in ∂x:

$$\frac{-\partial P_i(x,t)}{\partial x} = \frac{P_i(x,t) - P_i(x+\partial x,t)}{\partial x}$$

$$g(x,t) = \frac{-\partial P_i(x,t)\,/\,(h f_L)}{F\,\partial x} = \frac{\alpha P_i(x,t)}{F h f_L}$$

Absorption Zone — External Short-Circuit Current

Quantum efficiency, power decay, and generation rate:

$$P_i(x,t) = P_e(t)\,(1 - R_P)\,\mathrm{e}^{-\alpha(x+w_A)}$$

$$g(x,t) = \frac{\alpha P_i(x,t)}{F h f_L} = \frac{\alpha P_e(t)}{F h f_L}(1 - R_P)\,\mathrm{e}^{-\alpha(x+w_A)}$$

$$\eta = (1 - R_P)\left(1 - \mathrm{e}^{-\alpha w_A}\right)$$

$$eFg(x,t) = \frac{\eta e}{h f_L}\,P_e(t)\,\frac{\alpha\,\mathrm{e}^{-\alpha(x+w_A)}}{1 - \mathrm{e}^{-\alpha w_A}}$$

A system of differential equations follows:

$$\frac{1}{v_p}\frac{\partial i_p(x,t)}{\partial t} + \frac{\partial i_p(x,t)}{\partial x} = eFg(x,t), \qquad i_p(x,t) = Fep(x,t)v_p,$$

$$\frac{1}{v_n}\frac{\partial i_n(x,t)}{\partial t} - \frac{\partial i_n(x,t)}{\partial x} = eFg(x,t), \qquad i_n(x,t) = Fen_T(x,t)v_n,$$

$$i(t) = \frac{1}{w_A}\int_{-w_A}^{0} \left[\, i_n(x,t) + i_p(x,t) \,\right] \mathrm{d}x$$

nip-Diode — External Short-Circuit Current — Static Case

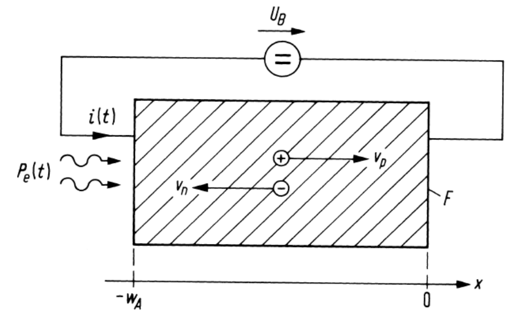

Generation rate, $\partial/\partial t = 0$:

$$eFg(x) = \frac{\eta e}{hf_L} P_e \frac{\alpha\, \mathrm{e}^{-\alpha(x+w_A)}}{1-\mathrm{e}^{-\alpha w_A}}$$

System of differential equations, $\partial/\partial t = 0$:

$$\frac{1}{v_p}\frac{\partial i_p(x,t)}{\partial t} + \frac{\partial i_p(x,t)}{\partial x} = eFg(x,t), \qquad i_p(x,t) = Fep(x,t)v_p,$$

$$\frac{1}{v_n}\frac{\partial i_n(x,t)}{\partial t} - \frac{\partial i_n(x,t)}{\partial x} = eFg(x,t), \qquad i_n(x,t) = Fen_T(x,t)v_n,$$

Minority current injection neglected, $i_p(-w_A) = 0$, $i_n(0) = 0$:

$$i = i_p(0) = i_n(-w_A) = \int_{-w_A}^{0} eFg(x)\,\mathrm{d}x = \frac{\eta e}{hf_L}P_e\,, \qquad i = \frac{\eta e}{hf_L}P_e = SP_e$$

Each absorbed photon generates electron-hole pair $\rightarrow$ transport of one elementary charge e through external circuit.
Rate of generated charges $i/e = \eta P_e/(hf_L)$ photon absorption rate.

Band Structure of Direct and Indirect Semiconductors

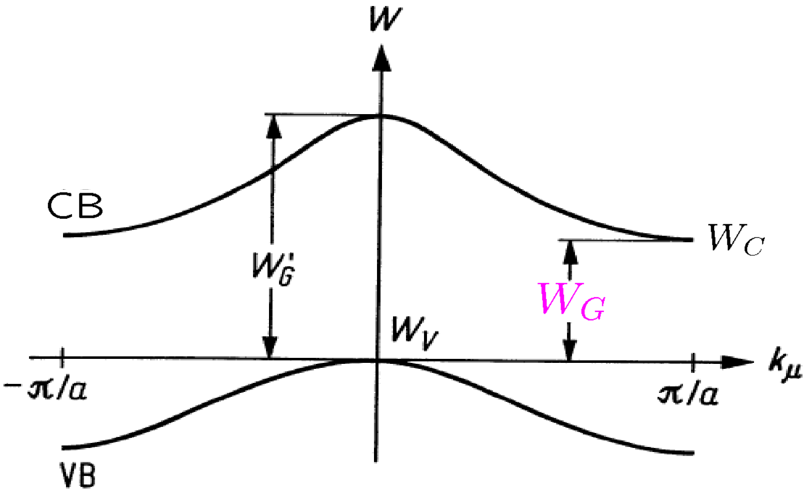

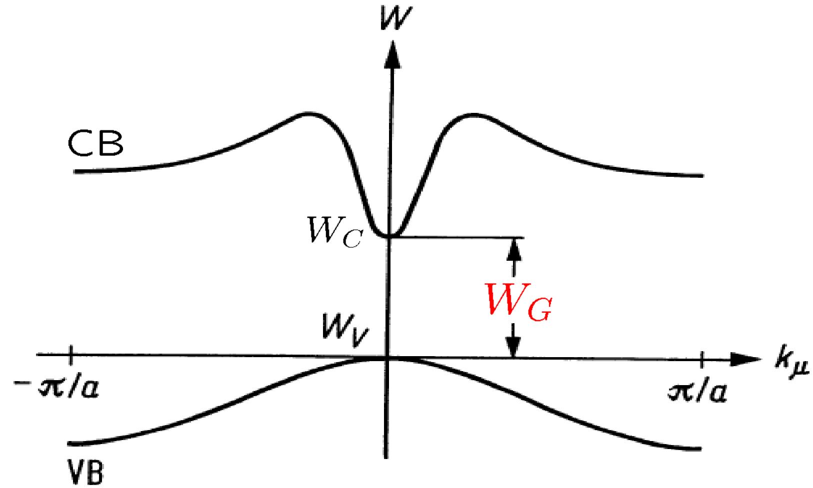

Indirect semicond. Smallest transition energy W_G for crystal momentum diff. $\Delta k_\mu = \pi/a$. Phonon required as collision partner → Radiative transition unlikely. Examples: Elemental semiconductors Si, Ge

$$W_G = \begin{cases} 0.67\,\text{eV} \mathrel{\widehat{=}} 1.85\,\mu\text{m} & (\text{Ge}) \\ 1.13\,\text{eV} \mathrel{\widehat{=}} 1.10\,\mu\text{m} & (\text{Si}) \end{cases}$$

$$W'_G = \begin{cases} 0.8\ \ \text{eV} \mathrel{\widehat{=}} 1.55\,\mu\text{m} & (\text{Ge}) \\ 3.4\ \ \text{eV} \mathrel{\widehat{=}} 0.36\,\mu\text{m} & (\text{Si}) \end{cases}$$

Direct semicond. Smallest transition energy W_G for crystal momentum difference $\Delta k_\mu = 0$. No collision partner required → Radiative transition likely. Examples: Compounds GaAs, InP, InGaAs

$$W_G = \begin{cases} 1.42\,\text{eV} \mathrel{\widehat{=}} 0.87\,\mu\text{m} & (\text{GaAs}) \\ 1.80\,\text{eV} \mathrel{\widehat{=}} 0.69\,\mu\text{m} & (\text{Ga}_{0.7}\text{Al}_{0.3}\text{As}) \\ 0.75\,\text{eV} \mathrel{\widehat{=}} 1.65\,\mu\text{m} & (\text{In}_{0.53}\text{Ga}_{0.47}\text{As}) \\ 1.35\,\text{eV} \mathrel{\widehat{=}} 0.92\,\mu\text{m} & (\text{InP}) \end{cases}$$

Absorption Constants

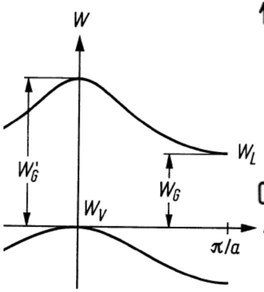

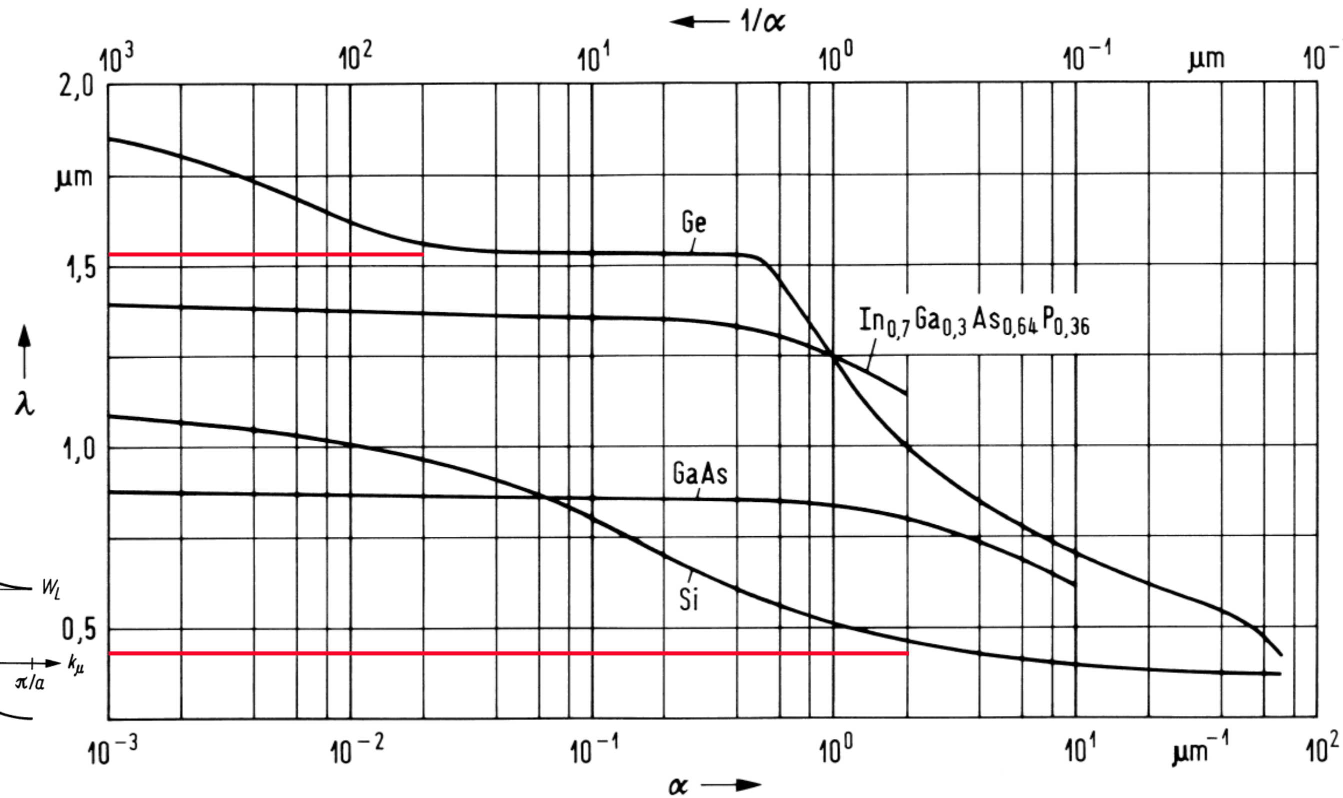

Wavelength dependence of the absorption constant α (penetration depth $1/\alpha$) for several semiconductor materials

$$W_G = \begin{cases} 0{,}67\,\text{eV} \mathrel{\widehat{=}} 1{,}85\,\mu\text{m} & (\text{Ge}) \\ 1{,}13\,\text{eV} \mathrel{\widehat{=}} 1{,}10\,\mu\text{m} & (\text{Si}) \end{cases}$$

$$W_G' = \begin{cases} 0{,}8\ \ \text{eV} \mathrel{\widehat{=}} 1{,}55\,\mu\text{m} & (\text{Ge}) \\ 3{,}4\ \ \text{eV} \mathrel{\widehat{=}} 0{,}36\,\mu\text{m} & (\text{Si}) \end{cases}$$

$$W_G = \begin{cases} 1{,}42\,\text{eV} \mathrel{\widehat{=}} 0{,}87\,\mu\text{m} & (\text{GaAs}) \\ 1{,}80\,\text{eV} \mathrel{\widehat{=}} 0{,}69\,\mu\text{m} & (\text{Ga}_{0,7}\text{Al}_{0,3}\text{As}) \\ 0{,}75\,\text{eV} \mathrel{\widehat{=}} 1{,}65\,\mu\text{m} & (\text{In}_{0,53}\text{Ga}_{0,47}\text{As}) \\ 1{,}35\,\text{eV} \mathrel{\widehat{=}} 0{,}92\,\mu\text{m} & (\text{InP}) \end{cases}$$

pin Photodiode — Dynamics

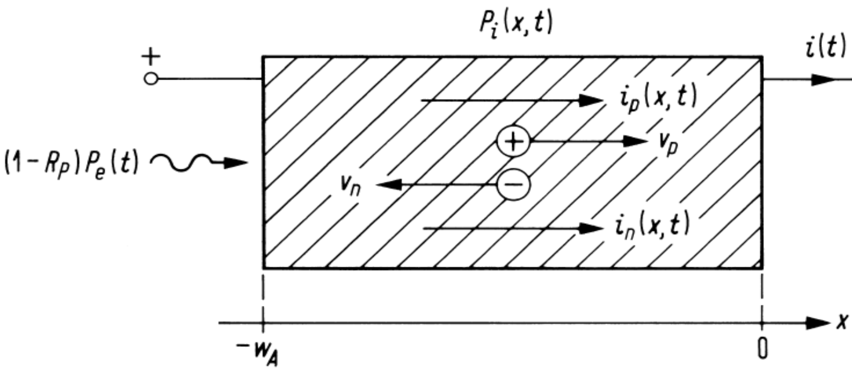

$$\eta = (1 - R_P)\left(1 - \mathrm{e}^{-\alpha w_A}\right)$$

$$eFg(x,t) = \frac{\eta e}{h f_L} P_e(t) \frac{\alpha\, \mathrm{e}^{-\alpha(x+w_A)}}{1 - \mathrm{e}^{-\alpha w_A}}$$

Absorption layer of a pin-photodiode. P_e incicent external light power, R_P power reflection coefficient, $i(t)$ external short-circuit current, P_i internal optical power; i_p, i_n convection currents of electrons and holes; v_p, v_n saturation drift velocities, w_A length of absorption region

Differential equations to be solved for ext. short-circuit current:

$$\frac{1}{v_p}\frac{\partial i_p(x,t)}{\partial t} + \frac{\partial i_p(x,t)}{\partial x} = eFg(x,t), \qquad i_p(x,t) = Fep(x,t)v_p,$$

$$\frac{1}{v_n}\frac{\partial i_n(x,t)}{\partial t} - \frac{\partial i_n(x,t)}{\partial x} = eFg(x,t), \qquad i_n(x,t) = Fen_T(x,t)v_n,$$

$$i(t) = \frac{1}{w_A}\int_{-w_A}^{0} \left[\, i_n(x,t) + i_p(x,t)\,\right] \mathrm{d}x$$

pin Photodiode — Dynamics. Impulse Response (1)

Integrate over interval $-\Delta t \le t \le \Delta t$, current before δ-impulse of generation rate $g(x,t) \sim \delta(t)$ is zero, spatial dependency of time integral of finite current disappears for $\Delta t \to 0$, i. e.,

$$\int_{-\Delta t}^{+\Delta t} \frac{\partial i_p}{\partial x} \,\mathrm{d}t = \frac{\partial}{\partial x} \int_{-\Delta t}^{+\Delta t} i_p \,\mathrm{d}t \to 0 \quad \text{for} \quad \Delta t \to 0,$$

because $i_p(x,t)$ has no singularity in time, and free charge carriers disappear, $P_e(t) = \delta(t)$,

$$\frac{1}{v_p} \int_{-\Delta t}^{+\Delta t} \frac{\partial i_p}{\partial t} \,\mathrm{d}t + \int_{-\Delta t}^{+\Delta t} \frac{\partial i_p}{\partial x} \,\mathrm{d}t = \frac{\eta e}{h f_L} \frac{\alpha\, \mathrm{e}^{-\alpha(x+w_A)}}{1-\mathrm{e}^{-\alpha w_A}} \int_{-\Delta t}^{+\Delta t} \delta(t) \,\mathrm{d}t \quad \text{f. } \Delta t \to 0\,,$$

$$\frac{1}{v_p}\Big(i_p(x,+0) - \underbrace{i_p(x,-0)}_{=0}\Big) + \underbrace{\frac{\partial}{\partial x} \int_{-\Delta t}^{+\Delta t} i_p(x,t) \,\mathrm{d}t}_{=0 \text{ für } \Delta t \to 0} = \frac{\eta e}{h f_L} \frac{\alpha\, \mathrm{e}^{-\alpha(x+w_A)}}{1-\mathrm{e}^{-\alpha w_A}}$$

pin Photodiode — Dynamics. Impulse Response (2)

$$\frac{1}{v_p}\Big(i_p(x,+0) - \underbrace{i_p(x,-0)}_{=0}\Big) + \underbrace{\frac{\partial}{\partial x}\int_{-\Delta t}^{+\Delta t} i_p(x,t)\,\mathrm{d}t}_{=0 \text{ für } \Delta t \to 0} = \frac{\eta e}{h f_L}\,\frac{\alpha\,\mathrm{e}^{-\alpha(x+w_A)}}{1-\mathrm{e}^{-\alpha w_A}}$$

Limit $\Delta t \to 0$ leads to „convection currents" at time $t = +0$ (IC).

$i_p(x,+0) = i_n(x,+0)$ holds because carriers are generated by pairs:

$$\frac{1}{v_p} i_p(x,+0) = \frac{1}{v_n} i_n(x,+0) = \frac{\eta e}{h f_L}\,\frac{\alpha \exp\left[-\alpha(x+w_A)\right]}{1-\exp\left(-\alpha w_A\right)}$$

$g(x,t) = 0$ f. $t > 0$. Homogeneous DE solved by arbitrary functions:

$$\frac{1}{v_p}\frac{\partial i_p}{\partial t} + \frac{\partial i_p}{\partial x} = 0 \longrightarrow i_p(x,t) = i_p(x - v_p t),\quad i_n(x,t) = i_n(x + v_n t),$$

$$\frac{\partial i_p}{\partial t} = \frac{\partial i_p(x-v_p t)}{\partial (x-v_p t)}\,\frac{\partial (x-v_p t)}{\partial t} = -v_p \frac{\partial i_p(x-v_p t)}{\partial (x-v_p t)},$$

$$\frac{\partial i_p}{\partial x} = \frac{\partial i_p(x-v_p t)}{\partial (x-v_p t)}\,\frac{\partial (x-v_p t)}{\partial x} = \frac{\partial i_p(x-v_p t)}{\partial (x-v_p t)}$$

pin Photodiode — Impulse Response Strong Absorption

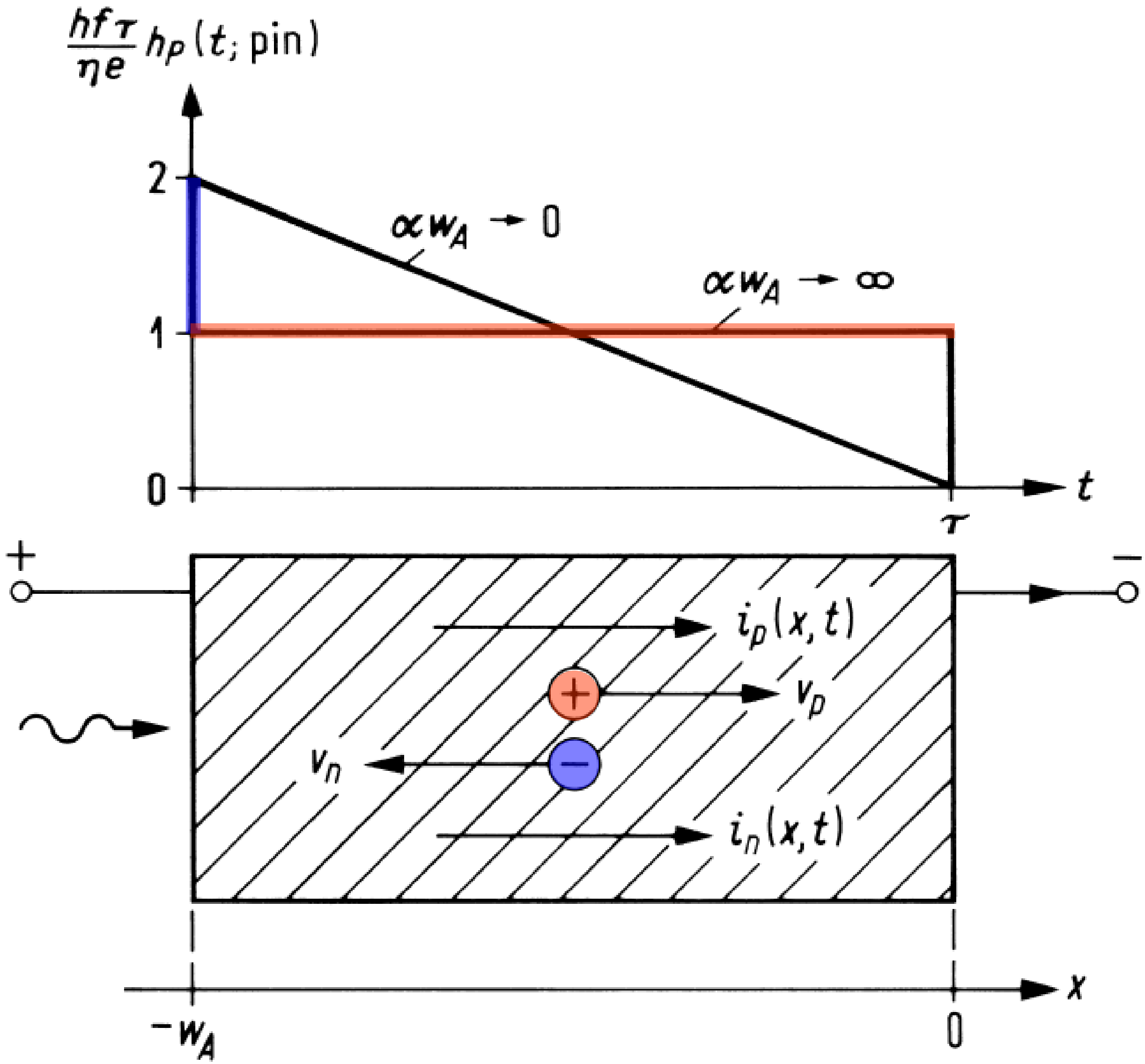

pin Photodiode — Impulse Response Weak Absorpt. ($v_n = v_p$)

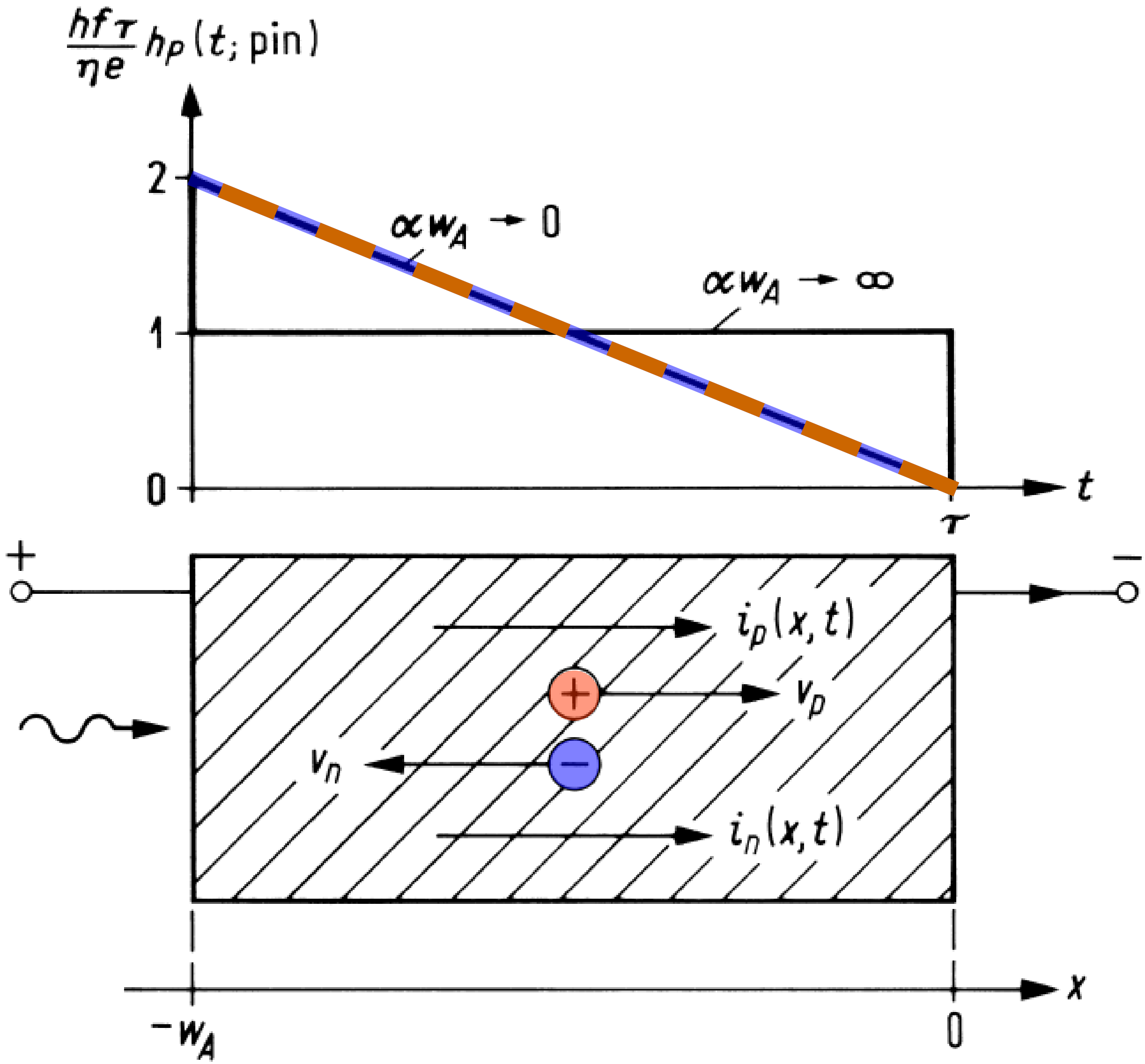

pin Photodiode — Impulse Response Fair Absorpt. ($v_n = v_p$)

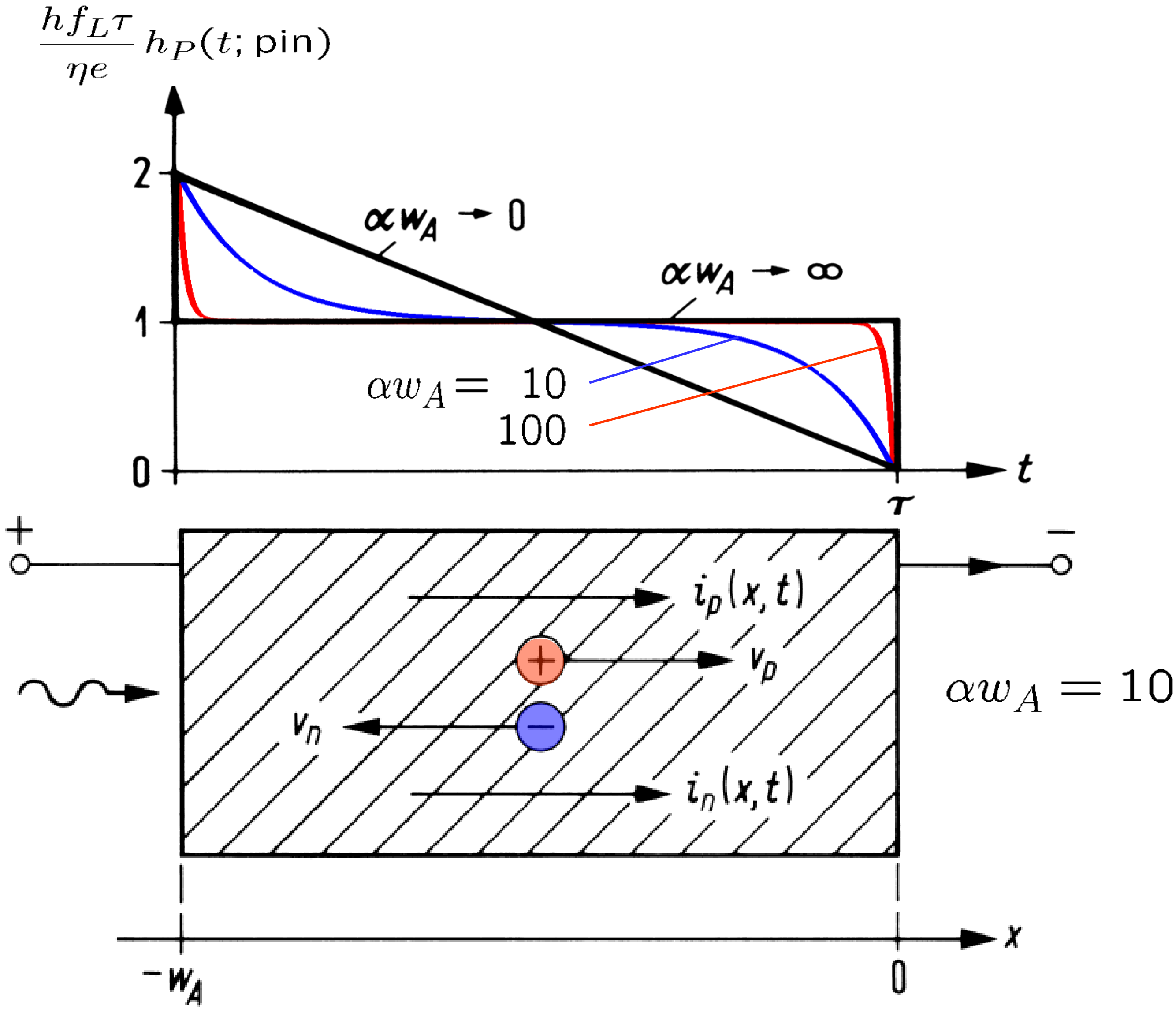

LECTURE 15

pin Photodiode — Transit Time Cutoff Frequency

Short-circuit current spectrum $I(f;\text{pin})$ for light power:

$$P_e(t) = P_0 + P_1 \cos(\omega t) \quad (P_0 \geq P_1)$$

Limiting cases strong and weak absorption, for weak absorption $\tau_n = \tau_p = \tau$ holds:

$$\frac{I(f;\text{pin})}{I(0;\text{pin})} = \mathrm{e}^{-\mathrm{j}\omega\tau_p/2}\,\frac{\sin(\omega\tau_p/2)}{\omega\tau_p/2} \qquad \text{für } \alpha w_A \to \infty$$

$$\frac{I(f;\text{pin})}{I(0;\text{pin})} = \frac{1}{\mathrm{j}\omega\tau/2}\left[1 - \mathrm{e}^{-\mathrm{j}\omega\tau/2}\,\frac{\sin(\omega\tau/2)}{\omega\tau/2}\right] \qquad \text{für } \alpha w_A \to 0$$

3-dB cutoff frequency from $\left|\frac{I(f_{3\text{dB}};\text{pin})}{I(0;\text{pin})}\right| = \frac{1}{\sqrt{2}}$:

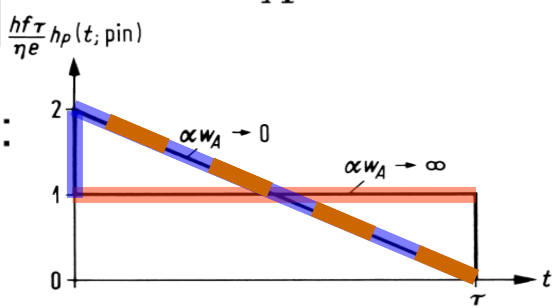

$$f_{3\text{dB}} = \begin{cases} 0.44/\tau_p & \text{for } \alpha w_A \to \infty \\ 0.55/\tau & \text{für } \alpha w_A \to 0, \quad \tau_n = \tau_p = \tau \end{cases}$$

pin Photodiode — Quantum Efficiency

Quantum efficiency for weak absorption $\alpha w_A \to 0$:

$$\eta = \frac{P_i(-w_A,t) - P_i(0,t)}{P_e(t)} = (1-R_P)\left(1 - \mathrm{e}^{-\alpha w_A}\right) \underset{\alpha w_A \to 0}{=} (1-R_P)\alpha w_A$$

3-dB cutoff frequency for $\alpha w_A \to 0$:

$$f_{3\mathrm{dB}} = 0.55/\tau$$

Product of quantum efficiency and cutoff frequency:

$$\eta f_{3\mathrm{dB}} = 0.55\,(1 - R_P)\,\alpha v \qquad \text{for } \alpha w_A \to 0$$

$\eta f_{3\mathrm{dB}}$ depends for $R_P = 0$ only on material properties α, v (power attenuation constant, saturation drift velocities of carriers).

For InGaAs at $\lambda = 1.55\,\mu\mathrm{m}$ ($\alpha = 0.68\,\mu\mathrm{m}^{-1}$, $v = (v_n + v_p)/2 = 56.5\,\mu\mathrm{m/ns}$): $\eta f_{3\mathrm{dB}} = 21\,\mathrm{GHz}$; at $\lambda = 1.36\,\mu\mathrm{m}$ ($\alpha = 1.16\,\mu\mathrm{m}^{-1}$, $v = 56.5\,\mu\mathrm{m}\,/\,\mathrm{ns}$): $\eta f_{3\mathrm{dB}} = 36\,\mathrm{GHz}$.

pin Photodiode — Edge Coupling (1)

For $\alpha w_A \to 0$ better performance achieved by irradiating light $\|$ to pn-junction into absorption zone.

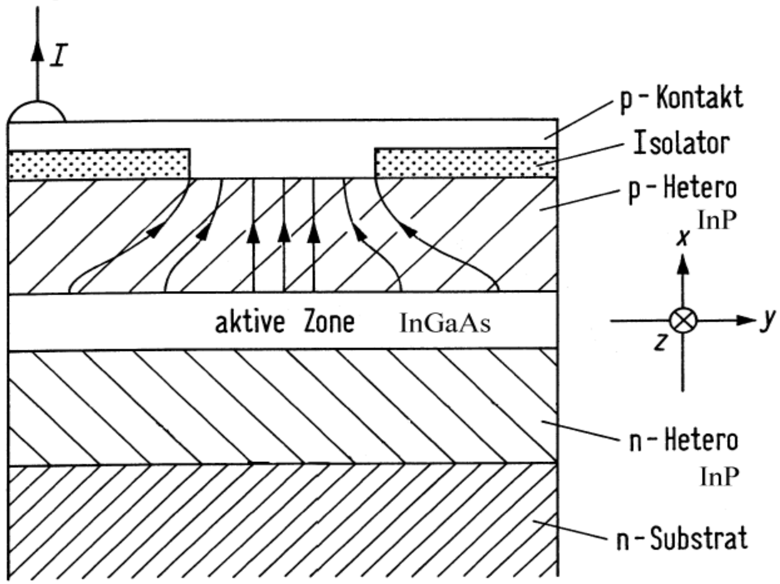

- act. InGaAs absorption zone
- n-InP/p-InP hetero layers
- reverse voltage
- InP/InGaAs/InP slab WG

Pin-diode with edge-coupling of light, w_A is the height of the active zone. x-axis: direction of current flow; z-axis: direction of light propagation (Aktive Zone = active zone, p-Kontakt = p-contact, Isolator = insulator, n-substrat = n-substrate).

For InGaAs layer with thickness $w_A = 0.2\,\mu\text{m}$: Field confinement factor $\Gamma = \dfrac{\text{power in core}}{\text{power in cross-section}} = 0.4$

This means difficult coupling conditions because of small WG cross-section!

pin Photodiode — Edge Coupling (2)

Eff. absorption constant $\alpha\Gamma$ for vertical fundamental mode. Length L of absorption zone in z-direction, coupling efficiency η_{coupl}. Quantum efficiency:

$$\eta = \eta_{\text{coupl}} \left(1 - \mathrm{e}^{-\alpha\Gamma L}\right)$$

Quantum efficiency ($\alpha = 0.68\,\mu\text{m}^{-1}$, $\Gamma = 0.4$, $L > 10\,\mu\text{m}$):

$$\eta \approx \eta_{\text{coupl}} \qquad \text{because} \qquad \mathrm{e}^{-\alpha\Gamma L} < 0.066$$

$\eta_{\text{coupl}} \approx 0.5$ realistic. Transit-time cutoff frequency for <u>small</u> w_A:

$$f_{3\text{dB}} = 0.55/\tau \quad \text{for } \alpha w_A \to 0, \quad \tau_n = \tau_p = \tau$$

$\eta \approx 0.5$ independently of $f_{3\text{dB}}$ and λ. With $w_A = 0.2\,\mu\text{m}$:

$$f_{3\text{dB}} = 124\,\text{GHz}$$

pin Photodiode — Devices, Si Planar and InGaAs-Mesa (1)

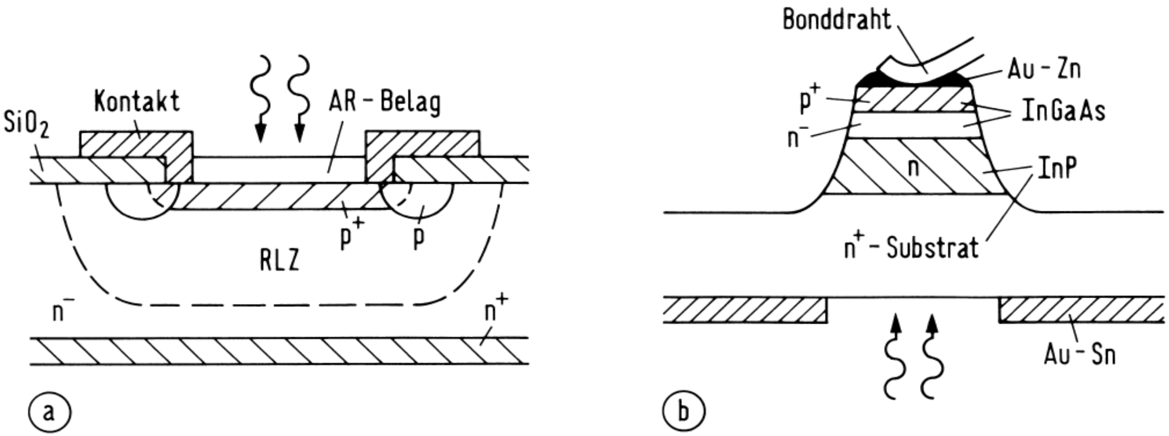

Operation for

$0.92\,\mu\text{m} < \lambda < 1.65\,\mu\text{m}$

Cutoff frequency

$65\ldots100\,\text{GHz}$

for $L_S \leq 0.2\,\text{nH}$

Pin-photodiodes. (a) Planar Si photodiode (b) InGaAs/InP photodiode with mesa structure and illumination through the InP substrate (AR-Belag = anti-reflection coating, RLZ Raumladungszone = depletion region, Kontakt = contact. Bonddraht = bond wire).

Abrupt pn-junction. Doping concentrations n_A, n_D, intrinsic n_i, temperature voltage $U_T = kT/e$, inbuilt voltage U_D, space charge region reverse voltage $U > 0$, junction width w, capacitance C_{sp}:

$$w = \sqrt{\frac{2\epsilon_0\epsilon_r(U_D + U)}{e}\left(\frac{1}{n_A} + \frac{1}{n_D}\right)},$$

$$C_{\text{sp}} = \frac{\epsilon_0\epsilon_r F}{w}, \qquad U_D = U_T \ln\frac{n_A n_D}{n_i^2}.$$

pin Photodiode — Devices, Si Planar (2)

- Short-λ mostly Si, absorption length $1/\alpha = 15\,\mu$m @ $\lambda = 0.85\,\mu$m $\rightarrow \eta \approx 0.5$
- AR coating SiO_2, Si_3N_4. Light in thin ($< 1\,\mu$m) cover layer hardly absorbed. Absorption zone from n$^-$-material ($n_D = 13 \times 10^{14}\,\text{cm}^{-3}$)
- Light in direction of faster carriers (Si: n_T; InGaAs: p)
- p guard ring to prevent breakdown at edges
- Width space-charge region $10\,\mu$m for $U = 10\,$V, $n_D = 1.3 \times 10^{14}\,\text{cm}^{-3} \ll n_A$, $\epsilon_0 = 8.85 \times 10^{-12}\,\text{Fm}^{-1}$, $\epsilon_r = 11.7$
- With $v = (v_n + v_p)/2 = 64\,\mu$m / ns the transit-time cutoff frequency is near 3 GHz:

$$\eta f_{3\text{dB}} = 0.55\,(1 - R_P)\,\alpha v$$

- $F = (200\,\mu\text{m})^2 \mathrel{\widehat{=}} (16\,\mu\text{m diameter})$, $R_S + R_a = 60\,\Omega \rightarrow RC$ cutoff frequency 6.4 GHz $\rightarrow$ transit-time limited

pin Photodiode — Devices, InGaAs Planar (3)

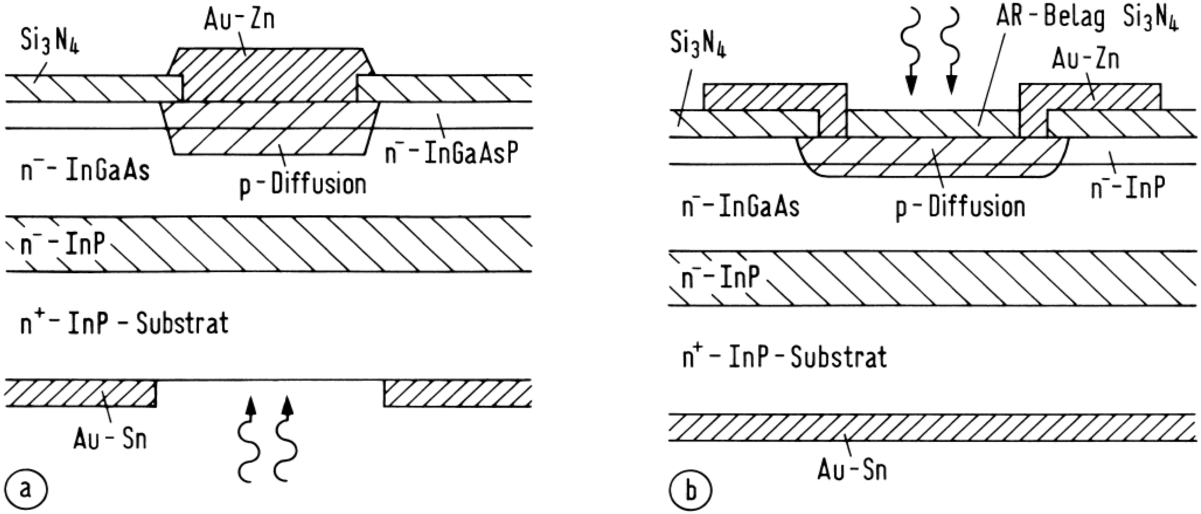

Planar InGaAs/InP pin-photodiodes. (a) Illumination through the substrate (b) illumination from top, AR-Belag = anti-reflection coating

Design of Photodetectors: Overview

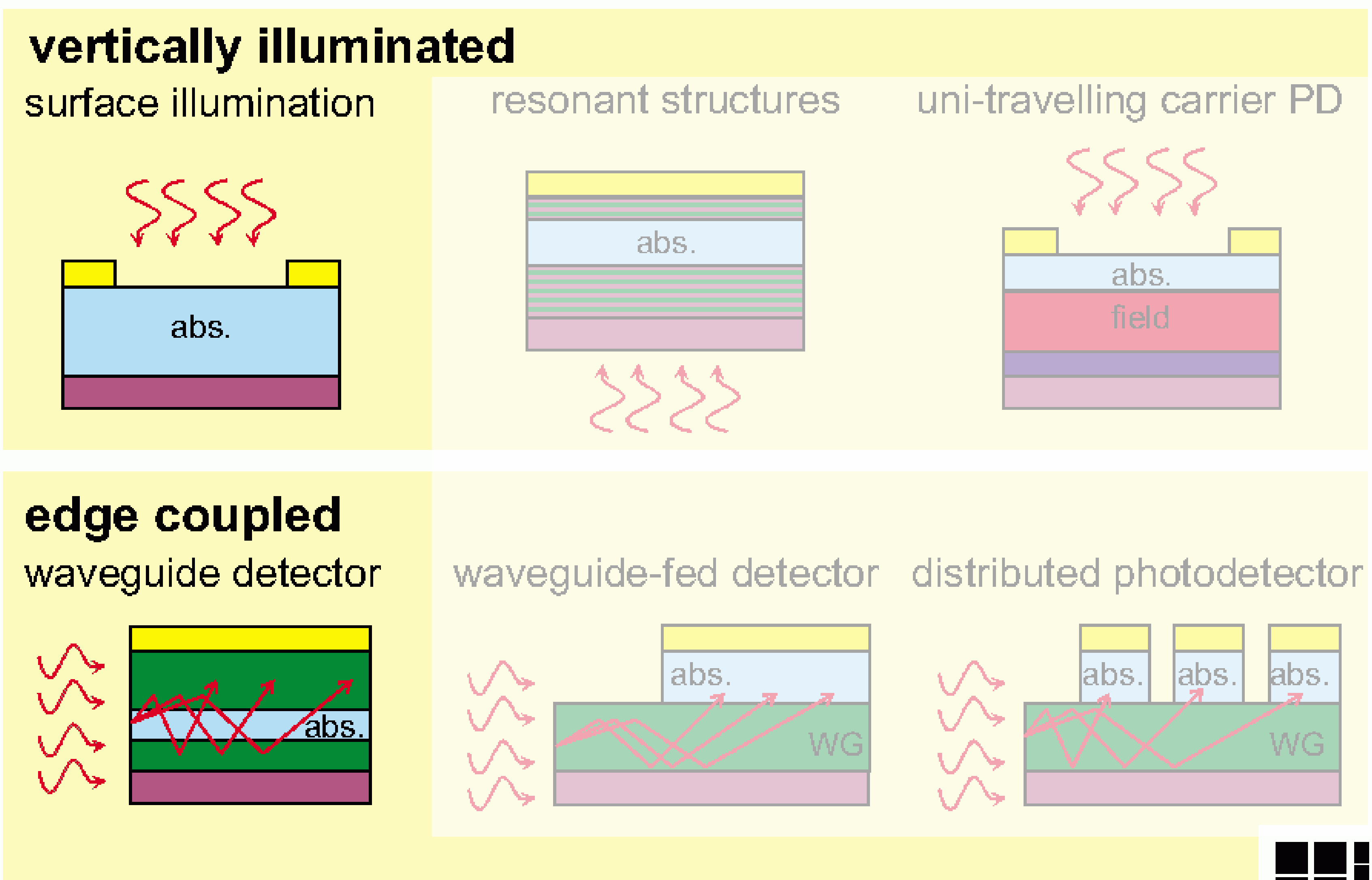

Shot Noise

Shot noise, if quantization of charges manifest:

1. Transition of charges across junctions
2. Transition of charges between electrodes in vacuum
3. Generation of charges through inner photoelectric effect

If RV "carrier number in observation time" statistically independent, then Poisson probability that for $\bar{n}$ (average) n photons:

$$p_n(n) = \frac{\bar{n}^n}{n!}\mathrm{e}^{-\bar{n}}, \qquad \sigma_n^2 = \overline{(n-\bar{n})^2} = \overline{\delta n^2} = \overline{n^2} - (\bar{n})^2 = \bar{n}$$

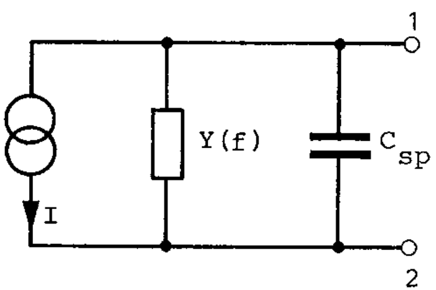

Small-signal equivalent circuit of a pn-junction with shot noise current I. Diffusion admittance $Y(f)$, junction capacitance C_{sp}

Shot noise, two- and one-sided power spectrum:

$$\Theta_i(f) = \bar{i}^{\,2}\delta(f) + e\bar{i}\,,$$
$$w_i(f) = 2\bar{i}^{\,2}\delta(f) + 2e\bar{i}\,.$$

Current generator with RMS phasor I in Δf:

$$\overline{|I|^2} = 2e\bar{i}\Delta f$$

Thermal Noise

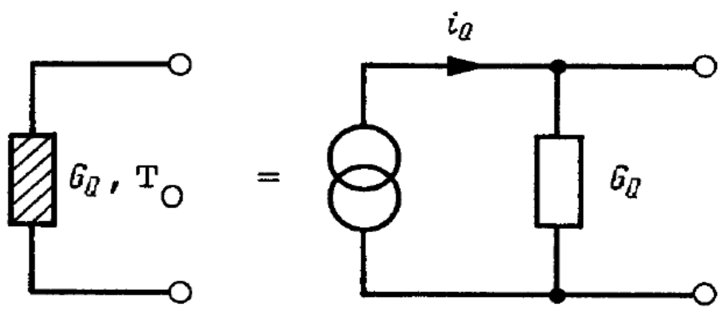

Equivalent circuit of a conductance G_Q with thermal noise

Temperature T, electrons move randomly → random current, even without voltage. PD load resistance at amplifier input adds noise → thermal noise, Johnson or Nyquist noise.

RMS noise phasors discussed in previous slide. Equivalent short-circuit noise phasor i_Q of conductance G_Q at temperature T_0 has an expectation $\overline{i_Q} = 0$ and a second moment:

$$\overline{|i_Q|^2} = 4kT_0G_Q\,\mathrm{d}f, \qquad T_0 = 293\,\mathrm{K}$$

Shot noise for comparison:

$$\overline{|i_{RD}|^2} = 2e\bar{i}\,\mathrm{d}f$$

Amplifier Noise Figure

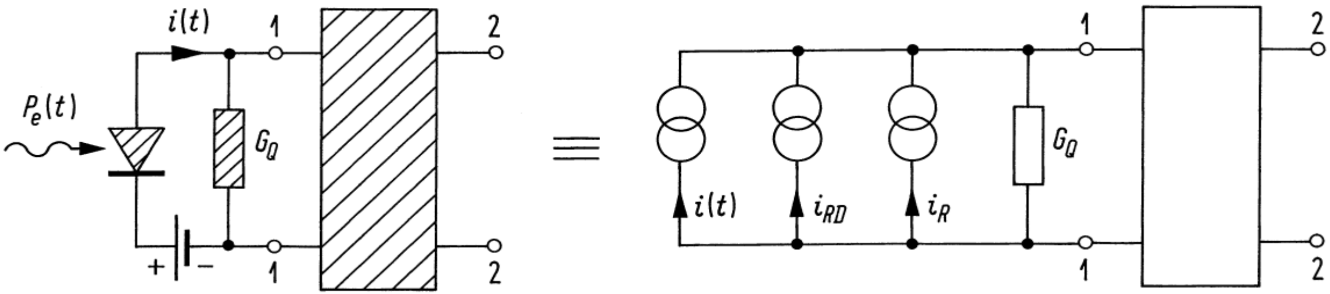

Fig. 7.1. Schematic of an optical receiver with pin-photodiode, source conductance G_Q and amplifier (noisy components are hatched). i_{RD} specifies the shot noise of the pin-photodiode, i_R represents the noise of the source conductance and of the amplifier

Electronic amplifier connected to source with admittance $Y_Q = G_Q + \mathrm{j}\, B_Q$. Amplifier noise described by fictitious increase of actual conductance temperature T_0 to temperature $FT_0 = T_0 + T_R$, then amplifier (noise temperature T_R) regarded as noiseless. Equivalent short-circuit noise current:

$$\overline{|i_R|^2} = 4k\,(FT_0)\,G_Q\,\mathrm{d}f, \qquad F = \frac{\overline{|i_R|^2}}{\overline{|i_Q|^2}} = 1 + \frac{T_R}{T_0},$$

$$F = \frac{\text{total output noise power in }\ \mathrm{d}f}{\text{total output noise power for noiseless two-port in }\ \mathrm{d}f}$$

pin Photodiode Receiver Limits

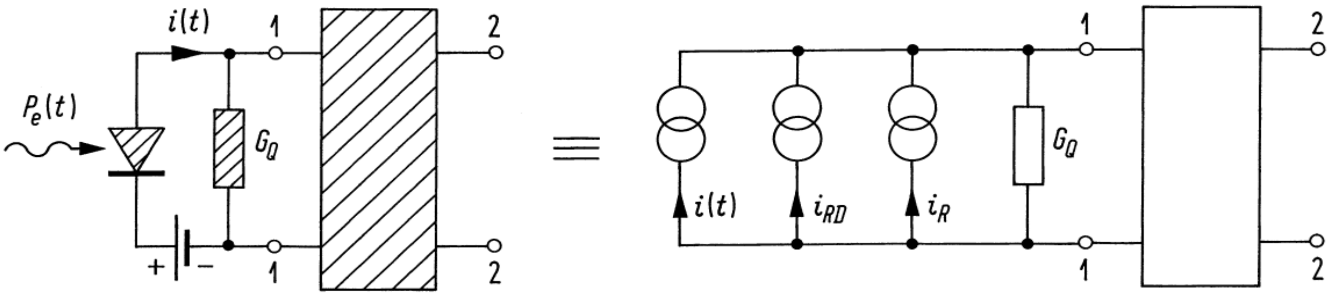

Fig. 7.1. Schematic of an optical receiver with pin-photodiode, source conductance G_Q and amplifier (noisy components are hatched). i_{RD} specifies the shot noise of the pin-photodiode, i_R represents the noise of the source conductance and of the amplifier

Noise sources uncorrelated $\to$ noise powers added. Average signal current $i_S \equiv \overline{i} = S\overline{P_e}$, $S = \eta e/(hf_L)$. SNR γ for direct reception in el. bandwidth d$f = B$ ($\overline{|i_{RD}|^2} = 2ei_S B$, $\overline{|i_R|^2} = 4kFT_0 G_Q B$):

$$\gamma = \frac{P_S}{P_R} = \frac{i_S^2}{\overline{|i_{RD}|^2} + \overline{|i_R|^2}} = \frac{\eta \overline{P_e}}{2hf_L B} \frac{1}{1 + 4kFT_0 G_Q/(2ei_S)}$$

If thermally limited $\overline{|i_R|^2} \gg \overline{|i_{RD}|^2}$. Shot noise limit $\overline{|i_{RD}|^2} \gg \overline{|i_R|^2}$:

$$\gamma_{\mathrm{max}} = \frac{\eta \overline{P_e}}{hf_L \times \left(2B = f_t = \frac{1}{T_t}\right)} = \eta N_e \quad \text{(shot-noise limit, } \frac{4kFT_0 G_Q}{2ei_S} \ll 1\text{)}$$

pin Photodiode Quantum (Shot) Noise Limit

$$\gamma = \frac{P_S}{P_R} = \frac{\overline{i_S^2}}{\overline{|i_{RD}|^2} + \overline{|i_R|^2}} = \frac{\eta \overline{P_e}}{2hf_L B} \frac{1}{1 + 4kFT_0 G_Q/(2ei_S)}$$

$$\gamma_{\text{max}} = \frac{\eta \overline{P_e}}{hf_L \cdot 2B} = \eta N_e \qquad \text{(shot-noise limited, } \frac{4kFT_0 G_Q}{2ei_S} \ll 1\text{)}$$

Bit period $T_t = 1/f_t = 1/(2B)$. Energy per 1-bit $\overline{P_e} T_t \rightarrow$ number of received photons $N_e = \overline{P_e} T_t/(hf_L)$ (absorbed: ηN_e). SNR $= 20\,\text{dB}$ for $N_e \approx 100$ photons ($\eta \approx 1$). Several 1 000 photons required for $\gamma \mathrel{\widehat{=}} 20\,\text{dB}$ when thermal noise dominating. At $1.55\,\mu\text{m}$, receiver operating at $f_t = 10\,\text{Gbit/s}$, $N_e = 100$ when $\overline{P_e} \approx 130\,\text{nW}$.

El. ampl. noise prevents shot noise limit for pin-PD receiver. With OA, i_S large enough. Noise added (minimum for direct reception $F = 2$). Shot-noise limited SNR somewhat smaller, but achievable:

$$\gamma_{\text{OA max}} = \frac{1}{2} \frac{\overline{P_e}}{hf_L \cdot 2B} = \frac{\gamma_{\text{max}}}{2\eta} = \frac{1}{2} N_e$$

Eye Diagram

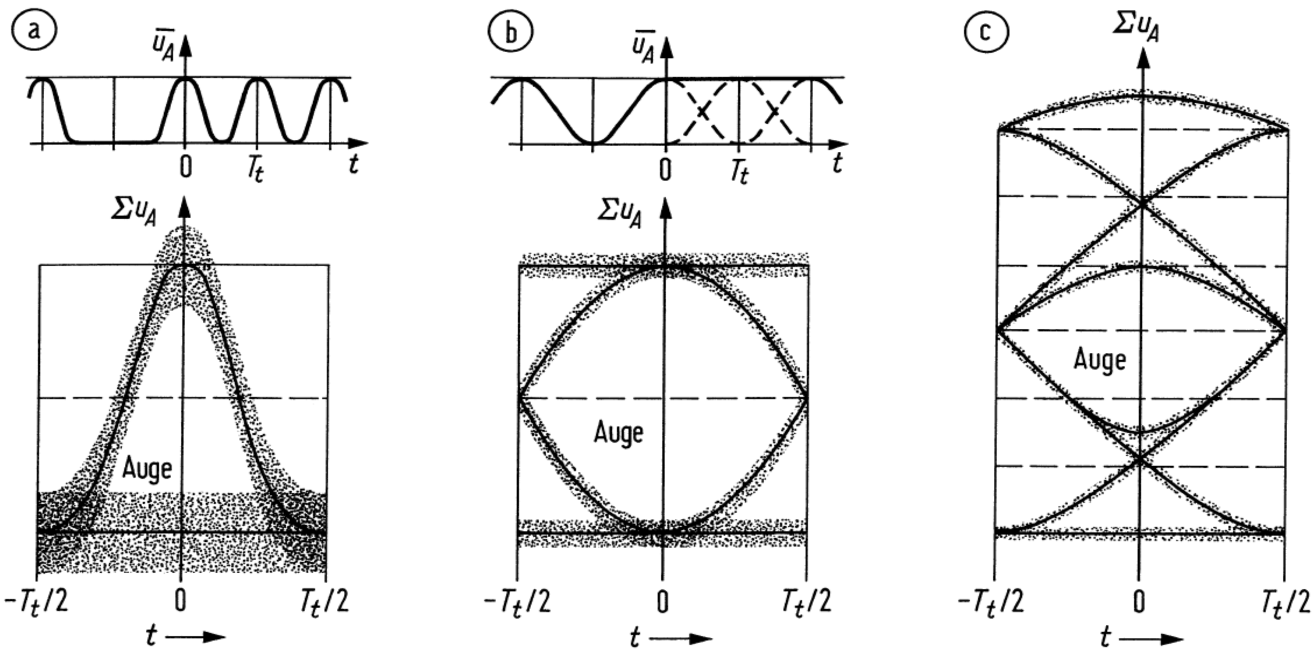

Fig. 7.2. Eye diagrams for RZ (return to zero) pulses, sampling time $t = 0$; solid lines: without noise. (a) large noise, no impulse overlap (b) optimum case: small noise, impulse overlap, but no intersymbol interference at sampling time (c) low noise, strong impulse overlap, strong intersymbol interference at sampling time. Auge = eye

Detection Errors by Noise (1)

Voltage at decision circuit ($u(t) \equiv u_A(t)$):

$$u(t) = u_{R0}(t) \qquad \text{(0-bit received)},$$
$$u(t) = u_{R1}(t) + u_1 h_A(t) \quad \text{(1-bit received)}.$$

Gaussian noise voltages with expectation zero $u_{R0}(t)$, $u_{R1}(t)$. Equalizer produces impulse $h_A(t)$, normalized such that $h_A(0) = 1$ at sampling time $t = 0$. Expectation u_1 at sampling time.

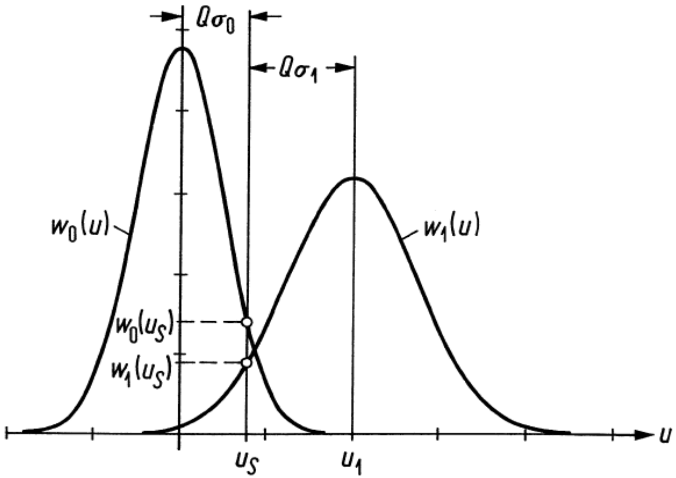

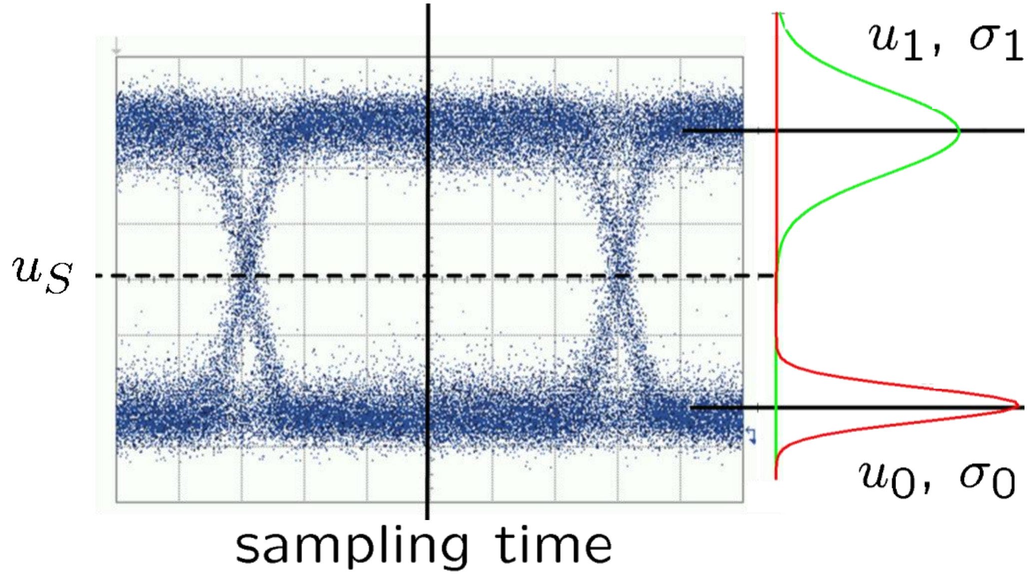

Probability densities $w_0(u)$, $w_1(u)$ of the sampled input voltage of the decision circuit for the receive symbols zero, one. σ_0, σ_1 standard deviations, u_1 expectation of voltage for a received one, u_S specific choice of decision threshold fixed by the bit error parameter Q

Detection Errors by Noise (2)

Probability density functions (pdf) for decision circuit voltages at sampling time $w_0(u)$, $w_1(u)$ (0 and 1 received, respectively):

$$w_0(u) = \frac{1}{\sqrt{2\pi\sigma_0^2}} \exp\left(-\frac{u^2}{2\sigma_0^2}\right), \qquad \overline{u} = 0, \quad \overline{(u-\overline{u})^2} = \overline{u_{R0}^2} = \sigma_0^2,$$

$$w_1(u) = \frac{1}{\sqrt{2\pi\sigma_1^2}} \exp\left[-\frac{(u-u_1)^2}{2\sigma_1^2}\right], \quad \overline{u} = u_1, \quad \overline{(u-\overline{u})^2} = \overline{u_{R1}^2} = \sigma_1^2.$$

$\sigma_1^2 > \sigma_0^2$, because logical 1 transmitted with higher power $\rightarrow$ larger PD shot noise. Usually, $1 < \sigma_1^2/\sigma_0^2 \leq 2$.

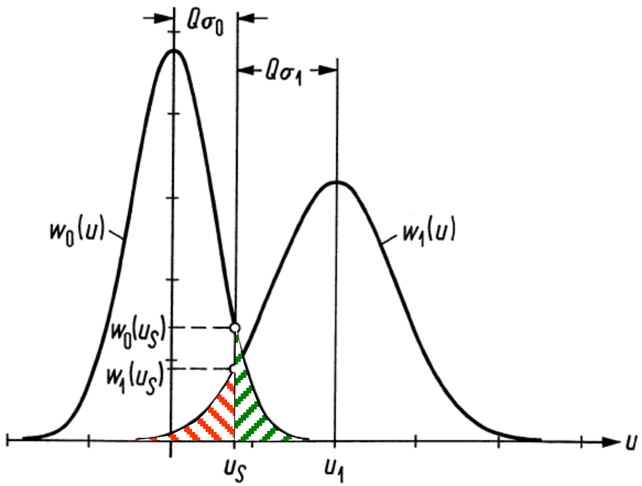

Zero: $u < u_S$. One: $u > u_S$. Prob. that 1 wrong: $p(\text{1d}|\text{0r})$; 0 wrong: $p(\text{0d}|\text{1r})$. Receiving prob. $p(\text{0r})$, $p(\text{1r})$. Bit error probability (BER, bit error ratio):

$$\text{BER} = p(\text{1r})p(\text{0d}|\text{1r}) + p(\text{0r})p(\text{1d}|\text{0r}),$$
$$p(\text{0r}) + p(\text{1r}) = 1$$

Detection Errors by Noise (3)

Minimum bit error probability:

$$\mathrm{BER} = p(1\mathrm{r}) \int_{-\infty}^{u_S} w_1(u)\,\mathrm{d}u + p(0\mathrm{r}) \int_{u_S}^{\infty} w_0(u)\,\mathrm{d}u\,,$$

$$\frac{\partial\,\mathrm{BER}}{\partial u_S} = p(1\mathrm{r}) w_1(u_S) - p(0\mathrm{r}) w_0(u_S) \stackrel{!}{=} 0\,,$$

$$\rightarrow p(1\mathrm{r}) w_1(u_S) = p(0\mathrm{r}) w_0(u_S)$$

Optimum threshold (note: $u_S - u_1 = \pm\sqrt{(u_S - u_0)^2}$):

$$p(1\mathrm{r}) \frac{1}{\sqrt{2\pi\sigma_1^2}} \exp\left(-\frac{(u_S - u_1)^2}{2\sigma_1^2}\right) = p(0\mathrm{r}) \frac{1}{\sqrt{2\pi\sigma_0^2}} \exp\left(-\frac{(u_S - u_0)^2}{2\sigma_0^2}\right)$$

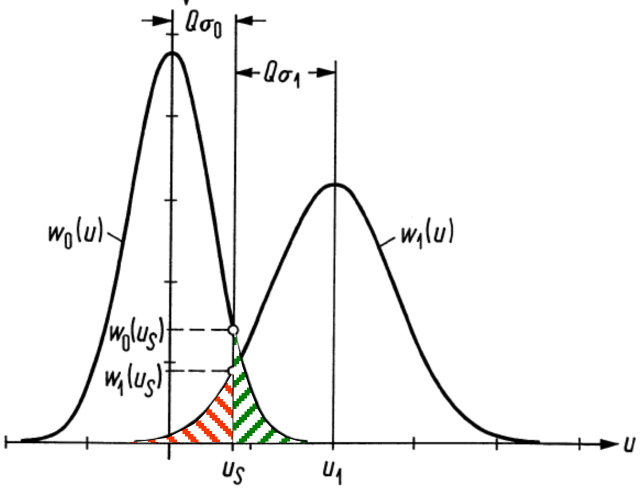

Threshold $u_S = \frac{\sigma_0\,u_1 + \sigma_1\,u_0}{\sigma_0 + \sigma_1}$, if $\frac{p(1\mathrm{r})}{\sigma_1} = \frac{p(0\mathrm{r})}{\sigma_0}$.

In practice:

$$1 < \sigma_1/\sigma_0 \leq \sqrt{2}\,, \qquad \sigma_1 \approx \sigma_0$$

$$p(1\mathrm{r}) = \frac{\sigma_1}{\sigma_0} p(0\mathrm{r}) \gtrapprox p(0\mathrm{r}),$$

$$p(1\mathrm{r}) \approx p(0\mathrm{r}) \approx 1/2$$

Bit-Error Parameter (Signal Quality Factor) and SNR

Connection between SNR γ at decision circuit (mean and RMS value measured) and bit error parameter Q?

No intersymbol interference, bit rate f_t, clock period $T_t = 1/f_t$, el. signal bandwidth $B = f_t/2$. Average el. power at decision circuit:

$$P = \frac{1}{2}\left\{\frac{1}{T_t}\int_{-T_t/2}^{+T_t/2}\overline{[u_1 h_A(t) + \underbrace{u_{R1}(t)}_{\overline{u_{R1}}=0}\,]^2}\,\mathrm{d}t + \frac{1}{T_t}\int_{-T_t/2}^{+T_t/2}\overline{u_{R0}^2(t)}\,\mathrm{d}t\right\}$$

$$= \frac{u_1^2}{2} I(h_A) + \frac{1}{2}(\sigma_0^2 + \sigma_1^2), \qquad I(h_A) = \frac{1}{T_t}\int_{-T_t/2}^{+T_t/2} h_A^2(t)\,\mathrm{d}t \approx \tfrac{1}{2}$$

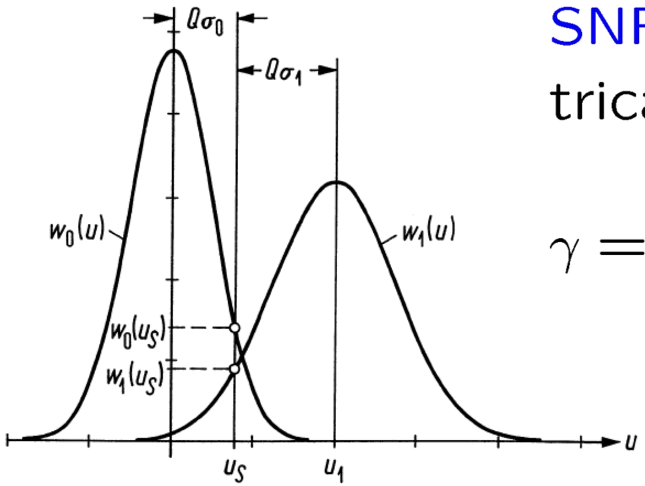

SNR follows, with $u_1 = (\sigma_0 + \sigma_1)Q$ and electrical signal power P_S to noise power P_R:

$$\gamma = \frac{P_S}{P_R} = \frac{u_1^2 I(h_A)/2}{(\sigma_0^2 + \sigma_1^2)/2} = Q^2\frac{(\sigma_0 + \sigma_1)^2 I(h_A)}{\sigma_0^2 + \sigma_1^2}$$

$$= (0.97\ldots 1) \times Q^2, \quad \rightarrow \quad \boxed{\gamma = \frac{P_S}{P_R} = Q^2}$$

BER and Power Penalty (1)

Compensation of additional noise (noise power P_{Rz}) by an increase of signal power $P_S \to P_{S+}$ possible?

$$\gamma = Q^2 = \frac{P_S}{P_R} = \frac{P_{S+}}{P_R + P_{Rz}}, \quad \gamma_+ = Q_+^2 = \frac{P_{S+}}{P_R}, \quad \mathrm{BER}_+ = \frac{1}{2}\,\mathrm{erfc}\left(\frac{Q_+}{\sqrt{2}}\right)$$

γ_+, Q_+, BER_+ for P_{S+} without additional noise.

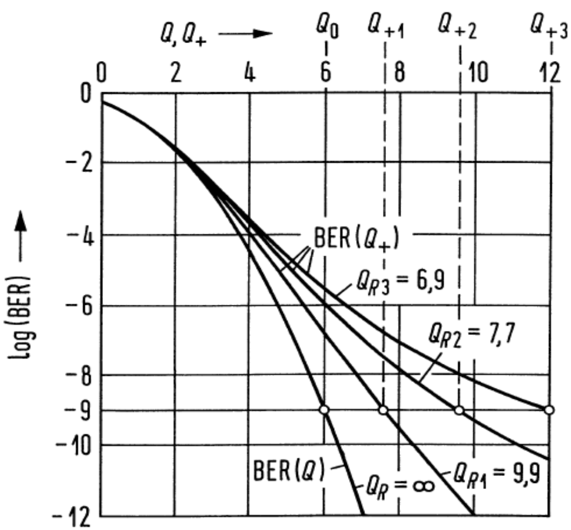

Additive noise: Compensation by increase of opt. input power P_{opt} always possible. El. signal $P_S \sim (P_{\mathrm{opt}})^2$. Power penalty:

$$p_B = 10\ \lg\left(\frac{P_{\mathrm{opt}+}}{P_{\mathrm{opt}}}\right) = 5\ \lg\left(\frac{P_{S+}}{P_S}\right)$$
$$= 10\ \lg\left(\frac{Q_+}{Q}\right) = 5\ \lg\left(1 + \frac{P_{Rz}}{P_R}\right)$$

Fig. 7.4. Bit error probability from Eq. (7.27) as a function of the bit error parameters Q (denoted as BER(Q)) and Q_+ (denoted as BER(Q_+)) for various values of the residual bit error parameter Q_R

BER and Power Penalty (2)

Multiplicative noise: Noise power $P_{Rz} = \frac{1}{\gamma_R} \cdot P_S = \frac{1}{Q_R^2} \cdot P_S$ compensatable by increased signal power $P_S \to P_{S+}$?

$$\gamma = Q^2 = \frac{P_S}{P_R} = \frac{P_{S+}}{P_R + P_{Rz}} = \frac{P_{S+}}{P_R + P_{S+}/Q_R^2} = \frac{Q_+^2 Q_R^2}{Q_+^2 + Q_R^2} \underset{P_{S+}\to\infty}{=} Q_R^2$$

γ_+, Q_+, BER_+ for P_{S+} without additional noise.

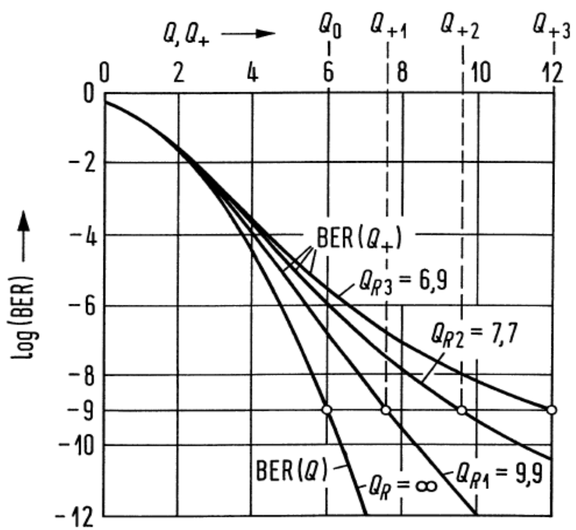

Compensation with increased opt. input power P_{opt} not complete. El. signal $P_S \sim (P_{\text{opt}})^2$. Power penalty, floor BER:

$$p_B = 10 \lg\left(\frac{P_{\text{opt}+}}{P_{\text{opt}}} = \frac{Q_+}{Q}\right) = 5 \lg\left(\frac{Q_R^2}{Q_R^2 - Q^2}\right),$$

$$\mathrm{BER}_R = \frac{1}{2}\operatorname{erfc}\left(\frac{Q_R}{\sqrt{2}}\right)$$

Fig. 7.4. Bit error probability from Eq. (7.27) as a function of the bit error parameters Q (denoted as $\mathrm{BER}(Q)$) and Q_+ (denoted as $\mathrm{BER}(Q_+)$) for various values of the residual bit error parameter Q_R

Limiting Sensitivity for Direct Detection (1)

No electron. noise. PD $\eta = 1$. Zero: $\overline{N_{e\,0}} = 0$. One: $\overline{N_e} \neq 0$. Prob. $p(1\text{d}|0\text{r}) = 0$ that 0 wrongly detected as 1. Threshold $u_S \to u_S = 0$. Only logical 1 perturbed, $p(0\text{d}|1\text{r}) \neq 0$. Poisson probability of photons:

$$p_{N_e}(N_e) = \frac{\overline{N_e}^{N_e}}{N_e!}\,\mathrm{e}^{-\overline{N_e}}, \qquad \overline{\delta N_e^2} = \overline{N_e}, \qquad (\overline{N_e} \text{ arbitrary})$$

$p_{N_S}(N_e = 0)$ is probability that logical 1 with $\overline{N_e} > 0$ wrongly detected as logical 0:

$$p_{N_e}(0) = \frac{\overline{N_e}^{\,0}}{0!}\,\mathrm{e}^{-\overline{N_e}} = \mathrm{e}^{-\overline{N_e}} > 0$$

schematic showing Poisson *probability* (not pdf)

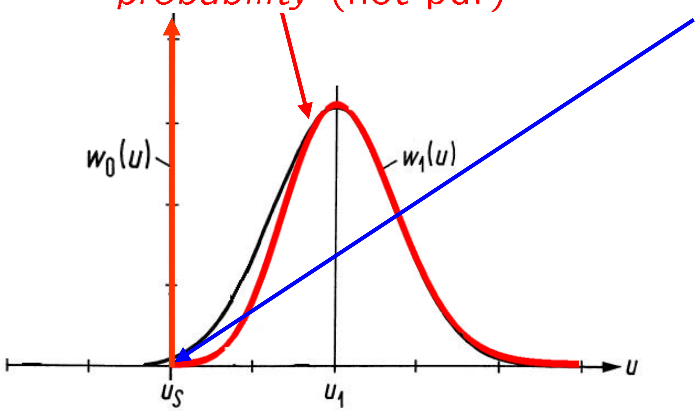

Poisson probability is discrete, therefore probability density function:

$$w_{N_e}(N_e) = \sum_{N_e'=0}^{\infty} p_{N_e}(N_e)\,\delta(N_e - N_e')$$

Limiting Sensitivity for Direct Detection (2)

Prob. One: $p(1\mathrm{r}) = 1/2$. Because of Poisson statistics, prob. that One $\to$ Zero: $p(0\mathrm{d}|1\mathrm{r}) = p_{N_{e\,1}}(0) = \mathrm{e}^{-\overline{N_e}}$. BER:

$$\mathrm{BER} = \overbrace{p(1\mathrm{r})}^{1/2}\,\overbrace{p(0\mathrm{d}|1\mathrm{r})}^{\exp(-\overline{N_e})} + \overbrace{p(0\mathrm{r})}^{1/2}\,\overbrace{p(1\mathrm{d}|0\mathrm{r})}^{0}, \qquad \to \qquad \boxed{\mathrm{BER} = \frac{1}{2}\mathrm{e}^{-\overline{N_e}}}$$

$$p(0\mathrm{r}) + p(1\mathrm{r}) = 1\,,$$

For bit error probability $\mathrm{BER} = 10^{-9}$ therefore:

$$\overline{N_e} = -\ln\left(2\times 10^{-9}\right) = 20 \qquad \to \qquad \boxed{\overline{N_e} = 20 \quad \text{for} \quad \mathrm{BER} = 10^{-9}}$$

schematic showing Poisson *probability* (not pdf)

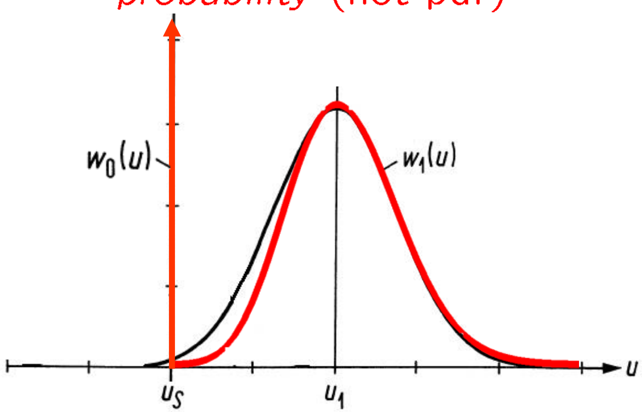

Photons for One ($w(1\mathrm{r}) = 1/2$). On average:

$$\overline{N_{e\,\mathrm{bit}}} = \overbrace{\overline{N_e}}^{20}\,\overbrace{p(1\mathrm{r})}^{1/2} + \overbrace{N_{e\,0}}^{0}\,\overbrace{p(0\mathrm{r})}^{1/2}$$

$$\overline{N_{e\,\mathrm{bit}}} = 10 \quad \text{for} \quad \mathrm{BER} = 10^{-9}$$

Realized: $N_{e\,\mathrm{bit}} = 4\,000$ (pin-PD), $N_{e\,\mathrm{bit}} = 150$ (APD), 152 (pin & OA)

Measured Sensitivities for Direct Detection

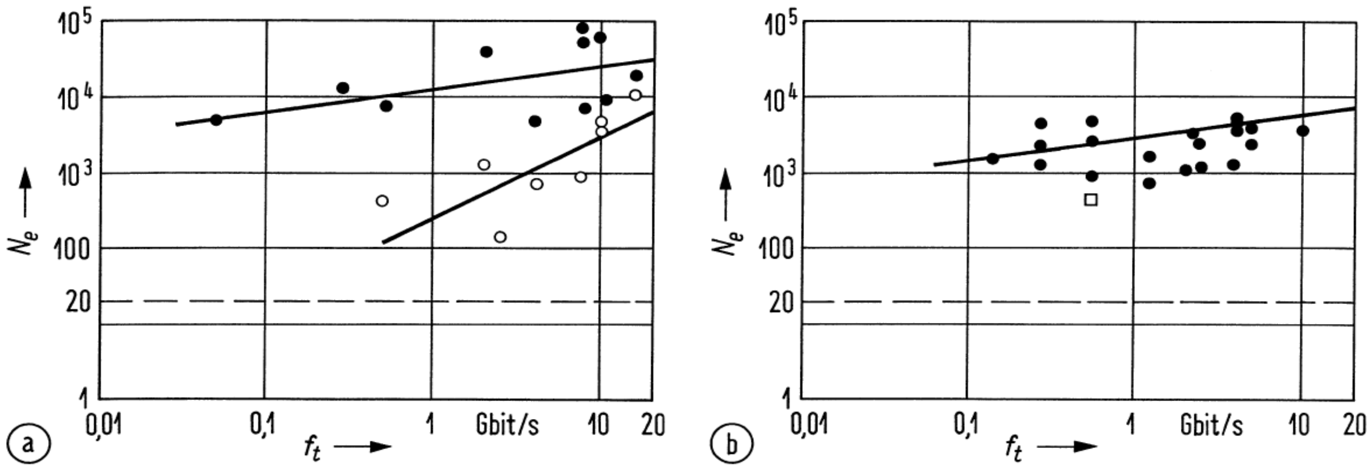

Fig. 7.5. Measured minimum received photon numbers N_e for a 1 bit (η not known, BER $= 10^{-9}$). Quantum limit $N_e = 20$, $\eta = 1$ (– – –). (a) pin-photodiode $\lambda = 1.3$; $1.55\,\mu$m (●), pin-photodiode with optical amplifier (○) (b) avalanche photodiode (APD) $\lambda = 1.55\,\mu$m (●), $\lambda = 0.85\,\mu$m (□)

END OF LECTURES